Universität Bremen

Metabolism of iron and iron oxide nanoparticles in glial cells

Dissertation

zur Erlangung des Grades eines Doktors der Naturwissenschaften
des Fachbereichs 2 Biologie/Chemie
Universität Bremen

2011

vorgelegt von
Michaela C. Hohnholt

Dekan: Prof. Dr. S. Kelm

1. Gutachter: Prof. Dr. R. Dringen

2. Gutachter: Prof. Dr. S. Kelm

Hiermit versichere ich, die vorliegende Dissertationsarbeit selbstständig und nur unter Verwendung der angegebenen Hilfsmittel angefertigt zu haben. Diese Arbeit wurde zuvor nicht an anderer Stelle eingereicht.

Bremen, Juni 2011

(Michaela C. Hohnholt)

Table of content

I   Acknowledgment

I would like to gratefully thank Prof. Dr. Ralf Dringen for giving me the opportunity to work on my doctoral thesis under his supervision. I would like to acknowledge the support he provided with his incredible knowledge in biochemistry and brain cells, advice for practical work as well as for writing manuscripts and funding applications. His amazing enthusiasm for scientific research was a constant and enormous encouragement during my doctoral thesis.

I would like to thank Prof. Dr. Soerge Kelm very much for being the second referee of my thesis.

My special thanks to Mark Geppert for a very successful cooperation during my thesis and providing the nanoparticles I used in my thesis. I would like to express my gratitude to the other coauthors of the publications in this thesis.

I would like to thank all members of the Dringen group for their continuous advice, help and support in laboratory work and scientific discussions. Many thanks go to Monika Cox and Yvonne Köhler for their excellent management of the Dringen laboratory. Furthermore, I would like to acknowledge the help and support of all present doctoral students of the Dringen group, Dr. Maike M. Schmidt and Yvonne Köhler for support and advice during the writing of this thesis.

The graduate school nanoToxCom offered me the opportunity to broaden my scientific horizon in various research fields from ecology to risk assessment with seminars on scientific methods, numerous guest talks and scientific discussions.

I would like to thank the "Zentrale Forschungsförderung" of the University of Bremen for the financial support during my thesis.

To my father, brother, partner and close friends, thank you so much for your endless love and support especially during the ups and downs of the emotional roller coaster of this doctoral thesis.

II   Structure of this thesis

This thesis investigated the two glial cell types oligodendroglial cells and astrocytes. The Results subchapter 2.1. contains results obtained on OLN-93 cells. The first manuscript describes the iron metabolism of OLN-93 cells (chapter 2.1.1.) that was not submitted so far for publication. In this chapter, figures and tables are placed at the respective position in the text. The Results subchapter 2.1. contains in addition one accepted publication on the proliferation of OLN-93 cells (chapter 2.1.2.) and two submitted manuscripts describing the consequences of an exposure of OLN-93 cells to iron oxide nanoparticles (chapters 2.1.3. and 2.1.4.). The Results subchapter 2.2. consists of three accepted publications on the viability and iron accumulation of iron oxide nanoparticles-exposed cultured astrocytes.

Accepted publications are inserted as portable document format. The two submitted manuscripts were adapted to the layout of this thesis and the figures, tables and their legends were placed directly after the results chapter. Otherwise are the submitted manuscripts shown in the present thesis identical to the versions that were submitted for publication.

For each accepted publication and submitted manuscript in this thesis, the contributions of the authors are listed on the first page of the respective chapter.

III   Summary

Iron is an essential metal for mammalian cells catalyzing redox reactions in various metabolic pathways. However, iron can also induce cellular damage due to increased formation of reactive oxygen species (ROS). Among the different brain cell types, oligodendrocytes produce and maintain the myelin sheaths around neuronal axons whereas brain astrocytes participate in a variety of different brain functions such as synaptic signal transduction, regulation of metal homeostasis and detoxification of xenobiotics. In brain, these cells may encounter iron oxide nanoparticles (Fe-NP), since Fe-NP are extensively investigated for biomedical applications.

This thesis investigated the metabolism of iron and Fe-NP in glial cells. The oligodendroglial OLN-93 cells express the mRNAs of the protein transferrin, transferrin-receptor and divalent metal transporter 1 for iron uptake as well as the iron storage protein ferritin. The proliferation of these cells depended on the availability of extracellular iron and can be inhibited by iron chelators. Furthermore, OLN-93 cells accumulated substantial amounts of iron from low molecular weight iron salts and Fe-NP. The cell viability was not compromised despite of high intracellular iron concentrations. Moreover, exposure to Fe-NP hardly affected the metabolism of OLN-93 cells. Intracellularly, iron was mobilized from Fe-NP by OLN-93 cells as demonstrated by the increase in proliferation following iron restriction, by the upregulation of ferritin and by the inhibition of Fe-NP-dependent ROS formation by a cell-membrane-permeable iron chelator.

Also primary astrocytes took up Fe-NP as shown by increased cellular iron contents and electron microscopy. Both OLN-93 cells and astrocytes accumulated iron from Fe-NP in comparable amounts, showed similar time- and concentration-dependencies of iron accumulation and stored iron in ferritin. These observations suggest that the uptake and the cellular fate of Fe-NP are similar in OLN-93 cells and astrocytes.

IV Zusammenfassung

Eisen ist ein essentielles Metall für Säugetierzellen, welches Redoxreaktion in verschiedenen Stoffwechselwegen katalysiert. Allerdings kann Eisen auch durch die erhöhte Bildung von reaktiven Sauerstoffspezies Zellschädigungen induzieren. Unter den verschiedenen Gehirnzelltypen haben Oligodendrozyten die Funktion der Produktion und Aufrechterhaltung der Myelinscheiden um die neuronalen Axone, wohingegen Astrocyten an einer Vielzahl von Funktion im Gehirn beteiligt sind, wie zum Beispiel an der synaptischen Signalübertragung, an der Regulation des Metallstoffwechsels und an der Entgiftung von Fremdstoffen. Im Gehirn könnten diese Zellen Eisenoxid-Nanopartikeln ausgesetzt sein, da Eisenoxid-Nanopartikel weitgehend für biomedizinische Anwendungen untersucht werden.

In dieser Dissertationsarbeit wurde der Metabolismus von Eisen und Eisenoxid-Nanopartikeln in glialen Zellen untersucht. The oligodendroglialen OLN-93 Zellen exprimieren die mRNA der Proteine Transferrin, des Transferrin-Rezeptors und des divalenten Metall Transporters 1 zur Eisenaufnahme und auch die des Eisenspeicherproteins Ferritin. Die Proliferation dieser Zellen war von der Verfügbarkeit von extrazellulärem Eisen abhängig und konnte durch Eisenchelatoren inhibiert werden. Desweiteren akkumulierten OLN-93 Zellen substanzielle Mengen Eisen aus niedermolekularen Eisensalzen und Eisenoxid-Nanopartikeln. Die Zellvitalität wurde ungeachtet der hohen intrazellulären Eisenkonzentrationen nicht beeinträchtigt. Darüber hinaus beeinflusste die Exposition mit Eisenoxid-Nanopartikeln kaum den Stoffwechsel von OLN-93 Zellen. Intrazellulär wurde Eisen aus Eisenoxid-Nanopartikeln von OLN-93 Zellen mobilisiert, was anhand der gesteigerten Proliferation unter Eisenmangelbedigungen, der Hochregulierung von Ferritin und der Inhibition der Eisenoxid-Nanopartikel-abhängigen ROS Bildung durch einen Zellmembran-permeablen Eisenchelator gezeigt wurde.

Auch primäre Astrocyten nahmen Eisenoxid-Nanopartikel auf, welches mittels der gesteigerten zellulären Eisengehalte und Elektronenmikroskopie gezeigt wurde. Beide, OLN-93 Zellen und Astrocyten, akkumulierten Eisen aus Eisenoxid-Nanopartikeln in vergleichbaren Mengen, zeigten ähnliche Zeit- und Konzentrationsabhängigkeiten der Eisenaufnahme und speicherten Eisen in Ferritin. Diese Beobachtungen lassen darauf schließen, dass die Aufnahme und das zelluläre Schicksal von Eisenoxid-Nanopartikeln in OLN-93 Zellen und Astrocyten ähnlich sind.

V   Abbreviations

ABCB7	ATP-binding cassette transporter for iron-sulfur clusters
ABC-transporters	ATP-binding cassette transporter
AD	Alzheimer´s disease
ANOVA	analysis of variance
APC	astrocyte-rich primary cultures
APP	amyloid precursor protein
ATP	adenosine triphosphate
BBB	blood brain barrier
bp	base pairs
C	control
cDNA	complementary deoxyribonucleic acid
CHX	cycloheximide
cm	centimeter
cm^2	square centimeter
CNS	central nervous system
CNP	2´,3´-cyclic nucleotide-3´-phosphohydrolase
Cp	ceruloplasmin
Da	dalton
Dcytb	duodenal cytochrome b
DFX	deferoxamine
DMEM	Dulbecco´s modified Eagle´s medium
DMT1	divalent metal transporter 1
DMSA	dimercaptosuccinic acid
DNA	deoxyribonucleic acid
DNTB	5,5´-dithio-bis(2-nitrobenzoic acid)
dNTP	deoxynucleotide triphosphate
EC50	half maximal effect concentration
EGFR	epidermal growth factor receptor
et al.	latin for *et alii*, and others
F	forward primer sequence
FAC	ferric ammonium citrate
FCS	fetal calf serum
Fe-NP	iron oxide nanoparticles
Fe-S cluster	iron-sulfur cluster
Fig./Figs.	figure/figures
Fpn	ferroportin
Ft-H	heavy chain of ferritin
Ft-L	light chain of ferritin
g	acceleration of gravity
G	glycosylphosphatidylinositol
GalC	galactosylceramides
G-Cp	glycosylphosphatidylinositol-anchored form of ceruloplasmin
GPx	glutathione peroxidase
GSH	glutathione
GSSG	glutathione disulfide
h	hour/hours
H-ferritin	heavy chain-rich ferritin

HEF	hemochromatosis protein
HEPES	N-(2-hydroxyethyl)piperazine-N´-(2-ethanesulfonic acid)
IB	incubation buffer
IgG	Immunoglobulin G
IRE	iron responsive element
IREG1	ferroportin
IRP1	iron regulatory protein 1
IRP2	iron regulatory protein 2
k	kilo
K_M	Michaelis-Menten-constant
L	liter
LDH	lactate dehydrogenase
L-ferritin	light chain-rich ferritin
M	molar (moles/L)
MAG	myelin-associated glycoprotein
MBP	myelin basic protein
mg	milligram
min	minute/minutes
mL	milliliter
mM	millimolar (millimoles/L)
MOG	myelin/oligodendrocyte glycoprotein
MRI	magnetic resonance imaging
MS	multiple sclerosis
MTT	3-(4,5-dimethylthiazol-2-yl)-2,5-diphenyl tetrasodium bromide
mRNA	messenger ribonucleic acid
n	number of experiments
$NADH/NAD^+$	nicotinamide adenine dinucleotide, reduced/oxidized
$NADPH/NADP^+$	nicotinamide adenine dinucleotide phosphate, reduced/oxidized
nm	nanometer
nmol	nanomole
NCAM	neural cell adhesion molecule
O	OLN-93 cells
PBS	phosphate-buffered saline
PCR	polymerase chain reaction
PD	Parkinson´s disease
PEG	polyethylene glycol
PI	propidium iodide
PSA-NCAM	polysialylated neural cell adhesion molecule
PLP	proteolipid protein
PDGFR α	platelet-derived growth factor α-receptor
R	reverse primer sequence
RNA	ribonucleic acid
ROOH	organic peroxides
ROS	reactive oxygen species
RT-PCR	reverse transcriptase-polymerase chain reaction
SDCT	sodium-dependent carboxylate transporter
SOD	superoxide dismutase
Tab	table
TBS	tris-buffered saline
TBST	tris-buffer saline containing 0.1% (w/v) Tween 20
Tf	transferrin

TfR	transferrin receptor
Tim-2	T cell immunoglobulin-domain and mucin-domain 2
TNB	5-thio-2-nitrobenzoate
U	unit (μmol/min)
v	volume
v_{max}	maximum velocity
w	weight
β-A	β-actin
°C	degree Celsius
μg	microgram
μL	microliter
μm	micrometer
μM	micromolar (micromoles/L)

1. Introduction

Content of the chapter

1.1. Glial cells

1.1.1. Oligodendrocytes

1.1.2. OLN-93 cells as model system for oligodendroglial precursor cells

1.1.3. Astrocytes

1.2. Iron

1.2.1. Iron, iron-mediated oxidative stress and antioxidative defense mechanisms

1.2.2. Iron metabolism of the brain

1.2.3. Oligodendrocytes and iron

1.2.4. Iron metabolism of cultured astrocytes

1.3. Nanoparticles

1.3.1. Magnetic iron oxide nanoparticles

1.3.2. Uptake mechanisms of iron oxide nanoparticles

1.3.3. Potential toxicity of iron oxide nanoparticles

1.3.4. Intracellular fate of iron oxide nanoparticles

1.3.5. Iron oxide nanoparticles cross the blood brain barrier

1.3.6. Effects of iron oxide nanoparticles on glial cells

1.4. Aim of the thesis

1.5. References

1. Introduction

1.1. Glial cells

The central nervous system (CNS) consists of different cell types which act in concert to enable the brain to fulfill its function of information processing (Bullock *et al.* 2005). Brain cells are divided into excitable neurons and non-excitable glial cells (Verkhratsky and Butt 2007). The neurons perform the signal transduction along their axons and for their survival and function the presence of glial cells is crucial (Eroglu and Barres 2010, Piaton *et al.* 2010). Interestingly, the glial cell population accounts for more than 90% of all human brain cells (Verkhratsky and Butt 2007) and can be further divided into oligodendrocytes (see chapter 1.1.1.), astrocytes (see chapter 1.1.3.), immune-competent microglial cells (Graeber and Streit 2010) and some other cell types such as ependymal cells (Verkhratsky and Butt 2007) and pericytes (Krueger and Bechmann 2010).

1.1.1. Oligodendrocytes

<u>Functions and development of oligodendrocytes in the brain</u>

Oligodendrocytes are the myelin-forming cells of the brain. The myelin sheath is an insulating layer around the axons of neurons to maximize the conduction velocity of electrical signals (Emery 2010, Miron *et al.* 2011). Two myelin segments are separated from each other by the nodes of Ranvier, in which sodium channels are clustered. The propagation of electric signals from one node to the next strongly increases the conduction velocity of myelinated axons (Baumann and Pham-Dinh 2001, McTigue and Tripathi 2008). However, the oligodendroglial myelin sheath is not only a passive insulation layer, as oligodendrocytes and neuronal axons also interact with each other. For example, factors released from oligodendrocytes support axonal survival (Nave 2010) and oligodendrocytes respond to factors derived from axons (Nave and Trapp 2008). Moreover, one oligodendrocyte myelinates several axons (Miron *et al.* 2011) and one axon is myelinated by different oligodendrocytes (Baumann and Pham-Dinh 2001).

The development of the brain is a chronology of complex processes which are determined and influenced by intrinsic and environmental factors (Stiles and Jernigan 2010). Neurons develop from neural progenitor cells predominately prenatally, whereas glial progenitor cell

2

proliferation also begins prenatally but extends until adulthood (Stiles and Jernigan 2010). Oligodendrocyte precursor cells originate from the subventricular zone and migrate through the CNS to reach all brain areas and mature into myelin forming cells (Bradl and Lassmann 2010). Each of the developmental stages of oligodendrocytes is characterized by the expression of different marker proteins. Oligodendroglial precursor cells express the polysialylated neural cell adhesion molecule (PSA-NCAM) and a splicing variant of the proteolipid protein (PLP) gene product DM-20 (Baumann and Pham-Dinh 2001, Bradl and Lassmann 2010). The next developmental stage is the oligodendrocyte progenitor cell, which is characterized by a bipolar morphology and by expression of NG2 proteoglycan, platelet-derived growth factor α-receptor (PDGFRα) and the ganglioside GD3 (Baumann and Pham-Dinh 2001, McTigue and Tripathi 2008, Jakovcevski *et al.* 2009). Cells in this developmental stage are able to migrate and proliferate (Baumann and Pham-Dinh 2001, McTigue and Tripathi 2008, Jakovcevski *et al.* 2009). After arrival at their final place in the brain, oligodendrocyte progenitor cells develop multiple processes and express a protein that can be detected by the antibody O4 (Baumann and Pham-Dinh 2001, Jakovcevski *et al.* 2009). The subsequent developmental stage is the immature oligodendrocyte. These cells express galactosylceramides (GalC) and 2′,3′-cyclic nucleotide-3′-phosphohydrolase (CNP) as the first myelin specific markers (Baumann and Pham-Dinh 2001, Bradl and Lassmann 2010). Finally, mature oligodendrocytes are characterized by the expression of myelin basic protein (MBP), myelin-associated glycoprotein (MAG), PLP and myelin/oligodendrocyte glycoprotein (MOG; Baumann and Pham-Dinh 2001, Jakovcevski *et al.* 2009). The above list of markers of the oligodendrocyte lineage is not complete and for a detailed overview, the reader is referred to more comprehensive reviews (Baumann and Pham-Dinh 2001, Jakovcevski *et al.* 2009, Bradl and Lassmann 2010).

Structure of myelin and its function for saltatory conduction

The myelin sheath is an extension of the plasma membrane of mature oligodendrocytes, which envelopes the neuronal axon in a spiral that appears as electron-dense and electron-light concentric rings on electron microscopical pictures (Baumann and Pham-Dinh 2001, Nave 2010). The dry mass of the myelin sheaths consists of 70% lipids, in which glycosphingolipids such as GalC are especially enriched, and 30% proteins, such as MBP, PLP, CNP, MAG and MOG (Baumann and Pham-Dinh 2001, Baron and Hoekstra 2010).

The process of myelination itself is partly regulated by the activity of the axon, since the blockage of axonal activity, for example by inhibition of action potentials, inhibits also the

myelination (Bradl and Lassmann 2010). Furthermore, the assembly of the myelin sheath is a complex process, since biosynthesis and transport of the myelin proteins to the plasma membrane are accomplished by different ways for each of the different proteins (Baron and Hoekstra 2010, Bradl and Lassmann 2010). For example, the messenger ribonucleic acid (mRNA) of MBP is transported to the plasma membrane, where the protein is synthesized, whereas the PLP protein is synthesized in the rough endoplasmic reticulum and is transported as protein in vesicles to its destination (Baron and Hoekstra 2010, Bradl and Lassmann 2010).

Demyelinating diseases and remyelination

Oligodendrocytes and myelin are very important for brain functioning and the destruction of these cells or of the myelin sheaths can cause several diseases, such as leukodystropies (Mar and Noetzel 2010, Nave 2010) and multiple sclerosis (MS; Trapp and Nave 2008).

MS is an immune-mediated, demyelinating disease which causes neurological disabilities in young adults starting between 20 and 30 years of age (Compston and Coles 2008, Trapp and Nave 2008). Ten years after onset of the disease, 50% of MS patients are unable to perform household/employment responsibilities, whereas 25 years after disease onset, the same percentage of MS patients is not ambulatory. In addition to these limitations in the daily life, the average lifespan of MS patients is reduced by 7 to 8 years (Trapp and Nave 2008). The presence of lymphocytes and monocytes is observed in the CNS of MS patients and the presence of these cells may cause the observed inflammation of the CNS (Compston and Coles 2008, Nave 2010). In addition, transected axons are found in lesions in the brains of MS patients and the frequency of axonal transection and the degree of inflammation correlate very well (Nave 2010). The inflammation can directly cause damage of demyelinated axons, for example by interference with the blood supply or by glutamate-mediated excitotoxicity (Nave 2010). Although, the exact mechanism of demyelination is still not clear, the inflammatory environment of infiltrating lymphocytes might recruit microglial cells. These microglial cells might then become activated and could propagate lethal signals to oligodendrocytes and/or myelin (Compston and Coles 2008). It is currently under debate whether immune-mediated inflammation or the death of oligodendrocytes is the initiating event causing MS (Nakahara *et al.* 2010).

In addition, the demyelination of axons leads to a number of changes in the axonal metabolism, such as alterations of the expression and the position of sodium channels, impairment of the protein transport system along the axon and decreased ATP production,

which together could cause the malfunction of axons in MS patients (Piaton *et al.* 2010). The disease progress of most MS patients is characterized by periods of recurrent and reversible neurological disabilities. The recovery phase between relapses is mediated by remyelination (Trapp and Nave 2008). Remyelination is a process that restores the myelin sheaths of demyelinated axons (Piaton *et al.* 2010) and re-establishes the saltatory conduction of axons (Franklin and Ffrench-Constant 2008). Such as the initial myelination during the development of the CNS, the remyelination process also requires the migration of oligodendrocyte precursor cells to the respective axons (Franklin and Ffrench-Constant 2008, Bruce *et al.* 2010, Piaton *et al.* 2010). This process is achieved by a population of adult oligodendrocyte precursor cells in the brain, which upon activation proliferate and migrate to the lesion site, where this cell population differentiates and finally remyelinates the axons in a process that is similar to the initial myelination (Franklin and Ffrench-Constant 2008, Bruce *et al.* 2010). The understanding of the remyelination process is important for potential clinical remyelination therapy strategies for treatment of MS patients. The enhancement of remyelination as treatment of demyelination has already been tested in animal models of demyelinating diseases (Franklin and Ffrench-Constant 2008).

1.1.2.   OLN-93 cells as model system for oligodendroglial precursor cells

OLN-93 cells have been introduced as model cell line for oligodendrocytes in 1996 by Richter-Landsberg and Heinrich (Richter-Landsberg and Heinrich 1996). These cells have been derived from spontaneously transformed primary rat brain glial cell cultures. Their ability to proliferate and their expression of markers of oligodendroglial progenitor cells (for example NCAM) suggest that OLN-93 cells are in an early developmental stage of the oligodendroglial lineage. In addition to NCAM, OLN-93 cells express galactocerebrosides, MBP, PLP and MAG, which indicates that these cells are orientated towards a later developmental stage. Because OLN-93 cells do not express astroglial cell markers, these cells can be used as a model for oligodendrocyte precursor cells (Richter-Landsberg and Heinrich 1996). Since their first introduction in 1996 (Richter-Landsberg and Heinrich 1996), OLN-93 cells have been used as model system in various studies. Table 1 lists currently available studies on OLN-93 cells and sorts the reports into research areas to give an overview about the use of OLN-93 cells in research. So far, OLN-93 cells were mainly used in studies on oxidative stress and oligodendroglial differentiation.

Table 1: Overview about research topics of studies on OLN-93 cells.

Research topic	References
Oxidative stress	Kameshwar-Rao *et al.* 1999, Uberti *et al.* 1999, Brand *et al.* 2000, Brand *et al.* 2001, Ernst *et al.* 2004a, Ernst *et al.* 2004b, Van Meeteren *et al.* 2004, Brand and Yavin 2005, Stahnke *et al.* 2007, Brand *et al.* 2008, Brand *et al.* 2010
Oligodendrocyte differentiation	Jaquet *et al.* 1999, Strelau and Unsicker 1999, Robitzki *et al.* 2000, Hu *et al.* 2003, Nguyen *et al.* 2003, Van Meeteren *et al.* 2005, Zhang *et al.* 2005, Gerstner *et al.* 2006, Van Meeteren *et al.* 2006, Li *et al.* 2007, Buckinx *et al.* 2009, Chesik *et al.* 2010, Meng *et al.* 2010, Smolders *et al.* 2010
Consequences of xenobiotics exposure on cell metabolism	Burgmaier *et al.* 2000, Chesik and De Keyser 2010, Holzknecht and Rohl 2010, Thiessen *et al.* 2010, Steiner *et al.* 2011
Hypoxia research	Gerstner *et al.* 2006, Gerstner *et al.* 2007, Stark *et al.* 2008, Kaur *et al.* 2010
α-synuclein	Kragh *et al.* 2009, Riedel *et al.* 2009, Riedel *et al.* 2010, Riedel *et al.* 2011
Nanoparticles	Bastian *et al.* 2009, Hohnholt *et al.* 2010, Busch *et al.* 2011
Other topics	Mey and Hammelmann 2000, Mey and Henkes 2002, Plumb *et al.* 2002, Goldbaum *et al.* 2003, Dabouras *et al.* 2004, Wang *et al.* 2004, Gerstner *et al.* 2005, Gielen *et al.* 2005, Wejksza *et al.* 2005, Bauer and Richter-Landsberg 2006, Langer *et al.* 2006, Maier *et al.* 2006, Nie *et al.* 2006, Wejksza *et al.* 2006, Gielen *et al.* 2008, Steiner *et al.* 2008, Bolhuis and Richter-Landsberg 2010, Steiner *et al.* 2010

1.1.3. Astrocytes

Astrocytes outnumber neurons by over fivefold and fulfill a variety of different functions in the CNS (Kimelberg 2010, Sofroniew and Vinters 2010). During CNS development, the blood brain barrier (BBB) formation occurs at the same time as astrocyte differentiation, proposing a role of this cell type in the development of the BBB (Lee *et al.* 2009). Anatomically, astroglial endfeet envelope the blood vessels in the brain (Attwell *et al.* 2010), suggesting that astrocytes are involved in controlling the local blood flow according to regional energy metabolism (Koehler *et al.* 2009, Attwell *et al.* 2010, Carmignoto and Gómez-Gonzalo 2010). Furthermore, astrocytes have been shown to contribute to the support and maintenance of the BBB, for example by tightening tight junctions and influencing the expression of transport proteins (Abbott *et al.* 2006, Lee *et al.* 2009). Moreover, astrocytes participate in synaptogenesis (Fellin 2009, Pfrieger 2010) and astroglial processes also envelope synapses (Sofroniew and Vinters 2010). By the expression of uptake transporters for neurotransmitters near the synapses, astrocytes contribute to the clearance and recycling of neurotransmitters (Eulenburg and Gomeza 2010). Also for the normal function of synaptic signalling, a tight regulation of ion concentrations in the synaptic environment is crucial (Deitmer and Rose 2010). Astrocytes have been shown to participate in the regulation of fluid, ion and pH homeostasis of the brain (Obara *et al.* 2008, Deitmer and Rose 2010). Moreover, astrocytes synthesize and release gliotransmitters, which influence neighboring cells to promote physiological processes (Parpura and Zorec 2010).

Metabolic coupling has been described between neurons and astrocytes. For example, astrocytes metabolize glucose to lactate, release it and subsequently lactate could be taken up and used as energy substrate by neurons (Magistretti 2006, Barros and Deitmer 2010). In addition to lactate, astrocytes provide neurons with precursors for the synthesis of the antioxidant glutathione (Dringen and Hirrlinger 2003, Banerjee *et al.* 2008). Metabolic cooperation between astrocytes and neurons has also been shown for amino acids (Yudkoff *et al.* 1994, Bixel and Hamprecht 1995, Bixel *et al.* 1997, Dringen *et al.* 1998) as well as other metabolites (Auestad *et al.* 1991, Bixel and Hamprecht 1995, Brand *et al.* 1998, Dringen *et al.* 1998). Furthermore, astrocytes also play an important role in the metal homeostasis of the brain (Tiffany-Castiglioni and Qian 2001, Dringen *et al.* 2007). In view of this broad diversity of astrocyte functions in brain metabolism, they are considered to play a crucial role in brain homeostasis.

1.2. Iron

1.2.1. Iron, iron-mediated oxidative stress and antioxidative defense mechanisms

Iron is an important nutrient for mammals, because it plays a crucial role in various metabolic processes. In the physiological environment, iron can exist as ferrous (Fe^{2+}) or ferric (Fe^{3+}) iron and is thus able to facilitate redox reactions (Moos and Morgan 2000). Ferrous iron is bound in haemoglobin and enables the transport of oxygen in the red blood cells from lungs to other tissues. In this protein, the ferrous iron ion is tightly incorporated into the protoporphyrin IX structure and can reversibly bind molecular oxygen (Jensen 2009). To catalyze redox reactions, iron is also incorporated in proteins and enzymes participating in many different pathways of the cellular metabolism such as the respiratory chain (Babcock 1999), the tricarboxylic acid cycle (Rouault and Tong 2008) and the cell proliferation (Stubbe 1998). The final enzyme of the respiratory chain, cytochromoxidase, contains heme-bound iron and cytochrome c-bound iron for the reduction of molecular oxygen (O_2) to water (Babcock 1999). Furthermore, iron is incorporated in the iron-sulfur (Fe-S) clusters which are assemblies of iron atoms connected with sulfur atoms, for example [2Fe-2S] or [4Fe-4S]. These clusters are part of enzymes, for example of aconitase and succinate dehydrogenase (Rouault and Tong 2008) and enable one electron transfer reactions. Another example for the important role of iron in the cellular metabolism is its essential function as cofactor of the enzyme ribonucleotide reductase, which catalyzes the rate limiting step of deoxyribonucleic acid (DNA) synthesis (Stubbe 1998, Stubbe and van der Donk 1998). The mammalian ribonucleotide reductase contains a tyrosyl radical adjacent to a diferric cluster in the active center (Stubbe and van der Donk 1998). The presence of iron in this enzyme is considered to be the reason for the iron dependency of cell proliferation (Thelander *et al.* 1983, Lederman *et al.* 1984, Brodie *et al.* 1993, Nyholm *et al.* 1993, Green *et al.* 2001).

The iron uptake in mammals is regulated in a coordinated manner by the hepatic hormone hepcidin, whose secretion by hepatocytes depends on the availability of iron (Rouault and Cooperman 2006, Knutson 2010). Hepcidin binds to the cellular iron exporter ferroportin of the intestinal duodenal epithelial cells and induces internalization and degradation of ferroportin. This leads to decreased iron absorption from the diet into the blood (Rouault and Cooperman 2006, Knutson 2010). The CNS, the retina and the testis are considered to be the only organs of the mammalian body, which are excluded from this control of iron metabolism
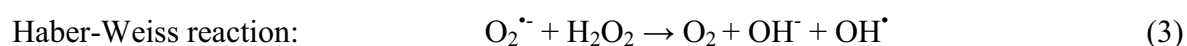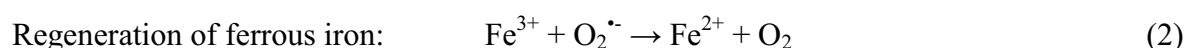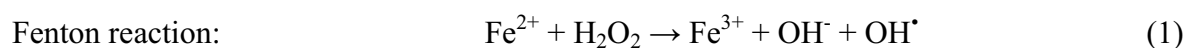
by hepcidin, because they are protected by barriers (Rouault and Cooperman 2006). However, the presence of hepcidin in the brain has been shown and suggests that hepcidin is also involved in regulation of the brain iron metabolism (Clardy *et al.* 2006, Zechel *et al.* 2006, Du *et al.* 2011).

The daily human iron intake is approximately 17.7 mg per adult man and day and 12.7 mg per adult woman and day from the diet as heme-bound or non-heme-bound iron in the intestinal duodenum (Lieu *et al.* 2001, Mackenzie and Garrick 2005, Valerio 2007, Knutson 2010). This uptake needs to be tightly regulated since both, iron deficiency and iron overload, are associated with human diseases such as anaemia and hemochromatosis (O'Neil and Powell 2005, Zimmermann and Hurrell 2007, Darshan *et al.* 2010). The negative effects of iron are attributed to its ability to catalyze the formation of reactive oxygen species (ROS) by the Fenton reaction (reaction 1; Halliwell and Gutteridge 1984, Kehrer 2000).

<u>Iron-mediated oxidative stress</u>

The normal cellular metabolism generates ROS by various reactions such as autoxidation of molecules, as product of enzymatic reactions and especially as by-product of the respiratory chain in mitochondria (Kehrer 2000, Halliwell 2006). The term ROS refers to a collective of oxygen-containing radicals (for example superoxide ($O_2^{\bullet-}$) and the hydroxyl radical ($OH^{\bullet}$)) and non-radicals (for example hydrogen peroxide (H_2O_2) and organic peroxides (ROOH); Halliwell 2006). In the respiratory chain, molecular oxygen is converted to water via a four electron reduction, but about 1-4% of the oxygen escapes the respiratory chain in a partially reduced state (Jezek and Hlavata 2005, Kell 2009). This incomplete reduction of molecular oxygen is the reason for a continuous production of superoxide and hydrogen peroxide in cells. Ferrous iron which is not tightly bound in a redox-inactive environment can directly react with hydrogen peroxide in the Fenton reaction (reaction 1) and catalyze the formation of highly reactive hydroxyl radicals. The ferric iron can be reduced to ferrous iron by superoxide (reaction 2) or by other intracellular reducing agents such as ascorbate (Kell 2009), thereby regenerating the ferrous iron. The cycling of iron within reaction 1 and 2 is called the iron-catalyzed Haber-Weiss reaction (reaction 3; Kehrer 2000).

Fenton reaction: $\qquad\qquad Fe^{2+} + H_2O_2 \rightarrow Fe^{3+} + OH^- + OH^{\bullet}$ (1)

Regeneration of ferrous iron: $\qquad Fe^{3+} + O_2^{\bullet-} \rightarrow Fe^{2+} + O_2$ (2)

Haber-Weiss reaction: $\qquad\quad O_2^{\bullet-} + H_2O_2 \rightarrow O_2 + OH^- + OH^{\bullet}$ (3)

Introduction

One possible reaction of the hydroxyl radical in cells is its addition to bases or deoxyribose sugars of the DNA, forming lesion of the DNA strands (Evans *et al.* 2004, Halliwell 2006). In lipids, the hydroxyl radical can abstract an hydrogen radical from carbon-hydrogen bonds forming carbon radicals, which can further react with molecular oxygen, subsequently leading to lipid peroxidation. Lipid peroxidation alters membrane properties that can affect the cellular metabolism (Valko *et al.* 2004, Davies 2005, Niki 2009, Adibhatla and Hatcher 2010). In addition, hydroxyl radicals can oxidize proteins that can subsequently accumulate and are considered to contribute to disease development and aging (Chang *et al.* 2000, Dunlop *et al.* 2009).

The low level of ROS that is continually produced by the normal cellular oxygen metabolism is usually captured by cellular antioxidant mechanisms thereby preventing damage to bio-molecules (Limon-Pacheco and Gonsebatt 2009). However, oxidative stress occurs when the level of ROS increases and overwhelms the cellular antioxidant defence mechanisms (Kehrer 2000, Halliwell and Gutteridge 2007). Under these circumstances, major damage to bio-molecules can occur and thereby finally cause cell death (Lushchak 2011).

Antioxidative defence mechanisms

The cellular metabolism has developed a variety of antioxidative mechanisms to cope with the continuous production of ROS (Halliwell and Gutteridge 2007, Battin and Brumaghim 2009, Flora 2009). These include low molecular weight antioxidant molecules, such as glutathione (GSH; Dringen 2000), ascorbic acid (Buettner 1993), vitamin E (Buettner 1993), uric acid (Limon-Pacheco and Gonsebatt 2009) and melatonin (Gupta *et al.* 2003, Srinivasan *et al.* 2005), as well as antioxidant enzymes such as superoxide dismutase (SOD; Fridovich 1995, Adam-Vizi 2005), superoxide reductase (Nivière and Fontecave 2004), catalase (Dringen *et al.* 2005, Battin and Brumaghim 2009), glutathione peroxidase (GPx; Dringen *et al.* 2005, Battin and Brumaghim 2009), thioredoxin (Nordberg and Arner 2001) and peroxiredoxin (Immenschuh and Baumgart-Vogt 2005, Rhee *et al.* 2005). These antioxidants and antioxidative enzymes act in a coordinated way to protect the cell against damage by ROS (Halliwell and Gutteridge 2007, Lushchak 2011). The brain seems to have a disadvantage concerning iron-mediated oxidative stress compared to other organs (Dringen 2000, Halliwell 2006), because it consumes a high amount of oxygen in relation to its weight, has higher iron levels, contains a high level of polyunsaturated fatty acids, which are prone to lipid peroxidation, has lower specific activities of SOD, catalase and GPx than other organs and contains autoxidizable neurotransmitters. Despite these disadvantages, the brain has high

amounts of low molecular weight antioxidants, for example ascorbate and GSH, and tightly regulates its metal homeostasis (Dringen 2000, Halliwell 2006).

Implication of iron in neurodegenerative diseases

The importance of the tight regulation of the iron metabolism and the detoxification of ROS is manifested by the association of an imbalance of iron metabolism with many human neurodegenerative diseases (Halliwell 2006, Benarroch 2009), iron related disorders (Valerio 2007, Lee and Beutler 2009) and the observation of increased iron contents in the elderly brain (Altamura and Muckenthaler 2009, Stankiewicz and Brass 2009, Crichton *et al.* 2011), which might be associated with age-related diseases (Stankiewicz and Brass 2009). An overview about selected neurodegenerative diseases that have been connected with alterations of iron metabolism is given in Table 2. The examples, Alzheimer´s disease (AD), Parkinson´s disease (PD) and MS will be described in more detail in the following paragraphs.

The characteristics of AD are senile plaques containing the extracellularly insoluble amyloid-β peptide and neurofibrillary tangles of aggregated and hyperphosphorylated microtubule-associated protein tau (Hardy and Selkoe 2002, Altamura and Muckenthaler 2009, Crews and Masliah 2010). Accumulation of iron has been observed in areas of amyloid-β depositions and in neurons with tangles, suggesting a possible connection of iron accumulation to the occurrence of amyloid-β depositions and of tangles (Altamura and Muckenthaler 2009, Benarroch 2009). Furthermore, iron affects the processing of the amyloid precursor protein. Low cellular iron levels are associated with an increased activity of furin, an enzyme participating in the processing of amyloid precursor protein, which subsequently stimulates the processing of amyloid precursor protein by the non-amyloidogenic pathway that precludes the deposition of amyloid-β (Zecca *et al.* 2004, Altamura and Muckenthaler 2009, Benarroch 2009). In contrast, high cellular iron levels have the opposite effect and increase the deposition of amyloid-β (Zecca *et al.* 2004, Altamura and Muckenthaler 2009, Benarroch 2009). In addition, AD patients and animal models of this disease are characterized by increased levels of oxidative stress in the brain, which might be a result of increased iron levels and/or alterations of the antioxidative system (Altamura and Muckenthaler 2009, Sultana and Butterfield 2010).

Table 2: Neurodegenerative disorders which are associated with alterations of the iron metabolism.

Disease	Disease hallmarks	Involvement of iron	Selected Reviews
Multiple sclerosis	Autoimmune-induced inflammation in the CNS Demyelination of axons Loss of oligodendrocytes and neurons	High levels of iron in the brain of patients	Levine and Chakrabarty 2004 Singh and Zamboni 2009
Alzheimer's disease	Formation and deposition of β-amyloid plaques/tau aggregates	Iron deposition in plaques Iron deposition in *temporal lope* mRNA of amyloid precursor protein contains iron responsive element	Mandel *et al.* 2007 Barnham and Bush 2008 Altamura and Muckenthaler 2009 Benarroch 2009 Stankiewicz and Brass 2009
Parkinson's disease	α-synuclein aggregation and formation of Lewy bodies Loss of dopaminergic neurons in *lateral substantia nigra pars compacta*	Iron deposition in *substantia nigra*	Benarroch 2009 Stankiewicz and Brass 2009
Neuroferritinopathy	Spherical ferritin and iron inclusions in different brain regions	Mutation of the ferritin light chain gene	Levi *et al.* 2005
Aceruloplasminemia	Absence of circulating ceruloplasmin Cerebellar iron deposition Purkinje cell loss	Mutation of the ceruloplasmin gene	Xu *et al.* 2004

PD is characterized by a selective loss of dopaminergic neurons of the *pars compacta* of the *substantia nigra*. Aggregates of α-synuclein (Lewy bodies) have been found in dopaminergic neurons in brains of PD patients as well as an elevated iron level (Altamura and Muckenthaler 2009, Benarroch 2009, Lee and Andersen 2010, Schulz-Schaeffer 2010). Iron can promote the formation of these aggregates and application of iron chelators to protect against α-synuclein aggregate formation was successful (Avramovich-Tirosh *et al.* 2008, Altamura and Muckenthaler 2009). Additionally, lipid peroxidation has been observed in animal models of PD, suggesting an involvement of iron-mediated oxidative stress in this disease (Altamura and Muckenthaler 2009).

MS is a demyelinating disease with axonal degeneration (chapter 1.1.1.; Trapp and Nave 2008). The brains of MS patients also have decreased levels of low molecular weight antioxidants, such as GSH and α-tocopherol. These low levels of antioxidants might be a consequence of an elevated ROS production by macrophages and activated microglial cells (Sayre *et al.* 2005). Abnormal deposits of iron in tissue and neurons of MS patients as well as elevated levels of ferritin have been found (Levine and Chakrabarty 2004), suggesting an important role of iron-mediated oxidative stress in the disease progression (Sayre *et al.* 2005).

The association of AD, PD and MS with increased iron levels in the affected brain areas strongly suggests a connection between an altered iron metabolism and these diseases. Further studies are necessary to elucidate this relationship in detail and to evaluate whether a therapeutical reduction of iron levels is indeed a beneficial treatment for patients (Altamura and Muckenthaler 2009).

1.2.2. Iron metabolism of the brain

The brain has a special position in the mammalian body, because it is separated from the systemic blood circulation in the body by the BBB. This barrier protects the brain against a variation of the blood plasma composition and against potentially toxic substances, thereby controlling the brain microenvironment (Abbott 2002, Abbott *et al.* 2010). Tight junctions between neighboring capillary endothelial cells limit uncontrolled entry of molecules into the brain. Only small and lipophilic molecules are able to diffuse through this barrier (Abbott 2002). The supply of the brain with essential nutrition such as glucose, amino acids and monocarboxylic acids is enabled by specific transport mechanisms (Qutub and Hunt 2005, Zlokovic 2008). Due to the important functions of iron in the cellular metabolism, brain iron metabolism and the transport of this metal into the brain have been extensively studied and

are subject of numerous reviews (Yokel 2006, Bressler *et al.* 2007, Moos *et al.* 2007, Benarroch 2009, Mills *et al.* 2010, Crichton *et al.* 2011). An overview about the expression of proteins involved in iron uptake and iron metabolism of capillary endothelial cells and astrocytes is shown in Figure 1.

In the blood and cerebrospinal fluid, iron occurs either bound to proteins as protein-bound iron or is present as non-protein-bound iron in low molecular weight complexes (Moos *et al.* 2007). The main carrier protein for iron is transferrin (Tf). Tf is present in blood plasma, lymph and cerebrospinal fluid in order to distribute this metal throughout the body (Figure 1; Moos and Morgan 2000, Garrick and Garrick 2009, Munoz *et al.* 2009). In addition to Tf, iron efficiently binds to the glycoproteins lactoferrin and melanotransferrin (Moos and Morgan 2000), of which lactoferrin is also present in the cerebrospinal fluid (Moos *et al.* 2007). Reactive microglial cells contain and release lactoferrin which has been suggested to be an iron source for dopaminergic neurons (Fillebeen *et al.* 2001). Moreover, the presence of melanotransferrin has been shown in human brain tissue (Rothenberger *et al.* 1996). The contributions of these proteins to the brain iron metabolism remain to be elucidated in more detail.

The main iron carrier protein Tf contains two iron binding sites and is also expressed in the brain (Bloch *et al.* 1985, Connor and Menzies 1990, Connor *et al.* 1990, Benkovic and Connor 1993, Moos *et al.* 2000). During early development, Tf expression increases on both the mRNA (Levin *et al.* 1984) and the protein level (Mollgard *et al.* 1987). The cellular uptake of Tf is mediated by binding of Tf to the transferrin receptor (TfR) and subsequent internalization of the Tf/TfR complex by receptor-mediated endocytosis into the cell (Ponka and Lok 1999, Lieu *et al.* 2001, Garrick and Garrick 2009). In endocytotic vesicles ferric iron is released from the Tf/TfR complex by a pH shift. The binding of ferric iron to Tf is almost irreversible at pH 7.4, but iron is readily released from the Tf/TfR complex by a pH below 6.5 that occurs in endocytotic vesicles (Moos and Morgan 2000, Lieu *et al.* 2001).

The uptake of iron by brain capillary endothelial cells via the Tf/TfR complex is considered to be the main entrance route of iron into the brain as shown in Figure 1 (Benarroch 2009, Garrick and Garrick 2009). Brain capillary endothelial cells contain Tf (Connor and Fine 1986, Mollgard *et al.* 1988) and so do oligodendrocytes and neurons *in vivo* (Oh *et al.* 1986). In contrast, expression of Tf has been controversially discussed for astrocytes *in vivo* (Dwork *et al.* 1988, Connor and Menzies 1990, Connor *et al.* 1990, Benkovic and Connor 1993, Moos *et al.* 2000), while microglial cells appear not to contain Tf (Moos *et al.* 2000).
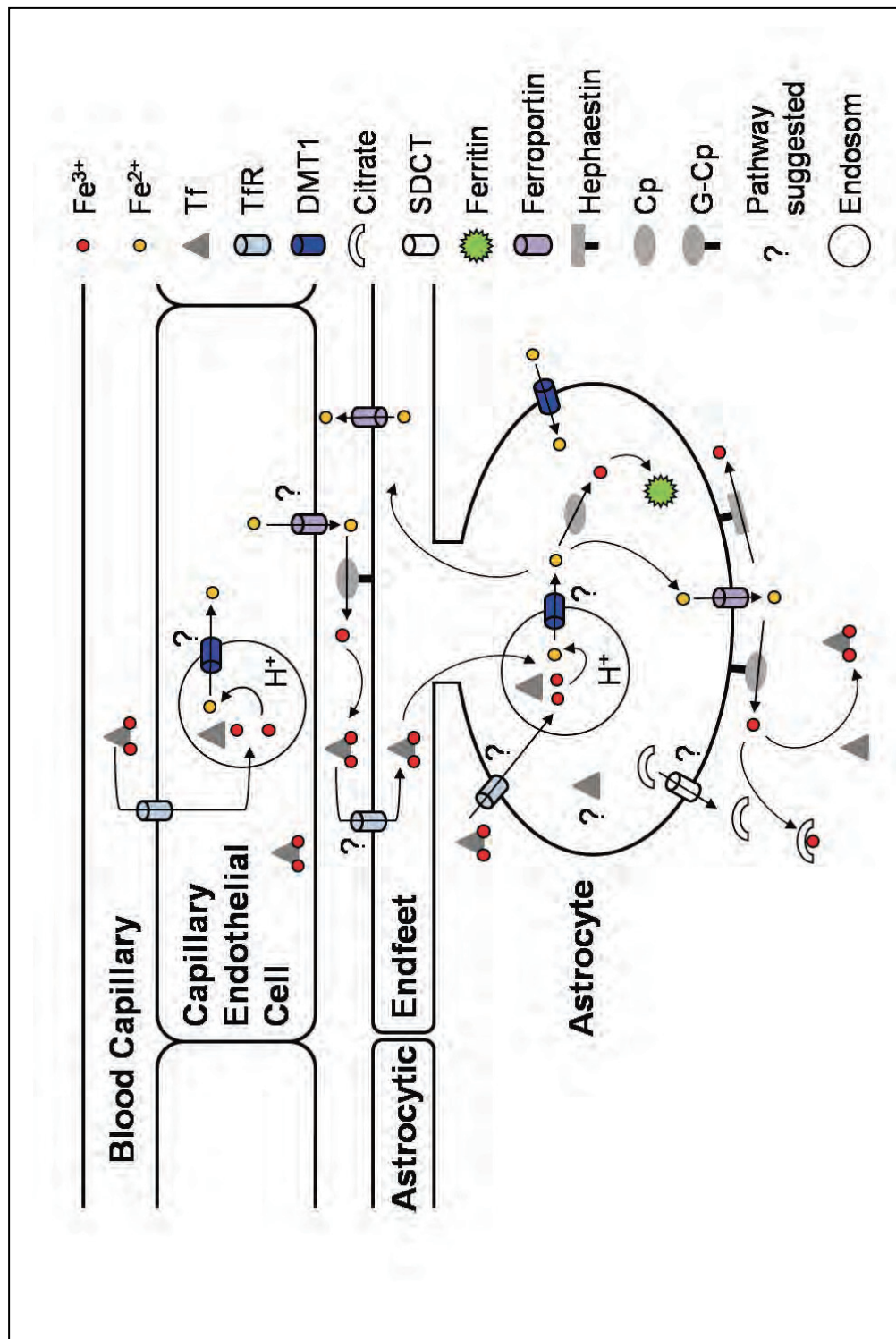
Figure 1: Iron transport from blood into brain. Uptake and metabolism of iron in capillary endothelial cells and astrocytes are based on the known expression of proteins of the iron metabolism in these cells. Abbreviations: Cp, ceruloplasmin; DMT1, divalent metal transporter 1; G-Cp, glycosylphosphatidylinositol-anchored form of Cp; SDCT, sodium-dependent carboxylate transporter; Tf, transferrin; TfR, transferrin receptor.

TfR is present in brain capillary endothelial cells, but it is hardly detectable in the brain tissue (Jefferies *et al.* 1984, Hulet *et al.* 1999a, Hulet *et al.* 2002). The presence of TfR has been discussed for astrocytes, oligodendrocytes and microglial cells (Lin and Connor 1989, Connor and Menzies 1995, Kaur and Ling 1995, Moos 1996), but it has not been finally proven *in vivo*. In contrast, presence of TfR has been documented in cultures of neurons, astrocytes and oligodendrocytes, suggesting that this receptor takes part in the iron accumulation by cultured brain cells (Oh *et al.* 1986, Qian *et al.* 1999, Moos *et al.* 2000, Hoepken *et al.* 2004, Hoepken 2005, Ortiz *et al.* 2005, Salvador 2010). After uptake and iron release, the iron-free Tf/TfR complex is shuttled back to the plasma membrane for reutilization (Moos and Morgan 2000, Lieu *et al.* 2001), while ferric iron is reduced and ferrous iron is transported from the endocytotic vesicles to the cytosol by the divalent metal transporter 1 (DMT1; Fleming *et al.* 1997, Gunshin *et al.* 1997, Fleming *et al.* 1998, Hentze *et al.* 2004). So far, no studies are available concerning the presence of DMT1 in vesicles of brain cells as shown before for other cell types (Gruenheid *et al.* 1999, Tabuchi *et al.* 2000). Therefore, it remains to be elucidated whether DMT1 is the transporter responsible for the iron export from vesicles in brain cells.

Besides the uptake of protein-bound iron, cells are able to internalize non-protein-bound iron as ferrous or ferric iron by various transport mechanisms. The uptake of low molecular weight iron has been suggested for neurons, astrocytes and oligodendrocytes in the brain (Moos *et al.* 2007, Salvador 2010) and several studies have shown that the uptake of non-transferrin-bound iron by cultured brain cells is possible (Oshiro *et al.* 1998, Takeda *et al.* 1998, Bishop *et al.* 2011).

The aforementioned DMT1 is a divalent metal transporter, which transports ferrous iron and other divalent metal ions out of vesicles (Fleming *et al.* 1997, Gunshin *et al.* 1997). In addition to this export, DMT1 has been suggested to transport iron across the plasma membrane of brain cells (Hentze *et al.* 2004, Jeong and David 2003). However, the initially described expression of this transporter in capillary endothelial cells (Burdo *et al.* 2001) was not confirmed in other studies (Wang *et al.* 2001, Moos and Morgan 2004). Thus, the contribution of DMT1 in the export of iron from endocytotic vesicles in capillary endothelial cells remains to be elucidated (Figure 1). Expression of DMT1 has been shown for neurons, astrocytes, oligodendrocytes and microglial cells *in vivo* (Moos *et al.* 2000, Burdo *et al.* 2001, Wang *et al.* 2001), although a recent study was unable to confirm the presence of DMT1 in oligodendrocytes in the *substantia nigra* (Song *et al.* 2007). In addition, DMT1 is expressed in cultured astrocytes (Jeong and David 2003) and cultured neurons (Roth *et al.* 2000, Du *et*

al. 2009), but no reports are available on its expression in cultured oligodendrocytes or microglial cells. The location of DMT1 in the plasma membrane of neurons (Roth *et al.* 2000) suggests that it could facilitate the uptake of ferrous iron into these cells, whereas other studies did not investigate the subcellular localization of DMT1 in the other brain cell types. Since iron is present in the extracellular environment predominantly as ferric iron, a reduction of iron prior to its DMT1-mediated transport across the plasma membrane would be necessary (Gunshin *et al.* 1997). The ferric reductase duodenal cytochrome b (Dcytb) is expressed by cultured astrocytes (Jeong and David 2003, Tulpule *et al.* 2010) and this enzyme could catalyze the reduction of ferric to ferrous iron. In addition, mouse cytochrome b561 and mouse and fly stromal cell-derived receptor 2 have been detected in brain slices (Vargas *et al.* 2003) and the latter also in cultured astrocytes (Tulpule *et al.* 2010). Both enzymes are candidates for catalyzing the reduction of ferric iron (Vargas *et al.* 2003).

In addition to DMT1, a β_3-integrin/mobilferrin transport system has been suggested for low molecular weight ferric iron (Conrad *et al.* 1994, Conrad *et al.* 2000), but the involvement of this transport mechanism in the uptake of ferric iron into brain cells remains to be investigated. The uptake of non-protein-bound iron from the extracellular fluid has been suggested to occur in the form of low molecular weight iron complexes with citrate, ascorbate or ATP (Moos and Morgan 1998, Takeda *et al.* 1998, Rouault and Cooperman 2006, Moos *et al.* 2007), which are potential molecules for iron chelation (Moos *et al.* 2007). In Figure 1, citrate is shown as one example. Furthermore, citrate, ascorbate and ATP have been shown to be released from astrocytes (Figure 1; Sonnewald *et al.* 1991, Guthrie *et al.* 1999, Lane and Lawen 2009). Citrate release by astrocytes may be mediated by sodium-dependent carboxylate transporters (SDCT; Yodoya *et al.* 2006), ascorbate release has been suggested to be mediated by volume-sensitive anion channels or exocytosis of ascorbate-containing vesicles (Lane and Lawen 2009) while ATP is released from astrocytes by regulated exocytosis from secretory vesicles or lysosomes (Parpura and Zorec 2010).

Intracellular iron metabolism and storage

After uptake into cells, iron can become part of the labile iron pool, which consists of chelatable and redox-active iron, or it can be stored in a redox-inactive form in the iron storage protein ferritin (Figure 1; Kakhlon and Cabantchik 2002, Petrat *et al.* 2002, Arosio *et al.* 2009). In iron-restricted conditions, both the cellular iron from the labile iron pool and from ferritin is used for cellular metabolism (Kakhlon and Cabantchik 2002). Ferritin is an almost spherical shell of 24 subunits of light (L) and heavy (H) ferritin protein chains and can

hold up to 4000 iron atoms (Arosio *et al.* 2009). The brain mostly contains H-chain-rich ferritin (H-ferritin) which is considered to possess antioxidative properties due to the ferroxidase activity of the H-chain (Lawson *et al.* 1989, Arosio *et al.* 2009, Snyder and Connor 2009). The proportion of L- to H-chains in ferritin depends on the tissue and cell type. In contrast to H-ferritin, ferritin rich in L-chains (L-ferritin) is considered to predominantly store iron (Arosio *et al.* 2009).

The presence of ferritin has been confirmed for neurons, astrocytes, oligodendrocytes and microglial cells *in vivo* (Connor *et al.* 1990, Benkovic and Connor 1993, Connor *et al.* 1994, Dickinson and Connor 1995, Cheepsunthorn *et al.* 1998, Moos *et al.* 2000) and also for cultures of these cell types (Qi and Dawson 1994, Regan *et al.* 2002, Hoepken *et al.* 2004, Hoepken 2005). Although all types of brain cells contain ferritin, the ratios of L- to H-ferritin differ between them. Microglial cells contain more L-ferritin, whereas neurons and oligodendrocytes express more H-ferritin than L-ferritin (Connor and Menzies 1996).

Mitochondria are important cellular organelles due to their function in different metabolic pathways and in iron metabolism (Richardson *et al.* 2010). The uptake of iron into mitochondria is mediated by mitoferrins, the mitochondrial iron transporters (Richardson *et al.* 2010). Recently, the ATP synthase complex has been shown to transport ferrous iron into isolated mitochondria (Kim and Song 2010). In addition, mitochondria are also able to store iron in mitochondrial ferritin (Santambrogio *et al.* 2007). However, no reports are available on iron exporters in mitochondria. The export of Fe-S clusters from mitochondria has been suggested to be mediated by the ABC (ATP-binding cassette) transporter B7. Furthermore, the heme-binding protein 1 and the ABC transporter B10 are considered as candidates for heme export from mitochondria (Anderson and Vulpe 2009, Richardson *et al.* 2010). Although, the presence of mitochondrial ferritin has been shown for brain cells (Santambrogio *et al.* 2007), no information is available about the regulation of this protein and potential differences in iron metabolism between peripheral mitochondria compared to those in brain.

Iron export

Ferroportin (metal transport protein 1 or IREG1) is the only known iron exporter (Figure 1; Garrick and Garrick 2009). This protein transports ferrous iron (Abboud and Haile 2000, Donovan *et al.* 2000, McKie *et al.* 2000) and is expressed in the brain tissue (Jiang *et al.* 2002). For brain capillary endothelial cells, the presence of this transporter was shown (Wu *et al.* 2004), although two other studies did not find ferroportin in capillary endothelial cells

(Burdo *et al.* 2001, Moos and Rosengren Nielsen 2006). Nevertheless, these cells are likely to release iron into the brain despite the unclear expression of ferroportin, since they have been shown to transport iron into the brain (Figure 1; Moos *et al.* 2007). Ferroportin expression was observed in astrocytes as well as in neurons, oligodendrocytes and microglial cells *in vivo* (Burdo *et al.* 2001, Wu *et al.* 2004) and in cultured neurons (Song *et al.* 2010) and cultured astrocytes (Jeong and David 2003). Since ferroportin transports ferrous iron, it is coupled to one of two extracellular ferroxidases ceruloplasmin (Cp) or hephaestin for the immediate extracellular oxidation of ferrous iron (Petrak and Vyoral 2005, De Domenico *et al.* 2008). Soluble Cp and its glycosylphosphatidylinositol-anchored form (G-Cp; Figure 1) have been shown to be expressed in astrocytes and neurons *in vivo* (Mollgard *et al.* 1988, Klomp *et al.* 1996, Patel and David 1997, Patel *et al.* 2000, Hwang *et al.* 2004), and for cultured astrocytes (Patel *et al.* 2000, Hwang *et al.* 2004). In contrast, both forms of Cp appear to be absent from oligodendrocytes and microglial cells (Mollgard *et al.* 1988). Hephaestin has been shown to be expressed in the brain (Qian *et al.* 2007) by neurons, astrocytes, oligodendrocytes and microglial cells (Wang *et al.* 2007) as well as in cultured neurons (Song *et al.* 2010) and cultured brain endothelial cells (Yang *et al.* 2011a).

Regulation of the iron metabolism

A tight regulation of the cellular iron metabolism is essential for cells to avoid iron deficiency or iron-mediated toxicity by excess of redox-active iron (Rouault 2006, Crichton *et al.* 2011). The regulation of iron metabolism is predominantly mediated by the iron regulatory protein (IRP) 1 and IRP2 which monitor the cytosolic iron level and both can regulate the expression of proteins, that are involved in iron metabolism (Hentze *et al.* 2004, Pantopoulos 2004, Rouault 2006). A low level of cellular iron facilitates the binding of an IRP to the iron responsive element (IRE) of the mRNA of proteins involved in iron metabolism, for example the mRNAs of ferritin or TfR. This low cellular iron level and binding of IRP to the ferritin mRNA inhibits ferritin synthesis (Rouault 2006). Binding of IRP to the mRNA of TfR protects the mRNA from degradation by endonucleases. This enhances the synthesis of TfR and can subsequently increase the uptake of iron by the Tf/TfR complex (Rouault 2006).

The involvement of the IRP/IRE system in regulation of the brain iron homeostasis has been observed in studies with transgenic mice that are either deficient of both copies of IRP2 (LaVaute *et al.* 2001) or deficient of one copy of IRP1 and both copies of IRP2 (Smith *et al.* 2004). In these animals, neurons and oligodendrocytes in different brain regions had excessive iron accumulations and the mice suffered from neurodegeneration. These

observations suggest that IRP1 and IRP2 are indeed involved in the regulation of the iron metabolism in the brain (LaVaute *et al.* 2001, Smith *et al.* 2004).

In vivo, the expression of IRP1 and IRP2 have been shown for astrocytes and IRP also modulates the expression of DMT1, suggesting that IRPs are involved in the regulation of the iron metabolism of astrocytes (Huang *et al.* 2006). Furthermore, neuronal cell cultures from IRP1 or IRP2 knockout mice had higher ferritin protein levels, hinting towards the involvement of IRPs in the regulation of neuronal iron metabolism (Regan *et al.* 2008). Oligodendrocytes contain IRP1 *in vivo* and in cell cultures (Leibold *et al.* 2001), but so far no reports are available concerning the regulation of the iron metabolism by the IRP/IRE system in microglial cells.

1.2.3.   Oligodendrocytes and iron

In the normal brain, oligodendrocytes appear to have the highest content of iron as shown by histochemical iron stainings (Dwork *et al.* 1988, Connor and Menzies 1990, Benkovic and Connor 1993, Connor *et al.* 1995, Connor and Menzies 1996). This high iron level might be related to the myelination process (Todorich *et al.* 2009). However, the specific iron content of cultured oligodendrocytes strongly differs between reports (Thorburne and Juurlink 1996, Hoepken 2005). This chapter summarizes the current knowledge on the iron metabolism of oligodendrocytes and the expression of proteins of the iron metabolism in these cells (Figure 2; Table 3).

The iron carrier protein Tf is present in oligodendrocytes *in vivo* (Bloch *et al.* 1985, Connor and Fine 1986, Connor and Menzies 1990, Connor *et al.* 1990, Benkovic and Connor 1993, Moos *et al.* 2000) and in cell cultures (Espinosa de los Monteros *et al.* 1988, Griot and Vandevelde 1988, Espinosa de los Monteros *et al.* 1990, Connor *et al.* 1993, Espinosa de los Monteros *et al.* 1994). Furthermore, Tf is synthesized and stored by oligodendrocytes (Bloch *et al.* 1985, De Arriba Zerpa *et al.* 2000) and the increase in the amount of Tf mRNA after birth has been connected to the maturation of oligodendrocytes (Bartlett *et al.* 1991). Cultured oligodendrocytes express the TfR (Espinosa de los Monteros and Foucaud 1987, Hoepken 2005, Ortiz *et al.* 2005). *In vivo*, TfR expression has only been shown for early developmental stages and the expression decreases with age (Lin and Connor 1989, Giometto *et al.* 1990, Connor and Menzies 1995). In contrast, two studies were unable to detect TfR in oligodendrocytes in the neonatal and adult brain *in vivo* (Kaur and Ling 1995, Moos 1996). Thus, the Tf/TfR complex might be predominantly involved in iron uptake by developing
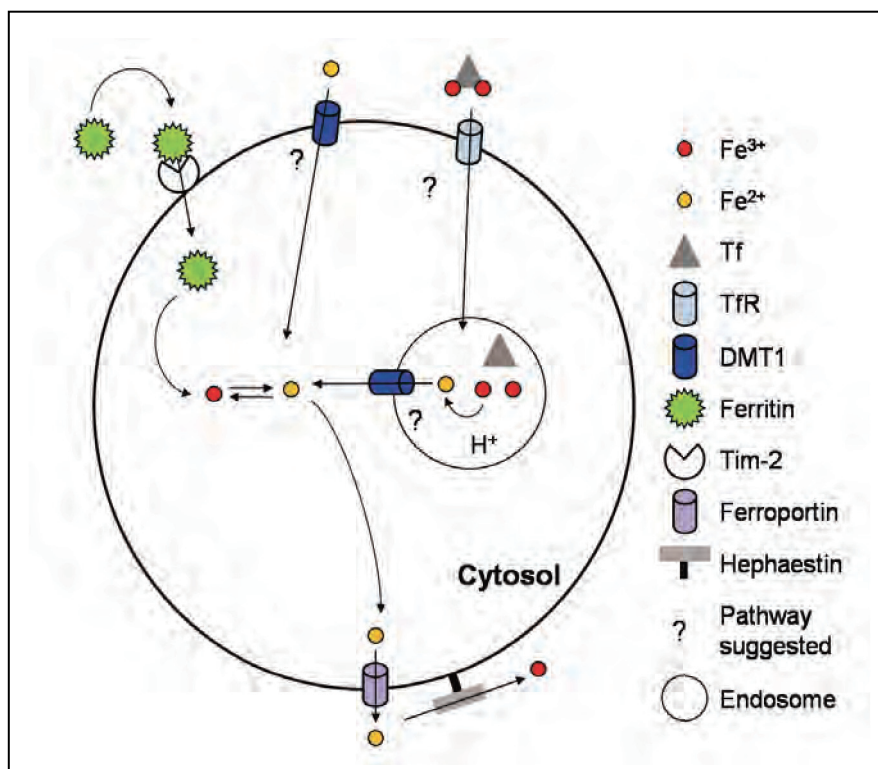
Figure 2: Iron transport and metabolism in oligodendrocytes in the brain based on the known expression of proteins of the iron metabolism. Abbreviation: Tim-2, T cell immunoglobulin-domain and mucin-domain 2.

oligodendrocytes (Todorich *et al.* 2009). Oligodendrocytes express the iron storage protein ferritin *in vivo* (Connor *et al.* 1990, Benkovic and Connor 1993, Connor *et al.* 1994, Connor and Menzies 1995, Blissman *et al.* 1996, Cheepsunthorn *et al.* 1998, Moos *et al.* 2000, Izawa *et al.* 2010) and in cell culture (Griot and Vandevelde 1988, Qi and Dawson 1994, Hoepken 2005). Although oligodendrocytes are able to express both ferritin chains (Connor *et al.* 1990, Benkovic and Connor 1993, Connor *et al.* 1994, Connor and Menzies 1995, Blissman *et al.* 1996, Cheepsunthorn *et al.* 1998, Moos *et al.* 2000, Izawa *et al.* 2010), they contain more H-ferritin than L-ferritin (Connor and Menzies 1996).

Ferritin upregulation has been shown for conditions of oxidative stress, suggesting that an increased iron storage capacity is important for the handling of oxidative stress by oligodendrocytes (Connor and Menzies 1996). Furthermore, H-ferritin has recently been suggested as an alternative extracellular iron source for Tf in oligodendrocytes that may be taken up selectively into these cells (Figure 2; Todorich *et al.* 2009).

Table 3: Presence of iron and proteins related to the iron metabolism in oligodendroglial cells.

Iron and proteins of the iron metabolism	In vivo		In vitro	
Iron	y	Dwork et al. 1988, Connor and Menzies 1990, Benkovic and Connor 1993, Connor et al. 1995, Connor and Menzies 1996	y	Thorburne and Juurlink 1996, Hoepken 2005
Ferritin (light and heavy chain)	y	Connor and Fine 1986, Connor et al. 1990, Benkovic and Connor 1993, Moos and Morgan 2000, Izawa et al. 2010	y	Griot and Vandevelde 1988, Qi and Dawson 1994, Hoepken 2005
Light chain	y	Connor et al. 1994, Connor and Menzies 1995, Cheepsunthorn et al. 1998	y	Hoepken 2005
Heavy chain	y	Connor et al. 1994, Connor and Menzies 1995, Blissman et al. 1996, Cheepsunthorn et al. 1998	y	Hoepken 2005
Ferritin binding site	y	Hulet et al. 1999a, Hulet et al. 1999b	y	Hulet et al. 2000, Hulet et al. 2002
Tim-2	y	Todorich et al. 2008	y	Todorich et al. 2008
IRP 1	y	Leibold et al. 2001	y	Leibold et al. 2001
IPR 2	-		-	

Presence confirmed (y), absence confirmed (n), presence unclear (±), presence or absence not reported so far (-).

Table 3 continued: Presence of iron and proteins related to the iron metabolism in oligodendroglial cells.

Iron and proteins of the iron metabolism	In vivo		In vitro	
TfR	Lin and Connor 1989, Connor and Menzies 1995	y	y	Espinosa de los Monteros and Foucaud 1987, Hoepken 2005, Ortiz et al. 2005
	Giometto et al. 1990	±		
	Kaur and Ling 1995, Moos 1996	n		
Tf	Bloch et al. 1985, Connor and Fine 1986, Connor and Menzies 1990, Connor et al. 1990, Benkovic and Connor 1993, Moos et al. 2000	y	y	Espinosa de los Monteros et al. 1988, Griot and Vandevelde 1988, Espinosa de los Monteros et al. 1990, Connor et al. 1993, Espinosa de los Monteros et al. 1994
DMT 1	Moos et al. 2000	y	-	
	Burdo et al. 2001	±		
	Song et al. 2007	n		
Cp	Mollgard et al. 1988	n	-	
G-Cp	Mollgard et al. 1988	n	-	
Hephaestin	Wang et al. 2007	y	-	
Ferroportin	Burdo et al. 2001, Wu et al. 2004, Wang et al. 2007	y	-	

Presence confirmed (y), absence confirmed (n), presence unclear (±), presence or absence not reported so far (-).

A H-ferritin receptor, that was initially found in white matter tracts (Hulet *et al.* 1999a, Hulet *et al.* 1999b) and later in cultured oligodendrocytes (Hulet *et al.* 2000, Hulet *et al.* 2002), has been identified as T cell immunoglobulin-domain and mucin-domain 2 (Tim-2; Hulet *et al.* 1999a, Chen *et al.* 2005). Blocking of this receptor prevents the binding of H-ferritin to oligodendrocytes in culture, confirming that Tim-2 is the receptor for H-ferritin (Figure 2; Todorich *et al.* 2008). Recently, Todorich *et al.* demonstrated that H-ferritin is taken up as iron source by cultured oligodendroglial cells, supporting cell survival in the absence of Tf and stimulating the differentiation process (Todorich *et al.* 2011). Currently, it is not clear whether H-ferritin in the brain might be derived from the blood by crossing the BBB (Fisher *et al.* 2007) or whether it is released by microglial cells (Zhang *et al.* 2006).

While iron uptake from ferritin or Tf has been demonstrated convincingly for oligodendrocytes, only little is known about uptake of non-protein-bound iron. The presence of DMT1 has been confirmed in one study (Moos *et al.* 2000), whereas other studies have not been able to support this observation (Burdo *et al.* 2001, Song *et al.* 2007) for oligodendrocytes *in vivo* (Figure 2). No literature data are available so far concerning the expression of DMT1 in cultured oligodendrocytes or the iron accumulation from low molecular weight iron sources. Therefore, the exact mechanism of non-protein-bound iron uptake by these cells remains to be elucidated.

Oligodendrocytes *in vivo* express the iron exporter ferroportin (Burdo *et al.* 2001, Wu *et al.* 2004, Wang *et al.* 2007) and the ferroxidase hephaestin (Wang *et al.* 2007), suggesting that the export of ferrous iron and subsequent extracellular oxidation of ferrous iron are mediated by ferroportin and hephaestin (Figure 2). Since ceruloplasmin and its G-anchored form have not been detected in oligodendrocytes *in vivo* (Mollgard *et al.* 1988), these ferroxidases do not appear to play a role in oligodendroglial iron metabolism.

Only a few reports are available about the regulation of oligodendroglial iron metabolism. The presence of IRP1 has been confirmed for oligodendrocytes *in vivo* and in cultured cells (Leibold *et al.* 2001), but no literature data are available on the expression of IRP2. Therefore, IRP1 might be the protein which regulates the expression of iron metabolism related proteins in oligodendrocytes.

Involvement of iron in myelin metabolism

Iron is an important cofactor for myelination (Connor and Menzies 1996, Ortiz *et al.* 2004) as demonstrated by the observation that the amount of myelin sheaths in iron deficient animals is

decreased and their composition is altered (Yu *et al.* 1986, Kwik-Uribe *et al.* 2000, Beard *et al.* 2003, Ortiz *et al.* 2004, Badaracco *et al.* 2008, Wu *et al.* 2008). Furthermore, the iron uptake of the brain is highest at the time of extensive myelination (Connor and Menzies 1996). Potential reason for this observation is that the syntheses of myelin proteins and lipids require a higher metabolic activity of oligodendrocytes compared to other brain cells (Piñero and Connor 2000). This was supported by the observations that oligodendrocytes have a increased oxygen consumption and ATP production and that oligodendrocytes are enriched with enzymes, which are participating in various metabolic pathways that contribute to ATP production and fatty acid synthesis (Connor and Menzies 1996, Lange and Que 1998, Piñero and Connor 2000, Baumann and Pham-Dinh 2001, McTigue and Tripathi 2008, Todorich *et al.* 2009).

Vulnerability of oligodendrocytes to iron-mediated oxidative stress

Oligodendrocytes are considered to be more vulnerable to iron-mediated oxidative stress compared to other types of brain cells due to their high metabolic activity and elevated iron content for the myelin synthesis (Connor and Menzies 1996, Piñero and Connor 2000, McTigue and Tripathi 2008, Todorich *et al.* 2009, Bradl and Lassmann 2010). However, cultured oligodendrocytes have been reported to efficiently dispose of exogenous hydrogen peroxide (Hirrlinger *et al.* 2002, Baud *et al.* 2004). The view on the antioxidative potential of these cells is controversially (Thorburne and Juurlink 1996, Back *et al.* 1998, Juurlink *et al.* 1998, Hirrlinger *et al.* 2002). Therefore, the hypothesis that oligodendrocytes have a greater risk to be damaged under conditions of increased oxidative stress and/or increased iron levels (McTigue and Tripathi 2008) needs to be reconsidered with respect to their iron and antioxidant defence mechanisms.

1.2.4. Iron metabolism of cultured astrocytes

Astrocytes are considered to play an important role in the brain iron metabolism, because they cover the brain capillary epithelial cells with their endfeet and therefore have a strategically important localization in the brain (Dringen *et al.* 2007). The expression of proteins of the iron metabolism in astrocytes is described in Figure 1 and the potential function of astrocytes in the brain iron metabolism has been reviewed by Dringen *et al.* (2007).

The uptake of protein-bound iron by cultured astrocytes has been shown to be mediated by the Tf/TfR complex, since astrocytes express the TfR in culture (Qian *et al.* 1999, Hoepken *et al.*

2004). In addition, the binding and uptake of Tf by cultured astrocytes has been demonstrated (Swaiman and Machen 1986, Qian *et al.* 1999, Qian *et al.* 2000). Furthermore, cultured astrocytes are able to accumulate iron from low molecular weight iron sources such as ferric chloride, ferric citrate, ferric ammonium citrate and ferric nitrilotriacetate (Swaiman and Machen 1985, Oshiro *et al.* 1998, Takeda *et al.* 1998, Jeong and David 2003, Hoepken *et al.* 2004, Lane *et al.* 2010, Bishop *et al.* 2011). Concerning the uptake mechanism of iron, a DMT1-independent transport of ferrous iron, an ascorbate-dependent ferrous iron uptake and an uptake mechanism of ferric iron have recently been suggested for astrocytes (Lane *et al.* 2010, Tulpule *et al.* 2010). Furthermore, astrocytes take up hemin by the heme transporter heme carrier protein 1 (Dang *et al.* 2010).

The iron metabolism of astrocytes appears to be regulated by the IRP/IRE system, since the expression of IRP1 and IRP2 has been shown (Irace *et al.* 2005). Furthermore, an alteration in their RNA-binding affinities of IRPs and of the expression of ferritin as response to hypoxia/reoxygenation has been shown in cultured astrocytes (Irace *et al.* 2005). In addition, astrocytes respond to hepcidin by a decreased expression of TfR1, DMT1, ferroportin, as well as by a reduced uptake of transferrin-bound and non-transferrin-bound iron, and by a lowered iron release (Du *et al.* 2011).

1.3. Nanoparticles

Nanotechnology covers the range from design to application of systems in the nanometer size, which have novel and/or superior characteristics (Soenen and De Cuyper 2010). In the last decade, this technology has gained an enormous interest because of the great variety of applications, ranging from electronics to health science (Silva 2006, Singh 2010). Nanoparticles are defined as particles and engineered materials in the size range of up to 100 nm in at least two dimensions (Silva 2006, Lewinski *et al.* 2008). These particles can consist of different materials, such as polymers, metals (for example iron, silver or gold), metal oxides (for example iron oxide, titanium dioxide or silica dioxide) or carbon (Cho *et al.* 2010, Fadeel and Garcia-Bennett 2010, Singh 2010). In the nanoscale, each of these materials has properties which are distinct from the properties of the bulk material. Accordingly, the reduction in particle size opens up new fields of application for a given material (Silva 2006, Gilmore *et al.* 2008). For example, semiconductor fluorescent quantum dots are widely used for visualization of molecular processes due to their stable fluorescent optical properties (Pathak *et al.* 2006). Carbon nanotubes are stiff, but also flexible and have electrical

properties which make them suitable as scaffolds for neuronal outgrowth (Malarkey and Parpura 2010). Polymer nanoparticles are widely used to encapsulate drugs for targeted delivery to a certain tissue (Gilmore *et al.* 2008).

Among these different materials, magnetic iron oxide nanoparticles have attracted much attention due to their great variety of applications in magnetic storage media, biosensing, drug delivery, hyperthermia, cell labeling and as contrast agents (Gupta and Gupta 2005, Laurent *et al.* 2008, Soenen and De Cuyper 2010). This chapter will focus on the current knowledge about magnetic iron oxide nanoparticles.

1.3.1.   Magnetic iron oxide nanoparticles

The synthesis of magnetic iron oxide nanoparticles (Fe-NP) can be accomplished by numerous methods such as coprecipitation of ferrous and ferric iron salts in basic aqueous solution, microemulsions, flow injection synthesis or electrospray synthesis (Laurent *et al.* 2008). After the synthesis, interactions of the particles with each other can lead to an increase of particle size due to aggregation and subsequent precipitation of particles in physiological media. To prevent this effect, Fe-NP can be coated with various substances (for example small molecules, polymers or proteins) to avoid the aggregation by steric and/or electrostatic repulsion (Gupta and Gupta 2005, Laurent *et al.* 2008).

Fe-NP are ideal contrast agents for magnetic resonance imaging (MRI) due to their very high relaxivity (Arbab *et al.* 2003, Laurent *et al.* 2008). The successful application of Fe-NP to enhance the contrast in MRI has been shown for brain glioma (Xie *et al.* 2011), the detection of labeled monocytes in an animal model of MS (Engberink *et al.* 2010), in animal models of AD (Beckmann *et al.* 2011) and for post-stroke neuroinflammation (Jin *et al.* 2009). Furthermore, Fe-NP with various different coatings have been developed for targeted delivery of anticancer drugs to the CNS and simultaneous visualization by MRI (Veiseh *et al.* 2009, Hadjipanayis *et al.* 2010, Veiseh *et al.* 2010, Yang *et al.* 2011b).

1.3.2.   Uptake mechanisms of iron oxide nanoparticles

In general, nanoparticles are considered to be taken up by endocytotic mechanisms (Hillaireau and Couvreur 2009, Zaki and Tirelli 2010), although there are only a few reports on the exact mechanisms. Several different endocytotic pathways are known and inhibitors for them are available, but the specificity of these inhibitors is limited and a given inhibitor usually blocks more than one pathway (Ivanov 2008, Zaki and Tirelli 2010). Literature reports have

suggested that different endocytotic pathways are involved together in the uptake of Fe-NP into mammalian cells (Kiessling *et al.* 2009, Xie *et al.* 2010). For example, caveolae-mediated endocytosis and macropinocytosis appear to be involved in Fe-NP uptake in BHK 21 cells (Arsianti *et al.* 2010), while scavenger receptor-mediated endocytosis, clathrin-mediated endocytosis and macropinocytosis are used for Fe-NP uptake in macrophages (Lunov *et al.* 2011). Electron microscopical pictures of cells that were exposed to various Fe-NP support the hypothesis of an endocytotic uptake process, since the Fe-NP are found within intracellular vesicles (Berg *et al.* 2010, Luciani *et al.* 2010, Soenen *et al.* 2011). Furthermore, the temperature-dependency of uptake processes indicates the presence of active and energy-dependent processes as shown before for protein-bound and non-protein-bound iron uptake (Trinder and Morgan 1998, Qian *et al.* 2000, Richardson 2001, Arredondo *et al.* 2008) and the uptake of Fe-NP (Kim *et al.* 2006, Pickard *et al.* 2010, Soenen *et al.* 2010).

1.3.3. Potential toxicity of iron oxide nanoparticles

The use of Fe-NP in clinical applications raises questions concerning potential toxic effects of the applied Fe-NP. Therefore, nanotoxicology and risk assessment of Fe-NP are increasingly studied and the subject of recent reviews (Nel *et al.* 2006, Singh and Nalwa 2007, Lewinski *et al.* 2008, Fadeel and Garcia-Bennett 2010, Oberdörster 2010).

The potential toxicity of Fe-NP on various kinds of cells has been investigated with a number of different cytotoxicity assays (Lewinski *et al.* 2008, Kroll *et al.* 2009, Marquis *et al.* 2009, Soenen and De Cuyper 2009). However, the results of these cytotoxicity assays need to be carefully interpreted and appropriate controls are mandatory, since nanoparticles have been shown to interfere with some assay components (Kroll *et al.* 2009, Marquis *et al.* 2009). Furthermore, the results of toxicity assays depend on factors such as physical and chemical properties of nanoparticles (Thorek and Tsourkas 2008), assessed time points (Pisanic *et al.* 2007), concentration of Fe-NP (Pisanic *et al.* 2007, Thorek and Tsourkas 2008) and the cell type tested (Ding *et al.* 2010, Kunzmann *et al.* 2011).

So far, Fe-NP are considered to be non-toxic and biocompatible and dextran-coated Fe-NP formulations (Endorem[®]/Feridex[®], Resovist[®] and Sinerem[®]) have been approved by the United States Food and Drug Administration for clinical application as MRI contrast agents (Soenen and De Cuyper 2009).

1.3.4.   Intracellular fate of iron oxide nanoparticles

So far, little is known about the fate of Fe-NP after the application and internalization into cells. Three studies have reported that Fe-NP with different coating materials release iron in a cell free system, that models the lysosomal environment by acidic pH and the presence of citrate (Arbab *et al.* 2005, Levy *et al.* 2010, Soenen *et al.* 2010). These observations raise the question of the effects of iron released from Fe-NP on the cells and their metabolism. In cells, iron derived from Fe-NP and/or the Fe-NP themselves are stainable by Prussian blue staining (Dunning *et al.* 2004, Soenen *et al.* 2010). The decrease in iron staining intensity, that has been observed over two weeks, demonstrates that at least the stainable cellular iron pool disappears with time from cells (Soenen *et al.* 2010).

Release of iron from Fe-NP would have physiological consequences, since ferritin and TfR expressions are regulated by the concentration of low molecular weight iron (chapter 1.2.2.; Rouault 2006). As response to the incubation of cells with Fe-NP, an upregulation of the ferritin expression and a transient alteration of the TfR expression have been observed (Pawelczyk *et al.* 2006, Schäfer *et al.* 2007, Raschzok *et al.* 2010, Soenen *et al.* 2010), as well as an accelerated cell proliferation (Huang *et al.* 2009). These reports demonstrate that at least some iron ions are released intracellularly from Fe-NP.

1.3.5.   Iron oxide nanoparticles cross the blood brain barrier

Fe-NP have been considered for different applications in neuroscience (Cooper and Nadeau 2009, Suh *et al.* 2009). For such applications, peripheral administration of Fe-NP requires crossing of the Fe-NP through the BBB. Table 4 lists selected studies that have demonstrated the presence of Fe-NP in the brain after peripheral administration, supporting the hypothesis that Fe-NP are able to cross the BBB.

1.3.6.   Effects of iron oxide nanoparticles on glial cells

Clinical applications of Fe-NP require the exposure of tissue and cells to Fe-NP (Bhaskar *et al.* 2010, Yang 2010). Many studies have investigated the effects of Fe-NP on brain cells in culture, but most of the studies deal with the labeling of cells with Fe-NP, for example for subsequent transplantation into the brain to support CNS regeneration and remyelination processes (Dunning *et al.* 2004) or for the replacement of dopaminergic neurons in patients

with PD (Focke *et al.* 2008). In this chapter, only the effects of Fe-NP on oligodendroglial and astrocyte cultures will be described (Tables 5 and 6).

The literature about the effects of Fe-NP on oligodendroglial cells is summarized in Table 5. Taken together, these studies have reported the uptake of Fe-NP into viable oligodendroglial cells. This suggests that oligodendroglial cells are able to cope well with the applied Fe-NP. Fe-NP-labeled oligodendroglial cells, which were then transplanted into the brains of rats, were detectable by MRI and these cells have been reported to remain viable and to be able to proliferate and myelinate axons (Bulte *et al.* 1999, Franklin *et al.* 1999, Dunning *et al.* 2004). The oligodendroglial cell line OLN-93 has been shown to be able to take up different kinds of nanoparticles, including Fe-NP and the involvement of a phagocytotic uptake process was suggested. Toxicity was observed for cobalt-doped tungsten carbide nanoparticles and attributed to the combination of particles and cobalt ions (Bastian *et al.* 2009, Busch *et al.* 2011). Therefore, also this oligodendroglial cell line seems to cope well with Fe-NP.

Some reports are also available that have studied the consequences of an application of Fe-NP on astrocytes (Table 6). Fe-NP are taken up by astroglial cells via clathrin-mediated endocytosis and via macropinocytosis (Pickard *et al.* 2010). Only one study reported a reduction of astrocyte viability after exposure to Fe-NP (Au *et al.* 2007). Therefore, cultured astrocytes also seem to cope well with the applied Fe-NP.

Table 4: Selected studies which have shown the presence of Fe-NP in the brain after peripheral application.

Type of coating	Animal model	Method used to demonstrate crossing of BBB	Reference
Dextran labeled with Cy5.5	Rats	MRI contrast enhancement / Prussian Blue staining / Fe-NP present in microglia cells	Kircher et al. 2003
Dextran	Mice	MRI contrast enhancement	Claes et al. 2008
Pluronic F-127 and oleic acid	Rats	Detection of iron in brain homogenates	Jain et al. 2008
Coating of PEGylated-chitosan branched copolymer coupled to chlorotoxin and Cy5.5 fluorophore	Mice	Biophonic imaging	Veiseh et al. 2009
Methoxy poly(ethyleneglycol)-poly(β-aminoester)/(amido amine)	Rats	MRI contrast enhancement	Gao et al. 2010
PEGylated polyamidoamine conjugated with fluorescein	Rats	Detection by confocal microscopy / Transmission electron microscopy	Ku et al. 2010
Myristoylated polyarginine peptide labeled with Cy5.5	Mice	MRI contrast enhancement / Prussian blue staining / Fe-NP present in macrophages	Kumar et al. 2010
-	Mice	Detection of iron in brain homogenates	Wang et al. 2010
Dextran	Mice	MRI contrast enhancement / Fe-NP present in macrophages	Beckmann et al. 2011
DMSA coupled to lactoferrin	Rats	MRI contrast enhancement / Prussian blue staining	Xie et al. 2011

Abbreviations: DMSA, dimercaptosuccinic acid; MRI, magnetic resonance imaging; PEG, polyethylene glycol.

Table 5: Literature describing consequences of a treatment of oligodendroglial cells with Fe-NP.

Cell type	Coating material	Consequences	Reference
CG-4	OX26 coupled to dextran	Labeling of cells Maintenance of migratory and myelination capacity *in vivo*	Bulte *et al.* 1999
CG-4	-	Internalization of Fe-NP Detection of cells after transplantation *in vivo* by MRI	Franklin *et al.* 1999
CG-4	-	Labeling of cells Maintenance of cell viability and proliferation	Bulte *et al.* 2001
CG-4	-	Labeling of cells with aid of transfection agents	Frank *et al.* 2002
CG-4	Dextran	Labeling of cells with aid of transfection agents	Frank *et al.* 2003
Schwann cells, olfactory ensheading cells	Dextran	Labeling of cells Maintenance of cellular functions Detection of cells after transplantation *in vivo* by MRI	Dunning *et al.* 2004

Abbreviation: CG-4 cells, rat oligodendrocyte progenitor cells.

Table 6: Literature describing consequences of a treatment of cultured astroglial cells with Fe-NP.

Cell type	Coating material	Consequences	Reference
Primary astrocytes and C6 cells	Collagen	Application of a magnetic field induces mechanical stimulation of cells that leads to increased Ca^{2+} and Mn^{2+} influx when cytoplasmic $[Ca^{2+}]$ is low	Niggel et al. 2000
Primary astrocytes	-	Detachment of cells Mitochondrial uncoupling Maintenance of membrane integrity	Au et al. 2007
Astrocytes	Hemagglutinating virus of Japan envelope vector coupled to dextran	Labeling of cells Detection of cells after transplantation in vivo by MRI	Zhu et al. 2007
Secondary astrocytes	Dextran	Uptake of Fe-NP Maintenance of cell viability	Ding et al. 2010
Astrocytes	Epidermal growth factor receptor (EGFR) antibody	Fe-NP decreased viability of cells expressing EGFR, but not the viability of other cells Contrast enhancement in MRI	Hadjipanayis et al. 2010
Secondary astrocytes	-	Uptake of Fe-NP Uptake by macropinocytosis and clathrin-mediated endocytosis Maintenance of cell viability and differentiation ability	Pickard et al. 2010

Abbreviations: C6 cells, glioma cells; EGFR, epidermal growth factor receptor.

33

1.4.   Aim of the thesis

This thesis will investigate the iron metabolism and the effects of Fe-NP on brain glial cells. In the first part of the thesis, the iron metabolism of the OLN-93 cell line will be investigated. The iron metabolism of these cells will be characterized by investigating the expression of the mRNA of proteins involved in iron metabolism, the ability of OLN-93 cells to take up iron from low molecular weight iron salts, the influence of an alteration of the cellular iron content on cell viability and the synthesis of ferritin. Additionally, the consequences of absence or presence of iron on the proliferation of OLN-93 cells will be studied by application of various iron sources and/or iron chelators.

Furthermore, the consequences of Fe-NP on OLN-93 cells will be investigated concerning cell morphology, viability, cellular iron content, cellular glutathione content and the ability of Fe-NP to generate ROS. In addition, the availability of iron from Fe-NP for the cellular metabolism will be examined by making use of the dependency of cell proliferation and ferritin synthesis on the presence of low molecular weight iron.

Finally, the consequences of Fe-NP exposure on the cell viability and iron contents of astrocyte-rich primary cultures will be investigated and data obtained for OLN-93 cells and astrocyte cultures will be compared in order to identify differences or common mechanisms how different types of glial cells deal with Fe-NP.

1.5. References

Abbott NJ (2002) Astrocyte-endothelial interactions and blood-brain barrier permeability. J Anat 200:629-638.

Abbott NJ, Ronnback L, Hansson E (2006) Astrocyte-endothelial interactions at the blood-brain barrier. Nat Rev Neurosci 7:41-53.

Abbott NJ, Patabendige AA, Dolman DE, Yusof SR, Begley DJ (2010) Structure and function of the blood-brain barrier. Neurobiol Dis 37:13-25.

Abboud S, Haile DJ (2000) A novel mammalian iron-regulated protein involved in intracellular iron metabolism. J Biol Chem 275:19906-19912.

Adam-Vizi V (2005) Production of reactive oxygen species in brain mitochondria: contribution by electron transport chain and non-electron transport chain sources. Antioxid Redox Signal 7:1140-1149.

Adibhatla RM, Hatcher JF (2010) Lipid oxidation and peroxidation in CNS health and disease: from molecular mechanisms to therapeutic opportunities. Antioxid Redox Signal 12:125-169.

Altamura S, Muckenthaler MU (2009) Iron toxicity in diseases of aging: Alzheimer's disease, Parkinson's disease and atherosclerosis. J Alzheimers Dis 16:879-895.

Anderson GJ, Vulpe CD (2009) Mammalian iron transport. Cell Mol Life Sci 66:3241-3261.

Arbab AS, Bashaw LA, Miller BR, Jordan EK, Lewis BK, Kalish H, Frank JA (2003) Characterization of biophysical and metabolic properties of cells labeled with superparamagnetic iron oxide nanoparticles and transfection agent for cellular MR imaging. Radiology 229:838-846.

Arbab AS, Wilson LB, Ashari P, Jordan EK, Lewis BK, Frank JA (2005) A model of lysosomal metabolism of dextran coated superparamagnetic iron oxide (SPIO) nanoparticles: implications for cellular magnetic resonance imaging. NMR Biomed 18:383-389.

Arosio P, Ingrassia R, Cavadini P (2009) Ferritins: a family of molecules for iron storage, antioxidation and more. Biochim Biophys Acta 1790:589-599.

Arredondo M, Kloosterman J, Nunez S, Segovia F, Candia V, Flores S, Le Blanc S, Olivares M, Pizarro F (2008) Heme iron uptake by Caco-2 cells is a saturable, temperature

sensitive and modulated by extracellular pH and potassium. Biol Trace Elem Res 125:109-119.

Arsianti M, Lim M, Marquis CP, Amal R (2010) Polyethylenimine based magnetic iron-oxide vector: the effect of vector component assembly on cellular entry mechanism, intracellular localization, and cellular viability. Biomacromolecules 11:2521-2531.

Attwell D, Buchan AM, Charpak S, Lauritzen M, Macvicar BA, Newman EA (2010) Glial and neuronal control of brain blood flow. Nature 468:232-243.

Au C, Mutkus L, Dobson A, Riffle J, Lalli J, Aschner M (2007) Effects of nanoparticles on the adhesion and cell viability on astrocytes. Biol Trace Elem Res 120:248-256.

Auestad N, Korsak RA, Morrow JW, Edmond J (1991) Fatty acid oxidation and ketogenesis by astrocytes in primary culture. J Neurochem 56:1376-1386.

Avramovich-Tirosh Y, Amit T, Bar-Am O, Weinreb O, Youdim MB (2008) Physiological and pathological aspects of Aβ in iron homeostasis via 5'UTR in the APP mRNA and the therapeutic use of iron-chelators. BMC Neurosci 9 (Suppl 2):S2.

Babcock GT (1999) How oxygen is activated and reduced in respiration. Proc Natl Acad Sci USA 96:12971-12973.

Back SA, Gan X, Li Y, Rosenberg PA, Volpe JJ (1998) Maturation-dependent vulnerability of oligodendrocytes to oxidative stress-induced death caused by glutathione depletion. J Neurosci 18:6241-6253.

Badaracco ME, Ortiz EH, Soto EF, Connor J, Pasquini JM (2008) Effect of transferrin on hypomyelination induced by iron deficiency. J Neurosci Res 86:2663-2673.

Banerjee R, Vitvitsky V, Garg SK (2008) The undertow of sulfur metabolism on glutamatergic neurotransmission. Trends Biochem Sci 33:413-419.

Barnham KJ, Bush AI (2008) Metals in Alzheimer's and Parkinson's diseases. Curr Opin Chem Biol 12:222-228.

Baron W, Hoekstra D (2010) On the biogenesis of myelin membranes: sorting, trafficking and cell polarity. FEBS Lett 584:1760-1770.

Barros LF, Deitmer JW (2010) Glucose and lactate supply to the synapse. Brain Res Rev 63:149-159.

Bartlett WP, Li XS, Connor JR (1991) Expression of transferrin mRNA in the CNS of normal and jimpy mice. J Neurochem 57:318-322.

Bastian S, Busch W, Kuhnel D, Springer A, Meissner T, Holke R, Scholz S, Iwe M, Pompe W, Gelinsky M, Potthoff A, Richter V, Ikonomidou C, Schirmer K (2009) Toxicity of tungsten carbide and cobalt-doped tungsten carbide nanoparticles in mammalian cells *in vitro*. Environ Health Perspect 117:530-536.

Battin EE, Brumaghim JL (2009) Antioxidant activity of sulfur and selenium: a review of reactive oxygen species scavenging, glutathione peroxidase, and metal-binding antioxidant mechanisms. Cell Biochem Biophys 55:1-23.

Baud O, Greene AE, Li J, Wang H, Volpe JJ, Rosenberg PA (2004) Glutathione peroxidase-catalase cooperativity is required for resistance to hydrogen peroxide by mature rat oligodendrocytes. J Neurosci 24:1531-1540.

Bauer NG, Richter-Landsberg C (2006) The dynamic instability of microtubules is required for aggresome formation in oligodendroglial cells after proteolytic stress. J Mol Neurosci 29:153-168.

Baumann N, Pham-Dinh D (2001) Biology of oligodendrocyte and myelin in the mammalian central nervous system. Physiol Rev 81:871-927.

Beard JL, Wiesinger JA, Connor JR (2003) Pre- and postweaning iron deficiency alters myelination in sprague-dawley rats. Dev Neurosci 25:308-315.

Beckmann N, Gerard C, Abramowski D, Cannet C, Staufenbiel M (2011) Noninvasive magnetic resonance imaging detection of cerebral amyloid angiopathy-related microvascular alterations using superparamagnetic iron oxide particles in APP transgenic mouse models of Alzheimer's disease: application to passive Aβ immunotherapy. J Neurosci 31:1023-1031.

Benarroch EE (2009) Brain iron homeostasis and neurodegenerative disease. Neurology 72:1436-1440.

Benkovic SA, Connor JR (1993) Ferritin, transferrin, and iron in selected regions of the adult and aged rat brain. J Comp Neurol 338:97-113.

Berg JM, Ho S, Hwang W, Zebda R, Cummins K, Soriaga MP, Taylor R, Guo B, Sayes CM (2010) Internalization of carbon black and maghemite iron oxide nanoparticle mixture leads to oxidant production. Chem Res Toxicol 23:1874-1882.

Bhaskar S, Tian F, Stoeger T, Kreyling W, de la Fuente JM, Grazu V, Borm P, Estrada G, Ntziachristos V, Razansky D (2010) Multifunctional nanocarriers for diagnostics, drug delivery and targeted treatment across blood-brain barrier: perspectives on tracking and neuroimaging. Part Fibre Toxicol 7:3.

Bishop GM, Dang TN, Dringen R, Robinson SR (2011) Accumulation of non-transferrin-bound iron by neurons, astrocytes, and microglia. Neurotox Res 19:443-451.

Bixel MG, Hamprecht B (1995) Generation of ketone bodies from leucine by cultured astroglial cells. J Neurochem 65:2450-2461.

Bixel MG, Hutson SM, Hamprecht B (1997) Cellular distribution of branched-chain amino acid aminotransferase isoenzymes among rat brain glial cells in culture. J Histochem Cytochem 45:685-694.

Blissman G, Menzies S, Beard J, Palmer C, Connor J (1996) The expression of ferritin subunits and iron in oligodendrocytes in neonatal porcine brains. Dev Neurosci 18:274-281.

Bloch B, Popovici T, Levin MJ, Tuil D, Kahn A (1985) Transferrin gene expression visualized in oligodendrocytes of the rat brain by using in situ hybridization and immunohistochemistry. Proc Natl Acad Sci USA 82:6706-6710.

Bolhuis S, Richter-Landsberg C (2010) Effect of proteasome inhibition by MG-132 on HSP27 oligomerization, phosphorylation, and aggresome formation in the OLN-93 oligodendroglia cell line. J Neurochem 114:960-971.

Bradl M, Lassmann H (2010) Oligodendrocytes: biology and pathology. Acta Neuropathol 119:37-53.

Brand A, Leibfritz D, Hamprecht B, Dringen R (1998) Metabolism of cysteine in astroglial cells: synthesis of hypotaurine and taurine. J Neurochem 71:827-832.

Brand A, Gil S, Yavin E (2000) N-methyl bases of ethanolamine prevent apoptotic cell death induced by oxidative stress in cells of oligodendroglia origin. J Neurochem 74:1596-1604.

Brand A, Gil S, Seger R, Yavin E (2001) Lipid constituents in oligodendroglial cells alter susceptibility to H_2O_2-induced apoptotic cell death via ERK activation. J Neurochem 76:910-918.

Brand A, Yavin E (2005) Translocation of ethanolamine phosphoglyceride is required for initiation of apoptotic death in OLN-93 oligodendroglial cells. Neurochem Res 30:1257-1267.

Brand A, Schonfeld E, Isharel I, Yavin E (2008) Docosahexaenoic acid-dependent iron accumulation in oligodendroglia cells protects from hydrogen peroxide-induced damage. J Neurochem 105:1325-1335.

Brand A, Bauer NG, Hallott A, Goldbaum O, Ghebremeskel K, Reifen R, Richter-Landsberg C (2010) Membrane lipid modification by polyunsaturated fatty acids sensitizes oligodendroglial OLN-93 cells against oxidative stress and promotes up-regulation of heme oxygenase-1 (HSP32). J Neurochem 113:465-476.

Bressler JP, Olivi L, Cheong JH, Kim Y, Maerten A, Bannon D (2007) Metal transporters in intestine and brain: their involvement in metal-associated neurotoxicities. Hum Exp Toxicol 26:221-229.

Brodie C, Siriwardana G, Lucas J, Schleicher R, Terada N, Szepesi A, Gelfand E, Seligman P (1993) Neuroblastoma sensitivity to growth inhibition by deferrioxamine: evidence for a block in G1 phase of the cell cycle. Cancer Res 53:3968-3975.

Bruce CC, Zhao C, Franklin RJ (2010) Remyelination- an effective means of neuroprotection. Horm Behav 57:56-62.

Buckinx R, Smolders I, Sahebali S, Janssen D, Smets I, Ameloot M, Rigo JM (2009) Morphological changes do not reflect biochemical and functional differentiation in OLN-93 oligodendroglial cells. J Neurosci Methods 184:1-9.

Buettner GR (1993) The pecking order of free radicals and antioxidants: lipid peroxidation, α-tocopherol, and ascorbate. Arch Biochem Biophys 300:535-543.

Bullock TH, Bennett MV, Johnston D, Josephson R, Marder E, Fields RD (2005) The neuron doctrine, redux. Science 310:791-793.

Bulte JW, Zhang S, van Gelderen P, Herynek V, Jordan EK, Duncan ID, Frank JA (1999) Neurotransplantation of magnetically labeled oligodendrocyte progenitors: magnetic resonance tracking of cell migration and myelination. Proc Natl Acad Sci USA 96:15256-15261.

Bulte JW, Douglas T, Witwer B, Zhang SC, Strable E, Lewis BK, Zywicke H, Miller B, van Gelderen P, Moskowitz BM, Duncan ID, Frank JA (2001) Magnetodendrimers allow

endosomal magnetic labeling and *in vivo* tracking of stem cells. Nat Biotechnol 19:1141-1147.

Burdo JR, Menzies SL, Simpson IA, Garrick LM, Garrick MD, Dolan KG, Haile DJ, Beard JL, Connor JR (2001) Distribution of divalent metal transporter 1 and metal transport protein 1 in the normal and Belgrade rat. J Neurosci Res 66:1198-1207.

Burgmaier G, Schonrock LM, Kuhlmann T, Richter-Landsberg C, Bruck W (2000) Association of increased bcl-2 expression with rescue from tumor necrosis factor-α-induced cell death in the oligodendrocyte cell line OLN-93. J Neurochem 75:2270-2276.

Busch W, Bastian S, Trahorsch U, Iwe M, Kühnel D, Meißner T, Springer A, Gelinsky M, Richter V, Ikonomidou C (2011) Internalisation of engineered nanoparticles into mammalian cells *in vitro*: influence of cell type and particle properties. J Nanopart Res 13:293-310.

Carmignoto G, Gómez-Gonzalo M (2010) The contribution of astrocyte signalling to neurovascular coupling. Brain Res Rev 63:138-148.

Chang TC, Chou WY, Chang GG (2000) Protein oxidation and turnover. J Biomed Sci 7:357-363.

Cheepsunthorn P, Palmer C, Connor JR (1998) Cellular distribution of ferritin subunits in postnatal rat brain. J Comp Neurol 400:73-86.

Chen TT, Li L, Chung DH, Allen CD, Torti SV, Torti FM, Cyster JG, Chen CY, Brodsky FM, Niemi EC, Nakamura MC, Seaman WE, Daws MR (2005) TIM-2 is expressed on B cells and in liver and kidney and is a receptor for H-ferritin endocytosis. J Exp Med 202:955-965.

Chesik D, De Keyser J (2010) Progesterone and dexamethasone differentially regulate the IGF-system in glial cells. Neurosci Lett 468:178-182.

Chesik D, De Keyser J, Bron R, Fuhler GM (2010) Insulin-like growth factor binding protein-1 activates integrin-mediated intracellular signaling and migration in oligodendrocytes. J Neurochem 113:1319-1330.

Cho EC, Glaus C, Chen J, Welch MJ, Xia Y (2010) Inorganic nanoparticle-based contrast agents for molecular imaging. Trends Mol Med 16:561-573.

Claes A, Gambarota G, Hamans B, van Tellingen O, Wesseling P, Maass C, Heerschap A, Leenders W (2008) Magnetic resonance imaging-based detection of glial brain tumors in mice after antiangiogenic treatment. Int J Cancer 122:1981-1986.

Clardy SL, Wang X, Boyer PJ, Earley CJ, Allen RP, Connor JR (2006) Is ferroportin-hepcidin signaling altered in restless legs syndrome? J Neurol Sci 247:173-179.

Compston A, Coles A (2008) Multiple sclerosis. Lancet 372:1502-1517.

Connor JR, Fine RE (1986) The distribution of transferrin immunoreactivity in the rat central nervous system. Brain Res 368:319-328.

Connor JR, Menzies SL (1990) Altered cellular distribution of iron in the central nervous system of myelin deficient rats. Neuroscience 34:265-271.

Connor JR, Menzies SL (1995) Cellular management of iron in the brain. J Neurol Sci 134 (Suppl 1):33-44.

Connor JR, Menzies SL (1996) Relationship of iron to oligodendrocytes and myelination. Glia 17:83-93.

Connor JR, Menzies SL, St Martin SM, Mufson EJ (1990) Cellular distribution of transferrin, ferritin, and iron in normal and aged human brains. J Neurosci Res 27:595-611.

Connor JR, Roskams AJ, Menzies SL, Williams ME (1993) Transferrin in the central nervous system of the shiverer mouse myelin mutant. J Neurosci Res 36:501-507.

Connor JR, Boeshore KL, Benkovic SA, Menzies SL (1994) Isoforms of ferritin have a specific cellular distribution in the brain. J Neurosci Res 37:461-465.

Connor JR, Pavlick G, Karli D, Menzies SL, Palmer C (1995) A histochemical study of iron-positive cells in the developing rat brain. J Comp Neurol 355:111-123.

Conrad ME, Umbreit JN, Moore EG, Uzel C, Berry MR (1994) Alternate iron transport pathway mobilferrin and integrin in K562 cells. J Biol Chem 269:7169-7173.

Conrad ME, Umbreit JN, Moore EG, Hainsworth LN, Porubcin M, Simovich MJ, Nakada MT, Dolan K, Garrick MD (2000) Separate pathways for cellular uptake of ferric and ferrous iron. Am J Physiol Gastrointest Liver Physiol 279:767-774.

Cooper DR, Nadeau JL (2009) Nanotechnology for *in vitro* neuroscience. Nanoscale 1:183-200.

Crews L, Masliah E (2010) Molecular mechanisms of neurodegeneration in Alzheimer's disease. Hum Mol Genet 19:R12-R20.

Crichton RR, Dexter DT, Ward RJ (2011) Brain iron metabolism and its perturbation in neurological diseases. J Neural Transm 118:301-314.

Dabouras V, Rothermel A, Reininger-Mack A, Wien SL, Layer PG, Robitzki AA (2004) Exogenous application of glucose induces aging in rat cerebral oligodendrocytes as revealed by alteration in telomere length. Neurosci Lett 368:68-72.

Dang TN, Bishop GM, Dringen R, Robinson SR (2010) The putative heme transporter HCP1 is expressed in cultured astrocytes and contributes to the uptake of hemin. Glia 58:55-65.

Darshan D, Frazer DM, Anderson GJ (2010) Molecular basis of iron-loading disorders. Expert Rev Mol Med 12:e36.

Davies MJ (2005) The oxidative environment and protein damage. Biochim Biophys Acta 1703:93-109.

De Arriba Zerpa GA, Saleh MC, Fernandez PM, Guillou F, Espinosa de los Monteros A, de Vellis J, Zakin MM, Baron B (2000) Alternative splicing prevents transferrin secretion during differentiation of a human oligodendrocyte cell line. J Neurosci Res 61:388-395.

De Domenico I, McVey Ward D, Kaplan J (2008) Regulation of iron acquisition and storage: consequences for iron-linked disorders. Nat Rev Mol Cell Biol 9:72-81.

Deitmer JW, Rose CR (2010) Ion changes and signalling in perisynaptic glia. Brain Res Rev 63:113-129.

Dickinson TK, Connor JR (1995) Cellular distribution of iron, transferrin, and ferritin in the hypotransferrinemic (Hp) mouse brain. J Comp Neurol 355:67-80.

Ding J, Tao K, Li J, Song S, Sun K (2010) Cell-specific cytotoxicity of dextran-stabilized magnetite nanoparticles. Colloids Surf B Biointerfaces 79:184-190.

Donovan A, Brownlie A, Zhou Y, Shepard J, Pratt SJ, Moynihan J, Paw BH, Drejer A, Barut B, Zapata A, Law TC, Brugnara C, Lux SE, Pinkus GS, Pinkus JL, Kingsley PD, Palis J, Fleming MD, Andrews NC, Zon LI (2000) Positional cloning of zebrafish ferroportin1 identifies a conserved vertebrate iron exporter. Nature 403:776-781.

Dringen R (2000) Metabolism and functions of glutathione in brain. Prog Neurobiol 62:649-671.

Dringen R, Hirrlinger J (2003) Glutathione pathways in the brain. Biol Chem 384:505-516.

Dringen R, Pawlowski PG, Hirrlinger J (2005) Peroxide detoxification by brain cells. J Neurosci Res 79:157-165.

Dringen R, Verleysdonk S, Hamprecht B, Willker W, Leibfritz D, Brand A (1998) Metabolism of glycine in primary astroglial cells: synthesis of creatine, serine, and glutathione. J Neurochem 70:835-840.

Dringen R, Bishop GM, Koeppe M, Dang TN, Robinson SR (2007) The pivotal role of astrocytes in the metabolism of iron in the brain. Neurochem Res 32:1884-1890.

Du F, Qian ZM, Zhu L, Wu XM, Yung WH, Tsim TY, Ke Y (2009) L-DOPA neurotoxicity is mediated by up-regulation of DMT1-IRE expression. PLoS One 4:e4593.

Du F, Qian C, Ming Qian Z, Wu XM, Xie H, Yung WH, Ke Y (2011) Hepcidin directly inhibits transferrin receptor 1 expression in astrocytes via a cyclic AMP-protein kinase a pathway. Glia 59:936-945.

Dunlop RA, Brunk UT, Rodgers KJ (2009) Oxidized proteins: mechanisms of removal and consequences of accumulation. IUBMB Life 61:522-527.

Dunning MD, Lakatos A, Loizou L, Kettunen M, ffrench-Constant C, Brindle KM, Franklin RJ (2004) Superparamagnetic iron oxide-labeled schwann cells and olfactory ensheathing cells can be traced *in vivo* by magnetic resonance imaging and retain functional properties after transplantation into the CNS. J Neurosci 24:9799-9810.

Dwork AJ, Schon EA, Herbert J (1988) Nonidentical distribution of transferrin and ferric iron in human brain. Neuroscience 27:333-345.

Emery B (2010) Regulation of oligodendrocyte differentiation and myelination. Science 330:779-782.

Engberink RD, van der Pol SM, Walczak P, van der Toorn A, Viergever MA, Dijkstra CD, Bulte JW, de Vries HE, Blezer EL (2010) Magnetic resonance imaging of monocytes labeled with ultrasmall superparamagnetic particles of iron oxide using magnetoelectroporation in an animal model of multiple sclerosis. Mol Imaging 9:268-277.

Ernst A, Stolzing A, Sandig G, Grune T (2004a) Antioxidants effectively prevent oxidation-induced protein damage in OLN 93 cells. Arch Biochem Biophys 421:54-60.

Ernst A, Stolzing A, Sandig G, Grune T (2004b) Protein oxidation and the degradation of oxidized proteins in the rat oligodendrocyte cell line OLN 93-antioxidative effect of the intracellular spin trapping agent PBN. Brain Res Mol Brain Res 122:126-132.

Eroglu C, Barres BA (2010) Regulation of synaptic connectivity by glia. Nature 468:223-231.

Espinosa de los Monteros A, Foucaud B (1987) Effect of iron and transferrin on pure oligodendrocytes in culture; characterization of a high-affinity transferrin receptor at different ages. Brain Res 432:123-130.

Espinosa de los Monteros A, Chiapelli F, Fisher RS, de Vellis J (1988) Transferrin: an early marker of oligodendrocytes in culture. Int J Dev Neurosci 6:167-175.

Espinosa de los Monteros A, Kumar S, Scully S, Cole R, de Vellis J (1990) Transferrin gene expression and secretion by rat brain cells *in vitro*. J Neurosci Res 25:576-580.

Espinosa de los Monteros A, Sawaya BE, Guillou F, Zakin MM, de Vellis J, Schaeffer E (1994) Brain-specific expression of the human transferrin gene. similar elements govern transcription in oligodendrocytes and in a neuronal cell line. J Biol Chem 269:24504-24510.

Eulenburg V, Gomeza J (2010) Neurotransmitter transporters expressed in glial cells as regulators of synapse function. Brain Res Rev 63:103-112.

Evans MD, Dizdaroglu M, Cooke MS (2004) Oxidative DNA damage and disease: induction, repair and significance. Mutat Res 567:1-61.

Fadeel B, Garcia-Bennett AE (2010) Better safe than sorry: understanding the toxicological properties of inorganic nanoparticles manufactured for biomedical applications. Adv Drug Deliv Rev 62:362-374.

Fellin T (2009) Communication between neurons and astrocytes: relevance to the modulation of synaptic and network activity. J Neurochem 108:533-544.

Fillebeen C, Ruchoux MM, Mitchell V, Vincent S, Bena ssa M, Pierce A (2001) Lactoferrin is synthesized by activated microglia in the human substantia nigra and its synthesis by the human microglial CHME cell line is upregulated by tumor necrosis factor α or 1-methyl-4-phenylpyridinium treatment. Brain Res Mol Brain Res 96:103-113.

Fisher J, Devraj K, Ingram J, Slagle-Webb B, Madhankumar AB, Liu X, Klinger M, Simpson IA, Connor JR (2007) Ferritin: a novel mechanism for delivery of iron to the brain and other organs. Am J Physiol Cell Physiol 293:C641-C649.

Fleming MD, Trenor CC, 3rd, Su MA, Foernzler D, Beier DR, Dietrich WF, Andrews NC (1997) Microcytic anaemia mice have a mutation in Nramp2, a candidate iron transporter gene. Nat Genet 16:383-386.

Fleming MD, Romano MA, Su MA, Garrick LM, Garrick MD, Andrews NC (1998) Nramp2 is mutated in the anemic Belgrade (b) rat: evidence of a role for Nramp2 in endosomal iron transport. Proc Natl Acad Sci USA 95:1148-1153.

Flora SJ (2009) Structural, chemical and biological aspects of antioxidants for strategies against metal and metalloid exposure. Oxid Med Cell Longev 2:191-206.

Focke A, Schwarz S, Foerschler A, Scheibe J, Milosevic J, Zimmer C, Schwarz J (2008) Labeling of human neural precursor cells using ferromagnetic nanoparticles. Magn Reson Med 60:1321-1328.

Frank JA, Zywicke H, Jordan EK, Mitchell J, Lewis BK, Miller B, Bryant LH, Jr., Bulte JW (2002) Magnetic intracellular labeling of mammalian cells by combining (FDA-approved) superparamagnetic iron oxide MR contrast agents and commonly used transfection agents. Acad Radiol 9 (Suppl 2):S484-487.

Frank JA, Miller BR, Arbab AS, Zywicke HA, Jordan EK, Lewis BK, Bryant LH, Jr., Bulte JW (2003) Clinically applicable labeling of mammalian and stem cells by combining superparamagnetic iron oxides and transfection agents. Radiology 228:480-487.

Franklin RJ, Ffrench-Constant C (2008) Remyelination in the CNS: from biology to therapy. Nat Rev Neurosci 9:839-855.

Franklin RJ, Blaschuk KL, Bearchell MC, Prestoz LL, Setzu A, Brindle KM, ffrench-Constant C (1999) Magnetic resonance imaging of transplanted oligodendrocyte precursors in the rat brain. Neuroreport 10:3961-3965.

Fridovich I (1995) Superoxide radical and superoxide dismutases. Annu Rev Biochem 64:97-112.

Gao GH, Lee JW, Nguyen MK, Im GH, Yang J, Heo H, Jeon P, Park TG, Lee JH, Lee DS (2010) pH-responsive polymeric micelle based on PEG-poly(β-amino ester)/(amido

amine) as intelligent vehicle for magnetic resonance imaging in detection of cerebral ischemic area. J Control Release in press.

Garrick MD, Garrick LM (2009) Cellular iron transport. Biochim Biophys Acta 1790:309-325.

Gerstner B, Gratopp A, Marcinkowski M, Sifringer M, Obladen M, Buhrer C (2005) Glutaric acid and its metabolites cause apoptosis in immature oligodendrocytes: a novel mechanism of white matter degeneration in glutaryl-CoA dehydrogenase deficiency. Pediatr Res 57:771-776.

Gerstner B, Buhrer C, Rheinlander C, Polley O, Schüller A, Berns M, Obladen M, Felderhoff-Mueser U (2006) Maturation-dependent oligodendrocyte apoptosis caused by hyperoxia. J Neurosci Res 84:306-315.

Gerstner B, Sifringer M, Dzietko M, Schüller A, Lee J, Simons S, Obladen M, Volpe JJ, Rosenberg PA, Felderhoff-Mueser U (2007) Estradiol attenuates hyperoxia-induced cell death in the developing white matter. Ann Neurol 61:562-573.

Gielen E, Vercammen J, Sykora J, Humpolickova J, Vandeven M, Benda A, Hellings N, Hof M, Engelborghs Y, Steels P, Ameloot M (2005) Diffusion of sphingomyelin and myelin oligodendrocyte glycoprotein in the membrane of OLN-93 oligodendroglial cells studied by fluorescence correlation spectroscopy. CR Biol 328:1057-1064.

Gielen E, Smisdom N, De Clercq B, Vandeven M, Gijsbers R, Debyser Z, Rigo JM, Hofkens J, Engelborghs Y, Ameloot M (2008) Diffusion of myelin oligodendrocyte glycoprotein in living OLN-93 cells investigated by raster-scanning image correlation spectroscopy (RICS). J Fluoresc 18:813-819.

Gilmore JL, Yi X, Quan L, Kabanov AV (2008) Novel nanomaterials for clinical neuroscience. J Neuroimmune Pharmacol 3:83-94.

Giometto B, Bozza F, Argentiero V, Gallo P, Pagni S, Piccinno MG, Tavolato B (1990) Transferrin receptors in rat central nervous system. an immunocytochemical study. J Neurol Sci 98:81-90.

Goldbaum O, Oppermann M, Handschuh M, Dabir D, Zhang B, Forman MS, Trojanowski JQ, Lee VM, Richter-Landsberg C (2003) Proteasome inhibition stabilizes tau inclusions in oligodendroglial cells that occur after treatment with okadaic acid. J Neurosci 23:8872-8880.

Graeber MB, Streit WJ (2010) Microglia: biology and pathology. Acta Neuropathol 119:89-105.

Green DA, Antholine WE, Wong SJ, Richardson DR, Chitambar CR (2001) Inhibition of malignant cell growth by 311, a novel iron chelator of the pyridoxal isonicotinoyl hydrazone class: effect on the R2 subunit of ribonucleotide reductase. Clin Cancer Res 7:3574-3579.

Griot C, Vandevelde M (1988) Transferrin, carbonic anhydrase C and ferritin in dissociated murine brain cell cultures. J Neuroimmunol 18:333-340.

Gruenheid S, Canonne-Hergaux F, Gauthier S, Hackam DJ, Grinstein S, Gros P (1999) The iron transport protein NRAMP2 is an integral membrane glycoprotein that colocalizes with transferrin in recycling endosomes. J Exp Med 189:831-841.

Gunshin H, Mackenzie B, Berger UV, Gunshin Y, Romero MF, Boron WF, Nussberger S, Gollan JL, Hediger MA (1997) Cloning and characterization of a mammalian proton-coupled metal-ion transporter. Nature 388:482-488.

Gupta AK, Gupta M (2005) Synthesis and surface engineering of iron oxide nanoparticles for biomedical applications. Biomaterials 26:3995-4021.

Gupta YK, Gupta M, Kohli K (2003) Neuroprotective role of melatonin in oxidative stress vulnerable brain. Indian J Physiol Pharmacol 47:373-386.

Guthrie PB, Knappenberger J, Segal M, Bennett MV, Charles AC, Kater SB (1999) ATP released from astrocytes mediates glial calcium waves. J Neurosci 19:520-528.

Hadjipanayis CG, Machaidze R, Kaluzova M, Wang L, Schuette AJ, Chen H, Wu X, Mao H (2010) EGFRvIII antibody-conjugated iron oxide nanoparticles for magnetic resonance imaging-guided convection-enhanced delivery and targeted therapy of glioblastoma. Cancer Res 70:6303-6312.

Halliwell B (2006) Oxidative stress and neurodegeneration: where are we now? J Neurochem 97:1634-1658.

Halliwell B, Gutteridge JM (1984) Oxygen toxicity, oxygen radicals, transition metals and disease. Biochem J 219:1-14.

Halliwell B, Gutteridge JMC (2007) Free Radicals in Biology and Medicine. Oxford, UK: Oxford University Press.

Hardy J, Selkoe DJ (2002) The amyloid hypothesis of Alzheimer's disease: progress and problems on the road to therapeutics. Science 297:353-356.

Hentze MW, Muckenthaler MU, Andrews NC (2004) Balancing acts: molecular control of mammalian iron metabolism. Cell 117:285-297.

Hillaireau H, Couvreur P (2009) Nanocarriers´ entry into the cell: relevance to drug delivery. Cell Mol Life Sci 66:2873-2896.

Hirrlinger J, Resch A, Gutterer JM, Dringen R (2002) Oligodendroglial cells in culture effectively dispose of exogenous hydrogen peroxide: comparison with cultured neurones, astroglial and microglial cells. J Neurochem 82:635-644.

Hoepken HH (2005) Untersuchungen zum Eisenstoffwechsel neuraler Zellen (Dissertation). University of Tübingen, Tübingen.

Hoepken HH, Korten T, Robinson SR, Dringen R (2004) Iron accumulation, iron-mediated toxicity and altered levels of ferritin and transferrin receptor in cultured astrocytes during incubation with ferric ammonium citrate. J Neurochem 88:1194-1202.

Hohnholt M, Geppert M, Dringen R (2010) Effects of iron chelators, iron salts, and iron oxide nanoparticles on the proliferation and the iron content of oligodendroglial OLN-93 cells. Neurochem Res 35:1259-1268.

Holzknecht C, Rohl C (2010) Effects of methylprednisolone and glatiramer acetate on nitric oxide formation of cytokine-stimulated cells from the rat oligodendroglial cell line OLN-93. Neuroimmunomodulation 17:23-30.

Hu QD, Ang BT, Karsak M, Hu WP, Cui XY, Duka T, Takeda Y, Chia W, Sankar N, Ng YK, Ling EA, Maciag T, Small D, Trifonova R, Kopan R, Okano H, Nakafuku M, Chiba S, Hirai H, Aster JC, Schachner M, Pallen CJ, Watanabe K, Xiao ZC (2003) F3/contactin acts as a functional ligand for Notch during oligodendrocyte maturation. Cell 115:163-175.

Huang E, Ong WY, Go ML, Connor JR (2006) Upregulation of iron regulatory proteins and divalent metal transporter-1 isoforms in the rat hippocampus after kainate induced neuronal injury. Exp Brain Res 170:376-386.

Huang DM, Hsiao JK, Chen YC, Chien LY, Yao M, Chen YK, Ko BS, Hsu SC, Tai LA, Cheng HY, Wang SW, Yang CS (2009) The promotion of human mesenchymal stem

cell proliferation by superparamagnetic iron oxide nanoparticles. Biomaterials 30:3645-3651.

Hulet SW, Hess EJ, Debinski W, Arosio P, Bruce K, Powers S, Connor JR (1999a) Characterization and distribution of ferritin binding sites in the adult mouse brain. J Neurochem 72:868-874.

Hulet SW, Powers S, Connor JR (1999b) Distribution of transferrin and ferritin binding in normal and multiple sclerotic human brains. J Neurol Sci 165:48-55.

Hulet SW, Heyliger SO, Powers S, Connor JR (2000) Oligodendrocyte progenitor cells internalize ferritin via clathrin-dependent receptor mediated endocytosis. J Neurosci Res 61:52-60.

Hulet SW, Menzies S, Connor JR (2002) Ferritin binding in the developing mouse brain follows a pattern similar to myelination and is unaffected by the jimpy mutation. Dev Neurosci 24:208-213.

Hwang IK, Yoon DK, Yoo KY, Eum WS, Bahn JH, Kim DW, Kang JH, Kwon HY, Kang TC, Choi SY, Won MH (2004) Ischemia-related change of ceruloplasmin immunoreactivity in neurons and astrocytes in the gerbil hippocampus and dentate gyrus. Neurochem Int 44:601-607.

Immenschuh S, Baumgart-Vogt E (2005) Peroxiredoxins, oxidative stress, and cell proliferation. Antioxid Redox Signal 7:768-777.

Irace C, Scorziello A, Maffettone C, Pignataro G, Matrone C, Adornetto A, Santamaria R, Annunziato L, Colonna A (2005) Divergent modulation of iron regulatory proteins and ferritin biosynthesis by hypoxia/reoxygenation in neurones and glial cells. J Neurochem 95:1321-1331.

Ivanov AI (2008) Pharmacological inhibition of endocytic pathways: is it specific enough to be useful? Methods Mol Biol 440:15-33.

Izawa T, Yamate J, Franklin RJ, Kuwamura M (2010) Abnormal iron accumulation is involved in the pathogenesis of the demyelinating dmy rat but not in the hypomyelinating mv rat. Brain Res 1349:105-114.

Jain TK, Reddy MK, Morales MA, Leslie-Pelecky DL, Labhasetwar V (2008) Biodistribution, clearance, and biocompatibility of iron oxide magnetic nanoparticles in rats. Mol Pharm 5:316-327.

Jakovcevski I, Filipovic R, Mo Z, Rakic S, Zecevic N (2009) Oligodendrocyte development and the onset of myelination in the human fetal brain. Front Neuroanat 3:5.

Jaquet V, Pfend G, Tosic M, Matthieu JM (1999) Analysis of cis-acting sequences from the myelin oligodendrocyte glycoprotein promoter. J Neurochem 73:120-128.

Jefferies WA, Brandon MR, Hunt SV, Williams AF, Gatter KC, Mason DY (1984) Transferrin receptor on endothelium of brain capillaries. Nature 312:162-163.

Jensen FB (2009) The dual roles of red blood cells in tissue oxygen delivery: oxygen carriers and regulators of local blood flow. J Exp Biol 212:3387-3393.

Jeong SY, David S (2003) Glycosylphosphatidylinositol-anchored ceruloplasmin is required for iron efflux from cells in the central nervous system. J Biol Chem 278:27144-27148.

Jezek P, Hlavata L (2005) Mitochondria in homeostasis of reactive oxygen species in cell, tissues, and organism. Int J Biochem Cell Biol 37:2478-2503.

Jiang DH, Ke Y, Cheng YZ, Ho KP, Qian ZM (2002) Distribution of ferroportin1 protein in different regions of developing rat brain. Dev Neurosci 24:94-98.

Jin AY, Tuor UI, Rushforth D, Filfil R, Kaur J, Ni F, Tomanek B, Barber PA (2009) Magnetic resonance molecular imaging of post-stroke neuroinflammation with a P-selectin targeted iron oxide nanoparticle. Contrast Media Mol Imaging 4:305-311.

Juurlink BH, Thorburne SK, Hertz L (1998) Peroxide-scavenging deficit underlies oligodendrocyte susceptibility to oxidative stress. Glia 22:371-378.

Kakhlon O, Cabantchik ZI (2002) The labile iron pool: characterization, measurement, and participation in cellular processes. Free Radic Biol Med 33:1037-1046.

Kameshwar-Rao AS, Gil S, Richter-Landsberg C, Givol D, Yavin E (1999) H_2O_2-induced apoptotic death in serum-deprived cultures of oligodendroglia origin is linked to cell differentiation. J Neurosci Res 56:447-456.

Kaur C, Ling EA (1995) Transient expression of transferrin receptors and localisation of iron in amoeboid microglia in postnatal rats. J Anat 186 (Pt 1):165-173.

Kaur C, Sivakumar V, Ling EA (2010) Melatonin protects periventricular white matter from damage due to hypoxia. J Pineal Res 48:185-193.

Kehrer JP (2000) The Haber-Weiss reaction and mechanisms of toxicity. Toxicology 149:43-50.

Kell DB (2009) Iron behaving badly: inappropriate iron chelation as a major contributor to the aetiology of vascular and other progressive inflammatory and degenerative diseases. BMC Med Genomics 2:2.

Kiessling F, Huppert J, Zhang C, Jayapaul J, Zwick S, Woenne EC, Mueller MM, Zentgraf H, Eisenhut M, Addadi Y, Neeman M, Semmler W (2009) RGD-labeled USPIO inhibits adhesion and endocytotic activity of $\alpha_v\beta_3$-integrin-expressing glioma cells and only accumulates in the vascular tumor compartment. Radiology 253:462-469.

Kim JS, Yoon TJ, Yu KN, Noh MS, Woo M, Kim BG, Lee KH, Sohn BH, Park SB, Lee JK, Cho MH (2006) Cellular uptake of magnetic nanoparticle is mediated through energy-dependent endocytosis in A549 cells. J Vet Sci 7:321-326.

Kim M, Song E (2010) Iron transport by proteoliposomes containing mitochondrial F_1F_0 ATP synthase isolated from rat heart. Biochimie 92:333-342.

Kimelberg HK (2010) Functions of mature mammalian astrocytes: a current view. Neuroscientist 16:79-106.

Kircher MF, Mahmood U, King RS, Weissleder R, Josephson L (2003) A multimodal nanoparticle for preoperative magnetic resonance imaging and intraoperative optical brain tumor delineation. Cancer Res 63:8122-8125.

Klomp LW, Farhangrazi ZS, Dugan LL, Gitlin JD (1996) Ceruloplasmin gene expression in the murine central nervous system. J Clin Invest 98:207-215.

Knutson MD (2010) Iron-sensing proteins that regulate hepcidin and enteric iron absorption. Annu Rev Nutr 30:149-171.

Koehler RC, Roman RJ, Harder DR (2009) Astrocytes and the regulation of cerebral blood flow. Trends Neurosci 32:160-169.

Kragh CL, Lund LB, Febbraro F, Hansen HD, Gai WP, El-Agnaf O, Richter-Landsberg C, Jensen PH (2009) α-Synuclein aggregation and ser-129 phosphorylation-dependent cell death in oligodendroglial cells. J Biol Chem 284:10211-10222.

Kroll A, Pillukat MH, Hahn D, Schnekenburger J (2009) Current *in vitro* methods in nanoparticle risk assessment: limitations and challenges. Eur J Pharm Biopharm 72:370-377.

Krueger M, Bechmann I (2010) CNS pericytes: concepts, misconceptions, and a way out. Glia 58:1-10.

Ku S, Yan F, Wang Y, Sun Y, Yang N, Ye L (2010) The blood-brain barrier penetration and distribution of PEGylated fluorescein-doped magnetic silica nanoparticles in rat brain. Biochem Biophys Res Commun 394:871-876.

Kumar M, Medarova Z, Pantazopoulos P, Dai G, Moore A (2010) Novel membrane-permeable contrast agent for brain tumor detection by MRI. Magn Reson Med 63:617-624.

Kunzmann A, Andersson B, Thurnherr T, Krug H, Scheynius A, Fadeel B (2011) Toxicology of engineered nanomaterials: focus on biocompatibility, biodistribution and biodegradation. Biochim Biophys Acta 1810:361-373.

Kwik-Uribe CL, Gietzen D, German JB, Golub MS, Keen CL (2000) Chronic marginal iron intakes during early development in mice result in persistent changes in dopamine metabolism and myelin composition. J Nutr 130:2821-2830.

Lane DJ, Lawen A (2009) Ascorbate and plasma membrane electron transport-enzymes vs efflux. Free Radic Biol Med 47:485-495.

Lane DJ, Robinson SR, Czerwinska H, Bishop GM, Lawen A (2010) Two routes of iron accumulation in astrocytes: ascorbate-dependent ferrous iron uptake via the divalent metal transporter (DMT1) plus an independent route for ferric iron. Biochem J 432:123-132.

Lange SJ, Que L, Jr. (1998) Oxygen activating nonheme iron enzymes. Curr Opin Chem Biol 2:159-172.

Langer AK, Poon HF, Munch G, Lynn BC, Arendt T, Butterfield DA (2006) Identification of AGE-modified proteins in SH-SY5Y and OLN-93 cells. Neurotox Res 9:255-268.

Laurent S, Forge D, Port M, Roch A, Robic C, Vander Elst L, Muller RN (2008) Magnetic iron oxide nanoparticles: synthesis, stabilization, vectorization, physicochemical characterizations, and biological applications. Chem Rev 108:2064-2110.

LaVaute T, Smith S, Cooperman S, Iwai K, Land W, Meyron-Holtz E, Drake SK, Miller G, Abu-Asab M, Tsokos M, Switzer R, 3rd, Grinberg A, Love P, Tresser N, Rouault TA (2001) Targeted deletion of the gene encoding iron regulatory protein-2 causes

misregulation of iron metabolism and neurodegenerative disease in mice. Nat Genet 27:209-214.

Lawson DM, Treffry A, Artymiuk PJ, Harrison PM, Yewdall SJ, Luzzago A, Cesareni G, Levi S, Arosio P (1989) Identification of the ferroxidase centre in ferritin. FEBS Lett 254:207-210.

Lederman HM, Cohen A, Lee JW, Freedman MH, Gelfand EW (1984) Deferoxamine: a reversible S-phase inhibitor of human lymphocyte proliferation. Blood 64:748-753.

Lee PL, Beutler E (2009) Regulation of hepcidin and iron-overload disease. Annu Rev Pathol 4:489-515.

Lee DW, Andersen JK (2010) Iron elevations in the aging parkinsonian brain: a consequence of impaired iron homeostasis? J Neurochem 112:332-339.

Lee HS, Han J, Bai HJ, Kim KW (2009) Brain angiogenesis in developmental and pathological processes: regulation, molecular and cellular communication at the neurovascular interface. FEBS J 276:4622-4635.

Leibold EA, Gahring LC, Rogers SW (2001) Immunolocalization of iron regulatory protein expression in the murine central nervous system. Histochem Cell Biol 115:195-203.

Levi S, Cozzi A, Arosio P (2005) Neuroferritinopathy: a neurodegenerative disorder associated with L-ferritin mutation. Best Pract Res Clin Haematol 18:265-276.

Levin MJ, Tuil D, Uzan G, Dreyfus JC, Kahn A (1984) Expression of the transferrin gene during development of non-hepatic tissues: high level of transferrin mRNA in fetal muscle and adult brain. Biochem Biophys Res Commun 122:212-217.

Levine SM, Chakrabarty A (2004) The role of iron in the pathogenesis of experimental allergic encephalomyelitis and multiple sclerosis. Ann NY Acad Sci 1012:252-266.

Levy M, Lagarde F, Maraloiu VA, Blanchin MG, Gendron F, Wilhelm C, Gazeau F (2010) Degradability of superparamagnetic nanoparticles in a model of intracellular environment: follow-up of magnetic, structural and chemical properties. Nanotechnology 21:395103-395114.

Lewinski N, Colvin V, Drezek R (2008) Cytotoxicity of nanoparticles. Small 4:26-49.

Li W, Zhang B, Tang J, Cao Q, Wu Y, Wu C, Guo J, Ling EA, Liang F (2007) Sirtuin 2, a mammalian homolog of yeast silent information regulator-2 longevity regulator, is an

oligodendroglial protein that decelerates cell differentiation through deacetylating α-tubulin. J Neurosci 27:2606-2616.

Lieu PT, Heiskala M, Peterson PA, Yang Y (2001) The roles of iron in health and disease. Mol Aspects Med 22:1-87.

Limon-Pacheco J, Gonsebatt ME (2009) The role of antioxidants and antioxidant-related enzymes in protective responses to environmentally induced oxidative stress. Mutat Res 674:137-147.

Lin HH, Connor JR (1989) The development of the transferrin-transferrin receptor system in relation to astrocytes, MBP and galactocerebroside in normal and myelin-deficient rat optic nerves. Brain Res Dev Brain Res 49:281-293.

Luciani N, Wilhelm C, Gazeau F (2010) The role of cell-released microvesicles in the intercellular transfer of magnetic nanoparticles in the monocyte/macrophage system. Biomaterials 31:7061-7069.

Lunov O, Zablotskii V, Syrovets T, Rocker C, Tron K, Nienhaus GU, Simmet T (2011) Modeling receptor-mediated endocytosis of polymer-functionalized iron oxide nanoparticles by human macrophages. Biomaterials 32:547-555.

Lushchak VI (2011) Adaptive response to oxidative stress: bacteria, fungi, plants and animals. Comp Biochem Physiol C Toxicol Pharmacol 153:175-190.

Mackenzie B, Garrick MD (2005) Iron Imports. II. Iron uptake at the apical membrane in the intestine. Am J Physiol Gastrointest Liver Physiol 289:981-986.

Magistretti PJ (2006) Neuron-glia metabolic coupling and plasticity. J Exp Biol 209:2304-2311.

Maier O, van der Heide T, Johnson R, de Vries H, Baron W, Hoekstra D (2006) The function of neurofascin155 in oligodendrocytes is regulated by metalloprotease-mediated cleavage and ectodomain shedding. Exp Cell Res 312:500-511.

Malarkey EB, Parpura V (2010) Carbon nanotubes in neuroscience. Acta Neurochir Suppl 106:337-341.

Mandel S, Amit T, Bar-Am O, Youdim MB (2007) Iron dysregulation in Alzheimer's disease: multimodal brain permeable iron chelating drugs, possessing neuroprotective-neurorescue and amyloid precursor protein-processing regulatory activities as therapeutic agents. Prog Neurobiol 82:348-360.

Mar S, Noetzel M (2010) Axonal damage in leukodystrophies. Pediatr Neurol 42:239-242.

Marquis BJ, Love SA, Braun KL, Haynes CL (2009) Analytical methods to assess nanoparticle toxicity. Analyst 134:425-439.

McKie AT, Marciani P, Rolfs A, Brennan K, Wehr K, Barrow D, Miret S, Bomford A, Peters TJ, Farzaneh F, Hediger MA, Hentze MW, Simpson RJ (2000) A novel duodenal iron-regulated transporter, IREG1, implicated in the basolateral transfer of iron to the circulation. Mol Cell 5:299-309.

McTigue DM, Tripathi RB (2008) The life, death, and replacement of oligodendrocytes in the adult CNS. J Neurochem 107:1-19.

Meng J, Xia W, Tang J, Tang BL, Liang F (2010) Dephosphorylation-dependent inhibitory activity of juxtanodin on filamentous actin disassembly. J Biol Chem 285:28838-28849.

Mey J, Hammelmann S (2000) OLN-93 oligodendrocytes synthesize all-trans-retinoic acid *in vitro*. Cell Tissue Res 302:49-58.

Mey J, Henkes L (2002) Retinoic acid enhances leukemia inhibitory factor expression in OLN-93 oligodendrocytes. Cell Tissue Res 310:155-161.

Mills E, Dong XP, Wang F, Xu H (2010) Mechanisms of brain iron transport: insight into neurodegeneration and CNS disorders. Future Med Chem 2:51-73.

Miron VE, Kuhlmann T, Antel JP (2011) Cells of the oligodendroglial lineage, myelination, and remyelination. Biochim Biophys Acta 1812:184-193.

Mollgard K, Stagaard M, Saunders NR (1987) Cellular distribution of transferrin immunoreactivity in the developing rat brain. Neurosci Lett 78:35-40.

Mollgard K, Dziegielewska KM, Saunders NR, Zakut H, Soreq H (1988) Synthesis and localization of plasma proteins in the developing human brain. integrity of the fetal blood-brain barrier to endogenous proteins of hepatic origin. Dev Biol 128:207-221.

Moos T (1996) Immunohistochemical localization of intraneuronal transferrin receptor immunoreactivity in the adult mouse central nervous system. J Comp Neurol 375:675-692.

Moos T, Morgan EH (1998) Evidence for low molecular weight, non-transferrin-bound iron in rat brain and cerebrospinal fluid. J Neurosci Res 54:486-494.

Moos T, Morgan EH (2000) Transferrin and transferrin receptor function in brain barrier systems. Cell Mol Neurobiol 20:77-95.

Moos T, Trinder D, Morgan EH (2000) Cellular distribution of ferric iron, ferritin, transferrin and divalent metal transporter 1 (DMT1) in substantia nigra and basal ganglia of normal and β2-microglobulin deficient mouse brain. Cell Mol Biol (Noisy-le-grand) 46:549-561.

Moos T, Morgan EH (2004) The significance of the mutated divalent metal transporter (DMT1) on iron transport into the Belgrade rat brain. J Neurochem 88:233-245.

Moos T, Rosengren Nielsen T (2006) Ferroportin in the postnatal rat brain: implications for axonal transport and neuronal export of iron. Semin Pediatr Neurol 13:149-157.

Moos T, Rosengren Nielsen T, Skjorringe T, Morgan EH (2007) Iron trafficking inside the brain. J Neurochem 103:1730-1740.

Munoz M, Villar I, Garcia-Erce JA (2009) An update on iron physiology. World J Gastroenterol 15:4617-4626.

Nakahara J, Aiso S, Suzuki N (2010) Autoimmune versus oligodendrogliopathy: the pathogenesis of multiple sclerosis. Arch Immunol Ther Exp 58:325-333.

Nave KA (2010) Myelination and support of axonal integrity by glia. Nature 468:244-252.

Nave KA, Trapp BD (2008) Axon-glial signaling and the glial support of axon function. Annu Rev Neurosci 31:535-561.

Nel A, Xia T, Mädler L, Li N (2006) Toxic potential of materials at the nanolevel. Science 311:622-627.

Nguyen D, Höpfner M, Zobel F, Henke U, Scherubl H, Stangel M (2003) Rat oligodendroglial cell lines express a functional receptor for the chemokine CCL3 (macrophage inflammatory protein-1alpha). Neurosci Lett 351:71-74.

Nie DY, Ma QH, Law JW, Chia CP, Dhingra NK, Shimoda Y, Yang WL, Gong N, Chen QW, Xu G, Hu QD, Chow PK, Ng YK, Ling EA, Watanabe K, Xu TL, Habib AA, Schachner M, Xiao ZC (2006) Oligodendrocytes regulate formation of nodes of Ranvier via the recognition molecule OMgp. Neuron Glia Biol 2:151-164.

Niggel J, Sigurdson W, Sachs F (2000) Mechanically induced calcium movements in astrocytes, bovine aortic endothelial cells and C6 glioma cells. J Membr Biol 174:121-134.

Niki E (2009) Lipid peroxidation: physiological levels and dual biological effects. Free Radic Biol Med 47:469-484.

Nivière V, Fontecave M (2004) Discovery of superoxide reductase: an historical perspective. J Biol Inorg Chem 9:119-123.

Nordberg J, Arner ES (2001) Reactive oxygen species, antioxidants, and the mammalian thioredoxin system. Free Radic Biol Med 31:1287-1312.

Nyholm S, Mann GJ, Johansson AG, Bergeron RJ, Graslund A, Thelander L (1993) Role of ribonucleotide reductase in inhibition of mammalian cell growth by potent iron chelators. J Biol Chem 268:26200-26205.

O'Neil J, Powell L (2005) Clinical aspects of hemochromatosis. Semin Liver Dis 25:381-391.

Obara M, Szeliga M, Albrecht J (2008) Regulation of pH in the mammalian central nervous system under normal and pathological conditions: facts and hypotheses. Neurochem Int 52:905-919.

Oberdörster G (2010) Safety assessment for nanotechnology and nanomedicine: concepts of nanotoxicology. J Intern Med 267:89-105.

Oh TH, Markelonis GJ, Royal GM, Bregman BS (1986) Immunocytochemical distribution of transferrin and its receptor in the developing chicken nervous system. Brain Res 395:207-220.

Ortiz E, Pasquini JM, Thompson K, Felt B, Butkus G, Beard J, Connor JR (2004) Effect of manipulation of iron storage, transport, or availability on myelin composition and brain iron content in three different animal models. J Neurosci Res 77:681-689.

Ortiz EH, Pasquini LA, Soto EF, Pasquini JM (2005) Apotransferrin and the cytoskeleton of oligodendroglial cells. J Neurosci Res 82:822-830.

Oshiro S, Nozawa K, Cai Y, Hori M, Kitajima S (1998) Characterization of a transferrin-independent iron uptake system in rat primary cultured cortical cells. J Med Dent Sci 45:171-176.

Pantopoulos K (2004) Iron metabolism and the IRE/IRP regulatory system: an update. Ann NY Acad Sci 1012:1-13.

Parpura V, Zorec R (2010) Gliotransmission: exocytotic release from astrocytes. Brain Res Rev 63:83-92.

Patel BN, David S (1997) A novel glycosylphosphatidylinositol-anchored form of ceruloplasmin is expressed by mammalian astrocytes. J Biol Chem 272:20185-20190.

Patel BN, Dunn RJ, David S (2000) Alternative RNA splicing generates a glycosylphosphatidylinositol-anchored form of ceruloplasmin in mammalian brain. J Biol Chem 275:4305-4310.

Pathak S, Cao E, Davidson MC, Jin S, Silva GA (2006) Quantum dot applications to neuroscience: new tools for probing neurons and glia. J Neurosci 26:1893-1895.

Pawelczyk E, Arbab AS, Pandit S, Hu E, Frank JA (2006) Expression of transferrin receptor and ferritin following ferumoxides-protamine sulfate labeling of cells: implications for cellular magnetic resonance imaging. NMR Biomed 19:581-592.

Petrak J, Vyoral D (2005) Hephaestin-a ferroxidase of cellular iron export. Int J Biochem Cell Biol 37:1173-1178.

Petrat F, de Groot H, Sustmann R, Rauen U (2002) The chelatable iron pool in living cells: a methodically defined quantity. Biol Chem 383:489-502.

Pfrieger FW (2010) Role of glial cells in the formation and maintenance of synapses. Brain Res Rev 63:39-46.

Piaton G, Gould RM, Lubetzki C (2010) Axon-oligodendrocyte interactions during developmental myelination, demyelination and repair. J Neurochem 114:1243-1260.

Pickard MR, Jenkins SI, Koller CJ, Furness DN, Chari DM (2010) Magnetic nanoparticle labeling of astrocytes derived for neural transplantation. Tissue Eng Part C Methods 17:89-99.

Piñero DJ, Connor JR (2000) Iron in the brain: an important contributor in normal and diseased states. Neuroscientist 6:435-453.

Pisanic TR, 2nd, Blackwell JD, Shubayev VI, Finones RR, Jin S (2007) Nanotoxicity of iron oxide nanoparticle internalization in growing neurons. Biomaterials 28:2572-2581.

Plumb J, Duprex WP, Cameron CH, Richter-Landsberg C, Talbot P, McQuaid S (2002) Infection of human oligodendroglioma cells by a recombinant measles virus expressing enhanced green fluorescent protein. J Neurovirol 8:24-34.

Ponka P, Lok CN (1999) The transferrin receptor: role in health and disease. Int J Biochem Cell Biol 31:1111-1137.

Qi Y, Dawson G (1994) Hypoxia specifically and reversibly induces the synthesis of ferritin in oligodendrocytes and human oligodendrogliomas. J Neurochem 63:1485-1490.

Qian ZM, To Y, Tang PL, Feng YM (1999) Transferrin receptors on the plasma membrane of cultured rat astrocytes. Exp Brain Res 129:473-476.

Qian Z, Liao Q, To Y, Ke Y, Tsoi Y, Wang G, Ho K (2000) Transferrin-bound and transferrin free iron uptake by cultured rat astrocytes. Cell Mol Biol (Noisy-le-Grand) 46:541-548.

Qian ZM, Chang YZ, Zhu L, Yang L, Du JR, Ho KP, Wang Q, Li LZ, Wang CY, Ge X, Jing NL, Li L, Ke Y (2007) Development and iron-dependent expression of hephaestin in different brain regions of rats. J Cell Biochem 102:1225-1233.

Qutub AA, Hunt CA (2005) Glucose transport to the brain: a systems model. Brain Res Brain Res Rev 49:595-617.

Raschzok N, Muecke DA, Adonopoulou MK, Billecke N, Werner W, Kammer NN, Zielinski A, Behringer PA, Ringel F, Huang MD, Neuhaus P, Teichgraber U, Sauer IM (2010) *In vitro* evaluation of magnetic resonance imaging contrast agents for labeling human liver cells: implications for clinical translation. Mol Imaging Biol in press.

Regan RF, Kumar N, Gao F, Guo Y (2002) Ferritin induction protects cortical astrocytes from heme-mediated oxidative injury. Neuroscience 113:985-994.

Regan RF, Li Z, Chen M, Zhang X, Chen-Roetling J (2008) Iron regulatory proteins increase neuronal vulnerability to hydrogen peroxide. Biochem Biophys Res Commun 375:6-10.

Rhee SG, Chae HZ, Kim K (2005) Peroxiredoxins: a historical overview and speculative preview of novel mechanisms and emerging concepts in cell signaling. Free Radic Biol Med 38:1543-1552.

Richardson DR (2001) Iron and gallium increase iron uptake from transferrin by human melanoma cells: further examination of the ferric ammonium citrate-activated iron uptake process. Biochim Biophys Acta 1536:43-54.

Richardson DR, Lane DJ, Becker EM, Huang ML, Whitnall M, Rahmanto YS, Sheftel AD, Ponka P (2010) Mitochondrial iron trafficking and the integration of iron metabolism between the mitochondrion and cytosol. Proc Natl Acad Sci USA 107:10775-10782.

Richter-Landsberg C, Heinrich M (1996) OLN-93: a new permanent oligodendroglia cell line derived from primary rat brain glial cultures. J Neurosci Res 45:161-173.

Riedel M, Goldbaum O, Richter-Landsberg C (2009) α-Synuclein promotes the recruitment of tau to protein inclusions in oligodendroglial cells: effects of oxidative and proteolytic stress. J Mol Neurosci 39:226-234.

Riedel M, Goldbaum O, Schwarz L, Schmitt S, Richter-Landsberg C (2010) 17-AAG induces cytoplasmic α-synuclein aggregate clearance by induction of autophagy. PLoS One 5:e8753.

Riedel M, Goldbaum O, Wille M, Richter-Landsberg C (2011) Membrane lipid modification by docosahexaenoic acid (DHA) promotes the formation of α-synuclein inclusion bodies immunopositive for SUMO-1 in oligodendroglial cells after oxidative stress. J Mol Neurosci 43:290-302.

Robitzki A, Doll F, Richter-Landsberg C, Layer PG (2000) Regulation of the rat oligodendroglia cell line OLN-93 by antisense transfection of butyrylcholinesterase. Glia 31:195-205.

Roth JA, Horbinski C, Feng L, Dolan KG, Higgins D, Garrick MD (2000) Differential localization of divalent metal transporter 1 with and without iron response element in rat PC12 and sympathetic neuronal cells. J Neurosci 20:7595-7601.

Rothenberger S, Food MR, Gabathuler R, Kennard ML, Yamada T, Yasuhara O, McGeer PL, Jefferies WA (1996) Coincident expression and distribution of melanotransferrin and transferrin receptor in human brain capillary endothelium. Brain Res 712:117-121.

Rouault TA (2006) The role of iron regulatory proteins in mammalian iron homeostasis and disease. Nat Chem Biol 2:406-414.

Rouault TA, Cooperman S (2006) Brain iron metabolism. Semin Pediatr Neurol 13:142-148.

Rouault TA, Tong WH (2008) Iron-sulfur cluster biogenesis and human disease. Trends Genet 24:398-407.

Salvador GA (2010) Iron in neuronal function and dysfunction. BioFactors 36:103-110.

Santambrogio P, Biasiotto G, Sanvito F, Olivieri S, Arosio P, Levi S (2007) Mitochondrial ferritin expression in adult mouse tissues. J Histochem Cytochem 55:1129-1137.

Sayre LM, Moreira PI, Smith MA, Perry G (2005) Metal ions and oxidative protein modification in neurological disease. Ann Ist Super Sanità 41:143-164.

Schäfer R, Kehlbach R, Wiskirchen J, Bantleon R, Pintaske J, Brehm BR, Gerber A, Wolburg H, Claussen CD, Northoff H (2007) Transferrin receptor upregulation: *in vitro* labeling of rat mesenchymal stem cells with superparamagnetic iron oxide. Radiology 244:514-523.

Schulz-Schaeffer WJ (2010) The synaptic pathology of α-synuclein aggregation in dementia with Lewy bodies, Parkinson's disease and Parkinson's disease dementia. Acta Neuropathol 120:131-143.

Silva GA (2006) Neuroscience nanotechnology: progress, opportunities and challenges. Nat Rev Neurosci 7:65-74.

Singh S (2010) Nanomedicine-nanoscale drugs and delivery systems. J Nanosci Nanotechnol 10:7906-7918.

Singh S, Nalwa HS (2007) Nanotechnology and health safety-toxicity and risk assessments of nanostructured materials on human health. J Nanosci Nanotechnol 7:3048-3070.

Singh AV, Zamboni P (2009) Anomalous venous blood flow and iron deposition in multiple sclerosis. J Cereb Blood Flow Metab 29:1867-1878.

Smith SR, Cooperman S, Lavaute T, Tresser N, Ghosh M, Meyron-Holtz E, Land W, Ollivierre H, Jortner B, Switzer R, 3rd, Messing A, Rouault TA (2004) Severity of neurodegeneration correlates with compromise of iron metabolism in mice with iron regulatory protein deficiencies. Ann NY Acad Sci 1012:65-83.

Smolders I, Smets I, Maier O, vandeVen M, Steels P, Ameloot M (2010) Simvastatin interferes with process outgrowth and branching of oligodendrocytes. J Neurosci Res 88:3361-3375.

Snyder AM, Connor JR (2009) Iron, the substantia nigra and related neurological disorders. Biochim Biophys Acta 1790:606-614.

Soenen SJ, De Cuyper M (2009) Assessing cytotoxicity of (iron oxide-based) nanoparticles: an overview of different methods exemplified with cationic magnetoliposomes. Contrast Media Mol Imaging 4:207-219.

Soenen SJ, De Cuyper M (2010) Assessing iron oxide nanoparticle toxicity *in vitro*: current status and future prospects. Nanomedicine (Lond) 5:1261-1275.

Soenen SJ, Himmelreich U, Nuytten N, Pisanic TR, 2nd, Ferrari A, De Cuyper M (2010) Intracellular nanoparticle coating stability determines nanoparticle diagnostics efficacy and cell functionality. Small 6:2136-2145.

Soenen SJ, Brisson AR, Jonckheere E, Nuytten N, Tan S, Himmelreich U, De Cuyper M (2011) The labeling of cationic iron oxide nanoparticle-resistant hepatocellular carcinoma cells using targeted magnetoliposomes. Biomaterials 32:1748-1758.

Sofroniew MV, Vinters HV (2010) Astrocytes: biology and pathology. Acta Neuropathol 119:7-35.

Song N, Jiang H, Wang J, Xie JX (2007) Divalent metal transporter 1 up-regulation is involved in the 6-hydroxydopamine-induced ferrous iron influx. J Neurosci Res 85:3118-3126.

Song N, Wang J, Jiang H, Xie J (2010) Ferroportin 1 but not hephaestin contributes to iron accumulation in a cell model of Parkinson's disease. Free Radic Biol Med 48:332-341.

Sonnewald U, Westergaard N, Krane J, Unsgard G, Petersen SB, Schousboe A (1991) First direct demonstration of preferential release of citrate from astrocytes using [^{13}C]NMR spectroscopy of cultured neurons and astrocytes. Neurosci Lett 128:235-239.

Srinivasan V, Pandi-Perumal SR, Maestroni GJ, Esquifino AI, Hardeland R, Cardinali DP (2005) Role of melatonin in neurodegenerative diseases. Neurotox Res 7:293-318.

Stahnke T, Stadelmann C, Netzler A, Bruck W, Richter-Landsberg C (2007) Differential upregulation of heme oxygenase-1 (HSP32) in glial cells after oxidative stress and in demyelinating disorders. J Mol Neurosci 32:25-37.

Stankiewicz JM, Brass SD (2009) Role of iron in neurotoxicity: a cause for concern in the elderly? Curr Opin Clin Nutr Metab Care 12:22-29.

Stark S, Schüller A, Sifringer M, Gerstner B, Brehmer F, Weber S, Altmann R, Obladen M, Bührer C, Felderhoff-Mueser U (2008) Suramin induces and enhances apoptosis in a model of hyperoxia-induced oligodendrocyte injury. Neurotox Res 13:197-207.

Steiner J, Bernstein HG, Bogerts B, Gos T, Richter-Landsberg C, Wunderlich MT, Keilhoff G (2008) S100B is expressed in, and released from, OLN-93 oligodendrocytes: influence of serum and glucose deprivation. Neuroscience 154:496-503.

Steiner J, Schroeter ML, Schiltz K, Bernstein HG, Müller UJ, Richter-Landsberg C, Müller WE, Walter M, Gos T, Bogerts B, Keilhoff G (2010) Haloperidol and clozapine decrease S100B release from glial cells. Neuroscience 167:1025-1031.

Steiner J, Sarnyai Z, Westphal S, Gos T, Bernstein HG, Bogerts B, Keilhoff G (2011) Protective effects of haloperidol and clozapine on energy-deprived OLN-93 oligodendrocytes. Eur Arch Psychiatry Clin Neurosci in press.

Stiles J, Jernigan TL (2010) The basics of brain development. Neuropsychol Rev 20:327-348.

Strelau J, Unsicker K (1999) GDNF family members and their receptors: expression and functions in two oligodendroglial cell lines representing distinct stages of oligodendroglial development. Glia 26:291-301.

Stubbe J (1998) Ribonucleotide reductases in the twenty-first century. Proc Natl Acad Sci USA 95:2723-2724.

Stubbe J, van der Donk WA (1998) Protein radicals in enzyme catalysis. Chem Rev 98:705-762.

Suh WH, Suslick KS, Stucky GD, Suh YH (2009) Nanotechnology, nanotoxicology, and neuroscience. Prog Neurobiol 87:133-170.

Sultana R, Butterfield DA (2010) Role of oxidative stress in the progression of Alzheimer's disease. J Alzheimers Dis 19:341-353.

Swaiman KF, Machen VL (1985) Iron uptake by glial cells. Neurochem Res 10:1635-1644.

Swaiman KF, Machen VL (1986) Transferrin binding by mammalian cortical cells. Neurochem Res 11:1241-1248.

Tabuchi M, Yoshimori T, Yamaguchi K, Yoshida T, Kishi F (2000) Human NRAMP2/DMT1, which mediates iron transport across endosomal membranes, is localized to late endosomes and lysosomes in HEp-2 cells. J Biol Chem 275:22220-22228.

Takeda A, Devenyi A, Connor JR (1998) Evidence for non-transferrin-mediated uptake and release of iron and manganese in glial cell cultures from hypotransferrinemic mice. J Neurosci Res 51:454-462.

Thelander L, Graslund A, Thelander M (1983) Continual presence of oxygen and iron required for mammalian ribonucleotide reduction: possible regulation mechanism. Biochem Biophys Res Commun 110:859-865.

Thiessen A, Schmidt MM, Dringen R (2010) Fumaric acid dialkyl esters deprive cultured rat oligodendroglial cells of glutathione and upregulate the expression of heme oxygenase 1. Neurosci Lett 475:56-60.

Thorburne SK, Juurlink BH (1996) Low glutathione and high iron govern the susceptibility of oligodendroglial precursors to oxidative stress. J Neurochem 67:1014-1022.

Thorek DL, Tsourkas A (2008) Size, charge and concentration dependent uptake of iron oxide particles by non-phagocytic cells. Biomaterials 29:3583-3590.

Tiffany-Castiglioni E, Qian Y (2001) Astroglia as metal depots: molecular mechanisms for metal accumulation, storage and release. Neurotoxicology 22:577-592.

Todorich B, Zhang X, Slagle-Webb B, Seaman WE, Connor JR (2008) Tim-2 is the receptor for H-ferritin on oligodendrocytes. J Neurochem 107:1495-1505.

Todorich B, Pasquini JM, Garcia CI, Paez PM, Connor JR (2009) Oligodendrocytes and myelination: the role of iron. Glia 57:467-478.

Todorich B, Zhang X, Connor JR (2011) H-ferritin is the major source of iron for oligodendrocytes. Glia 59:927-935.

Trapp BD, Nave KA (2008) Multiple sclerosis: an immune or neurodegenerative disorder? Annu Rev Neurosci 31:247-269.

Trinder D, Morgan E (1998) Mechanisms of ferric citrate uptake by human hepatoma cells. Am J Physiol 275:279-286.

Tulpule K, Robinson SR, Bishop GM, Dringen R (2010) Uptake of ferrous iron by cultured rat astrocytes. J Neurosci Res 88:563-571.

Uberti D, Yavin E, Gil S, Ayasola KR, Goldfinger N, Rotter V (1999) Hydrogen peroxide induces nuclear translocation of p53 and apoptosis in cells of oligodendroglia origin. Brain Res Mol Brain Res 65:167-175.

Valerio LG (2007) Mammalian iron metabolism. Toxicol Mech Methods 17:497-517.

Valko M, Izakovic M, Mazur M, Rhodes CJ, Telser J (2004) Role of oxygen radicals in DNA damage and cancer incidence. Mol Cell Biochem 266:37-56.

Van Meeteren ME, Hendriks JJ, Dijkstra CD, van Tol EA (2004) Dietary compounds prevent oxidative damage and nitric oxide production by cells involved in demyelinating disease. Biochem Pharmacol 67:967-975.

Van Meeteren ME, Koetsier MA, Dijkstra CD, van Tol EA (2005) Markers for OLN-93 oligodendroglia differentiation. Brain Res Dev Brain Res 156:78-86.

Van Meeteren ME, Baron W, Beermann C, Dijkstra CD, van Tol EA (2006) Polyunsaturated fatty acid supplementation stimulates differentiation of oligodendroglia cells. Dev Neurosci 28:196-208.

Vargas JD, Herpers B, McKie AT, Gledhill S, McDonnell J, van den Heuvel M, Davies KE, Ponting CP (2003) Stromal cell-derived receptor 2 and cytochrome b561 are functional ferric reductases. Biochim Biophys Acta 1651:116-123.

Veiseh O, Sun C, Fang C, Bhattarai N, Gunn J, Kievit F, Du K, Pullar B, Lee D, Ellenbogen RG, Olson J, Zhang M (2009) Specific targeting of brain tumors with an optical/magnetic resonance imaging nanoprobe across the blood-brain barrier. Cancer Res 69:6200-6207.

Veiseh O, Kievit FM, Fang C, Mu N, Jana S, Leung MC, Mok H, Ellenbogen RG, Park JO, Zhang M (2010) Chlorotoxin bound magnetic nanovector tailored for cancer cell targeting, imaging, and siRNA delivery. Biomaterials 31:8032-8042.

Verkhratsky A, Butt A (2007) Glial Neurobiology. Chichester, UK: John Wiley & Sons Ltd.

Wang XS, Ong WY, Connor JR (2001) A light and electron microscopic study of the iron transporter protein DMT-1 in the monkey cerebral neocortex and hippocampus. J Neurocytol 30:353-360.

Wang Y, Richter-Landsberg C, Reiser G (2004) Expression of protease-activated receptors (PARs) in OLN-93 oligodendroglial cells and mechanism of PAR-1-induced calcium signaling. Neuroscience 126:69-82.

Wang J, Jiang H, Xie JX (2007) Ferroportin1 and hephaestin are involved in the nigral iron accumulation of 6-OHDA-lesioned rats. Eur J Neurosci 25:2766-2772.

Wang J, Chen Y, Chen B, Ding J, Xia G, Gao C, Cheng J, Jin N, Zhou Y, Li X, Tang M, Wang XM (2010) Pharmacokinetic parameters and tissue distribution of magnetic Fe_3O_4 nanoparticles in mice. Int J Nanomedicine 5:861-866.

Wejksza K, Rzeski W, Okuno E, Kandefer-Szerszen M, Albrecht J, Turski WA (2005) Demonstration of kynurenine aminotransferases I and II and characterization of kynurenic acid synthesis in oligodendrocyte cell line (OLN-93). Neurochem Res 30:963-968.

Wejksza K, Rzeski W, Turski WA, Hilgier W, Dybel A, Albrecht J (2006) Ammonia at pathophysiologically relevant concentrations activates kynurenic acid synthesis in cultured astrocytes and neurons. Neurotoxicology 27:619-622.

Wu LJ, Leenders AG, Cooperman S, Meyron-Holtz E, Smith S, Land W, Tsai RY, Berger UV, Sheng ZH, Rouault TA (2004) Expression of the iron transporter ferroportin in synaptic vesicles and the blood-brain barrier. Brain Res 1001:108-117.

Wu LL, Zhang L, Shao J, Qin YF, Yang RW, Zhao ZY (2008) Effect of perinatal iron deficiency on myelination and associated behaviors in rat pups. Behav Brain Res 188:263-270.

Xie J, Wang J, Niu G, Huang J, Chen K, Li X, Chen X (2010) Human serum albumin coated iron oxide nanoparticles for efficient cell labeling. Chem Commun 46:433-435.

Xie H, Zhu Y, Jiang W, Zhou Q, Yang H, Gu N, Zhang Y, Xu H, Yang X (2011) Lactoferrin-conjugated superparamagnetic iron oxide nanoparticles as a specific MRI contrast agent for detection of brain glioma *in vivo*. Biomaterials 32:495-502.

Xu X, Pin S, Gathinji M, Fuchs R, Harris ZL (2004) Aceruloplasminemia: an inherited neurodegenerative disease with impairment of iron homeostasis. Ann NY Acad Sci 1012:299-305.

Yang H (2010) Nanoparticle-mediated brain-specific drug delivery, imaging, and diagnosis. Pharm Res 27:1759-1771.

Yang WM, Jung KJ, Lee MO, Lee YS, Lee YH, Nakagawa S, Niwa M, Cho SS, Kim DW (2011a) Transient expression of iron transport proteins in the capillary of the developing rat brain. Cell Mol Neurobiol 31:93-99.

Yang X, Hong H, Grailer JJ, Rowland IJ, Javadi A, Hurley SA, Xiao Y, Yang Y, Zhang Y, Nickles RJ, Cai W, Steeber DA, Gong S (2011b) cRGD-functionalized, DOX-conjugated, and ^{64}Cu-labeled superparamagnetic iron oxide nanoparticles for targeted anticancer drug delivery and PET/MR imaging. Biomaterials 32:4151-4160.

Yodoya E, Wada M, Shimada A, Katsukawa H, Okada N, Yamamoto A, Ganapathy V, Fujita T (2006) Functional and molecular identification of sodium-coupled dicarboxylate transporters in rat primary cultured cerebrocortical astrocytes and neurons. J Neurochem 97:162-173.

Yokel RA (2006) Blood-brain barrier flux of aluminum, manganese, iron and other metals suspected to contribute to metal-induced neurodegeneration. J Alzheimers Dis 10:223-253.

Yu GS, Steinkirchner TM, Rao GA, Larkin EC (1986) Effect of prenatal iron deficiency on myelination in rat pups. Am J Pathol 125:620-624.

Yudkoff M, Daikhin Y, Lin ZP, Nissim I, Stern J, Pleasure D (1994) Interrelationships of leucine and glutamate metabolism in cultured astrocytes. J Neurochem 62:1192-1202.

Zaki NM, Tirelli N (2010) Gateways for the intracellular access of nanocarriers: a review of receptor-mediated endocytosis mechanisms and of strategies in receptor targeting. Expert Opin Drug Deliv 7:895-913.

Zecca L, Youdim MB, Riederer P, Connor JR, Crichton RR (2004) Iron, brain ageing and neurodegenerative disorders. Nat Rev Neurosci 5:863-873.

Zechel S, Huber-Wittmer K, von Bohlen und Halbach O (2006) Distribution of the iron-regulating protein hepcidin in the murine central nervous system. J Neurosci Res 84:790-800.

Zhang B, Cao Q, Guo A, Chu H, Chan YG, Buschdorf JP, Low BC, Ling EA, Liang F (2005) Juxtanodin: an oligodendroglial protein that promotes cellular arborization and 2',3'-cyclic nucleotide-3'-phosphodiesterase trafficking. Proc Natl Acad Sci USA 102:11527-11532.

Zhang X, Surguladze N, Slagle-Webb B, Cozzi A, Connor JR (2006) Cellular iron status influences the functional relationship between microglia and oligodendrocytes. Glia 54:795-804.

Zhu W, Li X, Tang Z, Zhu S, Qi J, Wei L, Lei H (2007) Superparamagnetic iron oxide labeling of neural stem cells and 4.7T MRI tracking *in vivo* and *in vitro*. J Huazhong Univ Sci Technolog Med Sci 27:107-110.

Zimmermann MB, Hurrell RF (2007) Nutritional iron deficiency. Lancet 370:511-520.

Zlokovic BV (2008) The blood-brain barrier in health and chronic neurodegenerative disorders. Neuron 57:178-201.

2. Results

2.1. Consequences of an exposure of OLN-93 cells to iron and/or iron oxide nanoparticles

2.2. Consequences of an exposure of cultured astrocytes to iron oxide nanoparticles

2.1. Consequences of an exposure of OLN-93 cells to iron and/or iron oxide nanoparticles

2.1.1. Iron metabolism of OLN-93 cells

2.1.2. Publication 1

Hohnholt M, Geppert M, Dringen R (2010) Effects of iron chelators, iron salts, and iron oxide nanoparticles on the proliferation and the iron content of oligodendroglial OLN-93 cells. Neurochem Res 35:1259-1268

2.1.3. Publication/Manuscript 2

Hohnholt MC, Geppert M, Dringen R; Mobilization of iron from iron oxide nanoparticles in oligodendroglial cells. *Revised manuscript submitted for publication*

2.1.4. Publication/Manuscript 3

Hohnholt MC, Dringen R; Iron-dependent formation of reactive oxygen species and glutathione depletion after accumulation of magnetic iron oxide nanoparticles by oligodendroglial cells. *Submitted for publication*

2.1.1. Iron metabolism of OLN-93 cells

Michaela C. Hohnholt

2.1.1.   Iron metabolism of OLN-93 cells

Michaela C. Hohnholt

2.1.1.1.   Abstract

OLN-93 cells are a well established cell culture model for oligodendroglial cells. Here, the iron metabolism of OLN-93 cells and the consequences of a treatment of these cells with low molecular weight iron and iron oxide nanoparticles (Fe-NP) were investigated. OLN-93 cells, which divide once every 22 ± 1 h, had a basal iron content of 29.9 ± 37.7 nmol/mg protein, a specific activity of the cellular enzyme lactate dehydrogenase (LDH) of 3.6 ± 1.8 µmol/(min × mg protein) and a specific content of the cellular antioxidant glutathione of 56.3 ± 12.7 nmol/mg protein. RT-PCR analysis revealed the presence of the mRNAs of transferrin, transferrin receptor, the divalent metal transporter 1, the heavy and light chains of the iron storage protein ferritin and the glycosylphosphatidylinositol-anchored form of the ferroxidase ceruloplasmin, while the mRNAs of the soluble ceruloplasmin and the iron exporter ferroportin were absent. Furthermore, viable OLN-93 cells were able to accumulate iron from the low molecular weight iron salt ferric ammonium citrate (FAC) as well as from Fe-NP and synthesized ferritin after application of FAC or Fe-NP. Taken together, these results show that viable OLN-93 cells possess the basic mechanisms for iron accumulation and storage, and are able to accumulate iron from Fe-NP.

2.1.1.2. Introduction

Iron is a very important metal for mammals, since it is involved in functions such as the reversible binding of molecular oxygen in red blood cells for its transport from lungs to other parts of the body (Jensen 2009) and the catalysis of redox reactions by enzymes of the respiratory chain (Babcock 1999). Moreover, iron is essential for ribonuclease reductase, which catalyzes the rate-limiting step of the DNA synthesis (Stubbe 1998, Stubbe and van der Donk 1998). However, when iron is present in a redox-active form, it can catalyze the formation of reactive oxygen species (ROS) by the Fenton reaction (Kell 2009). ROS, like the highly reactive hydroxyl radical, can react with proteins, DNA and lipids, subsequently leading to cell damage (Halliwell 2006, Kell 2009). As protection against ROS, cells possess a number of antioxidative defense mechanisms including low molecular weight antioxidants such as glutathione (Dringen 2000, Limon-Pacheco and Gonsebatt 2009) and antioxidant enzymes, such as catalase and glutathione peroxidase (Dringen *et al.* 2005, Battin and Brumaghim 2009).

The function of oligodendrocytes in the brain is the synthesis and maintenance of the myelin sheaths around neuronal axons for fast conduction velocities (Emery 2010, Miron *et al.* 2011). Myelin sheaths are extensions of the oligodendroglial cell membrane that are wrapped around the axons as an insulating layer (Baumann and Pham-Dinh 2001, Nave 2010). Oligodendroglial cells contain high amounts of lipids and proteins and are considered to have a high metabolic activity to enable the production of the amounts of proteins and lipids necessary to form myelin sheaths (Piñero and Connor 2000, Todorich *et al.* 2009).

Among the cells in the healthy brain, oligodendrocytes appear to contain the highest amounts of iron as shown by iron staining of brain slices (Dwork *et al.* 1988, Connor and Menzies 1990, Connor and Menzies 1996). This iron has been suggested to be required for their high metabolic activity (Piñero and Connor 2000, Todorich *et al.* 2009). Due to their high iron content, the high metabolic activity and the high amounts of lipids, oligodendrocytes are considered to be especially vulnerable to oxidative stress (McTigue and Tripathi 2008). In contrast to the high iron content of oligodendrocytes *in vivo* (Dwork *et al.* 1988, Connor and Menzies 1990, Connor and Menzies 1996), the reported levels of iron of this cell type in culture differs strongly between the two reports that are available (Thorburne and Juurlink 1996, Hoepken 2005). Although, cultured oligodendrocytes have been reported to have a high capacity to dispose exogenous applied hydrogen peroxide (Hirrlinger *et al.* 2002, Baud *et al.*

2004), little is known about their intracellular content of antioxidants (Thorburne and Juurlink 1996, Juurlink *et al.* 1998, Hirrlinger *et al.* 2002).

The uptake of iron into oligodendrocytes could be mediated by transferrin (Tf), since these cells in culture express this protein (Espinosa de los Monteros *et al.* 1988, Griot and Vandevelde 1988, Espinosa de los Monteros *et al.* 1990, Connor *et al.* 1993, Espinosa de los Monteros *et al.* 1994) and its receptor (Espinosa de los Monteros and Foucaud 1987, Ortiz *et al.* 2004, Hoepken 2005). Until now, there are no reports available concerning uptake mechanisms for non-protein-bound iron in oligodendrocytes, such as for example the divalent metal transporter 1 for ferrous iron (DMT1; Fleming *et al.* 1997, Gunshin *et al.* 1997).

Intracellularly, iron can be stored in the iron storage protein ferritin, which is a spherical protein consisting of the heavy (FtH) and light (FtL) ferritin chains (Arosio *et al.* 2009). Oligodendrocytes express the iron storage protein ferritin (Griot and Vandevelde 1988, Qi and Dawson 1994, Hoepken 2005) and the presence of both FtH and FtL has been confirmed on the RNA level (Hoepken 2005). The ratio of FtH to FtL is cell type specific and oligodendrocytes have been reported to contain ferritin that is rich in FtH (H-ferritin; Connor and Menzies 1996). Besides the function of iron storage, extracellular H-ferritin has been proposed to be an additional iron source for cultured oligodendrocytes and the expression of Tim-2 (T cell immunoglobulin-domain and mucin-domain 2) as receptor for H-ferritin has been confirmed (Todorich *et al.* 2008). In addition, the survival of cultured oligodendrocytes in the absence of Tf depends on the presence of H-ferritin and the uptake of iron contained in H-ferritin (Todorich *et al.* 2011).

The expression of the ferrous iron exporter ferroportin (Fpn) and the ferroxidases ceruloplasmin (Cp), its glycosylphosphatidylinositol-anchored form (G-Cp) or hephaestin, have not been reported so far for oligodendrocytes. Therefore, it remains to be elucidated, whether these cells are able to release ferrous iron and oxidize it extracellularly.

Nanoparticles are defined as particles which are in at least two dimensions smaller than 100 nm (Lewinski *et al.* 2008). This small size is the reason for an alteration of the material properties in comparison to the bulk material that opens up new application fields for nanoparticles (Silva 2006, Soenen and De Cuyper 2010). Among the various materials used, iron oxide nanoparticles (Fe-NP) are considered to be especially useful due to their magnetic properties that make them suitable for cell labeling and as contrast agent for magnetic resonance imaging (MRI; Arbab *et al.* 2003, Laurent *et al.* 2008, Soenen and De Cuyper 2010). Fe-NP have been used for the labeling of oligodendroglial progenitor cells and a

successful transplantation of these cells *in vivo* has been detected by MRI (Bulte *et al.* 1999, Franklin *et al.* 1999, Bulte *et al.* 2001, Dunning *et al.* 2004). However so far, little is known about the consequences of an exposure of oligodendroglial cells to Fe-NP.

OLN-93 cells are a cell culture model for oligodendrocytes and have been introduced by Richter-Landsberg and Heinrich in 1996. During their development, oligodendrocytes undergo different developmental stages characterized by different marker proteins (Baumann and Pham-Dinh 2001, McTigue and Tripathi 2008). Analysis of the protein expression for OLN-93 cells revealed that they express proteins that are typical for the developmental stage of oligodendroglial precursor cells (Richter-Landsberg and Heinrich 1996) as well as for early and later stages of the oligodendroglial lineage, such as the neural cell adhesion molecule and the myelin specific marker myelin basic protein, respectively (Richter-Landsberg and Heinrich 1996, Buckinx *et al.* 2009). OLN-93 cells have been used so far as model for oligodendroglial cells to study oligodendroglial differentiation processes (Chesik *et al.* 2010, Meng *et al.* 2010, Smolders *et al.* 2010), the effects of oxidative stress (Stahnke *et al.* 2007, Brand *et al.* 2008, Brand *et al.* 2010), the detoxification of xenobiotics (Thiessen *et al.* 2010) and the effects of nanoparticles (Bastian *et al.* 2009, Busch *et al.* 2011). However, so far little is known about the iron metabolism of OLN-93 cells. These cells contain iron and accumulate iron from ferrous sulfate (Brand *et al.* 2008). In addition, the expression of the mRNA of the iron transporter DMT1, transferrin receptor (TfR) and ferritin has been shown and the presence of the TfR protein has been confirmed (Brand *et al.* 2008). Therefore, OLN-93 cells may be able to take up transferrin-bound and non-transferrin-bound iron.

The present study investigates basal parameters of OLN-93 cells such as the morphology, the activity of the cellular enzyme lactate dehydrogenase (LDH) and the cellular contents of iron and of glutathione. Regarding iron metabolism, the expression of the mRNA of various proteins involved in iron metabolism was investigated to confirm their absence or presence in this cell type. To reveal the consequences of low molecular weight iron and Fe-NP on OLN-93 cells, the cells were exposed to ferric ammonium citrate (FAC) or Fe-NP. Despite the observed high amounts of iron accumulated by OLN-93 cells from these two iron sources within 24 h, the cells remained viable most likely due to the observed synthesis of ferritin after exposure to FAC or Fe-NP.

2.1.1.3.   Materials and methods

Materials

Fetal calf serum (FCS), penicillin/streptomycin and trypsin solution were obtained from Biochrom (Berlin, Germany). Dulbecco´s modified Eagle´s medium (DMEM) was purchased from Invitrogen (Karlsruhe, Germany). Deferoxamine, cycloheximide, dihydrorhodamine 123, 5,5´-dithio-bis(2-nitrobenzoic acid) (DTNB), dimercaptosuccinic acid (DMSA), neocuproine, sodium ascorbate, Tris, glycine, methanol and the mouse anti-α-tubulin antibody were from Sigma (Steinheim, Germany). Bovine serum albumin, NADH and NADPH were obtained from Applichem (Darmstadt, Germany). Glutathione reductase and glutathione disulfide (GSSG) were purchased from Roche Diagnostics (Mannheim, Germany). The goat anti-L-ferritin antibody, horse radish peroxidase-conjugated anti-goat-IgG and anti-mouse-IgG were from Dianova (Hamburg, Germany). 96-well microtiter plates and 5 cm dishes were obtained from Nunc (Roskilde, Denmark), 12-well cell culture plates from Greiner Bio-one (Frickenhausen, Germany) and 24-well plates from Starstedt (Nümbrecht, Germany). RNeasy® Mini Kit and RevertAid^{TM} H Minus First Strand cDNA Synthesis Kit were purchased from Qiagen (Hilden, Germany). DNA loading dye, Taq polymerase, the GeneRuler^{TM} 50 bp DNA ladder and the PageRuler^{TM} prestained protein ladder 170-10 kDa were purchased from Fermentas (St. Leon-Rot, Germany). The Hybond^{TM}-C Extra membrane, the ECL^{TM} Western Blotting Detection Kit, the ECL Advance^{TM} Western Blotting Detection Kit and the Hyperfilm^{TM} ECL membrane were obtained from GE Healthcare (Munich, Germany). All other chemicals of the highest purity available were from Fluka (Buchs, Switzerland), Merck (Darmstadt, Germany), Serva (Heidelberg, Germany) or Riedel-deHaen (Seelze, Germany).

Synthesis of Fe-NP

The Fe-NP used in this study were kindly provided by Mark Geppert. Synthesis and coating of these Fe-NP with dimercaptosuccinic acid (DMSA) were performed as described previously (Geppert *et al.* 2009, Geppert *et al.* 2011). In the following sections, Fe-NP denotes DMSA-coated iron oxide nanoparticles. The concentration of Fe-NP refers to the concentration of iron in the Fe-NP, not to the concentration of particles.

Cell cultures and experimental incubation

OLN-93 cells were grown in 175 cm^2 flasks in culture medium (DMEM with 10% FCS, 1 mM pyruvate, 20 U/mL of penicillin G and 20 μg/mL of streptomycin sulphate) in a Sanyo (Osaka, Japan) incubator in a humidified atmosphere with 10% CO_2 at 37°C. For seeding the cells, approximately 80-90% confluent cell cultures were washed with 25 mL pre-warmed (37°C) phosphate-buffered saline (PBS; 10 mM potassium phosphate buffer containing 150 mM NaCl, pH 7.4) and subsequently incubated with 10 mL 0.01% trypsin in PBS for 5 min at 37°C. The trypsinization process was stopped by adding 10 mL culture medium and the cell suspension was centrifuged at 4°C for 5 min at 400 g. Cells were then resuspended in culture medium and the number of cells was counted in a Neubauer cell counting chamber (Brand, Wertheim, Germany). After dilution of the cell suspension, 25,000 cells were seeded in wells of 12-well plates, 100,000 cells in wells of 24-well plates (glutathione measurement) or 250,000 cells in 5 cm dishes (mRNA extraction and Western blot analysis). Cell cultures were trypsinized at least twice a week. Passage numbers between 33 and 40 were used for experiments.

Astrocyte-rich primary cultures were used as positive control for RT-PCR. These cultures were prepared from brains of newborn Wistar rats by a method described previously (Hamprecht and Löffler 1985). 3,000,000 viable cells were seeded per 5 cm dish in 5 mL culture medium. The cultures were kept in a humidified atmosphere with 10% CO_2 at 37°C and the culture medium was renewed every seventh day. Confluent cultures were used for mRNA extraction at a culture age between 14 and 20 days. The cultures were kindly provided by the members of the group of Prof. Dr. Ralf Dringen.

All experiments were performed in culture medium and experimental incubations were started 16 to 20 hours after seeding. OLN-93 cells were washed with 1 mL (12-well dishes) or with 5 mL (5 cm dishes) pre-warmed (37°C) culture medium and incubated in 1 mL (12-well dishes) or 5 mL (5 cm dishes) culture medium without or with 1 mM of iron as ferric ammonium citrate (FAC) or Fe-NP in the absence or in the presence of 1 mM deferoxamine (DFX) or 10 μM cycloheximide (CHX). The solvent of CHX in the stock solution was ethanol and the final ethanol concentration in the culture medium was 1%. For all experiments with CHX, an appropriate control containing 1% ethanol was included. None of the data obtained for 1% ethanol-treated cells differed compared to the control without ethanol (data not shown).

The incubations were terminated by washing the cells twice with 1 mL (12-well dishes) or 5 mL (5 cm dishes) ice-cold PBS. For analysis of protein and iron contents and for Western

blots, cells were stored at -20°C until analysis. Determination of cellular and extracellular lactate dehydrogenase (LDH) activity, measurement of total glutathione, propidium iodide (PI) staining and mRNA extractions were performed immediately after termination of the experimental incubations.

Determination of LDH activity and protein content

The determination of the activity of the cytosolic enzyme LDH was performed as described previously (Dringen *et al.* 1998). After termination of experimental incubations, media and cell samples were used for LDH analysis. Cell lysates were obtained by incubation of the cells in 1 mL 1% Triton X-100 in culture medium for 30 min at room temperature. For the measurement of the LDH activity, 40 µL of media samples or cell lysates were diluted with 140 µL of LDH buffer (80 mM Tris-HCl buffer containing 200 mM NaCl, pH 7.2) in wells of a microtiter plate. The measurement was started by addition of 180 µL of a freshly prepared reaction mixture in LDH buffer to each well to obtain a final concentration of 1.8 mM sodium pyruvate and 0.22 mM NADH in each well. The decrease in absorption per time at 340 nm due to the oxidation of NADH was measured by a Sunrise microtiter plate photometer (Tecan, Crailsheim, Germany). As a blank, culture medium without and with 1% Triton X-100 was used for media and cell samples, respectively, and the decrease in absorption per time of the blanks was subtracted from slopes obtained for media and cell samples prior to calculation of the cellular LDH activity and the extracellular LDH activity. To analyze the cell viability, LDH activities were expressed as extracellular LDH activity in percent of the total LDH activity (cellular plus extracellular LDH activity).

The Lowry method (Lowry *et al.* 1951) was used to quantify the cellular protein content after solubilization of the cells in 100 µL (for initial protein content) or 150 µL (for 24 h values) 0.5 M NaOH for 2 h at room temperature on a horizontal shaker (Unimax 1010 Heidolph, Schwabach, Germany) in a water-saturated environment. Bovine serum albumin was used as standard.

PI staining

PI staining was performed to test for the membrane permeability according to a previously described method (Scheiber *et al.* 2010). Visualization of cell nuclei was accomplished by costaining with the membrane-permeable dye H33342. The cells were washed twice with 1 mL pre-warmed incubation buffer (IB; 20 mM HEPES, 145 mM NaCl, 1.8 mM $CaCl_2$, 5.4 mM KCl, 1 mM $MgCl_2$ and 5 mM glucose, pH 7.4) after the experimental incubation and
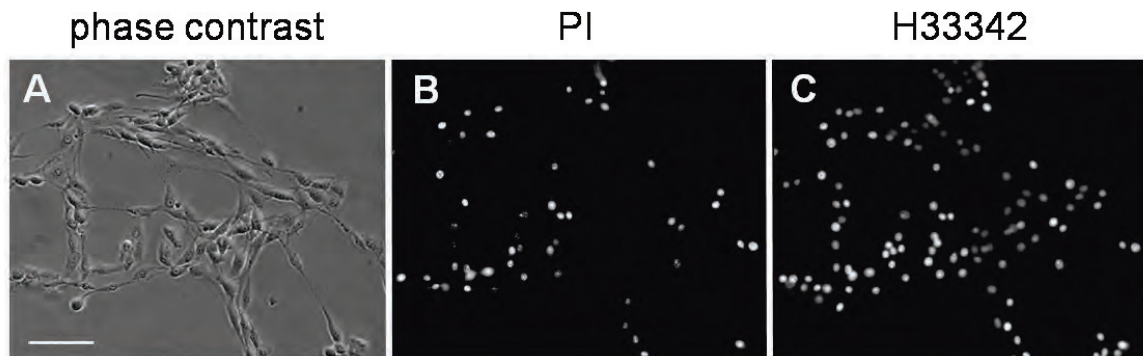
Figure 1: Membrane integrity of OLN-93 cells after permeabilization with 0.001% Triton X-100 in IB for 30 seconds. The phase contrast (A) and the PI staining (B) of OLN-93 cells are shown. In addition, the cell nuclei were costained with H33342 (C). Representative pictures were taken from cells of passage number 37. The scale bar in A applies to all panels and represents 100 µm.

subsequently incubated with 0.5 mL IB containing 5 µM PI and 10 µM H33342 for 15 min at 37°C. The incubation was terminated by washing the cells three times with 1 mL IB and the cells were immediately analyzed for fluorescence using a Nikon (Düsseldorf, Germany) TS2000U microscope. In Fig. 1, a positive PI staining of OLN-93 cells permeabilized with 0.001% Triton X-100 in IB for 30 seconds is shown.

Iron quantitation

The cellular iron content was quantified using a modification (Geppert *et al.* 2009) of the ferrozine method described previously (Riemer *et al.* 2004).

Cells treated without or with FAC or Fe-NP were solubilized in 100 µL (for initial iron content and for 24 h cell samples without extracellular iron applied) or in 1 mL (for 24 h cell samples with 1 mM FAC or Fe-NP in the absence or in the presence of DFX or CHX) of 50 mM NaOH at room temperature for 2 h in a water-saturated environment. Subsequently, 100 µL 10 mM HCl was added to the 100 µL NaOH in the wells or to 100 µL aliquots of cell lysates of FAC- or Fe-NP-exposed cells. 100 µL freshly prepared iron-releasing reagent (1:1 mixture of 1.4 M HCl and 4.5% $KMnO_4$ in water) was added to the cell lysates and incubated overnight at 60°C in a water-saturated atmosphere. For iron detection, 30 µL of a freshly prepared iron-detection reagent (6.5 mM ferrozine, 6.5 mM neocuproine, 2.5 M ammonium acetate and 1 M ascorbate) was added to the samples.

For analysis of the iron content of media samples, 200 µL culture medium that was not supplemented with iron was used and 25 µL of media supplemented with 1 mM FAC or Fe-NP was diluted with 75 µL 50 mM NaOH and 100 µM 10 mM HCl. 200 µL of medium or dilutions, respectively, were mixed with 100 µL iron-releasing reagent, incubated overnight at 60°C and 30 µL of freshly prepared iron-detection reagent was added.

As iron standards 100 µL of $FeCl_3$ (0-300 µM $FeCl_3$ in 10 mM HCl) were prepared and mixed with 100 µL 50 mM NaOH, 100 µL iron-releasing reagent and 30 µL iron-detection reagent. The iron-detection reagent was incubated at room temperature for 30 min and the absorbance of the ferrozine-iron complex was measured at 540 nm in 280 µL reaction mixtures in wells of microtiter plates by a microtiter plate photometer. For determination of the iron contents, the absorbance of reaction mixtures containing samples was compared to those containing iron standards (Fig. 2).
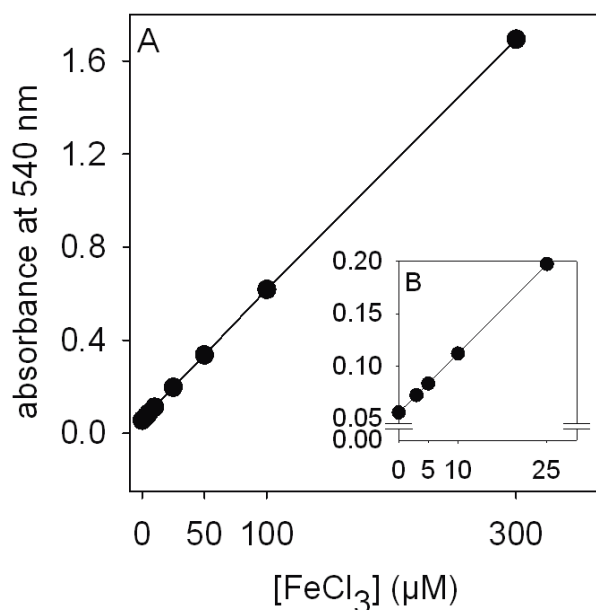
Figure 2: Detection of iron by the colorimetric assay. The concentration-dependent increase in absorbance of the ferrozine-iron complex at 540 nm after application of $FeCl_3$ standards (A: 0 to 300 µM; B: 0 to 25 µM) is shown. The correlation coefficients for both concentration ranges are $r^2 = 0.999$.

Glutathione quantification

The content of cellular total glutathione (GSx = amount of GSH plus twice the amount of glutathione disulfide (GSSG)) was determined as described previously (Dringen and Hamprecht 1996, Dringen *et al.* 1997) in microtiter plates according to the method that was

originally published by Tietze (1969). This assay is based on the reduction of 5,5´-dithio-bis-(2-nitrobenzoic acid) (DTNB) by GSH to 5-thio-2-nitrobenzoate (TNB). TNB can be detected by its absorbance at 405 nm. The specificity of this assay for the detection of reduced and oxidized glutathione is accomplished by the addition of glutathione reductase together with its cofactor NADPH. The reduction of DTNB oxidizes GSH to GSSG which is then recycled to GSH by glutathione reductase resulting in a cyclic assay and an increase in absorption at 405 nm with time. The rate limiting component under the conditions used is the amount of GSx and therefore the increase of absorption per time is proportional to the amount of GSx present in the reaction mixture.

After washing of OLN-93 cells in wells of 24-well plates twice with 1 mL ice-cold PBS, 500 µL 1% sulfosalicylic acid in H_2O was added per well and incubated for 10 min at 4°C. Subsequently, supernatants were mixed carefully and centrifuged for 1 min at 12,000 g. 10 µL of samples (cell lysates or GSSG standards) were diluted with 90 µL deionized water in wells of a 96-well plate and the measurement was started by addition of 100 µL of a reaction mixture containing 0.4 mM NADPH and 0.3 mM DTNB in 0.1 M phosphate buffer containing 1 mM ethylendiaminetetraacetic acid (pH 7.5). By comparison of the slope of samples with GSSG standards (0 to 100 pmol GSSG/10 µL; 100 pmol GSSG/10 µL corresponds to 200 pmol GSx/10 µL), the GSx concentrations of samples were calculated.

Reverse transcriptase-polymerase chain reaction (RT-PCR)

The total RNA of OLN-93 cells or astrocyte-rich primary cultures was extracted from 5 cm dishes with the RNeasy® Mini Kit according to the manufacturer´s instructions. The RevertAid[TM] H Minus First Strand cDNA Synthesis Kit was used to perform the reverse transcription according to the manufacturer´s instructions, using 4 µL RNA templates.

Table 1: Components of the PCR master mix.

Component	Final concentration	Volume
Taq buffer	1x	2 µL
MgCl$_2$	1.5 mM	1.2 µL
dNTP mix	0.25 mM	0.5 µL
Taq polymerase	0.05 U	0.2 µL
Sterile water	-	10.8 µL

Abbreviation: dNTP, deoxynucleotide triphosphate.

The amplification product of cDNA synthesized by reverse transcription was amplified by polymerase chain reaction (PCR). The PCR was performed in a total volume of 20 µL containing 15 µL master mix (Tab. 1), 0.5 µL forward primer, 0.5 µL reverse primer (0.25 µM final concentration of each primer; sequences according to Tab. 2) and 4 µL of cDNA or sterile water as negative control.

Table 2: PCR primers for the amplification of mRNA-derived cDNAs of proteins of the iron metabolism.

Gene product	Accession number	Sequence	Amplicon size (bp)
H-chain of ferritin	RNU58829	F: GTCTTGTTATTTTGACCGGG	443
		R: CGTCAGCTTAGCTCTCATCA	
L-chain of ferritin	NM_022500	F: TGGAGAAGAACCTGAACCAG	219
		R: CAAAGAGATACTCGCCCAGA	
Transferrin receptor	M58040	F: GCTCGTGGAGACTACTTCCG	311
		R: GCATTTGCAACTCCCTGAAT	
Transferrin	D38380	F: GGCATCAGACTCCAGCATCA	395
		R: TACCATCAGGGCACAGCAGC	
Divalent metal transporter 1	NM_013173	F: GTCACCGTCAGTATCCCAAG	470
		R: ATTGGCTTCTCGAACTTCCT	
Soluble ceruloplasmin	NM_012532	F: ATACATACCCCGATCACCCT	402
		R: TTTATTTCTTTCAGCCAGACTTAG	
G-anchored ceruloplasmin	AF202115	F: CTGCCATGTGACTGACCATA	243
		R: CTGAGGGACTGGTCTTGTTG	
Ferroportin	AF394785	F: TGTGTGTGATCTCCGTGTTC	365
		R: GAAATGCAGAAGGTCGAGAA	
β-Actin	V01217	F: GGGTCAGAAGGACTCCTACG	237
		R: GGTCTCAAACATGATCTGGG	

The indicated primers were described and previously used for analysis of mRNA isolated from astrocyte-rich primary cultures by RT-PCR (Korten 2004, Hoepken 2005). Abbreviations: bp, base pairs; F, forward primer sequence; G, gylcosylphosphatidylinositol; R, reverse primer sequence.

The cycling protocol was used as described previously (Hoepken 2005): 2 min at 94°C, followed by 35 cycles with 1 min at 94°C, 2 min at 58°C and 1 min at 72°C, followed by a final 10 min at 72°C. PCR products were separated on a 2.5% agarose gel in 40 mM

Tris/acetate buffer (pH 8.3) containing 1 mM ethylendiaminetetraacetic acid. The gel was stained with 1 µg/mL ethidium bromide in deionized water for 10 min and washed twice with deionized water for 15 min. Afterwards the gel was analyzed for the presence of cDNA amplification fragments with the DeVison G imaging system (Decon, Hohengandern, Germany).

Gel electrophoresis and Western blot analysis

For immunoblot analysis, cells incubated on 5 cm dishes were scraped of the dish in 1.4 mL PBS. The centrifugation for 1 min at 12,000 g resulted in a cell pellet which was lysed in deionized water (400 µL for control cells, 100 µL for cells incubated with DFX or CHX). The protein content of each sample was determined in aliquots of 10 µL of each cell lysate. After addition of 97.5 µL and 22.5 µL sample buffer (0.312 M Tris-HCl containing 10% sodium dodecylsulfate, 50% glycerine and 0.05% bromphenolblue, pH 6.8) to 390 µL and 90 µL cell lysates, respectively, the cell lysates were stored frozen at -20°C until further analysis. Protein separation was performed on a 12.5% polyacrylamide gel under reducing conditions (5 µL 20 mM dithiothreitol per lane) and electroblotted (Mini Trans-Blot® Electrophoretic Transfer Cell, BioRad, Hercules, USA) to a nitrocellulose membrane as previously described (Hoepken *et al.* 2004, Thiessen *et al.* 2010). Unspecific binding sites were blocked with 5% (w/v) milk powder (Heirler Cenovis, Radolfzell, Germany) in Tris-buffered saline (TBS, 10 mM Tris/HCl, 150 mM NaCl, pH 7.3) with 0.1% (w/v) Tween 20 (TBST) for 30 min. After incubation over night at 4°C with goat anti-L-ferritin antibody (1:500) or mouse anti-α-tubulin antibody (1:5,000) diluted in TBST containing 5% (w/v) milk powder on a roller shaker (IDL, Nidderau, Germany), the membrane was washed three times in TBST for 15 min and incubated for 1 h with horse radish peroxidase-conjugated anti-goat-IgG (1:10,000) or anti-mouse-IgG (1:20,000) diluted in TBST/5% (w/v) milk powder. After washing three times for 15 min with TBST, protein bands were visualized by enhanced chemiluminescence using an AGFA Curix 60 processor (Berlin, Germany). α-Tubulin was visualized by the ECL™ Western Blotting Detection Kit (1:1 mixture of solution A and B) and ferritin by the ECL Advance™ Western Blotting Detection Kit (25 µL of solution A and B, respectively, in 950 µL TBS).

Presentation of data

The data were obtained in three or more independent experiments on different passages of OLN-93 cells. The results are presented as means ± standard deviation. Pictures in figures that

show cell morphology and/or cell stainings are from a representative experiment that was reproduced at least twice with comparable results. Figures showing Western blot analysis and RT-PCR are from one representative experiment which was reproduced at least once with comparable results. Significance of differences between two sets of data was analyzed by the t-test and significance of differences between groups of data was analyzed by ANOVA followed by the Bonferroni post hoc test. $p > 0.05$ was considered as not significant.

2.1.1.4.   Results

Growth and morphology of OLN-93 cells

To investigate the proliferation of OLN-93 cells, cell density and morphology were monitored for up to three days after seeding of the cells in 12-well plates. The first picture, taken 20 h after seeding, was defined as 0 h time point (Fig. 3A) and revealed only a low number of cells that had a bipolar-shaped morphology with two processes per cell. After one additional day in culture, the cell density was increased and the majority of cells had also the bipolar shape
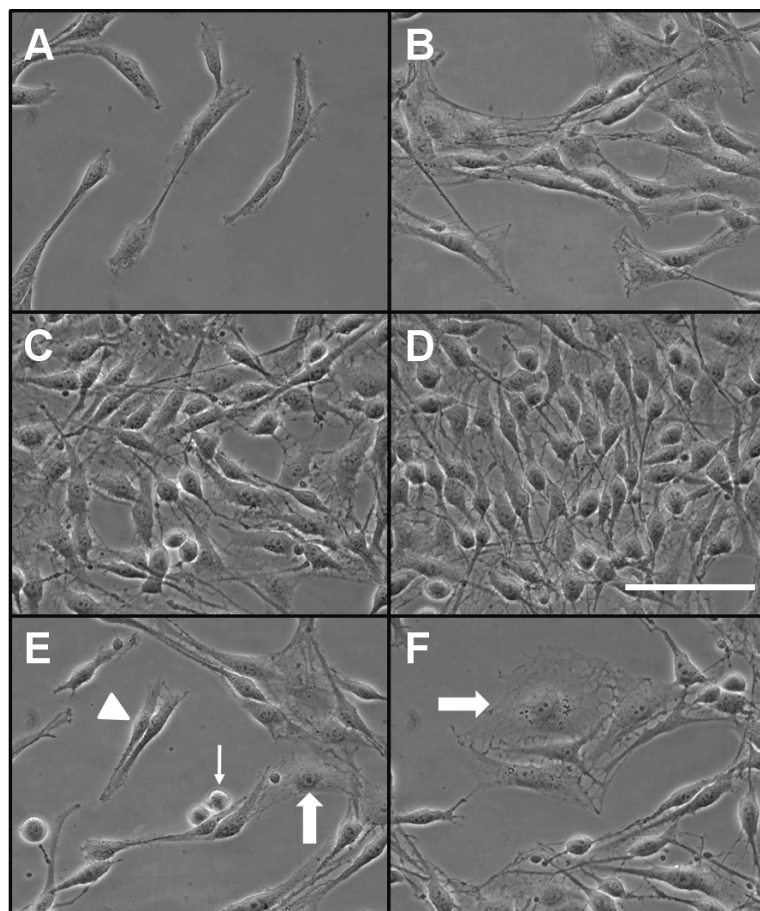
Figure 3: Morphology of OLN-93 cells. The 0 h time point was defined as 20 h after seeding of OLN-93 cells (passage 36; A). Further pictures were taken after 24 h (B,E), 48 h (C,F) and 72 h (D). The arrowhead in E shows two cells with bipolar shaped morphology, whereas the big arrows in E and F point to cells with flattened cytosol and the thin arrow in E indicates two cells with condensed cell bodies. The scale bar in D applies to all panels and represents 100 µm.

(Fig. 3B,E arrowhead). In addition, round-shaped cells with a condensed cell body were observed with usually two of them sitting next to each other, suggesting that these types of

cells might be products of cell division (Fig. 3E thin arrow). Some cells were observed which covered a bigger surface area of the well and appeared to be flattened with a widespread cytosol and a higher number of fine branches (Fig. 3B,E big arrow). The overall cell density increased further after 48 h and the cells covered about 70-80% of the bottom surface of a well (Fig. 3C,F). The cellular morphology after 48 h was comparable to the morphology seen at the 24 h time point, as most of the cells had a bipolar shape and some cells were flattened (Fig. 3F big arrow). After 72 h, OLN-93 cells covered almost completely the surface of the wells and the cells were tightly packed (Fig. 3D). The morphology was similar to the earlier time points, but hardly any cells appeared to have a flattened cytosol anymore which might be due to the high cell density. To elucidate the growth rate of OLN-93 cells, the doubling time was calculated from the increases of the cellular protein content with time (data not shown). From an exponentially fitted plot of the increases in cellular protein content with time, the doubling time of OLN-93 cells was calculated to be 22 ± 1 h (6 independent experiments performed in triplicates).

Basic parameters of OLN-93 cells

To further characterize OLN-93 cells, their specific iron content, specific LDH activity and specific GSx content were determined 20 h after seeding (Tab. 3). The basal iron content of OLN-93 cells was 29.9 ± 37.7 nmol/mg protein (Tab. 3). OLN-93 cells contained at these experimental conditions a specific LDH activity of 3.6 ± 1.8 µmol/(min × mg protein) and a specific GSx content of 56.3 ± 12.7 nmol/mg protein (Tab. 3). RT-PCR analyses were performed to demonstrate the presence of mRNA of different proteins involved in the iron metabolism in OLN-93 cells.

Table 3: Basic parameters of OLN-93 cells.

Parameter	Value	Unit	n
Iron content	29.9 ± 37.7 [A]	nmol/mg protein	49
LDH activity	3.6 ± 1.8	µmol/(min × mg protein)	70
GSx content	56.3 ± 12.7	nmol/mg protein	21

The data represent means ± standard deviation of data obtained from n experiments of cells of passages between 33 and 40. (A) In 7 of 49 experiments, exceptionally high specific iron contents above 60 nmol/mg protein were measured without obvious experimental explanations. These data caused the high standard deviation. Exclusion of these 7 values revealed a specific iron content of 16.0 ± 13.1 nmol/mg protein.

The amplification product for β-actin at approximately 240 base pairs (bp) confirmed that the transcription and amplification of the extracted mRNA was accomplished successfully (Fig. 4 first lane). Furthermore, signals of the expected sizes for the amplification products of the cDNA of Tf, TfR, DMT1, FtH, FtL and G-Cp were observed. In contrast, no amplification products were observed of Cp and Fpn. As negative control for all primer pairs used, the equivalent volume of cDNA was substituted by deionized water and the absence of any signal confirmed that the amplification product was indeed derived from the cDNA samples (data not shown). Since the presence of the mRNA of the Fpn protein has been reported for astrocytes (Jeong and David 2003, Korten 2004) mRNA was extracted from astrocyte-rich primary cultures and the presence of the mRNA of Fpn was successfully observed as positive control (data not shown).
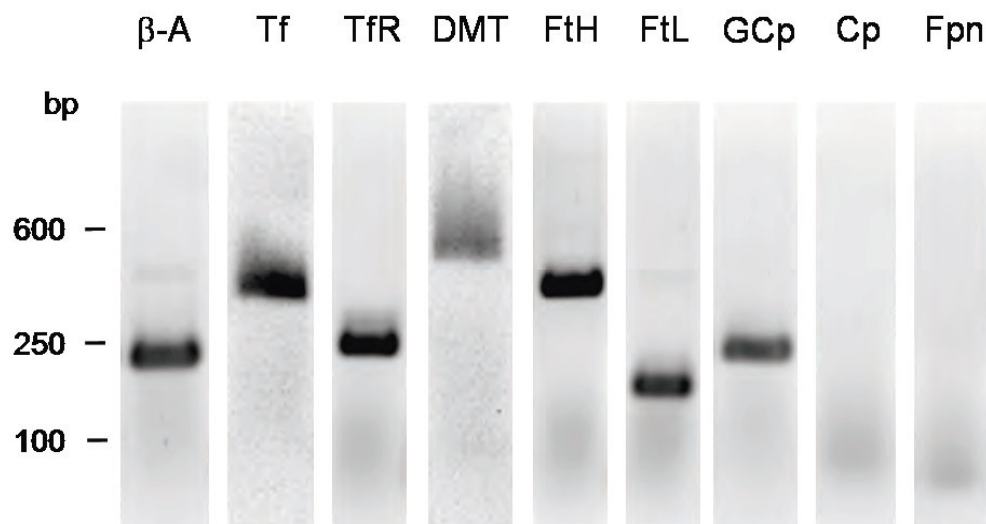
Figure 4: RT-PCR of mRNAs of proteins involved in the iron metabolism of OLN-93 cells. Selective primers were used to amplify specific DNA fragments from mRNA-derived cDNA of OLN-93 cell for β-actin (β-A), transferrin (Tf), transferrin receptor (TfR), divalent metal transporter 1 (DMT), heavy chain of ferritin (FtH), light chain of ferritin (FtL), glycosylphosphatidylinositol-anchored ceruloplasmin (GCp), soluble ceruloplasmin (Cp) or ferroportin (Fpn). Replacement of cDNA by sterile water did not result in any amplification product (data not shown).

Effects of FAC and Fe-NP on the morphology and viability of OLN-93 cells

To study the consequences of an application of iron either in form of low molecular weight iron (FAC) or in form of Fe-NP on OLN-93 cells, the cells were incubated with 1 mM FAC or 1 mM Fe-NP for 24 h in culture medium. In the absence of iron (control condition), the cellular morphology of control OLN-93 cells was bipolar and most cells had two processes

(Fig. 5A). The application of FAC did not lead to any obvious alterations in cell morphology compared to control cells (Fig. 5D). In contrast, cultures incubated with Fe-NP tended to have more flattened cells with a higher number of fine branches (Fig. 5G). Although, the cell density appeared to be lower in cultures exposed to 1 mM Fe-NP (Fig. 5G) compared to FAC-treated cells and controls, quantification of cellular protein contents as indicator for cell numbers after 24 h incubation with FAC or Fe-NP revealed no significant differences in
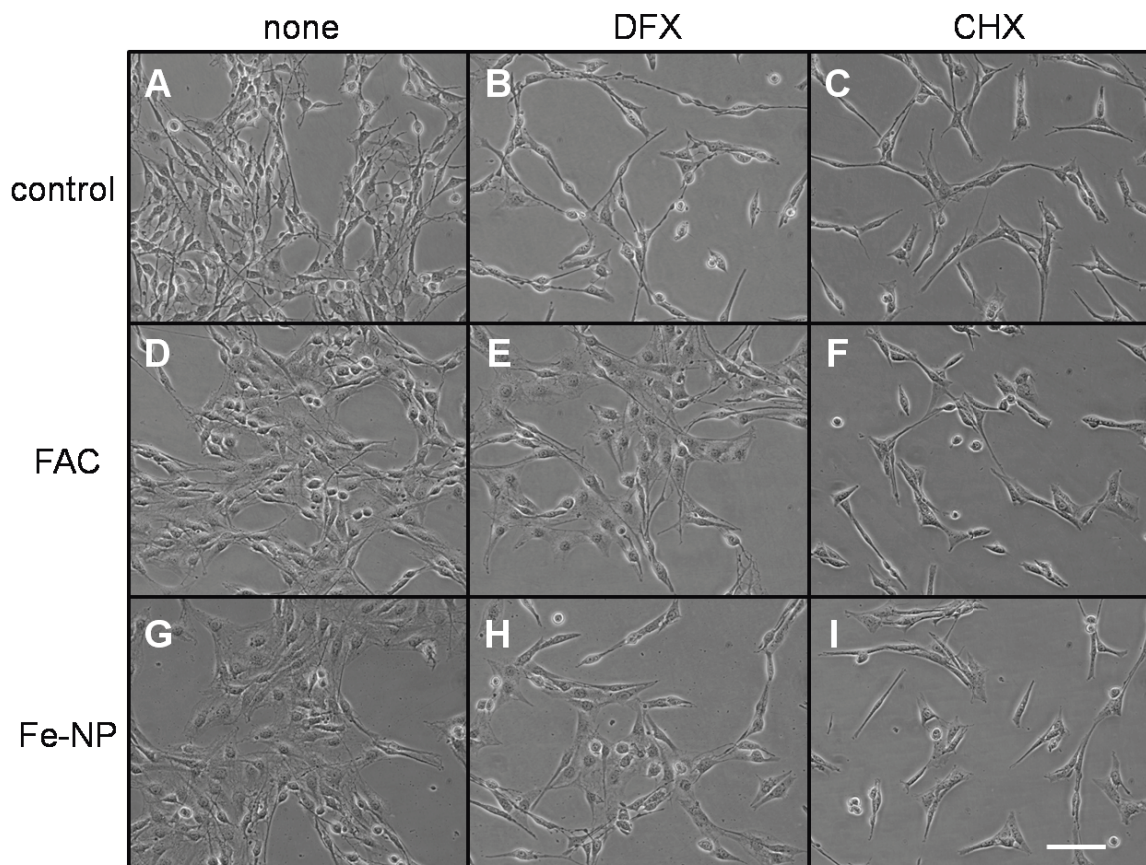

Figure 5: Morphology of OLN-93 cells (passage 37) after 24 h incubation without (control; A-C) or with 1 mM FAC (D-F) or 1 mM Fe-NP (G-I) in absence (A,D,G) or presence of 1 mM DFX (B,E,H) or 10 μM CHX (C,F,I). The scale bar in I applies to all panels and represents 100 μm.

comparison to control cells (Fig. 6B). To further investigate the influence of a treatment of OLN-93 cells with FAC or Fe-NP on the cell viability, the extracellular enzyme activity of the cytosolic enzyme LDH was measured. As shown in Fig. 6A, no significant increase in the extracellular LDH activities of OLN-93 cells exposed to FAC or Fe-NP for 24 h was observed.
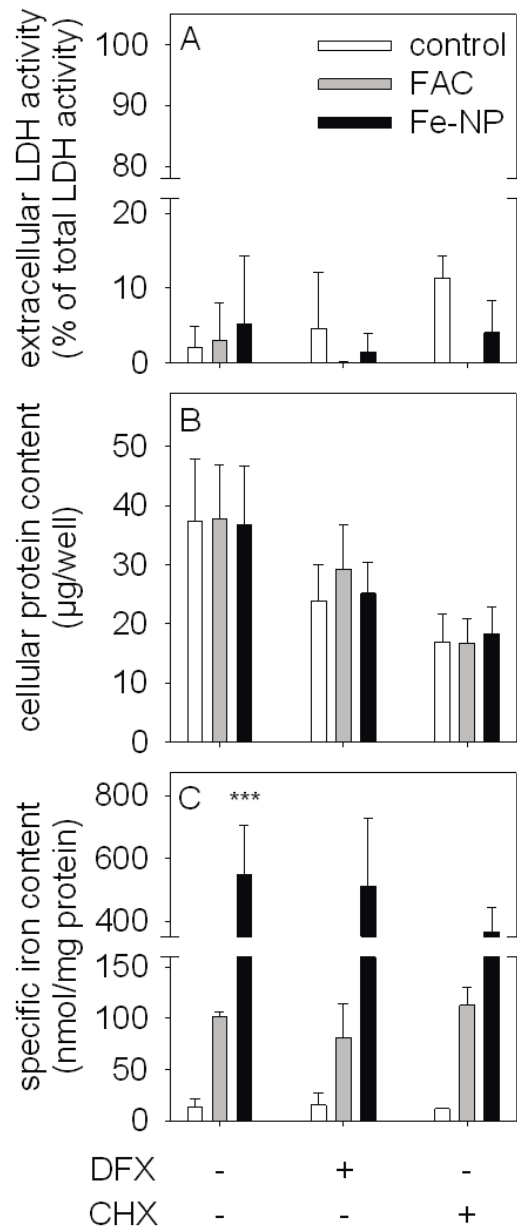
Figure 6: Extracellular LDH activity (A), cellular protein content (B) and specific iron content (C) of OLN-93 cells after 24 h incubation without (control) or with 1 mM FAC or 1 mM Fe-NP in the absence or the presence of 1 mM DFX or 10 μM CHX. The initial cellular protein content and the initial specific iron content were 16 ± 5 μg/well and 42.6 ± 16.2 nmol/mg protein, respectively. ANOVA followed by Bonferroni post hoc test was used for statistical analysis of the significance of differences of values compared to control (absence of FAC or Fe-NP) and is indicated by ***p<0.001.

This result was confirmed by data obtained from PI staining, as indicator for loss of membrane integrity, as no PI-positive cells were observed after incubation without (control) or with FAC or Fe-NP (Fig. 7A,G,M). To proof the presence of cells after treatment, the cell

nuclei were stained with H33342. The presence of a comparable amount of cell nuclei after incubation without (control) or with FAC or Fe-NP (Fig. 7D,J,P) demonstrated that these treatments did not cause detachment of cells from the culture wells.
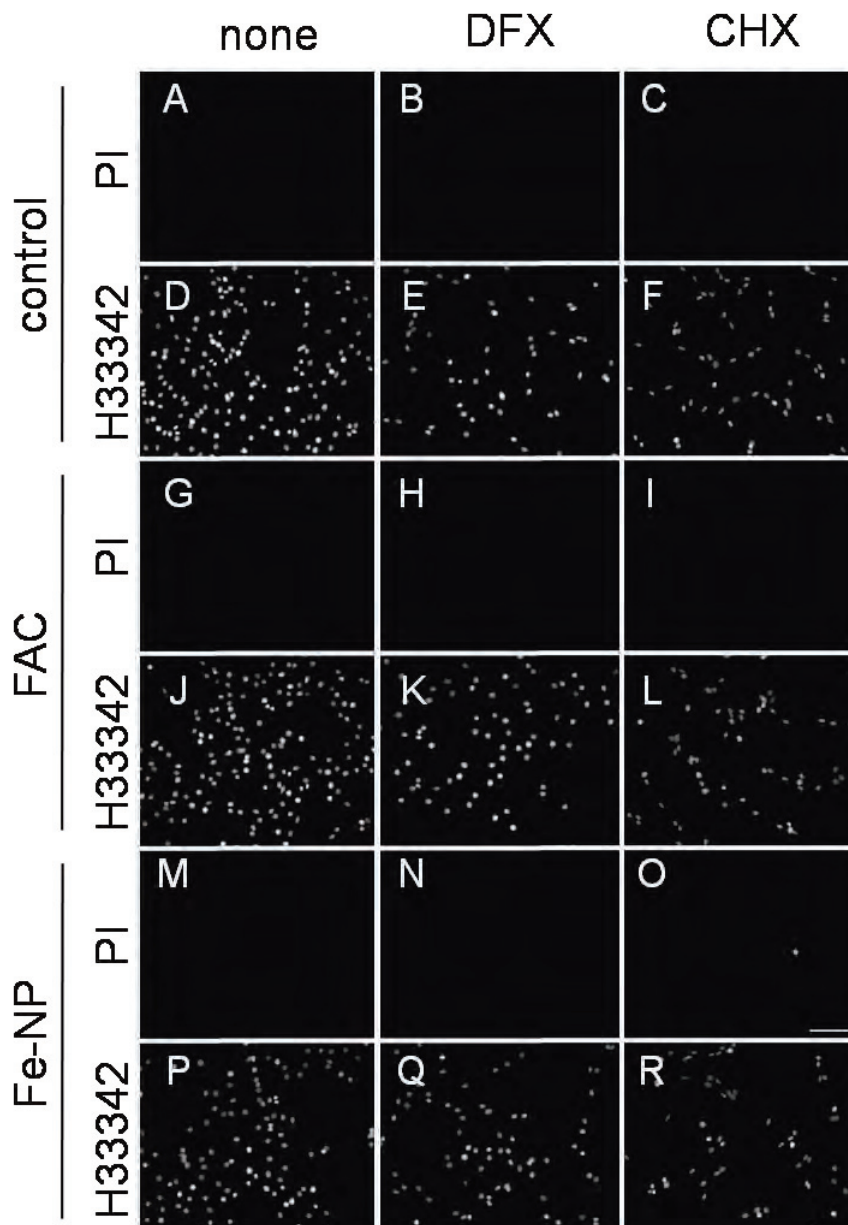
Figure 7: Membrane integrity of OLN-93 cells (passage 37) after 24 h incubation without (control; A-F) or with 1 mM FAC (G-L) or 1 mM Fe-NP (M-R) in the absence (none) or presence of 1 mM DFX or 10 μM CHX. To visualize the presence of the cells, the cell nuclei were stained with H33342 (D-F,J-L,P-R). The scale bar in O applies to all panels and represents 100 μm.

Iron accumulation of OLN-93 cells from FAC or Fe-NP

To study the iron accumulation in OLN-93 cells from FAC or Fe-NP, the specific iron contents after exposure to these compounds were determined (Fig. 6C). Within 24 h of incubation the specific iron content of control OLN-93 cells was lowered from an initial value of 42.6 ± 16.2 nmol/mg protein to 14.0 ± 7.1 nmol/mg protein, whereas the cellular iron content increased in the presence of FAC to 102 ± 4 nmol/mg and in the presence of Fe-NP to 548 ± 160 nmol/mg protein (Fig. 6C).

Upregulation of ferritin by OLN-93 cells

OLN-93 cells contain the mRNA of FtL and FtH (Fig. 4). To evaluate the potential of these cells to synthesize the iron storage protein ferritin, they were incubated in the absence or in the presence of FAC or Fe-NP for 24 h and cells were subsequently analyzed for the presence of ferritin (Fig. 8). In control cells incubated without an additional iron source, no ferritin signal was observed, indicating that these cells may contain at best a very low level of ferritin which is not detectable by the method used. In contrast, after 24 h exposure to 1 mM FAC or 1 mM Fe-NP, a prominent ferritin signal was observed, confirming that these cells are able to upregulate the synthesis of this protein.
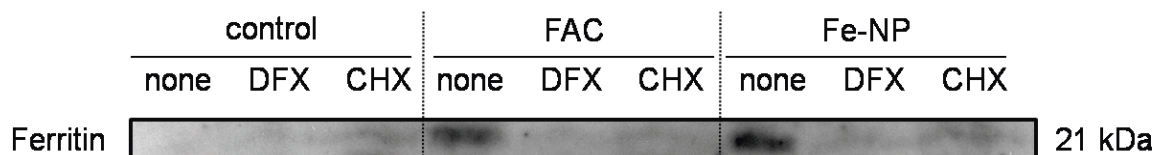
Figure 8: Western Blot for presence of the iron storage protein ferritin in OLN-93 cells. The cells (passage 35) were incubated for 24 h without (control) or with 1 mM FAC or 1 mM Fe-NP in the absence (none) or in the presence of 1 mM DFX or 10 μM CHX. 30 μg protein were loaded per lane.

Effects of DFX and CHX on OLN-93 cells

To evaluate the effects of iron chelation and inhibition of protein synthesis on OLN-93 cells, these cells were incubated without or with FAC or Fe-NP in the absence or presence of 1 mM DFX or 10 μM CHX for 24 h. Compared to control cells, DFX did not affect the cellular morphology (Fig. 5B,E,H), the cellular viability (Figs. 6A and 7B,H,N) nor the accumulation of iron from either FAC or Fe-NP (Fig. 6C). Also, presence of CHX did neither affect the cell morphology (Fig. 5C,F,I) nor caused an increase in extracellular LDH activity (Fig. 6A)

compared to control. Exposure of the cells to DFX and CHX led to hardly any PI-positive cells. However, DFX and CHX appeared to inhibit the proliferation of OLN-93 cells as shown by the lower cell density (Fig. 5B,C,E,F,H,I) and a lower cellular protein content per well (Fig. 6B) compared to the respective control, although the differences were not statistically significant after 24 h. Furthermore, DFX and CHX prevented the increases of the ferritin protein signal that was observed after treatment of OLN-93 cells with FAC or Fe-NP (Fig. 8).

2.1.1.5. Discussion

Morphology and basal parameters of OLN-93 cells

OLN-93 cells have been established as cell culture model of oligodendroglial precursor cells by Richter-Landsberg and Heinrich in 1996. The morphology of the majority of untreated OLN-93 cells observed in the present study corresponds to the reported bipolar shape of these cells (Richter-Landsberg and Heinrich 1996, Buckinx *et al.* 2009) and resembles the morphology of oligodendroglial precursor cells (McTigue and Tripathi 2008, Jakovcevski *et al.* 2009). However, a minority of cells showed a second distinct morphology that was characterized by a flattened cell body and a higher number of fine processes. OLN-93 cells have been reported before to undergo morphological changes such as flattening and appearance of many fine processes due to serum deprivation (0.5% FCS for 24 h) and these changes have been suggested to resemble more differentiated, immature oligodendrocytes (Kameshwar-Rao *et al.* 1999, Ernst *et al.* 2004, Buckinx *et al.* 2009). Although during the experimental incubation in the present study the applied FCS concentration was not lowered, these morphological changes were observed. Therefore a likely explanation might be a decrease in serum components during the incubation time due to uptake by cells that might cause this alteration at least of some cells. Since only a minority of cells altered their morphology and these morphological changes have been reported to reflect no biochemical or functional changes (Buckinx *et al.* 2009), they can be neglected. The morphology of OLN-93 cells that were exposed to Fe-NP changed in a similar manner whereas more cells seemed to be affected. Whether this observation is related to an alteration of the composition of the incubation medium or might be a consequence of Fe-NP on the cells by a different mechanism remains to be elucidated.

The calculated doubling time of OLN-93 cells of about 22 h is higher than the doubling time of 16-18 h which has been reported (Richter-Landsberg and Heinrich 1996). Reasons for this observation might be the long storage of cells frozen at -80°C, since cryopreservation induces certain stress on cells (Grout *et al.* 1990). Also, different culturing conditions are likely to affect the proliferation of OLN-93 cells, as for example naturally occurring variations of serum composition caused alterations in the proliferation rate of OLN-93 cells (data not shown).

The specific LDH activity of OLN-93 cells in the present study was 3.6 ± 1.8 μmol/(min × mg protein). This value is higher than those reported for rat oligodendrocytes in culture (0.5-

1.6 µmol/(min × mg protein); Cammer *et al.* 1982, Cammer and Zimmerman 1983, Minich *et al.* 2003). Since OLN-93 cells are immortalized and actively proliferating cells, the higher LDH activity might be due to the higher metabolic activity of proliferating cells compared to non-dividing cells (DeBerardinis *et al.* 2008), as it has been reported for liver and islet cells (Rasschaert and Malaisse 1995, Marin-Hernandez *et al.* 2006).

The total cellular GSx content of OLN-93 cells of 56.3 ± 12.7 nmol/mg protein is identical to values recently reported for untreated OLN-93 cells (Thiessen *et al.* 2010). Literature data on cellular GSH contents of cultured oligodendrocytes range between 6 and 33 nmol/mg protein (Thorburne and Juurlink 1996, Juurlink *et al.* 1998, Hirrlinger *et al.* 2002, Hemdan and Almazan 2007, Thiessen *et al.* 2010). Thus, OLN-93 cells appear to have a higher level of this low molecular weight thiol in comparison to cultured oligodendrocytes. This finding as well as the higher specific cellular LDH activity supports the hypothesis of a higher metabolic activity in the OLN-93 cell line compared to cells that were isolated freshly from tissue. Since higher metabolic activity has been suggested to be also connected with increased levels of ROS production in oligodendrocytes (McTigue and Tripathi 2008), a higher level of antioxidants may support survival of OLN-93 cells. Further investigations of the metabolic activity and antioxidant defense systems of OLN-93 cells would be necessary to verify this hypothesis.

Iron content and expression of proteins related to iron metabolism

OLN-93 cells contained a basal iron content of 29.9 ± 37.7 nmol/mg protein. The very high standard deviation reflects the unexpected high iron contents (>60 nmol/mg protein) found in 7 of 49 experiments. No experimental reason explained this variation in iron contents. Exclusion of these 7 values revealed a basal iron content of 16.0 ± 13.1 nmol/mg protein which corresponds well to the iron content of 15.4 ± 2.6 nmol/mg protein observed for cultured oligodendrocytes (Hoepken 2005). OLN-93 cells were found to express the mRNA of TfR as well as mRNA of the ferrous iron transporter DMT1, confirming literature data (Brand *et al.* 2008). Furthermore, presence of the mRNAs of Tf, FtH and FtL was found, as was expected from the known expression of these genes in cultured oligodendrocytes (Hoepken 2005). The presence of ferritin mRNA has been reported before for OLN-93 cells (Brand *et al.* 2008), although the authors did not discriminate between FtH and FtL. In addition, the mRNA of G-Cp was present in OLN-93 cells, while the mRNA of soluble Cp was not detected. It remains to be tested whether the method applied here is able to detect the presence of mRNA for Cp by using liver tissue (Aldred *et al.* 1987) or hepatocytes (Zhang *et*

al. 2004) as Cp-expressing positive controls. The Cp protein and G-Cp protein are absent from oligodendrocytes *in vivo* (Mollgard *et al.* 1988) although the expression of G-Cp mRNA in OLN-93 cells has been observed in the present study. However, the presence of the mRNA of G-Cp does not prove presence of the respective protein, since also the mRNA of the glial fibrillary acidic protein is present in OLN-93 cells, but not the corresponding protein (Buckinx *et al.* 2009). OLN-93 cells do not contain the mRNA of the iron exporter Fpn, although a signal was observed for mRNA extracted from astrocyte-rich primary cultures (data not shown), confirming the presence of Fpn mRNA in astroglial cells (Jeong and David 2003, Korten 2004). Since the presence of mRNA does not demonstrate the presence of the functional protein it would be important to further investigate also the presence of the protein DMT1 and G-Cp in OLN-93 cells.

Iron accumulation by OLN-93 cells

The initial decrease in cellular iron content of OLN-93 cells incubated in the absence of additional iron within the first 24 h of experimental incubation (from initial 42.6 ± 16.2 nmol/mg protein to 14.0 ± 7.1 nmol/mg protein at 24 h) is likely to be a consequence of the proliferation of the cells. Cells that have recently divided may need a given time to restore their specific iron content. Since the expression of TfR was shown to decrease by increasing cell density in human lung cancer cells and murine fibroblasts (Wang *et al.* 2005), a lower expression of TfR and therefore a lower iron uptake may be at least partly involved in the observed decrease of the specific iron content of OLN-93 cells. Differences in cellular iron content of OLN-93 cells that are altered by different incubation times in culture are likely not to affect the iron accumulation data obtained in the present study since all incubations were started during a short time frame of 16-20 h after seeding of cells. In contrast, this observation will become important when experimental incubations would be started at different time points after seeding or for pre-incubations for different time frames followed by post-incubations.

The low molecular weight iron complex FAC is a good extracellular iron source for brain cells (Hoepken *et al.* 2004, Bishop *et al.* 2011) and was therefore chosen as extracellular iron source for the present study. As OLN-93 cells have the potential to internalize different types of nanoparticles (Busch *et al.* 2011), Fe-NP were used as additional extracellular iron source. OLN-93 cells accumulated substantial amounts of iron from both FAC and Fe-NP, confirming literature data on iron accumulation of low molecular weight iron (Brand *et al.* 2008) and uptake of different types of nanoparticles by electron microscopy (Busch *et al.*

2011). The accumulation of iron from FAC might have been mediated by Tf, as Tf was present during the incubation in serum-containing culture medium (Garrick and Garrick 2009, Munoz *et al.* 2009). Surprisingly, OLN-93 cells accumulated about 5 times more iron from exogenous Fe-NP compared to incubation with the iron salt FAC. Oligodendrocytes have been reported to accumulated iron by the uptake of ferritin (Todorich *et al.* 2011), therefore the accumulation of the high amount of iron after exposure to Fe-NP suggests that OLN-93 cells might take up Fe-NP by a similar mechanism compared to ferritin. However, the colorimetric iron quantification used in the present study cannot discriminate between extracellularly bound and internalized iron. To discriminate between these two options, the temperature-dependency of the iron accumulation would have to be investigated (Trinder and Morgan 1998, Qian *et al.* 2000, Richardson 2001, Kim *et al.* 2006, Arredondo *et al.* 2008, Soenen *et al.* 2010, Pickard *et al.* 2011). This however was not feasible with the conditions used here, as the long incubation time of 24 h is very likely to compromise cell viability when performed at 4°C, at least in the absence of 10% CO_2 since no incubator was available for the present study that could be operated at 4°C with an atmosphere containing 10% CO_2. At least for Fe-NP discrimination between extracellularly bound and internalized Fe-NP could be studied by electron microscopy which would indicate Fe-NP as electron dense material (Berg *et al.* 2010, Luciani *et al.* 2010, Busch *et al.* 2011, Soenen *et al.* 2011).

The iron accumulation from FAC or Fe-NP was not influenced by the presence of the iron chelator DFX or by the protein biosynthesis inhibitor CHX (Siegel and Sisler 1963). DFX may not inhibit iron accumulation from FAC under the incubation conditions used here although the chelator was present in an equimolar concentration to FAC. Since DFX was suggested to be internalized by endocytosis (Keberle 1964, Halliwell and Gutteridge 2007) also the DFX-iron complex might be taken up by endocytosis in the high concentration that was applied here. It remains to be elucidated whether other iron chelators might inhibit the iron accumulation from FAC in the conditions used here. In addition, the absence of any alteration of iron accumulation in the presence of CHX shows that the iron accumulation does not require protein synthesis within this timeframe.

Cell proliferation and viability

The viability of OLN-93 cells as well as cell proliferation was not compromised by the presence of FAC or Fe-NP as was shown by the absences of any increases in extracellular LDH activity, the membrane permeability for PI as well as the cell density and cellular protein contents. This confirms literature data for OLN-93 cells treated with ferrous sulfate

(Brand *et al.* 2008) or different types of nanoparticles including iron oxide nanoparticles (Bastian *et al.* 2009, Busch *et al.* 2011).

Proliferation of cells is iron-dependent as it was previously reported for studies applying iron chelators (Lederman *et al.* 1984, Brodie *et al.* 1993, Cooper *et al.* 1996, Green *et al.* 2001), because the rate limiting step of DNA synthesis is catalyzed by the iron-containing enzyme ribonuclease reductase (Stubbe 1998, Stubbe and van der Donk 1998). The viability of OLN-93 cells was not compromised by incubation with DFX in the absence or in the presence of FAC or Fe-NP as shown by the lack of any increases in the extracellular LDH activity and the number of PI-positive cells. The decrease in cell density and cellular protein content in the presence of DFX suggests that the proliferation of OLN-93 cells is iron-dependent as assumed, although the decrease in cellular protein content did not reach the level of significance. In the presence of equimolar concentrations of DFX and FAC, no effect on cell proliferation would be expected since the chelator is supposed to be saturated with iron and iron from incubation medium should be available for the cells as it is in control conditions (absence of DFX and additional iron). In contrast to this hypothesis, in the presence of equimolar concentrations of DFX and FAC in the present study, the proliferation of OLN-93 cells was inhibited. A possible explanation might be a variation in the applied DFX concentration. A slightly higher DFX concentration compared to FAC would lead to a decreased availability of iron in the incubation medium and therefore explain the observed decrease in proliferation. Furthermore, the inhibition of proliferation by DFX alone was not statistically significant after 24 h incubation suggesting that the timeframe used in the present study might be too short to differentiate between the inhibition of proliferation by DFX and the absence of this observation in the presence of DFX and FAC. In contrast to the expected effect of FAC, Fe-NP are not assumed to overcome the inhibition of proliferation by DFX in equimolar concentrations. Under the assumption that iron is released from Fe-NP as observed in cell-free experiments within timeframes from days to weeks, no complete dissolution of Fe-NP is expected within 24 h (Arbab *et al.* 2005, Levy *et al.* 2010, Soenen *et al.* 2010). Therefore, the iron released from Fe-NP would be chelated by the excess of DFX since DFX is considered to be taken up by endocytosis (Lloyd *et al.* 1991) such as nanoparticles (Busch *et al.* 2011). Extracellular DFX could chelate the low molecular weight iron present in the incubation medium which is subsequently also unavailable for cellular proliferation.

The protein biosynthesis inhibitor CHX (Siegel and Sisler 1963) was expected to inhibit the proliferation of OLN-93 cells since this process requires *de novo* protein synthesis (Rao 1980). The cell viability was hardly affected by the coincubation with CHX in the presence of

either FAC or Fe-NP since any increases in extracellular LDH activity and no substantial increases in PI-positive cells were observed. As expected, the proliferation of OLN-93 cells was decreased in the presence of CHX alone or in combination with FAC or Fe-NP confirming that CHX indeed inhibits protein synthesis of OLN-93 cells.

Ferritin synthesis of OLN-93 cells

The upregulation of the iron storage protein ferritin was investigated by Western blot, because excess of iron is stored in ferritin in a redox-inactive form (Arosio *et al.* 2009). OLN-93 cells contain no detectable level of ferritin under basal culture conditions, but they were able to upregulate this protein within 24 h upon application of FAC. This was also observed in cultured oligodendrocytes (Qi and Dawson 1994, Qi *et al.* 1995). In addition to FAC, also the presence of Fe-NP induced synthesis of ferritin in OLN-93 cells. For other cell types, the alteration of ferritin and TfR protein levels as consequence to an exposure to Fe-NP was previously shown (Pawelczyk *et al.* 2006, Schäfer *et al.* 2007, Raschzok *et al.* 2010, Soenen *et al.* 2010). Since the synthesis of ferritin depends on the presence of low molecular weight iron (Arosio *et al.* 2009), the observed upregulation of ferritin also demonstrates that iron is released from Fe-NP after internalization. This is strongly supported by the observation that the upregulation of ferritin by FAC or Fe-NP was prevented by the iron chelator DFX. In OLN-93 cells, the release of iron is likely to occur in lysosomes since release of iron from Fe-NP with different coating materials has been shown in cell free experiments at acidic pH and in presence of citrate to model the lysosomal environment (Arbab *et al.* 2005, Levy *et al.* 2010, Soenen *et al.* 2010). The protein synthesis inhibitor CHX confirmed that ferritin upregulation is mediated by *de novo* synthesis of this protein as reported before for oligodendroglial cells (Qi and Dawson 1994) and astrocytes (Hoepken *et al.* 2004).

2.1.1.6. Conclusions

The present study investigated the basal iron metabolism of OLN-93 cells. OLN-93 cells not only contain iron but also the mRNA of Tf, TfR and DMT1, indicating that they might be able to accumulate Tf-bound iron as well as ferrous iron. Furthermore, these cells efficiently accumulated iron from FAC and Fe-NP and, despite of high amounts of accumulated iron, OLN-93 cells remained viable. As physiological consequence of the strong iron accumulation, upregulation of ferritin was observed which could be prevented by iron chelation and by inhibition of protein synthesis. Further studies will be necessary to identify the exact mechanisms of uptake of non-Tf-bound iron and of Fe-NP in OLN-93 cells. Also, it has to be further investigated whether these cells are able to export iron despite the absence of Fpn. In conclusion, OLN-93 cells seem to be suitable for studying the long term consequences of an exposure to Fe-NP, since these cells remain viable and are also able to store iron liberated from Fe-NP in ferritin.

2.1.1.7. References

Aldred AR, Grimes A, Schreiber G, Mercer JF (1987) Rat ceruloplasmin. molecular cloning and gene expression in liver, choroid plexus, yolk sac, placenta, and testis. J Biol Chem 262:2875-2878.

Arbab AS, Bashaw LA, Miller BR, Jordan EK, Lewis BK, Kalish H, Frank JA (2003) Characterization of biophysical and metabolic properties of cells labeled with superparamagnetic iron oxide nanoparticles and transfection agent for cellular MR imaging. Radiology 229:838-846.

Arbab AS, Wilson LB, Ashari P, Jordan EK, Lewis BK, Frank JA (2005) A model of lysosomal metabolism of dextran coated superparamagnetic iron oxide (SPIO) nanoparticles: implications for cellular magnetic resonance imaging. NMR Biomed 18:383-389.

Arosio P, Ingrassia R, Cavadini P (2009) Ferritins: a family of molecules for iron storage, antioxidation and more. Biochim Biophys Acta 1790:589-599.

Arredondo M, Kloosterman J, Nunez S, Segovia F, Candia V, Flores S, Le Blanc S, Olivares M, Pizarro F (2008) Heme iron uptake by Caco-2 cells is a saturable, temperature sensitive and modulated by extracellular pH and potassium. Biol Trace Elem Res 125:109-119.

Babcock GT (1999) How oxygen is activated and reduced in respiration. Proc Natl Acad Sci USA 96:12971-12973.

Bastian S, Busch W, Kuhnel D, Springer A, Meissner T, Holke R, Scholz S, Iwe M, Pompe W, Gelinsky M, Potthoff A, Richter V, Ikonomidou C, Schirmer K (2009) Toxicity of tungsten carbide and cobalt-doped tungsten carbide nanoparticles in mammalian cells *in vitro*. Environ Health Perspect 117:530-536.

Battin EE, Brumaghim JL (2009) Antioxidant activity of sulfur and selenium: a review of reactive oxygen species scavenging, glutathione peroxidase, and metal-binding antioxidant mechanisms. Cell Biochem Biophys 55:1-23.

Baud O, Greene AE, Li J, Wang H, Volpe JJ, Rosenberg PA (2004) Glutathione peroxidase-catalase cooperativity is required for resistance to hydrogen peroxide by mature rat oligodendrocytes. J Neurosci 24:1531-1540.

Baumann N, Pham-Dinh D (2001) Biology of oligodendrocyte and myelin in the mammalian central nervous system. Physiol Rev 81:871-927.

Berg JM, Ho S, Hwang W, Zebda R, Cummins K, Soriaga MP, Taylor R, Guo B, Sayes CM (2010) Internalization of carbon black and maghemite iron oxide nanoparticle mixture leads to oxidant production. Chem Res Toxicol 23:1874-1882.

Bishop GM, Dang TN, Dringen R, Robinson SR (2011) Accumulation of non-transferrin-bound iron by neurons, astrocytes, and microglia. Neurotox Res 19:443-451.

Brand A, Schonfeld E, Isharel I, Yavin E (2008) Docosahexaenoic acid-dependent iron accumulation in oligodendroglia cells protects from hydrogen peroxide-induced damage. J Neurochem 105:1325-1335.

Brand A, Bauer NG, Hallott A, Goldbaum O, Ghebremeskel K, Reifen R, Richter-Landsberg C (2010) Membrane lipid modification by polyunsaturated fatty acids sensitizes oligodendroglial OLN-93 cells against oxidative stress and promotes up-regulation of heme oxygenase-1 (HSP32). J Neurochem 113:465-476.

Brodie C, Siriwardana G, Lucas J, Schleicher R, Terada N, Szepesi A, Gelfand E, Seligman P (1993) Neuroblastoma sensitivity to growth inhibition by deferrioxamine: evidence for a block in G1 phase of the cell cycle. Cancer Res 53:3968-3975.

Buckinx R, Smolders I, Sahebali S, Janssen D, Smets I, Ameloot M, Rigo JM (2009) Morphological changes do not reflect biochemical and functional differentiation in OLN-93 oligodendroglial cells. J Neurosci Methods 184:1-9.

Bulte JW, Zhang S, van Gelderen P, Herynek V, Jordan EK, Duncan ID, Frank JA (1999) Neurotransplantation of magnetically labeled oligodendrocyte progenitors: magnetic resonance tracking of cell migration and myelination. Proc Natl Acad Sci USA 96:15256-15261.

Bulte JW, Douglas T, Witwer B, Zhang SC, Strable E, Lewis BK, Zywicke H, Miller B, van Gelderen P, Moskowitz BM, Duncan ID, Frank JA (2001) Magnetodendrimers allow endosomal magnetic labeling and *in vivo* tracking of stem cells. Nat Biotechnol 19:1141-1147.

Busch W, Bastian S, Trahorsch U, Iwe M, Kühnel D, Meißner T, Springer A, Gelinsky M, Richter V, Ikonomidou C (2011) Internalisation of engineered nanoparticles into mammalian cells *in vitro*: influence of cell type and particle properties. J Nanopart Res 13:293-310.

Cammer W, Zimmerman TR, Jr. (1983) Glycerolphosphate dehydrogenase, glucose-6-phosphate dehydrogenase, lactate dehydrogenase and carbonic anhydrase activities in oligodendrocytes and myelin: comparisons between species and CNS regions. Brain Res 282:21-26.

Cammer W, Snyder DS, Zimmerman TR, Jr., Farooq M, Norton WT (1982) Glycerol phosphate dehydrogenase, glucose-6-phosphate dehydrogenase, and lactate dehydrogenase: activities in oligodendrocytes, neurons, astrocytes, and myelin isolated from developing rat brains. J Neurochem 38:360-367.

Chesik D, De Keyser J, Bron R, Fuhler GM (2010) Insulin-like growth factor binding protein-1 activates integrin-mediated intracellular signaling and migration in oligodendrocytes. J Neurochem 113:1319-1330.

Connor JR, Menzies SL (1990) Altered cellular distribution of iron in the central nervous system of myelin deficient rats. Neuroscience 34:265-271.

Connor JR, Menzies SL (1996) Relationship of iron to oligodendrocytes and myelination. Glia 17:83-93.

Connor JR, Roskams AJ, Menzies SL, Williams ME (1993) Transferrin in the central nervous system of the shiverer mouse myelin mutant. J Neurosci Res 36:501-507.

Cooper CE, Lynagh GR, Hoyes KP, Hider RC, Cammack R, Porter JB (1996) The relationship of intracellular iron chelation to the inhibition and regeneration of human ribonucleotide reductase. J Biol Chem 271:20291-20299.

DeBerardinis RJ, Lum JJ, Hatzivassiliou G, Thompson CB (2008) The biology of cancer: metabolic reprogramming fuels cell growth and proliferation. Cell Metab 7:11-20.

Dringen R (2000) Metabolism and functions of glutathione in brain. Prog Neurobiol 62:649-671.

Dringen R, Hamprecht B (1996) Glutathione content as an indicator for the presence of metabolic pathways of amino acids in astroglial cultures. J Neurochem 67:1375-1382.

Dringen R, Kranich O, Hamprecht B (1997) The γ-glutamyl transpeptidase inhibitor acivicin preserves glutathione released by astroglial cells in culture. Neurochem Res 22:727-733.

Dringen R, Kussmaul L, Hamprecht B (1998) Detoxification of exogenous hydrogen peroxide and organic hydroperoxides by cultured astroglial cells assessed by microtiter plate assay. Brain Res Brain Res Protoc 2:223-228.

Dringen R, Pawlowski PG, Hirrlinger J (2005) Peroxide detoxification by brain cells. J Neurosci Res 79:157-165.

Dunning MD, Lakatos A, Loizou L, Kettunen M, ffrench-Constant C, Brindle KM, Franklin RJ (2004) Superparamagnetic iron oxide-labeled schwann cells and olfactory ensheathing cells can be traced *in vivo* by magnetic resonance imaging and retain functional properties after transplantation into the CNS. J Neurosci 24:9799-9810.

Dwork AJ, Schon EA, Herbert J (1988) Nonidentical distribution of transferrin and ferric iron in human brain. Neuroscience 27:333-345.

Emery B (2010) Regulation of oligodendrocyte differentiation and myelination. Science 330:779-782.

Ernst A, Stolzing A, Sandig G, Grune T (2004) Antioxidants effectively prevent oxidation-induced protein damage in OLN 93 cells. Arch Biochem Biophys 421:54-60.

Espinosa de los Monteros A, Foucaud B (1987) Effect of iron and transferrin on pure oligodendrocytes in culture; characterization of a high-affinity transferrin receptor at different ages. Brain Res 432:123-130.

Espinosa de los Monteros A, Chiapelli F, Fisher RS, de Vellis J (1988) Transferrin: an early marker of oligodendrocytes in culture. Int J Dev Neurosci 6:167-175.

Espinosa de los Monteros A, Kumar S, Scully S, Cole R, de Vellis J (1990) Transferrin gene expression and secretion by rat brain cells *in vitro*. J Neurosci Res 25:576-580.

Espinosa de los Monteros A, Sawaya BE, Guillou F, Zakin MM, de Vellis J, Schaeffer E (1994) Brain-specific expression of the human transferrin gene. similar elements govern transcription in oligodendrocytes and in a neuronal cell line. J Biol Chem 269:24504-24510.

Fleming MD, Trenor CC, 3rd, Su MA, Foernzler D, Beier DR, Dietrich WF, Andrews NC (1997) Microcytic anaemia mice have a mutation in Nramp2, a candidate iron transporter gene. Nat Genet 16:383-386.

Franklin RJ, Blaschuk KL, Bearchell MC, Prestoz LL, Setzu A, Brindle KM, ffrench-Constant C (1999) Magnetic resonance imaging of transplanted oligodendrocyte precursors in the rat brain. Neuroreport 10:3961-3965.

Garrick MD, Garrick LM (2009) Cellular iron transport. Biochim Biophys Acta 1790:309-325.

Geppert M, Hohnholt M, Gaetjen L, Grunwald I, Bäumer M, Dringen R (2009) Accumulation of iron oxide nanoparticles by cultured brain astrocytes. J Biomed Nanotechnol 5:285-293.

Geppert M, Hohnholt MC, Thiel K, Nürnberger S, Grunwald I, Rezwan K, Dringen R (2011) Uptake of dimercaptosuccinate-coated magnetic iron oxide nanoparticles by cultured brain astrocytes. Nanotechnology 22:145101-145111.

Green DA, Antholine WE, Wong SJ, Richardson DR, Chitambar CR (2001) Inhibition of malignant cell growth by 311, a novel iron chelator of the pyridoxal isonicotinoyl hydrazone class: effect on the R2 subunit of ribonucleotide reductase. Clin Cancer Res 7:3574-3579.

Griot C, Vandevelde M (1988) Transferrin, carbonic anhydrase C and ferritin in dissociated murine brain cell cultures. J Neuroimmunol 18:333-340.

Grout B, Morris J, McLellan M (1990) Cryopreservation and the maintenance of cell lines. Trends Biotechnol 8:293-297.

Gunshin H, Mackenzie B, Berger UV, Gunshin Y, Romero MF, Boron WF, Nussberger S, Gollan JL, Hediger MA (1997) Cloning and characterization of a mammalian proton-coupled metal-ion transporter. Nature 388:482-488.

Halliwell B (2006) Oxidative stress and neurodegeneration: where are we now? J Neurochem 97:1634-1658.

Halliwell B, Gutteridge JMC (2007) Free Radicals in Biology and Medicine. Oxford, UK: Oxford University Press.

Hamprecht B, Löffler F (1985) Primary glial cultures as a model for studying hormone action. Methods Enzymol 109:341-345.

Hemdan S, Almazan G (2007) Deficient peroxide detoxification underlies the susceptibility of oligodendrocyte progenitors to dopamine toxicity. Neuropharmacology 52:1385-1395.

Hirrlinger J, Resch A, Gutterer JM, Dringen R (2002) Oligodendroglial cells in culture effectively dispose of exogenous hydrogen peroxide: comparison with cultured neurones, astroglial and microglial cells. J Neurochem 82:635-644.

Hoepken HH, Korten T, Robinson SR, Dringen R (2004) Iron accumulation, iron-mediated toxicity and altered levels of ferritin and transferrin receptor in cultured astrocytes during incubation with ferric ammonium citrate. J Neurochem 88:1194-1202.

Hoepken HH (2005) Untersuchungen zum Eisenstoffwechsel neuraler Zellen (Dissertation). University of Tübingen, Tübingen.

Jakovcevski I, Filipovic R, Mo Z, Rakic S, Zecevic N (2009) Oligodendrocyte development and the onset of myelination in the human fetal brain. Front Neuroanat 3:5.

Jensen FB (2009) The dual roles of red blood cells in tissue oxygen delivery: oxygen carriers and regulators of local blood flow. J Exp Biol 212:3387-3393.

Jeong SY, David S (2003) Glycosylphosphatidylinositol-anchored ceruloplasmin is required for iron efflux from cells in the central nervous system. J Biol Chem 278:27144-27148.

Juurlink BH, Thorburne SK, Hertz L (1998) Peroxide-scavenging deficit underlies oligodendrocyte susceptibility to oxidative stress. Glia 22:371-378.

Kameshwar-Rao AS, Gil S, Richter-Landsberg C, Givol D, Yavin E (1999) H_2O_2-induced apoptotic death in serum-deprived cultures of oligodendroglia origin is linked to cell differentiation. J Neurosci Res 56:447-456.

Keberle H (1964) The biochemistry of desferrioxamine and its relation to iron metabolism. Ann NY Acad Sci 119:758-768.

Kell DB (2009) Iron behaving badly: inappropriate iron chelation as a major contributor to the aetiology of vascular and other progressive inflammatory and degenerative diseases. BMC Med Genomics 2:2.

Kim JS, Yoon TJ, Yu KN, Noh MS, Woo M, Kim BG, Lee KH, Sohn BH, Park SB, Lee JK, Cho MH (2006) Cellular uptake of magnetic nanoparticle is mediated through energy-dependent endocytosis in A549 cells. J Vet Sci 7:321-326.

Korten T (2004) Untersuchungen zum Eisentransport in Astrogliazellen (Diploma thesis). University of Tübingen, Tübingen.

Laurent S, Forge D, Port M, Roch A, Robic C, Vander Elst L, Muller RN (2008) Magnetic iron oxide nanoparticles: synthesis, stabilization, vectorization, physicochemical characterizations, and biological applications. Chem Rev 108:2064-2110.

Lederman HM, Cohen A, Lee JW, Freedman MH, Gelfand EW (1984) Deferoxamine: a reversible S-phase inhibitor of human lymphocyte proliferation. Blood 64:748-753.

Levy M, Lagarde F, Maraloiu VA, Blanchin MG, Gendron F, Wilhelm C, Gazeau F (2010) Degradability of superparamagnetic nanoparticles in a model of intracellular environment: follow-up of magnetic, structural and chemical properties. Nanotechnology 21:395103-395114.

Lewinski N, Colvin V, Drezek R (2008) Cytotoxicity of nanoparticles. Small 4:26-49.

Limon-Pacheco J, Gonsebatt ME (2009) The role of antioxidants and antioxidant-related enzymes in protective responses to environmentally induced oxidative stress. Mutat Res 674:137-147.

Lloyd JB, Cable H, Rice-Evans C (1991) Evidence that desferrioxamine cannot enter cells by passive diffusion. Biochem Pharmacol 41:1361-1363.

Lowry OH, Rosebrough NJ, Farr AL, Randall RJ (1951) Protein measurement with the Folin phenol reagent. J Biol Chem 193:265-275.

Luciani N, Wilhelm C, Gazeau F (2010) The role of cell-released microvesicles in the intercellular transfer of magnetic nanoparticles in the monocyte/macrophage system. Biomaterials 31:7061-7069.

Marin-Hernandez A, Rodriguez-Enriquez S, Vital-Gonzalez PA, Flores-Rodriguez FL, Macias-Silva M, Sosa-Garrocho M, Moreno-Sanchez R (2006) Determining and understanding the control of glycolysis in fast-growth tumor cells. Flux control by an over-expressed but strongly product-inhibited hexokinase. FEBS J 273:1975-1988.

McTigue DM, Tripathi RB (2008) The life, death, and replacement of oligodendrocytes in the adult CNS. J Neurochem 107:1-19.

Meng J, Xia W, Tang J, Tang BL, Liang F (2010) Dephosphorylation-dependent inhibitory activity of juxtanodin on filamentous actin disassembly. J Biol Chem 285:28838-28849.

Minich T, Yokota S, Dringen R (2003) Cytosolic and mitochondrial isoforms of NADP$^+$-dependent isocitrate dehydrogenases are expressed in cultured rat neurons, astrocytes, oligodendrocytes and microglial cells. J Neurochem 86:605-614.

Miron VE, Kuhlmann T, Antel JP (2011) Cells of the oligodendroglial lineage, myelination, and remyelination. Biochim Biophys Acta 1812:184-193.

Mollgard K, Dziegielewska KM, Saunders NR, Zakut H, Soreq H (1988) Synthesis and localization of plasma proteins in the developing human brain. integrity of the fetal blood-brain barrier to endogenous proteins of hepatic origin. Dev Biol 128:207-221.

Munoz M, Villar I, Garcia-Erce JA (2009) An update on iron physiology. World J Gastroenterol 15:4617-4626.

Nave KA (2010) Myelination and support of axonal integrity by glia. Nature 468:244-252.

Ortiz E, Pasquini JM, Thompson K, Felt B, Butkus G, Beard J, Connor JR (2004) Effect of manipulation of iron storage, transport, or availability on myelin composition and brain iron content in three different animal models. J Neurosci Res 77:681-689.

Pawelczyk E, Arbab AS, Pandit S, Hu E, Frank JA (2006) Expression of transferrin receptor and ferritin following ferumoxides-protamine sulfate labeling of cells: implications for cellular magnetic resonance imaging. NMR Biomed 19:581-592.

Pickard MR, Jenkins SI, Koller CJ, Furness DN, Chari DM (2011) Magnetic nanoparticle labeling of astrocytes derived for neural transplanation. Tissue Eng Part C Methods 17:89-99.

Piñero DJ, Connor JR (2000) Iron in the brain: an important contributor in normal and diseased states. Neuroscientist 6:435-453.

Qi Y, Dawson G (1994) Hypoxia specifically and reversibly induces the synthesis of ferritin in oligodendrocytes and human oligodendrogliomas. J Neurochem 63:1485-1490.

Qi Y, Jamindar TM, Dawson G (1995) Hypoxia alters iron homeostasis and induces ferritin synthesis in oligodendrocytes. J Neurochem 64:2458-2464.

Qian Z, Liao Q, To Y, Ke Y, Tsoi Y, Wang G, Ho K (2000) Transferrin-bound and transferrin free iron uptake by cultured rat astrocytes. Cell Mol Biol (Noisy-le-Grand) 46:541-548.

Rao PN (1980) The molecular basis of drug-induced G2 arrest in mammalian cells. Mol Cell Biochem 29:47-57.

Raschzok N, Muecke DA, Adonopoulou MK, Billecke N, Werner W, Kammer NN, Zielinski A, Behringer PA, Ringel F, Huang MD, Neuhaus P, Teichgraber U, Sauer IM (2010) *In vitro* evaluation of magnetic resonance imaging contrast agents for labeling human liver cells: implications for clinical translation. Mol Imaging Biol in press.

Rasschaert J, Malaisse WJ (1995) Activity of cytosolic and mitochondrial enzymes participating in nutrient catabolism of normal and tumoral islet cells. Int J Biochem Cell Biol 27:195-200.

Richardson DR (2001) Iron and gallium increase iron uptake from transferrin by human melanoma cells: further examination of the ferric ammonium citrate-activated iron uptake process. Biochim Biophys Acta 1536:43-54.

Richter-Landsberg C, Heinrich M (1996) OLN-93: a new permanent oligodendroglia cell line derived from primary rat brain glial cultures. J Neurosci Res 45:161-173.

Riemer J, Hoepken HH, Czerwinska H, Robinson SR, Dringen R (2004) Colorimetric ferrozine-based assay for the quantitation of iron in cultured cells. Anal Biochem 331:370-375.

Schäfer R, Kehlbach R, Wiskirchen J, Bantleon R, Pintaske J, Brehm BR, Gerber A, Wolburg H, Claussen CD, Northoff H (2007) Transferrin receptor upregulation: *in vitro* labeling of rat mesenchymal stem cells with superparamagnetic iron oxide. Radiology 244:514-523.

Scheiber IF, Schmidt MM, Dringen R (2010) Zinc prevents the copper-induced damage of cultured astrocytes. Neurochem Int 57:314-322.

Siegel MR, Sisler HD (1963) Inhibition of protein synthesis *in vitro* by cycloheximide. Nature 200:675-676.

Silva GA (2006) Neuroscience nanotechnology: progress, opportunities and challenges. Nat Rev Neurosci 7:65-74.

Smolders I, Smets I, Maier O, vandeVen M, Steels P, Ameloot M (2010) Simvastatin interferes with process outgrowth and branching of oligodendrocytes. J Neurosci Res 88:3361-3375.

Soenen SJ, De Cuyper M (2010) Assessing iron oxide nanoparticle toxicity *in vitro*: current status and future prospects. Nanomedicine (Lond) 5:1261-1275.

Soenen SJ, Himmelreich U, Nuytten N, Pisanic TR, 2nd, Ferrari A, De Cuyper M (2010) Intracellular nanoparticle coating stability determines nanoparticle diagnostics efficacy and cell functionality. Small 6:2136-2145.

Soenen SJ, Brisson AR, Jonckheere E, Nuytten N, Tan S, Himmelreich U, De Cuyper M (2011) The labeling of cationic iron oxide nanoparticle-resistant hepatocellular carcinoma cells using targeted magnetoliposomes. Biomaterials 32:1748-1758.

Stahnke T, Stadelmann C, Netzler A, Bruck W, Richter-Landsberg C (2007) Differential upregulation of heme oxygenase-1 (HSP32) in glial cells after oxidative stress and in demyelinating disorders. J Mol Neurosci 32:25-37.

Stubbe J (1998) Ribonucleotide reductases in the twenty-first century. Proc Natl Acad Sci USA 95:2723-2724.

Stubbe J, van der Donk WA (1998) Protein radicals in enzyme catalysis. Chem Rev 98:705-762.

Thiessen A, Schmidt MM, Dringen R (2010) Fumaric acid dialkyl esters deprive cultured rat oligodendroglial cells of glutathione and upregulate the expression of heme oxygenase 1. Neurosci Lett 475:56-60.

Thorburne SK, Juurlink BH (1996) Low glutathione and high iron govern the susceptibility of oligodendroglial precursors to oxidative stress. J Neurochem 67:1014-1022.

Tietze F (1969) Enzymic method for quantitative determination of nanogram amounts of total and oxidized glutathione: applications to mammalian blood and other tissues. Anal Biochem 27:502-522.

Todorich B, Zhang X, Slagle-Webb B, Seaman WE, Connor JR (2008) Tim-2 is the receptor for H-ferritin on oligodendrocytes. J Neurochem 107:1495-1505.

Todorich B, Pasquini JM, Garcia CI, Paez PM, Connor JR (2009) Oligodendrocytes and myelination: the role of iron. Glia 57:467-478.

Todorich B, Zhang X, Connor JR (2011) H-ferritin is the major source of iron for oligodendrocytes. Glia 59:927-935.

Trinder D, Morgan E (1998) Mechanisms of ferric citrate uptake by human hepatoma cells. Am J Physiol 275:279-286.

Wang J, Chen G, Pantopoulos K (2005) Inhibition of transferrin receptor 1 transcription by a cell density response element. Biochem J 392:383-388.

Zhang AS, Xiong S, Tsukamoto H, Enns CA (2004) Localization of iron metabolism-related mRNAs in rat liver indicate that HFE is expressed predominantly in hepatocytes. Blood 103:1509-1514.

2.1.2.   Publication 1

Hohnholt M, Geppert M, Dringen R

(2010)

Effects of iron chelators, iron salts, and iron oxide nanoparticles on the

proliferation and the iron content of oligodendroglial OLN-93 cells.

Neurochem Res 35:1259-1268

Contribution of Michaela C. Hohnholt:

- Performance of all experiments.
- Preparation of the first version of the manuscript.

Mark Geppert kindly provided the iron oxide nanoparticles.

ORIGINAL PAPER

Effects of Iron Chelators, Iron Salts, and Iron Oxide Nanoparticles on the Proliferation and the Iron Content of Oligodendroglial OLN-93 Cells

**Michaela Hohnholt · Mark Geppert ·
Ralf Dringen**

Abstract The oligodendroglial cell line OLN-93 was used as model system to investigate the consequences of iron deprivation or iron excess on cell proliferation. Presence of ferric or ferrous iron chelators inhibited the proliferation of OLN-93 cells in a time and concentration dependent manner, while the application of a molar excess of ferric ammonium citrate (FAC) prevented the inhibition of proliferation by the chelator deferoxamine. Proliferation of OLN-93 cells was not affected by incubation with 300 µM iron that was applied in the form of FAC, $FeCl_2$, ferrous ammonium sulfate or iron oxide nanoparticles, although the cells efficiently accumulated iron during exposure to each of these iron sources. The highest specific iron content was observed for cells that were exposed to the nanoparticles. These data demonstrate that the proliferation of OLN-93 cells depends strongly on the availability of iron and that these cells efficiently accumulate iron from various extracellular iron sources.

Keywords Oligodendrocytes · Iron · Proliferation · Deferoxamine · Iron oxide nanoparticles

Introduction

Iron is essential for cells as cofactor of various enzymes that are, for example, part of the respiratory chain or are required for DNA synthesis. However, excess of redox active iron in cells catalyses the production of hydroxyl radicals in the Fenton reaction which causes the oxidation of cellular macromolecules and can subsequently lead to cell death [1–3]. Therefore, iron uptake, cellular iron distribution and iron storage are tightly regulated.

Proliferation of cells depends on the availability of iron, since iron deprivation results in a G_1/S arrest of the cell cycle [4–7]. The molecular mechanism for this inhibition of proliferation is most likely the impairment of the synthesis of deoxyribonucleotides by the iron-dependent ribonucleotide reductase which limits DNA synthesis [8, 9]. Accordingly, the deprivation of iron, for instance by the iron chelator deferoxamine, has been reported to inhibit the proliferation of various types of cells [4, 10, 11]. In this context, deferoxamine has been tested with promising results as drug for the treatment of leukemia and neuroblastoma [11], and the use of iron chelators for the treatment of various cancers has been discussed [10, 12].

Iron staining of brain sections reveals that in the normal adult brain oligodendrocytes appear to be the cells that contain the highest amounts of iron [13, 14]. Therefore, these cells have to be especially equipped with mechanisms that catalyse iron uptake and allow save storage of iron to prevent iron-mediated toxicity. However, so far the mechanisms of iron uptake of oligodendrocytes have not been explored in full detail. Transferrin-dependent and transferrin-independent pathways are considered to mediate iron uptake in most cells [3, 15]. In the brain, oligodendrocytes express at best low amounts of immunodetectable transferrin receptors [16, 17]. In addition, at best a few

M. Hohnholt · M. Geppert · R. Dringen (✉)
Center for Biomolecular Interactions Bremen, University of
Bremen, P.O. Box 330440, 28334 Bremen, Germany
e-mail: ralf.dringen@uni-bremen.de

M. Hohnholt · M. Geppert · R. Dringen
Center for Environmental Research and Sustainable Technology,
University of Bremen, Bremen, Germany

R. Dringen
School of Psychology and Psychiatry, Monash University,
Clayton, VIC, Australia

🍎 Springer

oligodendrocytes were immunopositive for the divalent metal transporter 1 (DMT1) [18, 19]. These data suggest that transferrin-bound iron and ferrous iron are unlikely to be the predominant extracellular substrates for iron uptake into oligodendrocytes. Recently, H-ferritin was suggested as alternative extracellular source of iron for oligodendrocytes in vivo [17, 20].

In cell culture oligodendrocyte progenitor cells express transferrin receptor but the expression of this receptor is down regulated during differentiation to mature oligodendrocytes [16, 17, 21]. To study the consequences of both iron deprivation and application of an excess of iron on proliferation, viability and iron content of oligodendrocyte precursors, we have used cells of the oligodendroglial cell line OLN-93 [22] as model system. Here we report that membrane permeable and non-permeable iron chelators prevent the proliferation of OLN-93 cells, whereas an excess of iron does not affect proliferation or the viability of the cells, although the cells accumulated substantial amounts of iron from various extracellular iron sources, including iron oxide nanoparticles. Coincubation experiments revealed that the cellular iron accumulated after application of iron oxide nanoparticles plus low molecular weight iron sources was additive. Moreover, iron-treated OLN-93 cells contained higher levels than control cells of the iron storage protein ferritin, which is likely to contribute to the protection of the cells against iron-mediated oxidative damage.

Experimental Procedure

Materials

Fetal calf serum (FCS), penicillin/streptomycin and trypsin solution were obtained from Biochrom (Berlin, Germany). Dulbecco's modified Eagle's medium (DMEM) was from Gibco (Karlsruhe, Germany). Bathophenanthroline disulfonate (BPS), deferoxamine (DFX), neocuproine, paraformaldehyde, sodium ascorbate, and tris were purchased from Sigma (Steinheim, Germany). Bovine serum albumin and NADH were purchased from Applichem (Darmstadt, Germany). Goat anti-ferritin antibody and peroxidase-conjugated donkey anti-goat immunoglobuline G were obtained from Santa Cruz Biotechnology (Santa Cruz, USA) and Dianova (Hamburg, Germany), respectively. All other chemicals of the highest purity available were from Fluka (Buchs, Switzerland), Merck (Darmstadt, Germany), Serva (Heidelberg, Germany) or Riedel–de Haen (Seelze, Germany). 96-well microtiter plates were from Nunc (Wiesbaden, Germany) and 12-well cell culture plates from Greiner Bio-one (Frickenhausen, Germany). Citrate-coated

iron oxide nanoparticles (Fe-NP) were synthesized and characterised as previously described [23]. The given concentrations of Fe-NP reflect the concentration of the iron present in the nanoparticle preparation and not the concentration of particles.

Cell Cultures

OLN-93 cells [22] were grown in 175 cm^2 flasks in culture medium (90% DMEM, 10% FCS, 1 mM pyruvate, 20 units/mL penicillin G and 20 µg/mL streptomycin sulfate) in the humidified atmosphere of a Sanyo (Osaka, Japan) incubator with 10% CO_2. Approximately 80% confluent flasks were washed with 37°C warm phosphate-buffered saline (PBS, 10 mM potassium phosphate buffer pH 7.4, containing 150 mM NaCl). The cells were trypsinised with 0.01% trypsin in PBS for 5 min and centrifuged at 4°C for 5 min at 400g. Cells were resuspended in culture medium and 25,000 cells were seeded per well of 12-well culture dishes in 2 mL culture medium or 750,000 cells were seeded on 5 cm dishes in 5 mL culture medium. The cells were used for experiments 16-18 h after seeding. All data presented here were obtained on OLN-93 cells of passage numbers between 32 and 40.

Experimental Incubation

Cells were washed once with 2 mL (12-well dishes) or 5 mL (5 cm dishes) pre-warmed (37°C) culture medium. The main incubation of the cells was started by application of 1 mL (12-well dishes) or 5 mL (5 cm dishes) pre-warmed culture medium that contained iron chelators and/ or iron sources in the concentrations given in the figures and the table. After incubation of cells for the indicated incubation times at 37°C, the media were collected and the cells were washed twice with 2 mL (12-well dishes) or 5 mL (5 cm dishes) ice-cold PBS. Dry cells were stored frozen until further analysis of protein and iron contents. For analysis of the cellular activity of lactate dehydrogenase (LDH) the washed cells were immediately lysed with 1% Triton X-100 in culture medium. For cytochemical iron staining the cells were immediately fixated in 4% paraformaldehyde in 0.1 M potassium phosphate buffer (pH 7.4).

Iron Quantification and Perls' Iron Staining

The total iron content of media or cells was determined by a modification [23] of the ferrozine method previously described [24]. Ferric iron was visualized in cells by a modification of the histochemical Perls' stain [25, 26] as previously described [23].

Determination of Cell Viability, LDH Activity and Protein Content

Cell viability was analyzed by determining the activity of LDH in media and cell lysates using the microtiter plate assay described previously [27] with the modification that 20 or 40 μL of lysates or media were used. Extracellular LDH activity as indicator of a loss in cell viability was normalised to the sum of total (cellular plus extracellular) LDH found after a given treatment. Cellular LDH activity was calculated from the observed decrease in the NADH absorbance as described previously [28]. The protein content was determined after solubilisation of the cells in 0.5 M NaOH according to the Lowry method [29], using bovine serum albumin as a standard.

Gel Electrophoresis and Western Blotting

For immunoblot analysis, cells incubated on 5 cm dishes were scarped off in 1 mL PBS. After centrifugation (1 min; 12,000g), the cell pellet was lysed in water and 40 μg of lysate proteins were separated on a 12.5% polyacrylamide gel and electroblotted to a nitrocellulose membrane (GE Healthcare, Munich, Germany) as previously described [30]. Unspecific binding sites on the membrane were blocked with 5% milk powder in TBS (10 mM Tris/HCl, 150 mM NaCl, pH 7.3). The blocked membrane was incubated at 4°C over night with the ferritin antibody (1:250 in TBS) on a roller shaker (IDL, Nidderau, Germany). The membranes were washed with TBS containing 1% (v/v) Tween-20 and subsequently incubated with the peroxidase-conjugated secondary antibody (1:20,000 in TBS), washed with TBS and developed with the Amersham ECL advance Western blotting detection kit (GE Healthcare, Munich, Germany).

Presentation of Data

Experimental data are presented as means ± SD of values that were obtained in triplicates in 3 independent experiments on different passages of cells. Significance of differences between two sets of data was analyzed by unpaired t-test. Analysis of significance between groups of data was calculated by ANOVA followed by the Bonferroni *post-hoc* tests. $P > 0.05$ was considered as not significant.

Results

Effects of Iron Chelators on the Proliferation of OLN-93 Cells

OLN-93 cells proliferated efficiently during incubation for up to 72 h in serum-containing culture medium as demonstrated by the strong increases in cellular protein content from 11 ± 3 μg protein/well to 113 ± 23 μg protein/well (Fig. 1a) and in cellular LDH activity from 76 ± 5 nmol/(min × well) to 385 ± 18 nmol/(min × well) (Fig. 1b). In contrast, presence of 1,000 μM of the ferric iron chelator DFX under otherwise identical incubation conditions completely prevented the increases in protein content and LDH activity during incubation for 72 h (Fig. 1a, b). The morphology of the DFX-treated cells was not different to that of control cells (Fig. 1c–f), but the cell density of DFX-treated cultures (Fig. 1d, f) remained much lower than that of cultures which were incubated without the chelator (Fig. 1c, e). Thus, the differences in cellular protein content and cellular LDH activity reflect the density of the cells and were therefore considered as suitable indicators to investigate the consequences of iron chelators on the proliferation of OLN-93 cells. Since for DFX-treated cells no increase in the ratio of extracellular LDH activity to total (cells plus media) LDH activity was observed compared to that of cells incubated in the absence of DFX (data not shown), a DFX-induced loss in cell viability can be excluded as reason for the observed inhibition of cell proliferation.

Presence of DFX prevented the increases in cellular protein content and cellular LDH activity of OLN-93 cells in a concentration dependent manner. After 48 h of incubation, half-maximal effects were observed for DFX concentrations of about 50 μM (Fig. 2). Compared to controls (absence of DFX), none of these conditions caused any significantly elevated extracellular LDH activity (data not shown).

In addition to DFX, the membrane impermeable ferrous iron chelator bathophenanthroline disulfonate (BPS) prevented in a concentration of 500 μM the increases in cellular protein content and cellular LDH activity and caused only a moderate increase in extracellular LDH activity (Table 1). Also the membrane permeable ferrous iron chelators 1,10-phenanthroline and 2,2′-dipyridyl inhibited significantly the proliferation of OLN-93 cells compared to control cells that were treated with the solvent 1% DMSO in culture medium or to cells that were treated with the respective none-chelating analogs 4,7-phenanthroline or 4,4′-dipyridyl (Table 1). None of the membrane permeable iron chelators nor their structural analogs caused any significant increase in extracellular LDH activity compared to controls (Table 1), demonstrating that the viability of the cells was not affected by the experimental conditions used.

To test whether the inhibition of cell proliferation by DFX was indeed caused by iron deprivation, OLN-93 cells were incubated for 48 h with or without 100 μM DFX in the absence or presence of an excess of FAC (1,000 μM). In the absence of DFX, incubation of OLN-93 cells with FAC did not alter the cellular protein content compared to

Fig. 1 Consequences of an incubation of OLN-93 cells for the indicated incubation periods without (none) or with (1,000 μM) DFX on the cellular protein content (**a**), the cellular LDH activity (**b**) and the cell density (**c–f**)
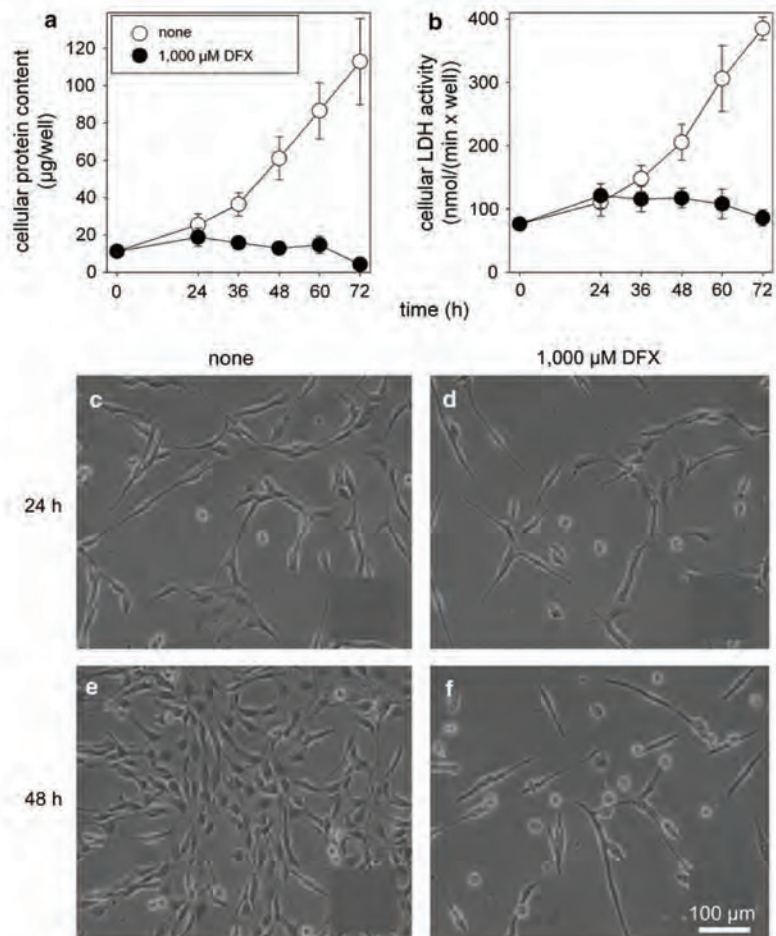
the FAC-free control (Fig. 3a), but significantly increased the cellular iron content per well (Fig. 3b) and the specific iron content of the cells (Fig. 3c). In contrast, presence of DFX in the absence of FAC prevented proliferation (Fig. 3a), whereas incubation of OLN-93 cells with a molar excess of FAC completely prevented the DFX-induced inhibition of proliferation (Fig. 3a), but did not significantly affect the amount of iron that was accumulated by the cells within 48 h (Fig. 3b, c).

Effects of Iron Supplementation on the Proliferation and the Ferritin Content of OLN-93 Cells

To test whether supplementation of the culture medium with additional iron would further accelerate or slow down the proliferation of OLN-93 cells, the cells were incubated without or with 100 or 1,000 μM iron in the form of the

soluble ferric iron complex FAC. Presence of FAC in these concentrations did not alter the increases in cellular protein content per well nor the cellular LDH activity compared to that of control cells during incubation for up to 72 h (Fig. 4). Also application of up to 300 μM of iron as $FeCl_2$, ferrous ammonium sulfate (FAS) or as iron oxide nanoparticles (Fe-NP) did not affect the increase in cellular protein content during a 48 h incubation of OLN-93 cells (Fig. 5a).

To test whether application of iron affects the cellular level of the iron storage protein ferritin, OLN-93 cells were incubated without or with FAC and the amount of cellular ferritin was analysed by Western blotting. OLN-93 cells that were incubated for 24 h without FAC hardly contained any detectable ferritin, whereas cells that were treated for 24 h with 500 μM FAC contained substantial amounts of ferritin, as indicated by the strong Western blot signal at a molecular mass of about 22 kDa (Fig. 6).
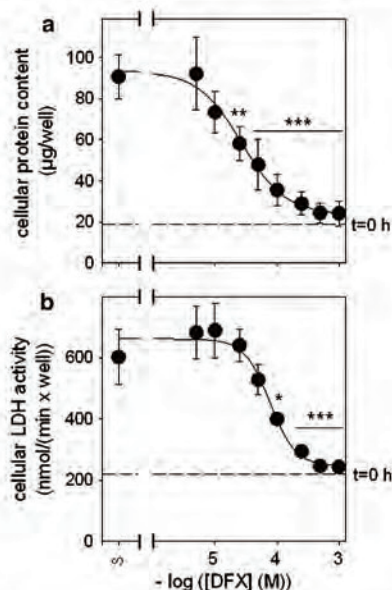
Fig. 2 Concentration dependency of the effects of DFX on the protein content (**a**) and the cellular LDH activity (**b**) of OLN-93 cell cultures. The cells were incubated for 48 h in the absence or presence of the indicated concentrations of DFX. The initial values for protein content (19 ± 3 µg/well) and cellular LDH activity (220 ± 85 nmol/min) are indicated by *dashed lines*. ANOVA was used for statistical analysis of the significance of differences compared to the data obtained for the absence of DFX (* $P < 0.05$, ** $P < 0.01$, and *** $P < 0.001$)

Iron Accumulation by OLN-93 Cells From Iron Salts and Iron Oxide Nanoparticles

After 48 h of incubation of OLN-93 cells in the presence of FAC, $FeCl_2$, FAS or Fe-NP, the cellular iron content was significantly increased in a concentration dependent manner from 10 ± 2 nmol/mg (absence of additional iron; 0 µM) to values of up to 159 ± 34 nmol/mg protein (300 µM Fe-NP) (Fig. 5b). Compared to the specific iron content of FAC-treated cells, the cellular iron contents of cells that had been exposed to 30, 100 or 300 µM iron in the form of Fe-NP was significantly increased by a factor between 2 and 3 (Fig. 5b). In contrast, incubation of the cells with the ferrous iron salts $FeCl_2$ or FAS resulted in a lower specific cellular iron content than those observed for FAC or Fe-NP treated cells, although this difference did not reach the level of significance (Fig. 5b).

To investigate potential interactions of Fe-NP and low molecular weight iron sources on OLN-93 cells, the cells were exposed to combinations of 300 µM iron as Fe-NP with 300 µM FAC, $FeCl_2$ or FAS. Neither the different iron sources alone nor their combinations affected the cellular protein content detected after 48 h of incubation (Fig. 7a) nor the viability of the cells (data not shown). Presence of FAC, $FeCl_2$ or FAS did not lower the strong accumulation of iron from Fe-NP (Fig. 7b). The specific iron contents of cells treated with Fe-NP plus low molecular weight iron salts were rather higher than those determined for cells that had been treated with Fe-NP alone (Fig. 7b), although the differences observed did not reach the level of significance.

Table 1 Effects of iron chelators on cellular protein content and LDH activity of OLN-93 cells

| Compound	Concentration (µM)	Cellular protein content (µg/well)	Cellular LDH activity (nmol/(min × well))	Extracellular LDH activity (nmol/(min × well))
None	0	91 ± 11	602 ± 91	31 ± 12
DFX	1,000	24 ± 6***	243 ± 3**	37 ± 1
BPS	500	26 ± 5***	320 ± 37**	54 ± 7*
None (DMSO)	0 (1%)	69 ± 21	630 ± 92	36 ± 7
4,7-phenanthroline	100	62 ± 8*	444 ± 52	41 ± 11
1,10-phenanthroline	100	19 ± 2***,###	229 ± 25***,##	37 ± 6
4,4'-dipyridyl	100	84 ± 13	622 ± 76	41 ± 15
2,2'-dipyridyl	100	23 ± 4***,###	267 ± 17***,##	44 ± 11

The cells were incubated without or with the indicated concentrations of chelators or non-chelating structural analogs for 48 h. The initial cellular protein content and cellular LDH activity were 19 ± 3 µg/well and 220 ± 85 nmol/(min × well), respectively. The incubation media with phenanthrolines or dipyridyls contained the solvent DMSO in culture medium in a final concentration of 1%. The data represent means $\pm$ SD of values that were obtained in three independent experiments. Statistical analysis of the significance of differences of data to those of the control condition (none or DMSO) were performed by ANOVA followed by Bonferroni post hoc test (* $P < 0.05$; ** $P < 0.01$; *** $P < 0.001$). Statistical analysis of the significance of differences of data from cells that were treated with the iron chelator 1,10-phenanthroline or 2,2'-dipyridyl and their respective none-chelating structural analogs was performed using the unpaired *t*-test (## $P < 0.01$; ### $P < 0.001$)
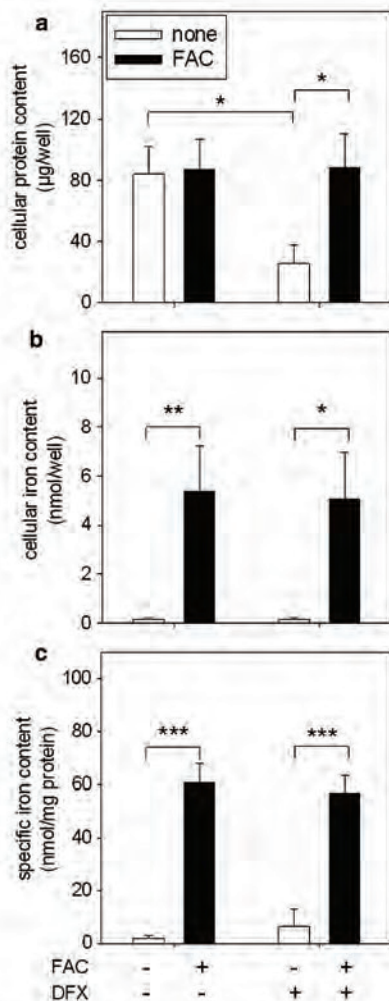
Fig. 3 Effects of DFX and/or FAC on the protein content (**a**), the cellular iron content (**b**) and the specific iron content (**c**) of OLN-93 cells. The cells were incubated for 48 h without or with 100 µM deferoxamine in the absence or presence of 1,000 µM FAC. The initial cellular protein content, the initial cellular iron content and the initial specific iron content were 25 ± 15 µg/well, 0.17 ± 0.08 nmol/well and 9.1 ± 7.8 nmol/mg, respectively. Statistical analysis of the significance of differences between two sets of data was performed by the unpaired t-test ($*\, P < 0.05$; $**\, P < 0.01$; $***\, P < 0.001$)

The strong cellular iron accumulation from Fe-NP was also visualized by the Perls' iron staining. OLN-93 cells that were incubated in the absence of iron did not show any detectable iron staining (Fig. 8a) and only some of the FAC-treated cells were slightly positive for iron after the staining (Fig. 8b), whereas Fe-NP-treated cells showed a dark staining which appeared to be localized predominantly in the cytosol around the nucleus (Fig. 8c).
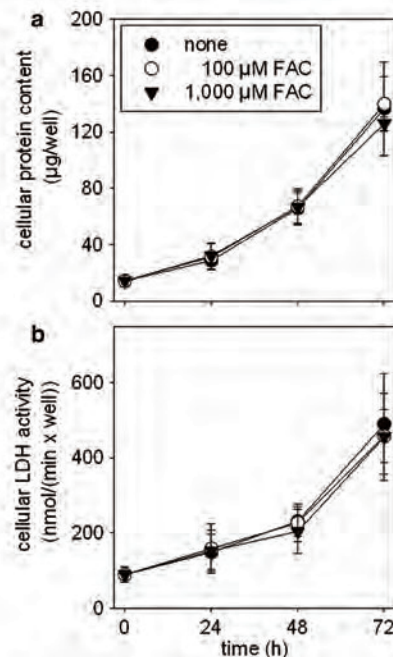
Fig. 4 Time dependent increases in cellular protein content (**a**) and cellular LDH activity (**b**) of OLN-93 cells after incubation without or with 100 or 1,000 µM FAC

Discussion

The consequences of an iron deprivation by iron chelators or of an iron supplementation of the incubation medium on the proliferation of OLN-93 cells was investigated. Under control conditions (absence of iron chelators and iron supplements), cell density, protein content and cellular LDH activity of OLN-93 cells that were incubated in serum-containing culture medium increased as expected from the known doubling time of 16–18 h for OLN-93 cells [22]. Therefore, cellular protein content and cellular LDH activity were considered as suitable indicators to quantify the proliferation of OLN-93 cells.

Ferrous and ferric iron chelators were applied to investigate whether the proliferation of OLN-93 cells depends on the availability of iron. All iron chelators applied prevented the proliferation of OLN-93 cells. Since chelator treatment did not substantially increase the extracellular LDH activity of OLN-93 cells, cell toxicity can be excluded as reason for the iron chelator-induced inhibition of proliferation.

The none-membrane permeable ferric iron chelator DFX completely prevented the increases in cellular protein content and in cellular LDH activity in a concentration dependent manner with half-maximal effects at a concentration of
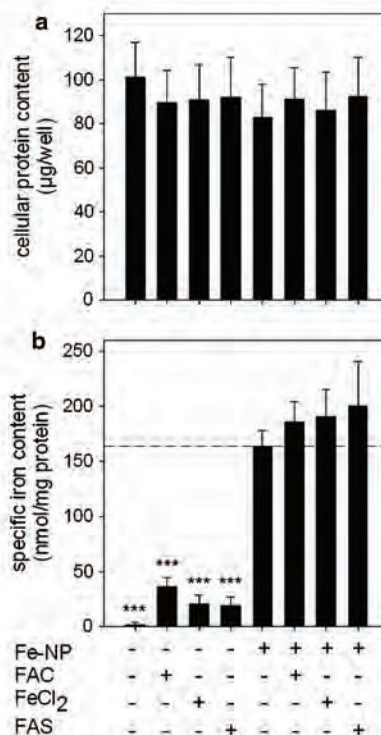
1265
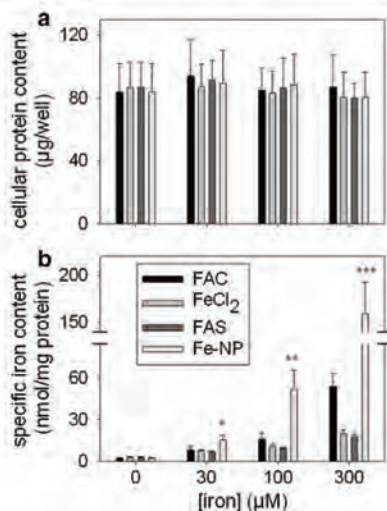
Fig. 5 Cellular protein content (**a**), and specific cellular iron content (**b**) of OLN-93 cells after 48 h incubation with the indicated concentrations of iron that were applied as FAC, $FeCl_2$, FAS or Fe-NP. The initial cellular protein content and the initial specific iron content were 25 ± 15 µg/well and 9.1 ± 7.8 nmol/mg, respectively. ANOVA was used for statistical analysis of the significance of differences compared to the data obtained from FAC-treated cells (* $P < 0.05$, ** $P < 0.01$, and *** $P < 0.001$)

Fig. 6 Western Blot analysis for the presence of ferritin in OLN-93 cells. The cells were incubated for 24 h without (none) or with 500 µM FAC before lysates of the cells were analysed for presence of ferritin

Fig. 7 Cellular protein content (**a**), and specific cellular iron content (**b**) of OLN-93 cells after 48 h incubation with iron (300 µM for each iron source indicated) that was applied as low molecular weight iron and/or as Fe-NP. The initial cellular protein content and the initial specific iron content were 18 ± 3 µg/well and 47.1 ± 44.7 nmol/mg, respectively. The *dashed line* in B indicates the specific iron content of cells that had been incubated with 300 µM Fe-NP in the absence of any low molecular weight iron. ANOVA was used for statistical analysis of the significance of differences compared to the data obtained from Fe-NP-treated cells (*** $P < 0.001$)

about 50 µM. This observation is consistent with literature data that demonstrate that DFX prevents cell proliferation of neuroblastoma cells [10], human B and T lymphocyte cell lines [5], T98 glioblastoma cells [4] and Jurkat cells [31], and demonstrates that also the proliferation of OLN-93 cells depends strongly on the availability of extracellular iron. The stability of the deferoxamine ferric iron complex is very high [32]. Therefore, DFX is likely to remove ferric iron from transferrin in the serum-containing culture medium, thereby preventing the access of OLN-93 cells to extracellular iron. The inhibition of cell proliferation by DFX was indeed due to iron deprivation, since a supplementation of the DFX-containing medium with an excess of FAC completely prevented the DFX-mediated inhibition of proliferation. This finding is consistent with literature data showing that the inhibition of the proliferation of human lymphocytes

by 100 µM DFX was also prevented by an excess of $FeCl_3$ [5].

In addition to DFX, the none-membrane permeable ferrous iron chelator BPS [33] as well as the membrane permeable ferrous iron chelators 1,10-phenanthroline and 2,2'-dipyridyl [34, 35] inhibited the proliferation of OLN-93 cells, while none-chelating structural analogs of the ferrous iron chelators had at best little effects on cell proliferation. BPS is considered as none-membrane permeable ferrous iron chelator and has been shown to limit iron accumulation in the human hepatoma cell line HuH7 [36] and iron-induced ferritin formation in CaCo-2 cells [37]. Also 1,10-phenanthroline and 2,2'-dipyridyl have been reported to prevent the uptake of iron into the human melanoma cell line SK-MEL-28 and in HuH7 cells [33, 36] and to prevent iron-mediated peroxide damage of cultured

🖄 Springer
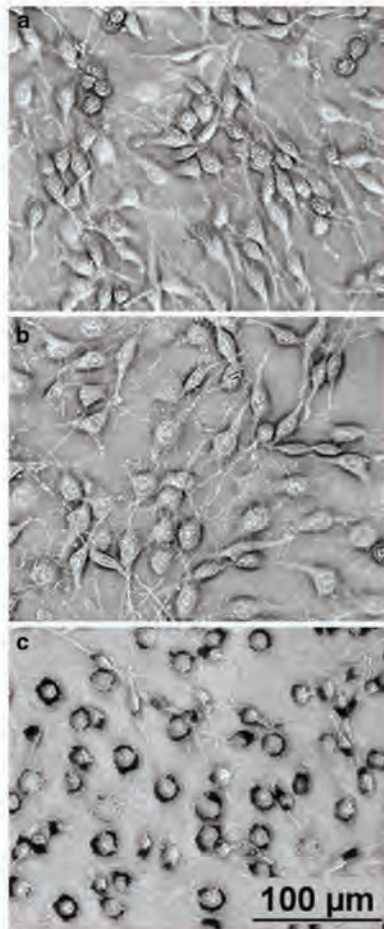
Fig. 8 Perls' iron staining of OLN-93 cells after incubation for 48 h without iron supplementation (**a**), or with 300 µM iron as FAC (**b**) or Fe-NP (**c**)

astrocytes [38]. Thus, the inhibition of proliferation of OLN-93 cells by BPS, 1,10-phenathroline and 2,2′-dipyridyl is likely to be a consequence of inhibition of iron uptake and/or chelation of intracellular iron that prevents the incorporation of iron in essential proteins. In this context, especially an impairment of the enzyme ribonucleotide reductase has to be considered, since the iron requirement of this enzyme that is essential for the generation of the deoxyribonucleoside triphosphates has been reported to be the reason for the observed inhibition of cell proliferation by iron chelators [6, 8, 9].

Results from the chelator experiments have clearly shown that the availability of iron is essential for the proliferation of OLN-93 cells. To test whether additional iron in the culture medium could accelerate cell proliferation,

various iron sources were added to the medium. As reported before for iron-exposed human lymphocytes [5], supplementation of culture medium of OLN-93 cells with FAC in a concentration of up to 1 mM did not further accelerate the increases in cellular protein content or cellular LDH activity of the cultures, nor did the application of ferrous iron salts or Fe-NP alter the proliferation of OLN-93 cells. These results demonstrate that serum-containing culture medium contains sufficient amounts of available iron to allow maximal proliferation of OLN-93 cells.

Incubation of OLN-93 cells with iron in low molecular weight form (FAC, FAS, $FeCl_2$) or as Fe-NP strongly increased the specific iron content of the cells in a concentration dependent manner, indicating that these cells have efficient uptake mechanisms for different extracellular iron sources. In addition, since the accumulation of cellular iron was neither accompanied by a loss in cell viability nor by a compromised proliferation, the accumulated iron appears to have been safely stored. Indeed, a strong increase in the cellular content of the iron storage protein ferritin was observed for OLN-93 cells that had been treated with FAC. This result suggests that OLN-93 cells store accumulated iron efficiently in redox inactive form in ferritin. This upregulation of cellular ferritin content is likely to protect the OLN-93 cells against iron-mediated toxicity as it has previously been reported for iron-treated astrocytes [30].

Iron can be transported into cells by transferrin-dependent or transferrin-independent mechanisms [15]. Since serum was present under the conditions used here, low molecular weight iron is likely to be bound to serum transferrin and subsequently taken up after binding to the transferrin receptor that is present in OLN-93 cells [39]. In addition to transferrin-dependent uptake, iron can be taken up in glial cells by various transferrin-independent mechanisms [3]. Indeed, also OLN-93 cells have been reported to accumulate iron after exposure to $FeSO_4$ [39]. One transporter that could be involved in iron accumulation from low molecular weight ferrous iron is DMT1 which is expressed in OLN-93 cells [39]. Whether this transporter contributes to the uptake of iron from exogenous ferrous iron under the conditions used here (48 h incubation) remains to be elucidated. Since ferrous iron is quickly oxidised to ferric iron in physiological media [40, 41], the iron applied as $FeCl_2$ or FAS to OLN-93 cells is likely to become quickly oxidised to ferric iron that subsequently may bind to transferrin. Alternatively, a DMT1-independent ferrous iron uptake [41] or a ferric iron uptake perhaps via β-integrin-mobilferrin or by a trivalent cation-specific transporter [42, 43] could contribute to the observed iron accumulation in OLN-93 cells from low molecular weight iron. The ability of OLN-93 cells to accumulate efficiently extracellular iron from various iron sources may reflect the

123

1267

ability of oligodendrocyte precursors to accumulate iron by multiple mechanisms. Recently, it has been suggested that oligodendrocyte precursor cells take up and store iron during proliferation and differentiation [44]. This could explain why oligodendrocytes in brain slices contain the highest level of stainable iron [13, 14].

Superparamagnetic iron oxide nanoparticles are currently under extensive investigations due to their application as contrast agents for magnetic resonance imaging in brain and for drug delivery to the brain [45–47]. However, so far little is known on the consequences of a treatment of different types of brain cells with such particles. Exposure of OLN-93 cells to Fe-NP did not cause any detectable loss in cell viability, change in morphology or impaired proliferation, although OLN-93 cells accumulated iron from Fe-NP more efficiently than from low molecular weight iron sources. This observation is consistent with results obtained for astrocyte-rich primary cultures [23]. The mechanisms involved in the accumulation of Fe-NP by cells have not been studied in detail so far. Presence of Fe-NP in intracellular vesicles suggests that endocytotic pathways are involved in the uptake of Fe-NP into cells [23, 48], while various other mechanisms have been reported to contribute to the uptake of low molecular weight iron into cells (see above). The observation that the iron accumulation of OLN-93 cells from Fe-NP and low molecular weight iron sources appears to be additive suggests that these cells possess independent mechanisms that are involved in the iron accumulation of iron from Fe-NP and from low molecular weight iron sources.

Perls' staining of OLN-93 cells after 48 h incubation with Fe-NP showed intense dark staining that was located around the nucleus of the cells. Such a perinuclear localisation of accumulated iron oxide nanoparticles has been shown for PC12 cells by transmission electron microscopy after exposure to anionic iron oxide nanoparticles and by a Prussian blue staining of Schwann cells and olfactory ensheathing cells incubated with dextran-coated superparamagnetic iron oxide [49, 50]. The localisation of the Perls' staining suggests that OLN-93 cells are able to efficiently take up intact Fe-NP or the iron from these particles. In contrast to cells that were exposed to Fe-NP, the iron staining of FAC-treated OLN-93 cells was at best weak. This is most likely due to insufficient sensitivity of the Perls' method used [23, 51].

In summary, iron chelators strongly inhibit the proliferation of OLN-93 cells in a time and concentration dependent manner demonstrating that the availability of iron is a critical component for the proliferation of these cells. In contrast, excess of extracellular iron does not accelerate proliferation nor does it damage the cells, although large amounts of iron are accumulated by OLN-93 cells. As a reaction to iron exposure OLN-93 cells increase their

content of ferritin, which stores iron efficiently in a redox-inactive form [30], thereby preventing iron-mediated oxidative damage. The strongest accumulation of iron in OLN-93 cells was observed after exposure of the cells to Fe-NP. The mechanism responsible for this accumulation is currently not clear, nor is known whether the accumulated Fe-NP is available for the cells, for example to support proliferation. If cells are able to utilize the iron from accumulated Fe-NP, such nanoparticles could be an interesting source to provide the cells with a depot of iron in a non-toxic form.

References

1. Galaris D, Skiada V, Barbouti A (2008) Redox signaling and cancer: the role of "labile" iron. Cancer Lett 266:21–29
2. Kruszewski M (2003) Labile iron pool: the main determinant of cellular response to oxidative stress. Mutat Res 531:81–92
3. Dringen R, Bishop GM, Koeppe M et al (2007) The pivotal role of astrocytes in the metabolism of iron in the brain. Neurochem Res 32:1884–1890
4. Brodie C, Siriwardana G, Lucas J et al (1993) Neuroblastoma sensitivity to growth inhibition by deferrioxamine: evidence for a block in G1 phase of the cell cycle. Cancer Res 53:3968–3975
5. Lederman HM, Cohen A, Lee JW et al (1984) Deferoxamine: a reversible S-phase inhibitor of human lymphocyte proliferation. Blood 64:748–753
6. Green DA, Antholine WE, Wong SJ et al (2001) Inhibition of malignant cell growth by 311, a novel iron chelator of the pyridoxal isonicotinoyl hydrazone class: effect on the R2 subunit of ribonucleotide reductase. Clin Cancer Res 7:3574–3579
7. Cooper CE, Lynagh GR, Hoyes KP et al (1996) The relationship of intracellular iron chelation to the inhibition and regeneration of human ribonucleotide reductase. J Biol Chem. 271:20291–20299
8. Thelander L, Graslund A, Thelander M (1983) Continual presence of oxygen and iron required for mammalian ribonucleotide reduction: possible regulation mechanism. Biochem Biophys Res Commun 110:859–865
9. Nyholm S, Mann GJ, Johansson AG et al (1993) Role of ribonucleotide reductase in inhibition of mammalian cell growth by potent iron chelators. J Biol Chem. 268:26200–26205
10. Dayani PN, Bishop MC, Black K et al (2004) Desferoxamine (DFO)-mediated iron chelation: rationale for a novel approach to therapy for brain cancer. J Neurooncol 67:367–377
11. Richardson DR (1997) Potential of iron chelators as effective antiproliferative agents. Can J Physiol Pharmacol 75:1164–1180
12. Yu Y, Kovacevic Z, Richardson DR (2007) Tuning cell cycle regulation with an iron key. Cell Cycle. 6:1982–1994
13. Connor JR, Menzies SL (1996) Relationship of iron to oligodendrocytes and myelination. Glia. 17:83–93
14. Benkovic SA, Connor JR (1993) Ferritin, transferrin, and iron in selected regions of the adult and aged rat brain. J Comp Neurol 338:97–113

15. Garrick MD, Garrick LM (2009) Cellular iron transport. Biochim Biophys Acta 1790:309–325

16. Hulet SW, Menzies S, Connor JR (2002) Ferritin binding in the developing mouse brain follows a pattern similar to myelination and is unaffected by the jimpy mutation. Dev Neurosci 24:208–213

17. Todorich B, Pasquini JM, Garcia CI et al (2009) Oligodendro-cytes and myelination: the role of iron. Glia. 57:467–478

18. Song N, Jiang H, Wang J et al (2007) Divalent metal transporter 1 up-regulation is involved in the 6-hydroxydopamine-induced ferrous iron influx. J Neurosci Res 35:3118–3126

19. Burdo JR, Menzies SL, Simpson IA et al (2001) Distribution of divalent metal transporter 1 and metal transport protein 1 in the normal and Belgrade rat. J Neurosci Res 66:1198–1207

20. Todorich B, Zhang X, Slagle-Webb B et al (2008) Tim-2 is the receptor for H-ferritin on oligodendrocytes. J Neurochem 107:1495–1505

21. Hulet SW, Hess EJ, Debinski W et al (1999) Characterization and distribution of ferritin binding sites in the adult mouse brain. J Neurochem 72:868–874

22. Richter-Landsberg C, Heinrich M (1996) OLN-93: a new per-manent oligodendroglia cell line derived from primary rat brain glial cultures. J Neurosci Res 45:161–173

23. Geppert M, Hohnholt M, Gaetjen L et al (2009) Accumulation of iron oxide nanoparticles by cultured brain astrocytes. J Biomed Nanotechnol. 5:285–293

24. Riemer J, Hoepken HH, Czerwinska H et al (2004) Colorimetric ferrozine-based assay for the quantitation of iron in cultured cells. Anal Biochem 331:370–375

25. Bishop GM, Robinson SR (2001) Quantitative analysis of cell death and ferritin expression in response to cortical iron: impli-cations for hypoxia-ischemia and stroke. Brain Res 907:175–187

26. Moos T, Mollgard K (1993) A sensitive post-DAB enhancement technique for demonstration of iron in the central nervous system. Histochemistry. 99:471–475

27. Dringen R, Kussmaul L, Hamprecht B (1998) Detoxification of exogenous hydrogen peroxide and organic hydroperoxides by cultured astroglial cells assessed by microtiter plate assay. Brain Res Brain Res Protoc. 2:223–228

28. Schmidt MM, Dringen R (2009) Differential effects of iodoa-cetamide and iodoacetate on glycolysis and glutathione metabo-lism of cultured astrocytes. Front Neuroenergetics. 1:1–10

29. Lowry OH, Rosebrough NJ, Farr AL et al (1951) Protein mea-surement with the Folin phenol reagent. J Biol Chem. 193:265–275

30. Hoepken HH, Korten T, Robinson SR et al (2004) Iron accu-mulation, iron-mediated toxicity and altered levels of ferritin and transferrin receptor in cultured astrocytes during incubation with ferric ammonium citrate. J Neurochem 88:1194–1202

31. Gharagozloo M, Khoshdel Z, Amirghofran Z (2008) The effect of an iron (III) chelator, silybin, on the proliferation and cell cycle of Jurkat cells: a comparison with desferrioxamine. Eur J Pharmacol 589:1–7

32. Keberle H (1964) The biochemistry of desferrioxamine and its relation to iron metabolism. Ann N Y Acad Sci 119:758–768

33. Richardson DR, Baker E (1994) Two saturable mechanisms of iron uptake from transferrin in human melanoma cells: the effect of transferrin concentration, chelators, and metabolic probes on transferrin and iron uptake. J Cell Physiol 161:160–168

34. Ware JL, Paulson DF, Webb KS (1984) 1, 10-Phenanthroline reversibility inhibits proliferation of two human prostate

carcinoma cell lines (PC-3 and DU145). Biochem Biophys Res Commun 124:538–543

35. Szuts D, Krude T (2004) Cell cycle arrest at the initiation step of human chromosomal DNA replication causes DNA damage. J Cell Sci 117:4897–4908

36. Trinder D, Morgan E (1998) Mechanisms of ferric citrate uptake by human hepatoma cells. Am J Physiol 275:G279–G286

37. Zhu L, Glahn RP, Yeung CK et al (2006) Iron uptake by Caco-2 cells from NaFeEDTA and FeSO4: Effects of ascorbic acid, pH, and a Fe(II) chelating agent. J Agric Food Chem 54:7924–7928

38. Liddell JR, Hoepken HH, Crack PJ et al (2006) Glutathione peroxidase 1 and glutathione are required to protect mouse astrocytes from iron-mediated hydrogen peroxide toxicity. J Neurosci Res 84:578–586

39. Brand A, Schonfeld E, Isharel I et al (2008) Docosahexaenoic acid-dependent iron accumulation in oligodendroglia cells pro-tects from hydrogen peroxide-induced damage. J Neurochem 105:1325–1335

40. Schroder I, Johnson E, de Vries S (2003) Microbial ferric iron reductases. FEMS Microbiol Rev 27:427–447

41. Tulpule K, Robinson SR, Bishop GM et al (2010) Uptake of ferrous iron by cultured rat astrocytes. J Neurosci Res 88:563–571

42. Attieh ZK, Mukhopadhyay CK, Seshadri V et al (1999) Cerulo-plasmin ferroxidase activity stimulates cellular iron uptake by a trivalent cation-specific transport mechanism. J Biol Chem. 274:1116–1123

43. Conrad ME, Umbreit JN, Moore EG et al (2000) Separate path-ways for cellular uptake of ferric and ferrous iron. Am J Physiol Gastrointest Liver Physiol. 279:G767–G774

44. Schonberg DL, McTigue DM (2009) Iron is essential for oligo-dendrocyte genesis following intraspinal macrophage activation. Exp Neurol 218:64–74

45. Islam T, Josepbson L (2009) Current state and future applications of active targeting in malignancies using superparamagnetic iron oxide nanoparticles. Cancer Biomark. 5:99–107

46. Ge Y, Zhang Y, Xia J et al (2009) Effect of surface charge and agglomerate degree of magnetic iron oxide nanoparticles on KB cellular uptake in vitro. Colloids Surf B Biointerfaces. 73:294–301

47. Weinstein JS, Varallyay CG, Dosa E et al (2010) Superpara-magnetic iron oxide nanoparticles: diagnostic magnetic resonance imaging and potential therapeutic applications in neurooncology and central nervous system inflammatory pathologies, a review. J Cereb Blood Flow Metab 30:15–35

48. Xie J, Wang J, Niu G et al (2010) Human serum albumin coated iron oxide nanoparticles for efficient cell labeling. Chem Com-mun (Camb). 46:433–435

49. Pisanic TR 2nd, Blackwell JD, Shubayev VI et al (2007) Nano-toxicity of iron oxide nanoparticle internalization in growing neurons. Biomaterials 28:2572–2581

50. Dunning MD, Lakatos A, Loizou L et al (2004) Superparamag-netic iron oxide-labeled Schwann cells and olfactory ensheathing cells can be traced in vivo by magnetic resonance imaging and retain functional properties after transplantation into the CNS. J Neurosci 24:9799–9810

51. Falangola MF, Lee SP, Nixon RA et al (2005) Histological co-localization of iron in Abeta plaques of PS/APP transgenic mice. Neurochem Res 30:201–205

2.1.3.   Publication/Manuscript 2

Hohnholt MC, Geppert M, Dringen R

Mobilization of iron from iron oxide nanoparticles in oligodendroglial cells.

Revised manuscript submitted for publication

Contribution of Michaela C. Hohnholt:

- Performance of experiments for Figs. 1A, C and E, and Figs. 2-7.
- Preparation of the first version of the manuscript.

Mark Geppert kindly provided the iron oxide nanoparticles and performed the MTT assay shown in Fig. 1D, the cell counting of PI-positive cells and H33342-stained cell nuclei for Figs. 1B and F as well as the counting of nigrosin-positive cells.

AB-11-403, revised version

Mobilization of iron from iron oxide nanoparticles in oligodendroglial cells

Michaela C. Hohnholt[a,b], Mark Geppert[a,b] and Ralf Dringen[a,b,c,*]

[a]Centre for Biomolecular Interactions Bremen, University of Bremen, PO. Box 330440, D-28334 Bremen, Germany.

[b]Centre for Environmental Research and Sustainable Technology, Leobener Straße, D-28359 Bremen, Germany.

[c]School of Psychology & Psychiatry, Monash University, Wellington Rd., Clayton, Victoria 3800, Australia.

Email:

Michaela C. Hohnholt: hohnholt@uni-bremen.de

Mark Geppert: mgeppert@uni-bremen.de

*Corresponding author:

Dr. Ralf Dringen

Centre for Biomolecular Interactions Bremen

University of Bremen

PO. Box 330440

D-28334 Bremen

Germany

Tel: +49-421-218-63230

Fax: +49-421-218-63244

Email: ralf.dringen@uni-bremen.de

Abstract

Magnetic iron oxide nanoparticles (IONP) are considered and used for many neurobiological approaches, although little is known so far on the fate of such particles in brain cells. To address these questions, we have exposed oligodendroglial OLN-93 cells to dimercaptosuccinate-coated IONP. Treatment of the cells strongly increased the specific cellular iron content proportional to the concentrations of IONP applied (0 to 1000 µM total iron as IONP) up to 300fold, but did not cause any acute cytotoxicity or induce oxidative stress. To investigate the potential of OLN-93 cells to liberate iron from the accumulated IONP, we have studied the upregulation of the iron storage protein ferritin and the cell proliferation as cellular processes that depend on the availability of low molecular weight iron. Presence of IONP caused a concentration-dependent increase in the amount of cellular ferritin and partially bypassed the inhibition of cell proliferation by the iron chelator deferoxamine. These data demonstrate that viable OLN-93 cells efficiently take up IONP and that these cells are able to use iron liberated from accumulated IONP for their metabolism.

Keywords: nanoparticles; iron; oligodendrocytes; ferritin; proliferation

1 Introduction

Magnetic iron oxide nanoparticles (IONP) are considered for various neurobiological and medical applications [1]. They have been used as contrast agent [2], as carriers for drug delivery [3], for cancer treatment by magnetic hyperthermia [4] and for neurotransplantation of magnetically labeled oligodendrocyte progenitors [5]. Recently was reported that IONP are able to cross the blood brain barrier and to enter the brain [6]. Therefore, the consequences of an application of IONP to the body and particularly to the brain are of special interest. IONP have the potential to harm cells, since they contain large amounts of iron. Iron-dependent formation of reactive oxygen species (ROS) by the Fenton reaction has been considered for the surface of nanoparticles [7]. However, such processes are likely to be accelerated, if iron is liberated from accumulated IONP, since low molecular weight iron catalyzes efficiently the generation of ROS [8, 9]. Such processes are important to be considered in the light of the reported high bioavailability of iron in nanosized iron oxide particles [10].

Iron is an essential cofactor for enzymes of the respiratory chain as well as for DNA synthesis and cell proliferation [11, 12]. Accordingly, removal of iron by application of iron chelators inhibits cell proliferation in a process that is bypassed by application of an excess of iron [13, 14]. In brain, iron-dependent processes appear to be especially important for oligodendrocytes, since these cells contain among the different types of brain cells the highest amount of iron [15, 16]. Since oligodendrocytes have a highly oxidative energy metabolism, these cells are considered as especially vulnerable to excess of iron which increases oxidative stress via the Fenton reaction [17, 18]. Thus, sufficient uptake and appropriate storage of iron by oligodendroglial cells is crucial to allow iron-dependent reactions while avoiding iron-catalyzed generation of ROS.

Oligodendroglial cell lines have been used to investigate the biocompatibility of nanoparticles, including IONP [13, 19, 20]. Such cells accumulate citrate-coated IONP and magnetodendrimers, but are not acutely damaged by the exposure to such particles [13, 20]. Iron can be released from IONP [21-23] and has the potential to harm cells, predominantly by the iron-catalyzed formation of ROS [22, 23]. Alternatively, IONP-derived low molecular weight iron can support iron-dependent cellular processes [24] and can also be stored in ferritin [25, 26]. For brain cells, no information is currently available on the intracellular metabolism of IONP, i.e., whether low molecular iron is liberated from accumulated IONP, is stored in ferritin and/or can be used for the cellular metabolism. To address such questions for oligodendroglial cells, we have used the oligodendroglial cell line OLN-93 [27] as model

system. Here we report that even high concentrations of dimercaptosuccinate (DMSA)-coated IONP are not toxic to OLN-93 cells, that these cells efficiently take up IONP and that they liberate iron from the accumulated nanoparticles and use it for their metabolism.

2 Materials and methods

2.1 Materials

Fetal calf serum, penicillin/streptomycin and trypsin solution were purchased from Biochrom (Berlin, Germany). Dulbecco´s modified Eagle´s medium was from Invitrogen (Karlsruhe, Germany). Deferoxamine (DFX), dihydrorhodamine 123, dimercaptosuccinic acid (DMSA), neocuproine, sodium ascorbate, sulfosalicylic acid, Tris, 5,5´-dithio-bis(2-nitrobenzoic acid), 3-(4,5-dimethylthiazol-2-yl)-2,5-diphenyltetrazoliumbromide (MTT), nigrosin and the mouse anti-α-tubulin antibody were obtained from Sigma (Steinheim, Germany). Bovine serum albumin, NADH and NADPH were purchased from Applichem (Darmstadt, Germany). Glutathione reductase and glutathione disulfide (GSSG) were purchased from Roche Diagnostics (Mannheim, Germany). Glucose was from Serva (Heidelberg, Germany) and saccharose and dimethyl sulfoxide (DMSO) from Janssen Chimica (Geel, Belgium). The goat anti-L-ferritin antibody, horse radish peroxidase-conjugated anti-goat-IgG and anti-mouse-IgG were from Dianova (Hamburg, Germany). All other chemicals of the highest purity available were from Fluka (Buchs, Switzerland), Merck (Darmstadt, Germany) or Riedel-deHaen (Seelze, Germany). 96-well microtitre plates and 5 cm dishes were from Nunc (Roskilde, Denmark) and 12-well cell culture plates from Greiner Bio-one (Frickenhausen, Germany).

The IONP used in the present report were synthesized, coated with DMSA and characterized as described previously [28, 29]. The obtained agglomerates of small IONP (diameter of 5-20 nm) have a monomodal particle size distribution with an average hydrodynamic diameter of around 60 nm. Dispersed in incubation buffer, the DMSA-coated IONP have a zeta-potential of -26 ± 3 mV [29]. Excess of unbound coating material was removed by centrifugation and redispersion of the particles. Prior to the dilution in culture medium, IONP were filtered with a 0.2 µm syringe sterile filter (Sartorius, Goettingen, Germany). The given concentrations of DMSA-coated IONP represent the concentrations of total iron contained in the particles applied and not the concentrations of particles.

2.2 Cell cultures and experimental incubation

OLN-93 cells (passage numbers between 32 and 40) were grown as described previously [30]. For experiments, 25,000 cells were seeded in wells of 12-well plates or 250,000 cells in 5 cm dishes. 16 to 18 hours after seeding, the cells were washed with 1 mL (12-well dishes) or with

5 mL (5 cm dishes) pre-warmed (37°C) culture medium (Dulbecco´s modified Eagle´s medium with 10% fetal calf serum, 20 U/mL of penicillin G and 20 µg/mL of streptomycin sulphate) and incubated in 1 mL (12-well dishes) or 5 mL (5 cm dishes) culture medium without or with DMSA-coated IONP and/or DFX. The incubations were terminated by washing the cells twice with 2 mL (12-well dishes) or 5 mL (5 cm dishes) ice-cold phosphate buffered saline (PBS; 10 mM potassium phosphate buffer, 150 mM NaCl, pH 7.4). If not stated otherwise, experiments were performed on cultures in wells of 12-well dishes.

2.3 Determination of cell viability

Cell viability was analyzed by determining the extracellular activity of the cytosolic enzyme lactate dehydrogenase (LDH) as well as the permeability of the cell membrane for propidium iodide or nigrosin. LDH activity in cell lysates and media was determined as described previously [31] in 40 µL of samples. Cell lysates were obtained by incubation of the cells in 1 mL 1% (w/v) Triton X-100 in culture medium for 30 min. Extracellular LDH activity was normalized to the total activity of LDH in cells plus medium. In cell lysates, LDH activity was not lowered during incubation for up to 48 h at 37°C in the incubator (data not shown). The membrane integrity was tested by staining with the membrane-impermeable dye propidium iodide (PI) as described previously [32]. After experimental incubations, the cells were washed twice with incubation buffer (IB; 20 mM HEPES, 145 mM NaCl, 1.8 mM CaCl$_2$, 5.4 mM KCl, 1 mM MgCl$_2$ and 5 mM glucose, pH 7.4) and incubated for further 15 min with 5 µM PI and 10 µM of the membrane-permeable dye H33342 (to stain all cell nuclei) in IB at 37°C. Subsequently the cells were washed three times with PBS and analyzed immediately for fluorescence on a Nikon (Düsseldorf, Germany) TS2000U microscope. Nigrosin staining of cells was performed according to a previously described method [33]. The cells were washed twice with IB and subsequently incubated with the membrane-impermeable black dye nigrosin (0.25% w/v) for 5 min at 37°C. Excess of the dye was removed by washing three times with IB and the cells were immediately analyzed by microscopy. The number of nigrosin-positive cells as percent of the total number of cells was evaluated. The number of nigrosin-positive cells per mm^2 was counted on phase contrast pictures taken at 200fold magnification and covering an area of 0.277 mm^2. From each of the three experiments performed three wells were analyzed.

2.4 Determination of cell proliferation

Cell proliferation was determined by quantitation of the cellular protein content and the cellular LDH activity per well as previously described [13] as well as by counting cell nuclei and by quantifying the ability of the cells to reduced MTT. Protein content was determined according to the Lowry method [34] using bovine serum albumin as a standard. The activity of cellular LDH was determined as described above in cell lysates that were obtained by incubation of the cells in 1 mL 1% Triton X-100. The MTT assay was performed as described recently [32]. Briefly, after experimental incubations, the cells were washed two times with 1 mL IB and incubated for 3 h at 37°C in 1 mL IB containing 2 mg/mL MTT. After washing twice with 1 mL IB, the cells were lysed in 0.5 mL DMSO for 30 min on a shaker. The absorbance at 540 nm was measured in 300 µL of cell lysate in a well of a microtiter plate. The number of cell nuclei per mm^2 was counted on pictures (taken at 200fold magnification and covering an area of 0.277 mm^2) obtained from H33342-stained cultures. From each of the three experiments performed three wells were analyzed.

2.5 Iron quantitation and cytochemical Perls´ iron staining

The iron content of cells before and after treatment with IONP was quantified using a modification [28] of the ferrozine method described previously [35]. Intracellular iron was visualized by the cytochemical Perls´ staining as described previously [28].

2.6 ROS staining

To detect intracellular ROS in OLN-93 cells, rhodamine 123 staining was used by a modification of a previously published method [8]. Following the experimental incubations, OLN-93 cells were washed twice with IB at 37°C and incubated for 3 h at 37°C in 0.5 mL IB containing 5 µg/mL dihydrorhodamine 123 and 10 µM H33342. After washing the cells twice with IB, the cells were fixed with 4% (w/v) paraformaldehyde in 0.1 M phosphate buffer (pH 7.2) at room temperature. Cells were subsequently washed three times with PBS and analyzed for fluorescence.

2.7 Glutathione quantification

Total cellular glutathione (GSx = amount of glutathione (GSH) plus twice the amount of GSSG) and GSSG were determined by the colorimetric Tietze assay in microtitre plates as

described previously [36]. The GSH content was calculated as difference between the values determined for GSx and GSSG.

2.8 Gel electrophoresis and Western blot

For immunoblot analysis, cells incubated on 5 cm dishes were scraped of the dish in 2 mL PBS. After centrifugation (1 min, 12,000 g), the cell pellet was lysed in water and the proteins of the lysate were separated on a 12.5% polyacrylamide gel and electroblotted to a nitrocellulose membrane as previously described [30]. After incubation over night at 4°C with goat anti-L-ferritin antibody (1:500) or mouse anti-α-tubulin antibody (1:5,000) diluted in TBST (10 mM Tris/HCl, 150 mM NaCl, 0.1% (w/v) Tween 20, pH 7.3) containing 5% (w/v) milk powder, the membrane was washed three times in TBST and incubated for 1 h with horse radish peroxidase-conjugated anti-goat-IgG (1:10,000) or anti-mouse-IgG (1:20,000) diluted in TBST/5% milk powder. After washing with TBST, protein bands were visualized by enhanced chemiluminescence (GE Healthcare, Buckinghamshire, UK).

2.9 Presentation of data

The data shown were obtained in at least three independent experiments on three different passages of OLN-93 cells. The results are presented as means ± standard deviation, if not stated otherwise. Pictures in figures that show stainings are from representative experiments that were reproduced at least twice with comparable results. Significance of differences between two sets of data was analyzed by the t-test and significance of differences between groups of data was analyzed by ANOVA followed by the Bonferroni post hoc test. p>0.05 was considered as not significant.

3 Results

3.1 Consequences of an exposure to IONP on the viability of OLN-93 cells

To test for the consequences of a treatment with IONP, OLN-93 cells were incubated in serum-containing medium for up to 72 h in the absence or the presence of IONP in concentrations of up to 1000 μM total iron. The viability of the cells was not affected by the presence of IONP as indicated by the absence of any significant increase in extracellular LDH activity (Fig. 1A). This was confirmed by the absence of any significant increase in the number of nigrosin-positive (data not shown) or PI-positive cells (Fig. 1B; Fig. 2) after exposure of OLN-93 cells for up to 72 h to IONP, while cells treated with Triton X-100 as positive control became PI-positive (Fig. 2I,J). Comparison of the total fluorescence intensity per picture of H33342-stained cells after incubation without or with IONP or Triton X-100 for the three independent experiments performed revealed no significant differences between the conditions used (data not shown).

3.2 Effects of IONP on the proliferation of OLN-93 cells

The cellular protein content, the MTT reduction capacity, the cellular LDH activity and the number of cell nuclei of IONP-treated OLN-93 cells were quantified as indicators of cell proliferation. In the absence of IONP, the cells proliferated as indicated by the strong increases in protein content per well (Fig. 1C), in the MTT reduction capacity (Fig. 1D), in the cellular LDH activity (Fig. 1E) and in the number of cell nuclei (Fig. 1F). Presence of IONP in concentrations of up to 1000 μM did not significantly affect these parameters during incubations for up to 72 h. However, at least for cells exposed for 48 h or 72 h to 1000 μM IONP proliferation appears to be to some extend lowered as demonstrated by around 20% lower numbers for all parameters investigated (Fig. 1C-F). However, these alterations did not reach the level of significance compared to the values obtained for control cells that had been incubated without IONP.

3.3 Increased iron contents of IONP-exposed OLN-93 cells

OLN-93 cells strongly accumulated iron from IONP as shown by a concentration-dependent increase in the specific cellular iron contents from 5 ± 5 nmol/mg protein (control cells incubated without IONP) to values of 36 ± 9 nmol/mg, 184 ± 37 nmol/mg and 957 ± 179 nmol/mg protein determined for cells that had been incubated with 100 μM, 300 μM and

1000 µM IONP for 24 h. Exposure of cells for 48 h resulted in similar specific cellular iron contents (Fig. 3A). The specific cellular iron content increased proportional to the concentrations of IONP applied with correlation coefficients of 0.988 (24 h) and 0.993 (48 h).

The accumulated iron of OLN-93 cells after exposure to IONP for 48 h was visualized by the cytochemical Perls´ staining (Fig. 4). While OLN-93 cells that had been incubated without IONP did hardly show any Perls´ detectable cellular iron (Fig. 4A), the dark Perls´ staining became more intense for cells exposed to increasing concentrations of IONP and was predominantly localized around the cell nuclei (Fig. 4B-D).

3.4 IONP-exposure induces synthesis of the iron storage protein ferritin

To test whether the strong iron accumulation by OLN-93 cells after application of IONP (Fig. 3A; Fig. 4) is accompanied by the synthesis of the iron storage protein ferritin, the cellular ferritin content was investigated by Western blotting after incubation of OLN-93 cells for 48 h in the absence or presence of IONP. While OLN-93 cells that had been incubated without IONP contained hardly any detectable ferritin, the intensity of the ferritin signal was strongly increased in a concentration-dependent manner after exposure of the cells to IONP (Fig. 5). Densitometric analysis of Western blots from three independent experiments revealed that compared to controls (absence of IONP; ferritin signal was $20 \pm 4\%$ of the α-tubulin signal) the cellular ferritin content was substantially increased in OLN-93 cells that had been exposed to IONP in concentrations of 100 µM (2fold), 300 µM (4fold) and 1000 µM (14fold) (Fig. 5B). This IONP-induced increase in the ferritin signal correlated well (correlation coefficient of 0.998) with the respective specific cellular iron content of IONP-treated cells. In addition, the upregulation of ferritin after exposure of OLN-93 cells for 48 h to IONP was almost completely prevented, if the cells were co-incubated with IONP and the iron chelator DFX (Fig. 5).

3.5 Iron from IONP is used by OLN-93 cells to bypass the deferoxamine-induced inhibition of proliferation

Presence of micromolar concentrations of the iron chelator DFX have been reported to inhibit the proliferation of OLN-93 cells [13]. To test whether the cellular iron found in IONP-treated cells is able to bypass the DFX-mediated inhibition of cell proliferation OLN-93 cells were co-incubated for 48 h with DFX and IONP. Neither the incubation of OLN-93 cells with DFX or IONP alone nor coincubation with DFX plus IONP in concentrations of up to 1000 µM compromized the cell viability as indicated by the absence of any increase in extracellular

LDH activity (Fig. 3B). In addition, presence of DFX did not significantly alter the specific cellular iron content determined for cells that had been exposed to IONP (Fig. 3A). However, compared to the protein content of cultures that were incubated for 48 h with DFX in the absence of IONP (33 ± 5 µg/well), the cellular protein content increased significantly to 52 ± 10 µg/well and 64 ± 13 µg/well for cells co-incubated with DFX plus 300 µM and 1000 µM IONP, respectively (Fig. 3C). Accordingly, the number of nuclei in cultures that had been treated with DFX in the presence of 1000 µM IONP was doubled compared to the respective control without IONP (Fig. 3D), demonstrating that cell proliferation occurred in the presence of DFX plus IONP.

3.6 Consequences of an IONP-treatment on the cellular GSH content and on radical formation

Oxidation of cellular GSH to GSSG and the accompanied alteration in the ratio of GSSG to GSH is considered as indicator for oxidative stress [37]. Therefore, GSH and GSSG levels were determined to investigate the potential of IONP to affect the GSH metabolism of OLN-93 cells. After 48 h incubation without IONP, OLN-93 cells had a specific cellular GSH content of around 40 nmol/mg protein and contained hardly any detectable GSSG (Fig. 6). Exposure of the cells to IONP in concentrations of up to 1000 µM for 48 h did not alter the specific GSH and GSSG contents of OLN-93 cells. The GSSG contents remained for all conditions investigated very low accounting for less than 3% of the values observed for GSH (Fig. 6).

Excess of redox active iron catalyzes the formation of ROS by the Fenton reaction [38, 39]. To test whether the high cellular iron content of IONP-treated OLN-93 cells (Fig. 3A) leads to an accelerated ROS production, the ROS-mediated oxidation of dihydrorhodamine 123 to the fluorescent rhodamine 123 in these cells was investigated. At best some basal signals for rhodamine 123 were observed for OLN-93 cells that had been incubated without IONP for 48 h (Fig. 7B) which were not intensified in cells that had been exposed to IONP in a concentration of 300 µM (Fig. 7E). In contrast, exposure of OLN-93 cells to 300 µM ferric ammonium citrate (FAC) caused a substantial increase in the production of cellular ROS (Fig. 7H).
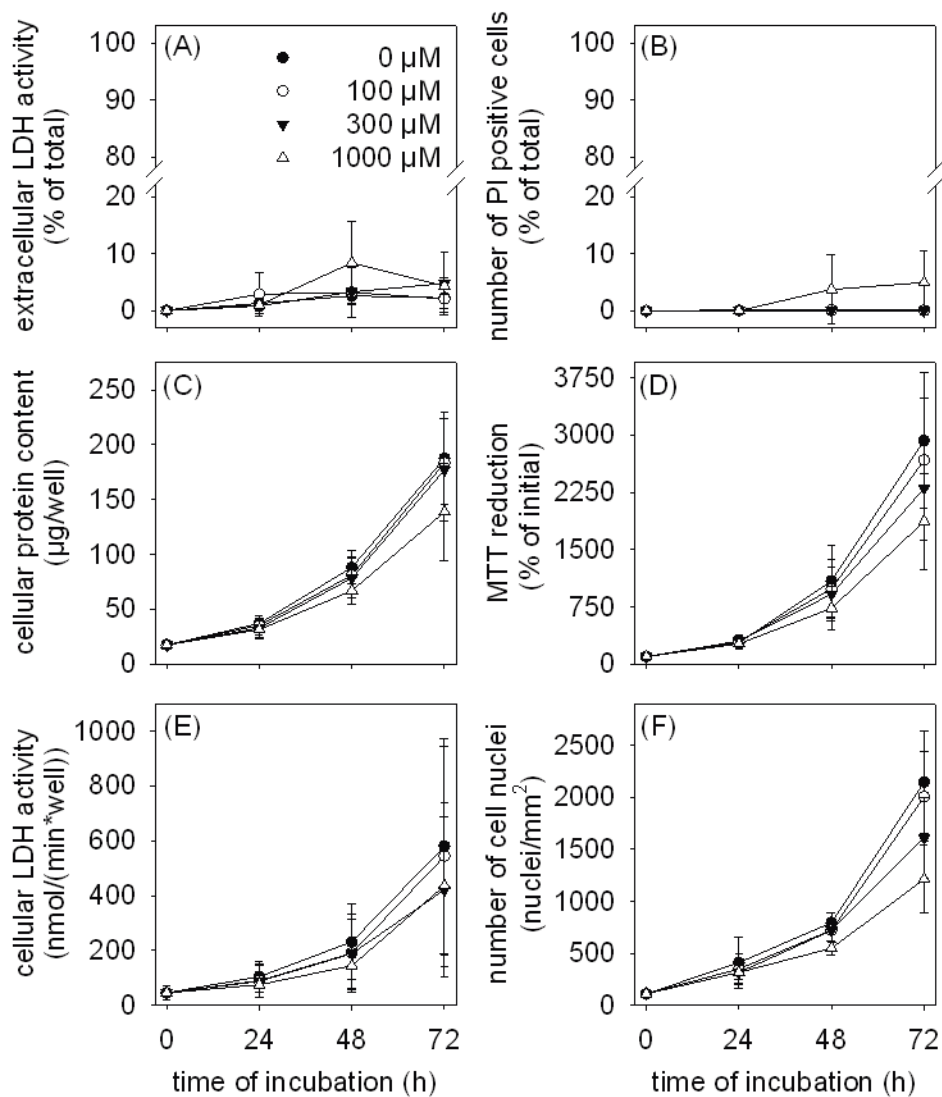
Figure 1. Consequences of an incubation of OLN-93 cells with IONP on cell viability and cell proliferation. The cells were incubated without (0 µM) or with IONP in the indicated concentrations for up to 72 h. At the indicated time points the extracellular LDH activity (A) and the number of PI-positive cells (B) were determined as indicators for cell viability and the cellular protein content (C), the MTT reduction capacity (D), the cellular LDH activity (E) and the number of H33342-stained cell nuclei (F) were determined as indicators for proliferation.
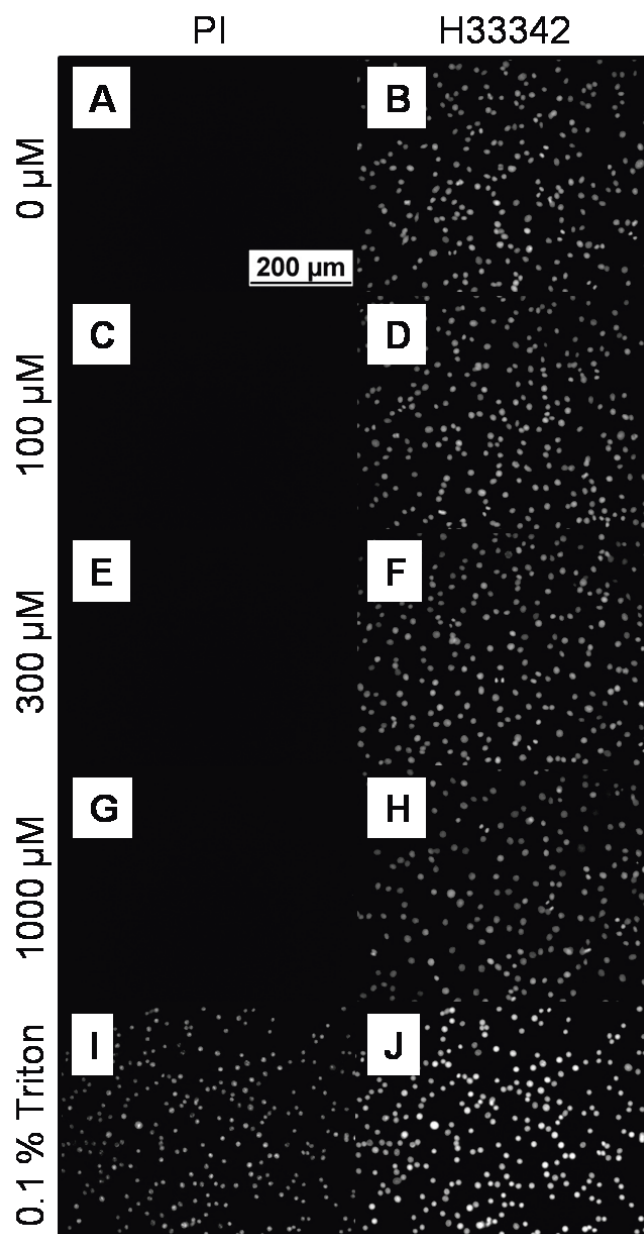
Figure 2. Plasma membrane integrity. OLN-93 cells were incubated for 48 h without (A,B) or with 100 μM (C,D), 300 μM (E,F) or 1000 μM (G,H) IONP. Subsequently, the cells were stained with PI to identify cells with compromized membrane integrity and with H33342 to visualize the nuclei of all cells present. As positive control for permeabilized cell membranes, cells were incubated for 2 min with 0.1% Triton X-100 prior to incubation with PI (I) and H33342 (J). The scale bar in A applies to all panels.
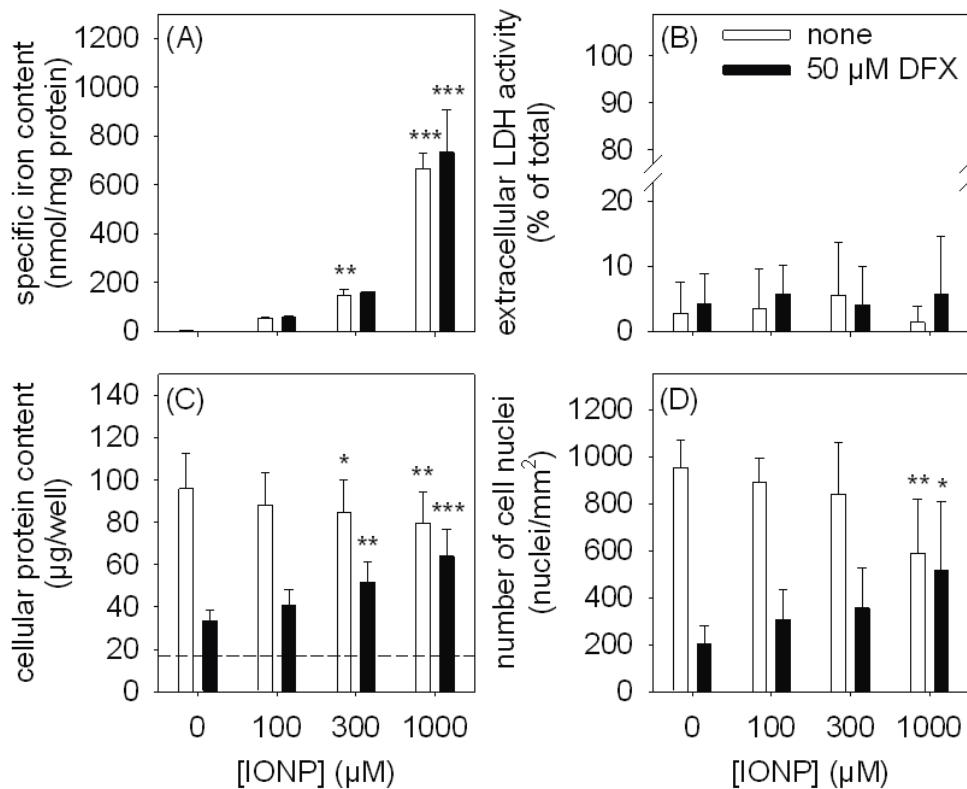
Figure 3. Presence of IONP bypasses the DFX-induced inhibition of proliferation. OLN-93 cells were incubated for 48 h without (none) or with 50 μM DFX in the absence (0 μM) or the presence of IONP in the indicated concentrations. Determined was the specific cellular iron content (A), the cell viability by measuring the extracellular LDH activity (B), the cellular protein content (C) and the number of H33342 stained nuclei (D). The initial cellular protein content of 17 ± 3 μg/well is indicated by a dashed line in C. The level of significance of values compared to those of the respective controls (absence of IONP) is indicated by *$p<0.05$, **$p<0.01$ or ***$p<0.001$.
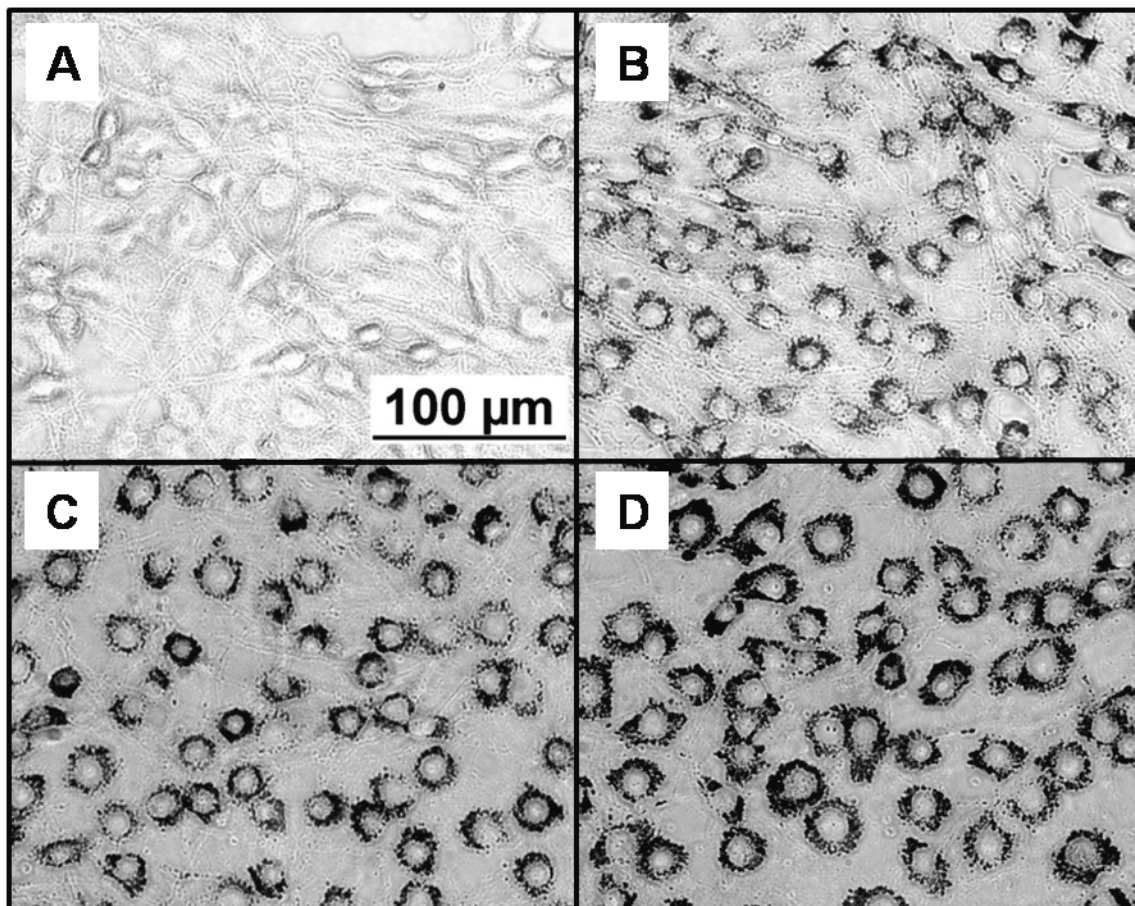
Figure 4. Perls´ staining for iron in OLN-93 cells that had been incubated for 48 h without (A) or with 100 µM (B), 300 µM (C) or 1000 µM (D) IONP. The scale bar in A applies to all panels.
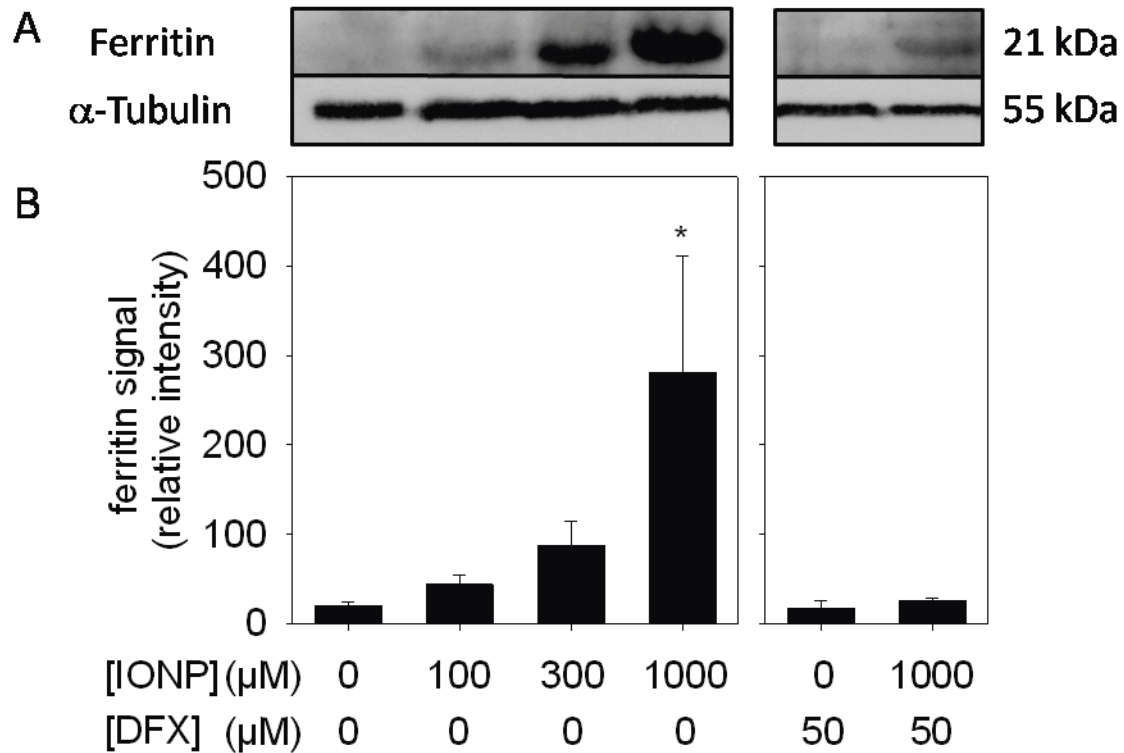
Figure 5. Western blot for the iron storage protein ferritin. OLN-93 cells were incubated for 48 h with IONP in the indicated concentrations. 40 µg of cell lysate protein were loaded per lane. A: Western blot of samples derived from a representative experiment. B: Densitometric analysis of the signal intensity normalized on the signal of α-tubulin in the respective sample. The data are presented as means ± SD of data from three independent experiments (absence of DFX) or as means ± difference to the mean values of data from two independent experiments (presence of DFX).
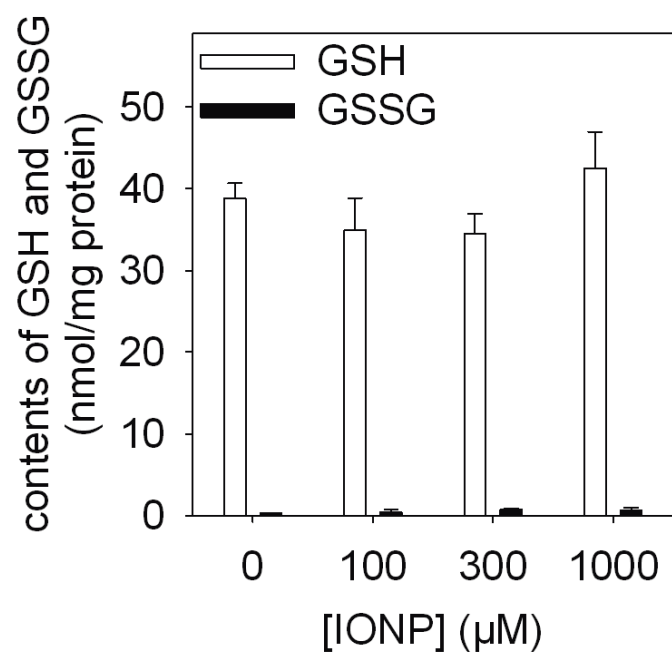
Figure 6. Specific contents of GSH and GSSG in OLN-93 cells after 48 h incubation in the absence (0 µM) or presence of IONP in the indicated concentrations.
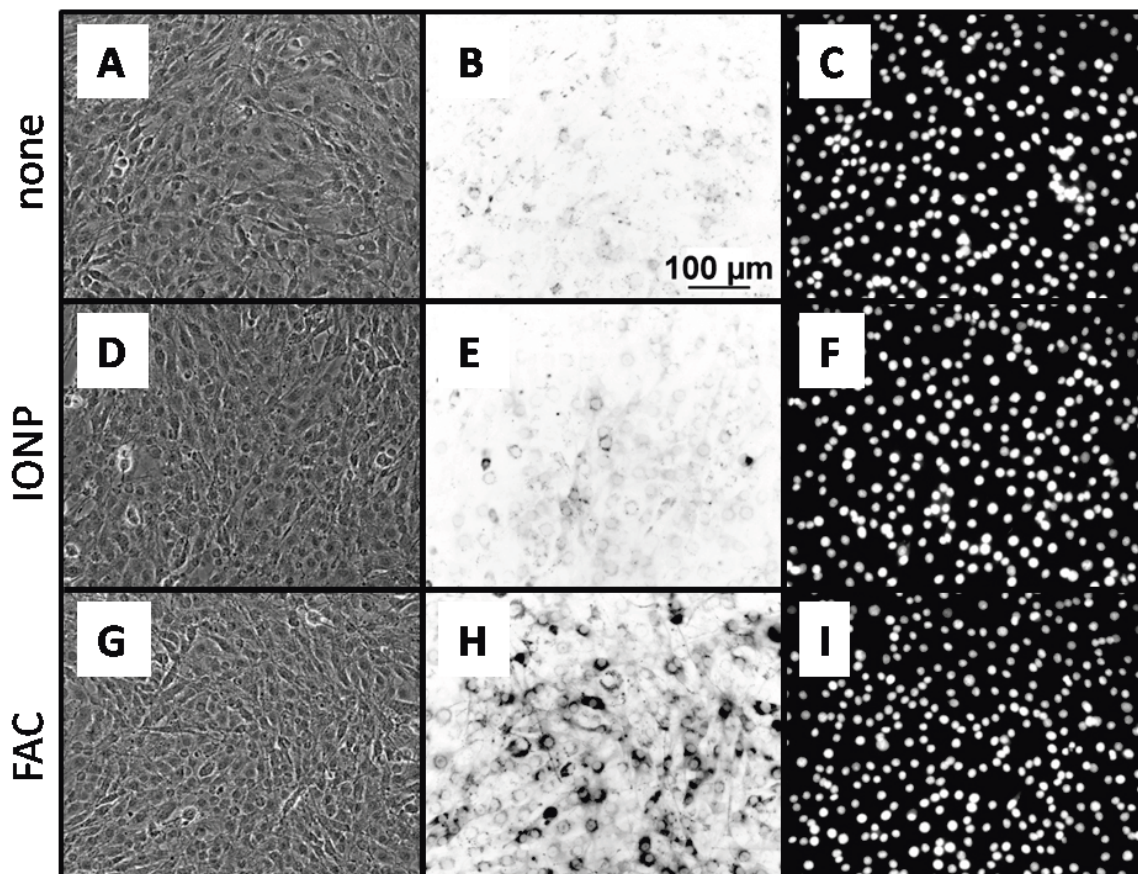
Figure 7. Staining for radicals in OLN-93 cells. The cells were incubated for 48 h without additional iron source (A-C), with 300 µM IONP (D-F) or with 300 µM FAC (G-I). Shown are phase contrast pictures of the cells (A,D,G), the fluorescence of rhodamine 123 (B,E,H) and the H33342-staining of cell nuclei (C,F,I). The size bar in B applies to all panels.

4 Discussion

The present study investigated the consequences of an exposure of OLN-93 cells to DMSA-coated IONP as well as the fate of the accumulated nanoparticles. IONP in concentrations of up to 1000 µM total iron did not compromise cell viability during an incubation of OLN-93 cells for up to 72 h and showed even in the highest concentration of IONP applied at best a mild effect on cell proliferation. The concentrations of IONP applied to OLN-93 cells (1000 µM IONP corresponds to 55 µg iron/mL) are in the concentration range suggested to be useful for in vitro tests [40]. However, these concentrations of IONP are substantially higher than those which are likely to be encountered by brain cells in vivo, since only a small proportion (around 50 µg/g brain tissue) of peripherally applied IONP (600 µg/g body weight) was found in mouse brain after 1 or 3 days [6]. Thus, the resistance of OLN-93 cells against toxicity by IONP, even after application of IONP in concentrations that are much higher than those expected for brain cells in vivo, suggests that oligodendroglial cells in brain may also have the potential to cope well with the IONP they will encounter after peripheral application of IONP.

The observed resistance of oligodendroglial cells against IONP-induced toxicity confirms literature data for nanosized iron particles [13, 20], but contrasts the observation that IONP are toxic and/or induce oxidative stress in various cell lines [41-43]. However, since IONP-treated OLN-93 cells did not suffer from a detectable increase in ROS production nor from a shift in the GSSG to GSH ratio, persistent oxidative stress appears not to be a consequence of the treatment, despite of the 300fold increase in the specific cellular iron content. Reasons for the resistance of OLN-93 cells towards acute IONP toxicity and for the absence of accelerated ROS-production could be the high antioxidative potential of oligodendroglial cells [44-46] as well as differences, compared to other more susceptible cell types, in the pathways involved in accumulation of IONP, in the velocity of liberation of iron from cellular IONP, as well as in the capacities to store or export IONP-derived iron. Whether the described intrinsic peroxidase activity of IONP [24, 47] may also be involved in prevention of a potential iron-mediated oxidative stress in IONP-treated OLN-93 cells, remains to be elucidated. In addition, our observations do not exclude that an initial transient increase in ROS formation may have occurred in IONP-treated OLN-93 cells, as very recently described for C17.2 neural progenitor cells [48].

Exposure of OLN-93 cells to 1000 µM DMSA-coated IONP lowered to some extent cell proliferation. Although this trend did not reach the level of significance in all experiments

performed, it was consistently observed for all proliferation assays applied. IONP have been reported to slow the proliferation of human lung alveolar carcinoma epithelial cells, normal human lung alveolar epithelial cells, human cervical adenocarcinoma epithelial cells, human osteosarcoma cells and mesenchymal stem cells [49, 50], although the proliferation of mesenchymal stromal cells was not influenced by IONP [51]. The observed moderate slow down of cell proliferation by IONP in OLN-93 cells could be a particle-effect, since neither the application of the coating material DMSA (data not shown) nor the presence of large amounts of low molecular weight iron [13] affected the proliferation of these cells. Potential reasons for a slowed cell proliferation during exposure to nanoparticles could be alterations of the cytoskeleton and the associated focal adhesion kinase-mediated signaling pathway which is known to diminish proliferation, as recently described for other cell types [52].

Incubation of OLN-93 cells with DMSA-coated IONP strongly increased the cellular iron content, as previously shown for oligodendroglial cells that had been exposed to citrate-coated IONP [13] or magnetodendrimers [20]. Under the conditions used, the cellular iron content increased proportional to the concentration of IONP applied up to 1000 µM which is consistent with results obtained for the uptake of citrate-coated IONP in OLN-93 cells [13] and astrocytes [53]. This observation does not exclude that a saturable mechanism is involved in the IONP uptake by OLN-93 cells, since also for cultured astrocytes DMSA-coated IONP had to be applied in concentrations higher than 1000 µM to observe saturation [29]. Interestingly, the specific iron contents observed after incubation of OLN-93 cells with IONP did not differ between cells that had been incubated for 24 h or 48 h, suggesting that steady state levels of cellular iron are established already within 24 h of incubation. Thus, under the conditions used each cell appears to be able to accumulate a given amount of iron which depends on the concentration of IONP applied. This view is supported by the linear increase in specific iron contents with the concentrations of IONP applied. The strong iron accumulation by OLN-93 cells was confirmed by cytochemical Perls´ staining for cellular iron. The observed perinuclear iron staining is consistent to literature data for cultured neural cells that had been exposed to different types of IONP [13, 53, 54].

The potential of OLN-93 cells to mobilize low molecular weight iron ions from accumulated IONP was investigated by quantifying ferritin contents and cell proliferation, since both ferritin synthesis and proliferation depend on the presence of low molecular weight iron [13, 55]. The strong accumulation of iron observed for IONP-treated OLN-93 cells was accompanied by a strong increase of the amount of the cellular iron storage protein ferritin. The cellular synthesis of ferritin depends on the incorporation of low molecular weight iron

into the iron-sulfur-cluster of the iron responsive protein (IRP), thereby preventing the binding of IRP to the iron responsive element in the ferritin mRNA and allowing translation of ferritin [55]. Thus, the increase in ferritin expression in OLN-93 cells after IONP exposure clearly demonstrates the presence of iron ions that have been liberated from the accumulated IONP and were subsequently incorporated into the IRP. An upregulation of ferritin has to our knowledge not been reported so far for neural cells, but human mesenchymal stem cells and liver cells are known to increase their ferritin contents after treatment with nanosized iron oxide [25, 26].

Exposure of OLN-93 cells to micromolar concentrations of DFX inhibits the proliferation without compromising cell viability in a process that is prevented by an excess of low molecular weight iron [13]. Likely reason for the DFX-induced inhibition of proliferation is the chelation of both low molecular weight iron and transferrin-bound iron from the incubation medium thereby making extracellular iron unavailable to support cell proliferation. The ability of DFX-treated OLN-93 cells to regain the potential to proliferate in the presence of IONP confirms the ability of OLN-93 cells to liberate and make use of iron from IONP. Such a process has also been suggested for the promotion of proliferation of human mesenchymal stem cells in the presence of IONP [24].

The strong iron accumulation from 1000 µM IONP was neither prevented by the presence of the iron chelator DFX in a concentration of 50 µM nor in a concentration of 1000 µM (data not shown). Since DFX prevents iron accumulation from low molecular weight iron [8, 56] but not from IONP [28], the strong iron accumulation after exposure of the cells to IONP is likely to be mediated by endocytotic particle uptake, as previously suggested [57] and recently demonstrated for other types of nanoparticles [19]. The low pH of the lysosomal compartment is likely to help mobilizing iron from IONP [21, 22, 24, 58]. From the lysosomal/endosomal compartment, ferrous iron could then be transported by the divalent metal transporter 1, which is expressed in OLN-93 cells [59], into the cytosol as it is known for iron that has entered the cells via transferrin receptor-mediated endocytosis [9], where it becomes available for incorporation into proteins and for storage in ferritin.

The amount of cellular iron correlated well with the level of ferritin in OLN-93 cells exposure to IONP, suggesting that the amount of iron liberated from the IONP depends on the amount of accumulated IONP. Presence of DFX prevented the IONP-induced upregulation of ferritin in OLN-93 cells, demonstrating that DFX had at least partial access to ferric iron that was liberated from IONP. DFX as charged molecule can hardly penetrate the cell membrane [60],

but has been suggested to enter cells by an endocytotic process [61]. Thus, after a co-incubation, iron may be liberated from IONP in the presence of DFX in the endosomal compartment. For each endosomal vesicle, the molar ratio of DFX to the iron liberated from IONP as well as the rate of reduction of ferric iron will determine how much ferrous iron is available in the DFX-dependent equilibrium between ferric and ferrous iron [62]. Thus, although IONP-derived ferric iron will be chelated by DFX, part of it is likely to be reduced to ferrous iron that cannot be chelated by DFX [63] and exported by DMT1 into the cytosol where it supports proliferation. Since ferritin upregulation takes only place if iron is present in excess in the cytosol [55], liberation of iron from IONP in presence of DFX in endosomal vesicles is likely to provide sufficient cytosolic ferrous iron to enable at least some proliferation, although the majority of IONP-derived ferric iron may be chelated in the endosomal compartment.

5 Conclusions

DMSA-coated IONP are efficiently taken up into viable oligodendroglial cells. The observation that IONP-derived iron bypasses the DFX-induced inhibition of proliferation demonstrates that OLN-93 cells mobilize iron from IONP. However, despite of the large amounts of accumulated iron, OLN-93 cells do not show substantial ROS production or an alteration in the cellular thiol reduction potential. Most likely, the strong upregulation of ferritin allows the cells to safely store only excess of iron liberated from the IONP that is not needed for proliferation, thereby preventing ROS formation by iron-mediated Fenton chemistry. Our data demonstrate for the first time that neural cells are able to liberate iron from accumulated IONP. Such processes have to be considered regarding the fate of magnetic IONP that will be applied to brain cells or to the brain for therapeutical or experiential reasons.

6 Acknowledgements

7 References

[1] Suh WH, Suslick KS, Stucky GD, Suh YH. Nanotechnology, nanotoxicology, and neuroscience. Prog Neurobiol 2009;87:133-170.

[2] Weinstein JS, Varallyay CG, Dosa E, Gahramanov S, Hamilton B, Rooney WD, et al. Superparamagnetic iron oxide nanoparticles: diagnostic magnetic resonance imaging and potential therapeutic applications in neurooncology and central nervous system inflammatory pathologies, a review. J Cereb Blood Flow Metab 2010;30:15-35.

[3] Chertok B, Moffat BA, David AE, Yu F, Bergemann C, Ross BD, et al. Iron oxide nanoparticles as a drug delivery vehicle for MRI monitored magnetic targeting of brain tumors. Biomaterials 2008;29:487-496.

[4] Jordan A, Scholz R, Maier-Hauff K, van Landeghem FK, Waldoefner N, Teichgraeber U, et al. The effect of thermotherapy using magnetic nanoparticles on rat malignant glioma. J Neurooncol 2006;78:7-14.

[5] Bulte JW, Zhang S, van Gelderen P, Herynek V, Jordan EK, Duncan ID, et al. Neurotransplantation of magnetically labeled oligodendrocyte progenitors: magnetic resonance tracking of cell migration and myelination. Proc Natl Acad Sci U S A 1999;96:15256-15261.

[6] Wang J, Chen Y, Chen B, Ding J, Xia G, Gao C, et al. Pharmacokinetic parameters and tissue distribution of magnetic Fe_3O_4 nanoparticles in mice. Int J Nanomedicine 2010;5:861-866.

[7] Nel A, Xia T, Mädler L, Li N. Toxic potential of materials at the nanolevel. Science 2006;311:622-627.

[8] Hoepken HH, Korten T, Robinson SR, Dringen R. Iron accumulation, iron-mediated toxicity and altered levels of ferritin and transferrin receptor in cultured astrocytes during incubation with ferric ammonium citrate. J Neurochem 2004;88:1194-1202.

[9] Galaris D, Pantopoulos K. Oxidative stress and iron homeostasis: mechanistic and health aspects. Crit Rev Clin Lab Sci 2008;45:1-23.

[10] Hilty FM, Arnold M, Hilbe M, Teleki A, Knijnenburg JT, Ehrensperger F, et al. Iron from nanocompounds containing iron and zinc is highly bioavailable in rats without tissue accumulation. Nat Nanotechnol 2010;5:374-380.

[11] Yu Y, Kovacevic Z, Richardson DR. Tuning cell cycle regulation with an iron key. Cell Cycle 2007;6:1982-1994.

[12] Rouault TA, Tong WH. Iron-sulfur cluster biogenesis and human disease. Trends Genet 2008;24:398-407.

[13] Hohnholt M, Geppert M, Dringen R. Effects of iron chelators, iron salts, and iron oxide nanoparticles on the proliferation and the iron content of oligodendroglial OLN-93 cells. Neurochem Res 2010;35:1259-1268.

[14] Lederman HM, Cohen A, Lee JW, Freedman MH, Gelfand EW. Deferoxamine: a reversible S-phase inhibitor of human lymphocyte proliferation. Blood 1984;64:748-753.

[15] Connor JR, Menzies SL. Relationship of iron to oligodendrocytes and myelination. Glia 1996;17:83-93.

[16] Benkovic SA, Connor JR. Ferritin, transferrin, and iron in selected regions of the adult and aged rat brain. J Comp Neurol 1993;338:97-113.

[17] McTigue DM, Tripathi RB. The life, death, and replacement of oligodendrocytes in the adult CNS. J Neurochem 2008;107:1-19.

[18] Bradl M, Lassmann H. Oligodendrocytes: biology and pathology. Acta Neuropathol 2010;119:37-53.

[19] Busch W, Bastian S, Trahorsch U, Iwe M, Kühnel D, Meißner T, et al. Internalisation of engineered nanoparticles into mammalian cells in vitro: influence of cell type and particle properties. J Nanopart Res 2011;13:293-310.

[20] Bulte JW, Douglas T, Witwer B, Zhang SC, Strable E, Lewis BK, et al. Magnetodendrimers allow endosomal magnetic labeling and in vivo tracking of stem cells. Nat Biotechnol 2001;19:1141-1147.

[21] Arbab AS, Wilson LB, Ashari P, Jordan EK, Lewis BK, Frank JA. A model of lysosomal metabolism of dextran coated superparamagnetic iron oxide (SPIO) nanoparticles: implications for cellular magnetic resonance imaging. NMR Biomed 2005;18:383-389.

[22] Levy M, Lagarde F, Maraloiu VA, Blanchin MG, Gendron F, Wilhelm C, et al. Degradability of superparamagnetic nanoparticles in a model of intracellular environment: follow-up of magnetic, structural and chemical properties. Nanotechnology 2010;21:395103-395114.

[23] Soenen SJ, Himmelreich U, Nuytten N, Pisanic TR, 2nd, Ferrari A, De Cuyper M. Intracellular nanoparticle coating stability determines nanoparticle diagnostics efficacy and cell functionality. Small 2010;6:2136-2145.

[24] Huang DM, Hsiao JK, Chen YC, Chien LY, Yao M, Chen YK, et al. The promotion of human mesenchymal stem cell proliferation by superparamagnetic iron oxide nanoparticles. Biomaterials 2009;30:3645-3651.

[25] Raschzok N, Muecke DA, Adonopoulou MK, Billecke N, Werner W, Kammer NN, et al. In vitro evaluation of magnetic resonance imaging contrast agents for labeling human liver cells: implications for clinical translation. Mol Imaging Biol 2010;in press.

[26] Pawelczyk E, Arbab AS, Pandit S, Hu E, Frank JA. Expression of transferrin receptor and ferritin following ferumoxides-protamine sulfate labeling of cells: implications for cellular magnetic resonance imaging. NMR Biomed 2006;19:581-592.

[27] Richter-Landsberg C, Heinrich M. OLN-93: a new permanent oligodendroglia cell line derived from primary rat brain glial cultures. J Neurosci Res 1996;45:161-173.

[28] Geppert M, Hohnholt M, Gaetjen L, Grunwald I, Bäumer M, Dringen R. Accumulation of iron oxide nanoparticles by cultured brain astrocytes. J Biomed Nanotechnol 2009;5:285-293.

[29] Geppert M, Hohnholt MC, Thiel K, Nürnberger S, Grunwald I, Rezwan K, et al. Uptake of dimercaptosuccinate-coated magnetic iron oxide nanoparticles by cultured brain astrocytes. Nanotechnology 2011;22:145101-145111.

[30] Thiessen A, Schmidt MM, Dringen R. Fumaric acid dialkyl esters deprive cultured rat oligodendroglial cells of glutathione and upregulate the expression of heme oxygenase 1. Neurosci Lett 2010;475:56-60.

[31] Dringen R, Kussmaul L, Hamprecht B. Detoxification of exogenous hydrogen peroxide and organic hydroperoxides by cultured astroglial cells assessed by microtiter plate assay. Brain Res Brain Res Protoc 1998;2:223-228.

[32] Scheiber IF, Mercer JF, Dringen R. Copper accumulation by cultured astrocytes. Neurochem Int 2010;56:451-460.

[33] Hamprecht B, Löffler F. Primary glial cultures as a model for studying hormone action. Methods Enzymol 1985;109:341-345.

[34] Lowry OH, Rosebrough NJ, Farr AL, Randall RJ. Protein measurement with the Folin phenol reagent. J Biol Chem 1951;193:265-275.

[35] Riemer J, Hoepken HH, Czerwinska H, Robinson SR, Dringen R. Colorimetric ferrozine-based assay for the quantitation of iron in cultured cells. Anal Biochem 2004;331:370-375.

[36] Dringen R, Hamprecht B. Glutathione content as an indicator for the presence of metabolic pathways of amino acids in astroglial cultures. J Neurochem 1996;67:1375-1382.

[37] Valko M, Leibfritz D, Moncol J, Cronin MT, Mazur M, Telser J. Free radicals and antioxidants in normal physiological functions and human disease. Int J Biochem Cell Biol 2007;39:44-84.

[38] Dringen R, Bishop GM, Koeppe M, Dang TN, Robinson SR. The pivotal role of astrocytes in the metabolism of iron in the brain. Neurochem Res 2007;32:1884-1890.

[39] Crichton RR, Wilmet S, Legssyer R, Ward RJ. Molecular and cellular mechanisms of iron homeostasis and toxicity in mammalian cells. J Inorg Biochem 2002;91:9-18.

[40] Soenen SJ, De Cuyper M. Assessing iron oxide nanoparticle toxicity in vitro: current status and future prospects. Nanomedicine (Lond) 2010;5:1261-1275.

[41] Choi JY, Lee SH, Na HB, An K, Hyeon T, Seo TS. In vitro cytotoxicity screening of water-dispersible metal oxide nanoparticles in human cell lines. Bioprocess Biosyst Eng 2010;33:21-30.

[42] Apopa PL, Qian Y, Shao R, Guo NL, Schwegler-Berry D, Pacurari M, et al. Iron oxide nanoparticles induce human microvascular endothelial cell permeability through reactive oxygen species production and microtubule remodeling. Part Fibre Toxicol 2009;6:1-14.

[43] Hussain SM, Hess KL, Gearhart JM, Geiss KT, Schlager JJ. In vitro toxicity of nanoparticles in BRL 3A rat liver cells. Toxicol In Vitro 2005;19:975-983.

[44] Hirrlinger J, Resch A, Gutterer JM, Dringen R. Oligodendroglial cells in culture effectively dispose of exogenous hydrogen peroxide: comparison with cultured neurones, astroglial and microglial cells. J Neurochem 2002;82:635-644.

[45] Baud O, Greene AE, Li J, Wang H, Volpe JJ, Rosenberg PA. Glutathione peroxidase-catalase cooperativity is required for resistance to hydrogen peroxide by mature rat oligodendrocytes. J Neurosci 2004;24:1531-1540.

[46] Back SA, Gan X, Li Y, Rosenberg PA, Volpe JJ. Maturation-dependent vulnerability of oligodendrocytes to oxidative stress-induced death caused by glutathione depletion. J Neurosci 1998;18:6241-6253.

[47] Gao L, Zhuang J, Nie L, Zhang J, Zhang Y, Gu N, et al. Intrinsic peroxidase-like activity of ferromagnetic nanoparticles. Nat Nanotechnol 2007;2:577-583.

[48] Soenen SJ, Himmelreich U, Nuytten N, De Cuyper M. Cytotoxic effects of iron oxide nanoparticles and implications for safety in cell labelling. Biomaterials 2011;32:195-205.

[49] Choi SJ, Oh JM, Choy JH. Toxicological effects of inorganic nanoparticles on human lung cancer A549 cells. J Inorg Biochem 2009;103:463-471.

[50] Jasmin, Torres AL, Nunes HM, Passipieri JA, Jelicks LA, Gasparetto EL, et al. Optimized labeling of bone marrow mesenchymal cells with superparamagnetic iron oxide nanoparticles and in vivo visualization by magnetic resonance imaging. J Nanobiotechnology 2011;9:4.

[51] Schmidtke-Schrezenmeier G, Urban M, Musyanovych A, Mailänder V, Rojewski M, Fekete N, et al. Labeling of mesenchymal stromal cells with iron oxide-poly(L-lactide) nanoparticles for magnetic resonance imaging: uptake, persistence, effetcs on cellular function and magnetic resonance imaging properties. Cytotherapy 2011;in press.

[52] Soenen SJ, Nuytten N, De Meyer SF, De Smedt SC, De Cuyper M. High intracellular iron oxide nanoparticle concentrations affect cellular cytoskeleton and focal adhesion kinase-mediated signaling. Small 2010;6:832-842.

[53] Hohnholt M, Geppert M, Nürnberger S, von Byern J, Grunwald I, Dringen R. Advanced biomaterials accumulation of citrate-coated magnetic iron oxide nanoparticles by cultured brain astrocytes. Adv Eng Mater 2010;12:B690-B694.

[54] Dunning MD, Lakatos A, Loizou L, Kettunen M, ffrench-Constant C, Brindle KM, et al. Superparamagnetic iron oxide-labeled Schwann cells and olfactory ensheathing cells can be traced in vivo by magnetic resonance imaging and retain functional properties after transplantation into the CNS. J Neurosci 2004;24:9799-9810.

[55] Arosio P, Ingrassia R, Cavadini P. Ferritins: a family of molecules for iron storage, antioxidation and more. Biochim Biophys Acta 2009;1790:589-599.

[56] Richardson DR, Baker E. Two saturable mechanisms of iron uptake from transferrin in human melanoma cells: the effect of transferrin concentration, chelators, and metabolic probes on transferrin and iron uptake. J Cell Physiol 1994;161:160-168.

[57] Bulte JW, Duncan ID, Frank JA. In vivo magnetic resonance tracking of magnetically labeled cells after transplantation. J Cereb Blood Flow Metab 2002;22:899-907.

[58] Weissleder R, Bogdanov A, Neuwelt EA, Papisov M. Long-circulating iron-oxides for MR imaging. Adv Drug Del Rev 1995;16:321-334.

[59] Brand A, Schonfeld E, Isharel I, Yavin E. Docosahexaenoic acid-dependent iron accumulation in oligodendroglia cells protects from hydrogen peroxide-induced damage. J Neurochem 2008;105:1325-1335.

[60] Halliwell B, Gutteridge JMC. Free radicals in biology and medicine. Fourth ed. Oxford: Oxford University Press; 2007.

[61] Lloyd JB, Cable H, Rice-Evans C. Evidence that desferrioxamine cannot enter cells by passive diffusion. Biochem Pharmacol 1991;41:1361-1363.

[62] Tulpule K, Robinson SR, Bishop GM, Dringen R. Uptake of ferrous iron by cultured rat astrocytes. J Neurosci Res 2010;88:563-571.

[63] Keberle H. The biochemistry of desferrioxamine and its relation to iron metabolism. Ann N Y Acad Sci 1964;119:758-768.

2.1.4. **Publication/Manuscript 3**

Hohnholt MC, Dringen R

Iron-dependent formation of reactive oxygen species and glutathione depletion

after accumulation of magnetic iron oxide nanoparticles

by oligodendroglial cells.

Submitted for publication

Contribution of Michaela C. Hohnholt:

- Performance of all experiments.
- Preparation of the first version of the manuscript.

Manuscript for J Nanopart Res

Iron-dependent formation of reactive oxygen species and glutathione depletion after accumulation of magnetic iron oxide nanoparticles by oligodendroglial cells

MICHAELA C. HOHNHOLT[1,2] and RALF DRINGEN[1,2,3]

[1]Centre for Biomolecular Interactions Bremen, University of Bremen, PO. Box 330440, D-28334 Bremen, Germany

[2]Centre for Environmental Research and Sustainable Technology, Leobener Straße, D-28359 Bremen, Germany

[3]School of Psychology & Psychiatry, Monash University, Wellington Rd., Clayton, Victoria 3800, Australia

Correspondance:

Dr. Ralf Dringen

Centre for Biomolecular Interactions Bremen

University of Bremen

PO. Box 330440

D-28334 Bremen

Germany

Tel: +49-421-218- 63230

Fax: +49-421-218-63244

Email: ralf.dringen@uni-bremen.de

Abstract

Magnetic iron oxide nanoparticles (IONP) are currently used for various neurobiological applications. To investigate the consequences of a treatment of brain cells with such particles, we have applied dimercaptosuccinate-coated IONP to oligodendroglial OLN-93 cells. After exposure to 4 mM iron applied as IONP, these cells increased their total specific iron content within 8 h almost 600fold from 7 to 4200 nmol/mg cellular protein. The strong iron accumulation was accompanied by a change in cell morphology, although the cell viability was not compromized. IONP treatment caused a concentration-dependent increase in the iron-dependent formation of reactive oxygen species and a decrease in the specific content of the cellular antioxidative tripeptide glutathione. During a 16 h recovery phase in IONP-free culture medium following exposure to IONP-treatment, OLN-93 cells maintained their high iron content and replenished their cellular glutathione content. These data demonstrate that viable OLN-93 cells have a remarkable potential to deal successfully with the consequences of an accumulation of large amounts of iron after exposure to IONP.

Keywords: GSH; magnetic iron oxide nanoparticles; oligodendrocytes; oxidative stress; radicals

Abbreviations: AA, amino acids; ANOVA, analysis of variance; BSO, buthionine sulfoximine; DMEM, Dulbecco´s modified Eagle´s medium; DMSA, dimercaptosuccinate; FCS, fetal calf serum; GSH, glutathione; GSSG, glutathione disulfide; GSx, total glutathione; IB, incubation buffer; IONP, iron oxide nanoparticles; LDH, lactate dehydrogenase; PBS, phosphate buffered saline; Phen, phenanthroline; PI, propidium iodide; ROS, reactive oxygen species

Introduction

Magnetic iron oxide nanoparticles (IONP) are currently used in neurobiology as contrast agent (Weinstein et al. 2010), as carriers for drug delivery (Chertok et al. 2008) and for cancer treatment by magnetic hyperthermia (Jordan et al. 2006). IONP have recently been reported to cross the blood-brain barrier and to enter the brain (Wang et al. 2010), but little is known on the toxicokinetic properties of IONP in the human body (Hagens et al. 2007) and on the safety of their application for the brain (Silva 2007; Yang 2010). Iron, which is likely to be released from IONP, has the potential to harm cells, since low molecular weight iron catalyzes the formation of reactive oxygen species (ROS) by the Fenton reaction (Galaris and Pantopoulos 2008; Hoepken et al. 2004). Additionally, it was suggested that the formation of ROS can also occur on the surface of nanoparticles (Nel et al. 2006). Indeed, several cell types have been shown to contain elevated levels of ROS after exposure to IONP (Apopa et al. 2009; Berg et al. 2010; Buyukhatipoglu and Clyne 2011; Soenen et al. 2011). This ROS production is likely to cause oxidative damage of biomolecules such as nucleic acids, proteins and lipids (Moller et al. 2010; Nel et al. 2006), if accelerated ROS generation induced by IONP is not compensated by a sufficient cellular antioxidative capacity.

Among the antioxidative molecules in brain cells, the tripeptide glutathione (GSH) appears to be especially important (Dringen and Hamprecht 1998; Hirrlinger and Dringen 2010). GSH reacts directly with radicals and is substrate of the glutathione peroxidase-dependent detoxification of peroxides (Dringen et al. 2005). In both processes GSH becomes oxidized to glutathione disulfide (GSSG) which is reduced in cells by glutathione reductase to regenerate GSH (Hirrlinger and Dringen 2010). In the brain, oligodendrocytes contain and need high amounts of iron (Benkovic and Connor 1993; Connor and Menzies 1996), but are also considered as prone to iron-mediated oxidative stress (Bradl and Lassmann 2010; McTigue and Tripathi 2008). To prevent oxidative damage, oligodendrocytes appear to be equipped with substantial antioxidative capacity. At least in culture, oligodendroglial cells detoxify hydrogen peroxides very efficiently and contain substantial amounts of GSH as well as high specific activities of the antioxidative enzymes glutathione peroxidase and glutathione reductase (Baud et al. 2004; Dringen et al. 2005; Hirrlinger et al. 2002a; Thiessen et al. 2010).

Oligodendroglial cells are known to accumulate IONP and other types of nanoparticles (Bulte et al. 2001; Busch et al. 2011; Hohnholt et al. 2010a). To investigate potential negative effects of an exposure of oligodendroglial cells to IONP, we have used the oligodendroglial cell line OLN-93 (Richter-Landsberg and Heinrich 1996) as model system. Here we report that the

accumulation of large amounts of iron in OLN-93 cells after exposure to dimercaptosuccinate (DMSA)-coated IONP is not acutely toxic but leads to changes in cell morphology, to an increase in iron-catalyzed cellular ROS production and to a decrease in the specific GSH content.

Methods

Materials

Fetal calf serum (FCS), penicillin/streptomycin and trypsin solution were obtained from Biochrom (Berlin, Germany). Dulbecco´s modified Eagle´s medium (DMEM) was from Invitrogen (Karlsruhe, Germany). Neocuproine, sodium ascorbate, Tris, 5,5´-dithio-bis(2-nitrobenzoic acid), dihydrorhodamine 123, DMSA and sulfosalicylic acid were purchased from Sigma (Steinheim, Germany). Bovine serum albumin, nicotinamide adenine dinucleotide and nicotinamide adenine dinucleotide phosphate were obtained from Applichem (Darmstadt, Germany). Glutathione reductase and GSSG were purchased from Roche Diagnostics (Mannheim, Germany). All other chemicals of the highest purity available were from Fluka (Buchs, Switzerland), Merck (Darmstadt, Germany) or Riedel-deHaen (Seelze, Germany). 96-well microtitre plates were from Nunc (Roskilde, Denmark) and 24-well cell culture plates from Sarstedt (Nümbrecht, Germany).

The IONP used in the present report were synthesized (Geppert et al. 2009) and coated with DMSA as described previously (Geppert et al. 2011). Dispersed in the incubation buffer used here, these DMSA-coated IONP have a monomodal size distribution with an average hydrodynamic diameter of 60 nm and a zeta-potential of -26 mV (Geppert et al. 2011). The given concentrations of DMSA-coated IONP represent the concentration of total iron contained in the particles applied and not the concentration of particles.

Cell cultures and experimental incubation

OLN-93 cells (passage numbers between 32 and 40) were cultured as described previously in culture medium (DMEM, 20 U/mL of penicillin G and 20 µg/mL of streptomycin sulphate) with 10% FCS (Hohnholt et al. 2010a; Thiessen et al. 2010). For experiments, 100,000 cells were seeded in wells of 24-well plates. 16 h to 18 h after seeding, the cells were washed twice with 1 mL pre-warmed (37°C) incubation buffer (IB; 20 mM HEPES, 145 mM NaCl, 1.8 mM $CaCl_2$, 5.4 mM KCl, 1 mM $MgCl_2$ and 5 mM glucose, pH 7.4) and incubated in 0.5 mL IB for up to 8 h in the presence or absence of DMSA-coated IONP and/or other compounds as indicated in the legends of the figures and tables. For recovery experiments, the IONP-containing IB was removed after 8 h of preincubation, the cells were washed with 1 mL pre-warmed (37°C) culture medium and incubated further for 16 h in 0.5 mL IONP-free culture medium in an incubator containing a humified atmosphere with 10% CO_2. All incubations

164

were terminated by washing the cells twice with 1 mL ice-cold phosphate buffered saline (PBS; 10 mM potassium phosphate buffer, 150 mM NaCl, pH 7.4).

Determination of cell viability and protein content

Cell viability was determined by comparison of the activity of the cytosolic enzyme lactate dehydrogenase (LDH) in the medium and in cell lysates as described previously (Dringen et al. 1998). The appearance of LDH in the extracellular medium is used as indicator for the loss of cell viability due to the complete loss of membrane integrity. The LDH activity of media samples was compared to the initial LDH activity of cells that had been lysed with 1% Trition X-100 in IB.

Permeability of cell membranes was also investigated by incubation of the cells with the membrane-impermeable dye propidium iodide (PI) and co-staining of all cell nuclei with the membrane-permeable dye H33342 as described previously (Scheiber et al. 2010). Briefly, the cells were washed twice with 1 mL IB and subsequently incubated for 15 min in IB containing 5 µM PI and 10 µM H33342. After washing three times with 1 mL PBS at room temperature, cells were immediately analyzed for fluorescence using a Nikon (Düsseldorf, Germany) TS2000U microscope. PI-positive nuclei indentify cells that have permeabilized membranes.

The content of cellular protein per well was determined according to the Lowry method (Lowry et al. 1951) using bovine serum albumin as a standard.

Quantification of iron and glutathione

The cellular iron content was quantified using a modification (Geppert et al. 2009) of the ferrozine-based colorimetric assay described previously (Riemer et al. 2004). The contents of cellular and extracellular total glutathione (GSx = amount of GSH plus twice the amount of GSSG) and GSSG were determined by the colorimetric Tietze assay with Ellman´s reagent in microtitre plates as described previously (Dringen and Hamprecht 1996; Dringen et al. 1997).

Staining for intracellular ROS

To detect intracellular ROS in OLN-93 cells, rhodamine 123 staining was performed by a modification of a previously published method (Hoepken et al. 2004). The non-fluorescent dihydrorhodamin 123 is oxidized by intracellular ROS to the fluorescent rhodamine 123. After a given experimental incubation, OLN-93 cells were washed twice with 1 mL IB and

incubated for 60 min at 37°C with 0.5 mL IB containing 5 µg/mL dihydrorhodamine 123 and 10 µM H33342. After washing twice with IB, the cells were fixed with 4% (w/v) paraformaldehyde in 0.1 M potassium phosphate buffer (pH 7.2) at room temperature. After washing the cells three times with PBS, they were analyzed for fluorescence.

Presentation of data

The results are presented as means ± standard deviation of at least three experiments performed on three different passages of OLN-93 cells. Figures that show cell morphology and/or cell stainings are derived from a representative experiment that was reproduced at least twice with comparable results. Significance of differences between two sets of data was analyzed by the t-test and significance of differences between groups of data was analyzed by analysis of variance (ANOVA) followed by the Bonferroni post hoc test. $p > 0.05$ was considered as not significant.

Results

Iron accumulation from IONP by OLN-93 cells

To test for the consequences of a treatment with IONP, OLN-93 cells were exposed for up to 8 h to IONP in various concentrations. Quantification of the cellular iron content revealed that the initial specific cellular iron content (7 ± 1 nmol/mg protein) remained unaltered, if the cells were incubated without IONP (Fig 1a). In contrast, exposure of cells to IONP caused a rapid and concentration-dependent increase of cellular iron levels. While the specific iron content of cells treated with 0.25 mM IONP increased almost linearly for up to 4 h and then remained almost constant at around 1000 nmol/mg protein, the cellular iron contents increased rapidly within 1 h after exposure to 1 mM and 4 mM IONP and increased slower within further 7 h to values of around 3000 nmol/mg protein and 4200 nmol/mg protein, respectively (Fig 1a).

Consequences of IONP treatment on cell viability and morphology

Despite of the high cellular iron contents of IONP-treated OLN-93 cells (Fig 1a), the cell viability appears not to be acutely compromized under these conditions as indicated by the absence of any significant increases in the extracellular activity of the cytosolic enzyme LDH (Fig 1b). This view was supported by PI staining that identifies cells with permeabilized membranes. Cultures incubated without or with 0.25 mM IONP hardly contained any PI-positive cells (Fig 2a,e), despite of the presence of a large number of cells that was demonstrated by H33342 staining (Fig 2b,f). The number of PI-positive cells was also very low in cultures exposed for 8 h to 1 mM IONP (Fig 2i) and increased at best slightly for cultures that had been treated with 4 mM IONP (Fig 2m).

Exposure of OLN-93 cells to IONP had severe consequences on the morphology of the cells. After 8 h incubation without IONP the cells had the typical bipolar shape of immature oligodendrocytes (Buckinx et al. 2009; Richter-Landsberg and Heinrich 1996) with elongated processes (Fig 3a). This morphology was not altered during incubation with 0.25 mM IONP (Fig 3c). In contrast, after incubation for 8 h in the presence of 1 mM or 4 mM IONP most cells had lost the initial bipolar shape and many cells contained bright intracellular vesicles (Fig 3e,g). The number and size of these vesicles were higher in cultures exposed to 4 mM IONP (Fig 3g) than in those treated with 1 mM IONP (Fig 3e).

Effects of IONP on the glutathione metabolism of OLN-93 cells

GSH is an important antioxidant that is present in millimolar concentrations in the cytosol of cells (Hirrlinger and Dringen 2010). To test whether exposure to IONP affects the GSH metabolism of OLN-93 cells, the cellular GSx content of IONP-treated cells was determined. In the absence of IONP, the specific GSx content was lowered during the first 2 h of incubation to 70% of the initial value, while additional incubation for up to 8 h decreased the specific GSx content at best slightly further to 60% of the initial content (Fig 1c). Exposure of OLN-93 cells to 0.25 mM IONP did not affect this alteration in the cellular GSx content, while incubation of OLN-93 cells with IONP in concentrations of 1 mM or 4 mM significantly lowered the specific cellular GSx contents compared to controls, reaching after 8 h of incubation 42% and 32% of the initial values, respectively (Fig 1c, Tab 1). The decline in the cellular GSx contents during incubation without or with IONP was not accompanied by any significant increase in the cellular level of GSSG (Tab 1), which remained for all conditions investigated below 8% of the respective GSx content. In addition, the loss of cellular GSx was not accompanied by any increase in the extracellular contents of GSx or GSSG (Tab 1). In contrast, compared to controls, the amounts of GSx determined in the media after 8 h of incubation were significantly lowered in a concentration-dependent manner by the presence of IONP (Tab 1).

To elucidate whether inactivation of GSH synthesis is involved in the observed loss of cellular GSx, OLN-93 cells were incubated with the GSH synthesis inhibitor buthionine sulfoximine (BSO) in the presence or the absence of the amino acids glutamate, cystine and glycine and/or 4 mM IONP (Fig 4). Presence of BSO during the incubation significantly lowered the cellular GSx content of cells that were treated without IONP (from 61% to 32% of the initial values) or with 4 mM IONP (from 33% to 8% of the initial values). In contrast, presence of amino acids maintained the cellular GSx content at the initial level during incubation in the absence or presence of IONP, while application of BSO completely prevented the preserving effect of amino acids on the cellular GSx content (Fig 4).

ROS production after exposure of OLN-93 cells to IONP

OLN-93 cells accumulated very high amounts of iron during exposure to IONP (Fig 1a). To test whether the accumulated iron is redox active, we investigated whether iron-mediated ROS production occurs in IONP-treated cells. In control cells that had been incubated for 8 h in the absence of IONP at best little ROS production was observed as indicated by the weak

rhodamine 123 staining (Fig 5b). Exposure of OLN-93 cells to 0.25 mM IONP did not increase this level of ROS production (Fig 5d), while many rhodamine 123-positive cells were present in cultures that had been exposed to 1 mM or 4 mM IONP (Fig 5f,h). In contrast to a treatment with IONP, a lowering of the cellular GSH content of OLN-93 cells by BSO did not cause any increase in the number of ROS-positive cells (data not shown).

Effects of iron chelators on the ROS production and on the GSH content of IONP-treated OLN-93 cells

To test whether the observed ROS formation in IONP-treated OLN-93 cells was an iron-dependent process, cells were coincubated with 4 mM IONP plus the membrane-permeable ferrous iron chelator 1,10-phenanthroline (Richardson and Baker 1994) or its non-chelating structural isomer 4,7-phenanthroline. Neither 1,10-phenathroline nor its isomer compromized cell viability as indicated by the absence of any significant increases in the extracellular LDH activity (Tab 2). Coincubation of OLN-93 cells with IONP plus 1,10-phenanthroline almost completely prevented the formation of ROS in IONP-treated cells (Fig 5j), while the non-chelating isomer 4,7-phenanthroline was unable to prevent ROS formation (Fig 5l). In contrast, presence of 1,10-phenanthroline (or its non-chelating isomer) did not prevent the other consequences of a treatment of OLN-93 cells with 4 mM IONP, such as the alteration in morphology (Fig 5i,k), the appearance of intracellular vesicles (Fig 5i,k) or the decline in the specific cellular GSx content (Tab 2).

Investigation of delayed consequences of an IONP treatment on OLN-93 cells

Treatment of OLN-93 cells with IONP caused an alteration of cell morphology, a strong accumulation of iron by the cells and a decline in cellular GSx (Figs 1 and 3). To test whether these consequences of a treatment of OLN-93 cells with IONP are maintained or reversible, the extracellular IONP were removed after a 8 h exposure and the cells were subsequently incubated in culture medium for further 16 h (recovery phase). The altered morphology of cells observed after incubation with 1 mM or 4 mM IONP (Fig 3e,g) remained during the recovery phase and the initial bipolar shape was not reestablished (Fig 3f,h), but the large bright intracellular vesicles that were observed after 8 h exposure to 4 mM IONP (Fig 3g) were hardly detectable anymore after 16 h recovery (Fig 3h). During the 16 h recovery phase, no increases in the extracellular LDH activity were observed for IONP-treated OLN-93 cells (data not shown), although the number of PI-positive cells was increased at least for cultures that had been exposed to 4 mM IONP (Fig 2o). In contrast, no increase in the number of PI-

positive cells was observed for cells after 16 h recovery following the treatment with 0.25 mM or 1 mM IONP (Fig 2g,k). The iron content of OLN-93 cells that had been pre-incubated for 8 h with IONP in various concentrations, was not lowered during the 16 h recovery phase (Fig 6a), while the cells had fully restored their initial cellular GSx content under these conditions (Fig 6b).
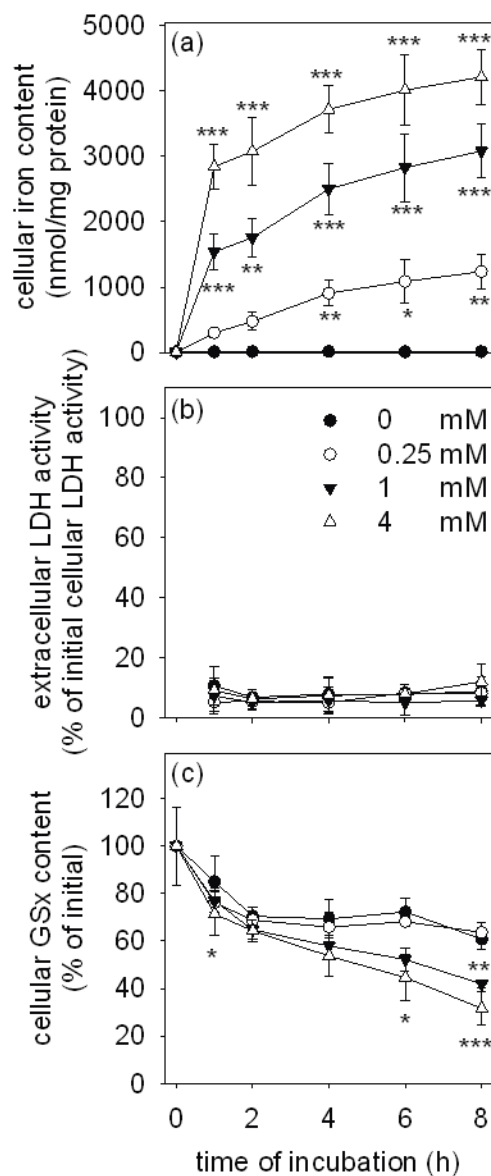
Fig 1 Effects of an IONP treatment of OLN-93 cells on the cellular iron content (a), the extracellular LDH activity (b) and the cellular GSx content (c). The cells were incubated without (0 mM) or with 0.25 mM, 1 mM or 4 mM IONP for up to 8 hours. The 100% GSx content corresponds to 47.0 ± 6.5 nmol/mg protein. The levels of significance of differences to controls (0 mM IONP) are indicated by *$p<0.05$, **$p<0.01$ and ***$p<0.001$.
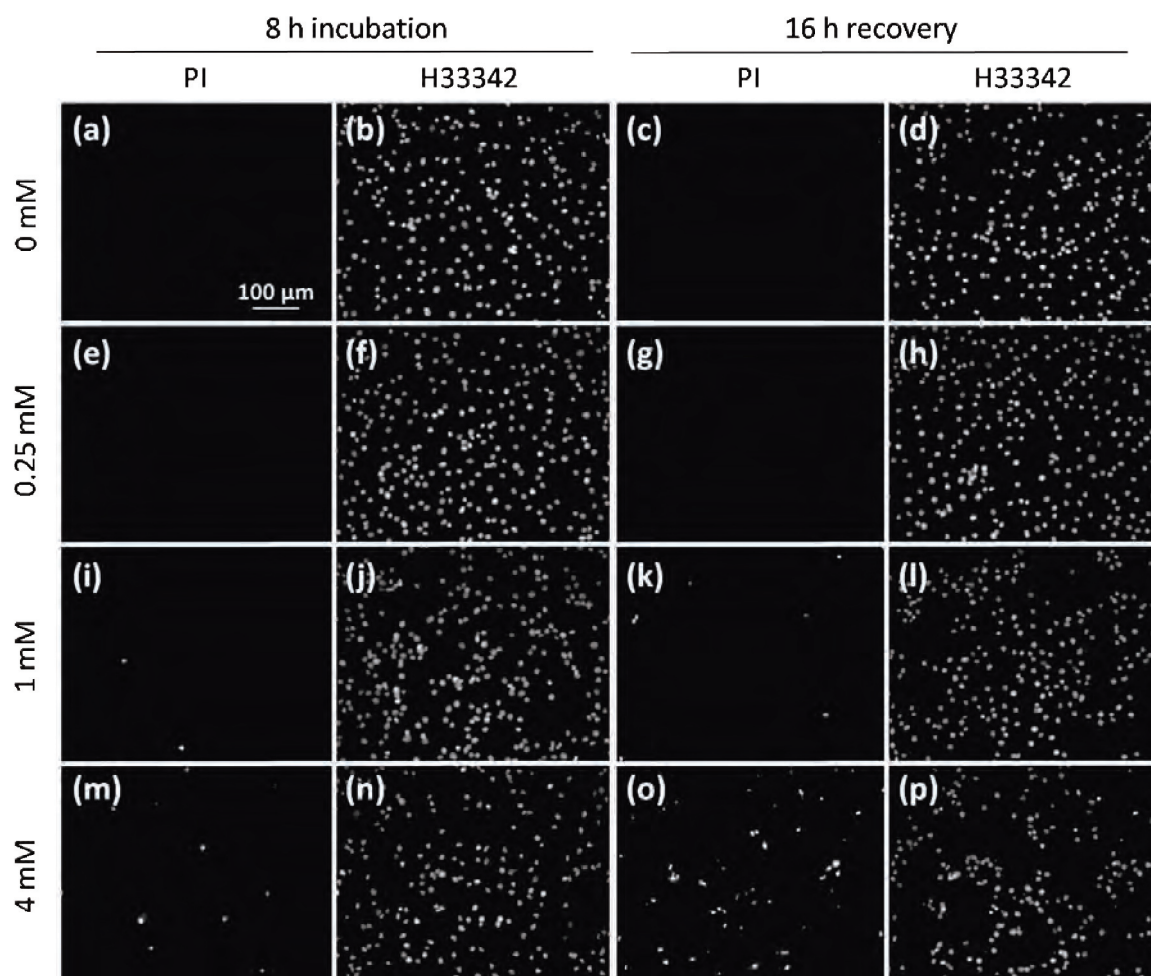
Fig 2 Membrane integrity of OLN-93 cells after exposure to IONP. The cells were stained with PI to identify cells with compromized membrane integrity and with H33342 to visualize the cell nuclei of all cells present. The cells were incubated for 8 h without (a-d) or with 0.25 mM (e-h), 1 mM (i-l) or 4 mM (m-p) IONP. Some cultures were directly analyzed (8 h incubation), while others were subsequently incubated for additional 16 h (recovery) in culture medium without IONP (16 h recovery). The size bar in (a) applies to all panels.

172
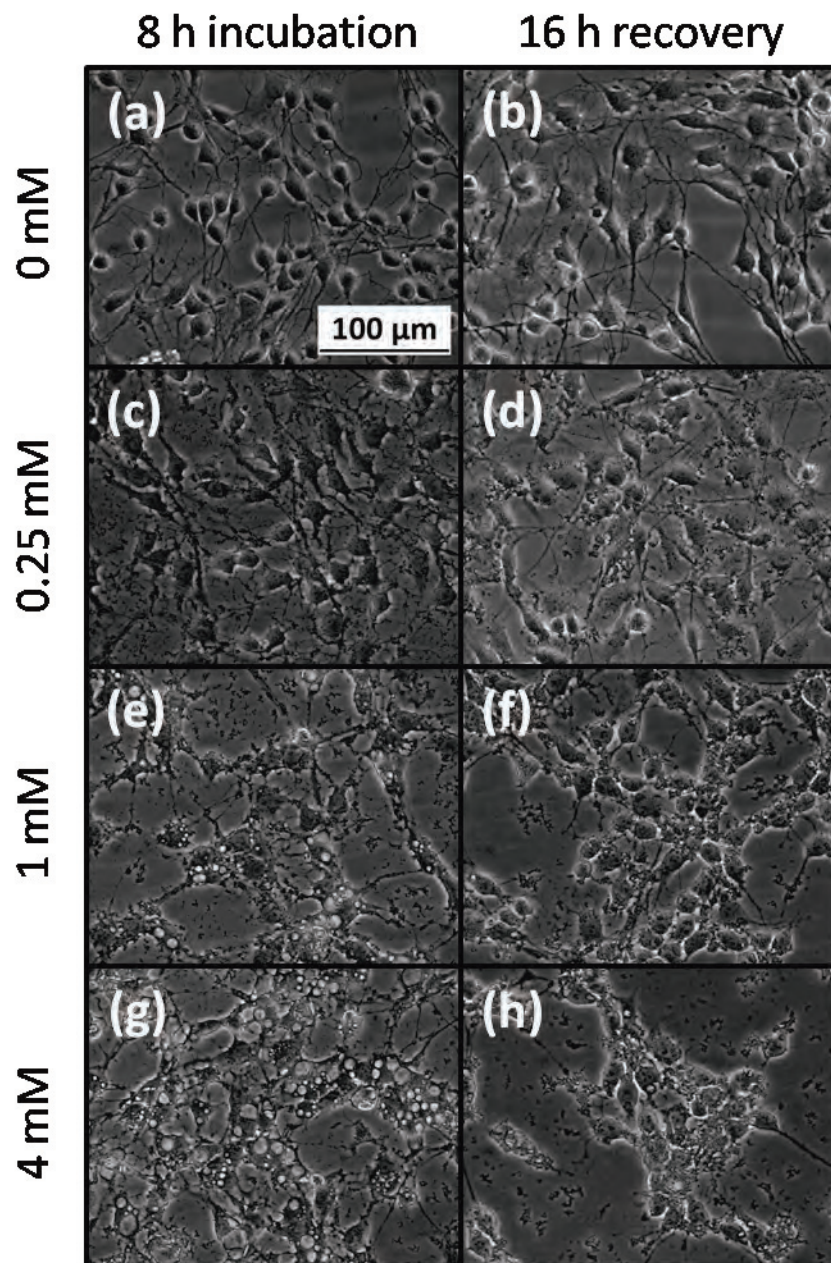
Fig 3 Cell morphology of OLN-93 cells after exposure to IONP. The cells were incubated for 8 h without (a,b) or with 0.25 mM (c,d), 1 mM (e,f) or 4 mM (g,h) IONP. Some cultures were directly analyzed for their morphology (8 h incubation; a,c,e,g), while others were subsequently incubated for additional 16 h in culture medium without IONP (16 h recovery; b,d,f,h). The size bar in (a) applies to all panels.
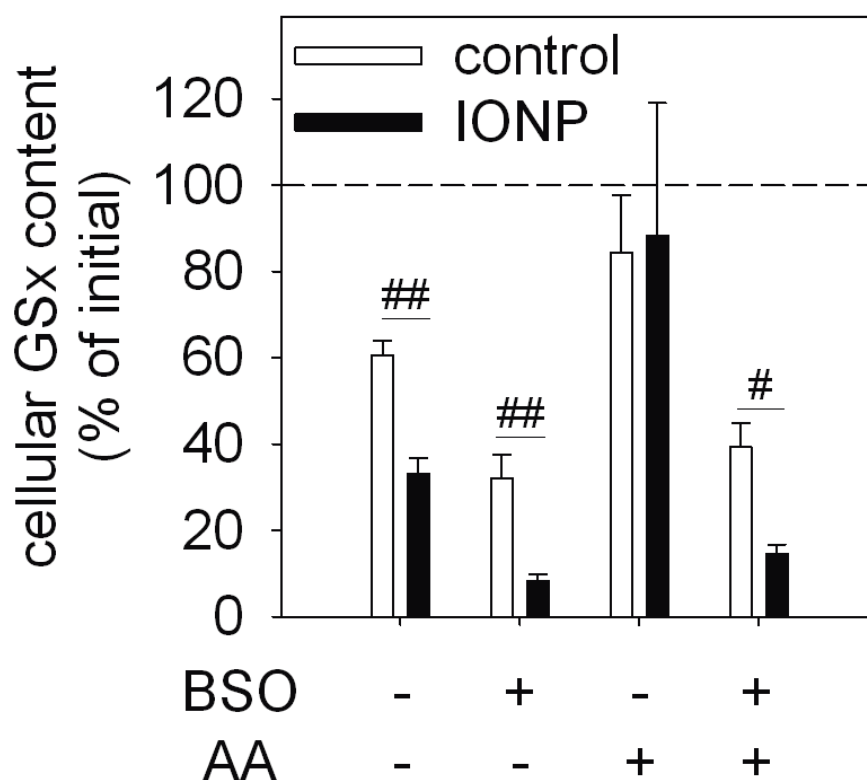
Fig 4 Effects of IONP, BSO and amino acids on the GSx content of OLN-93 cells. The cells were incubated for 8 h without (control) or with 4 mM IONP in the absence or the presence of BSO (0.1 mM) and/or amino acids (AA; 1 mM glutamate, 1 mM glycine and 0.1 mM cystine). The initial cellular GSx and protein contents were 52.5 ± 1.9 nmol/mg protein and 73 ± 24 μg/well, respectively. The levels of significance between cells that had been treated without and with IONP are indicated by [#]$p<0.05$ and [##]$p<0.01$.
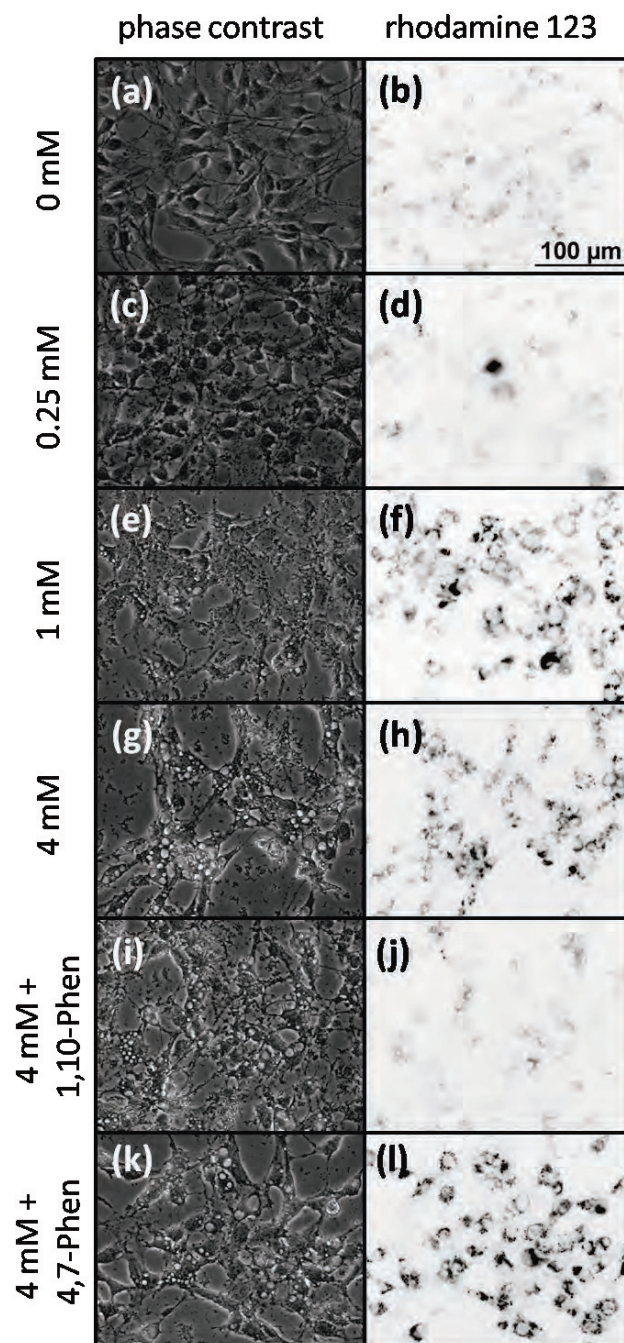
Fig 5 Rhodamine 123 staining for ROS in OLN-93 cells. The cells were incubated for 8 h without (a,b) or with 0.25 mM (c,d), 1 mM (e,f) or 4 mM IONP (g,h). Alternatively, cells were coincubated with 4 mM IONP plus either 100 μM 1,10-phenanthroline (1,10-Phen) (i,j) or 100 μM 4,7-phenanthroline (4,7-Phen) (k,l). The size bar in (b) applies to all panels.
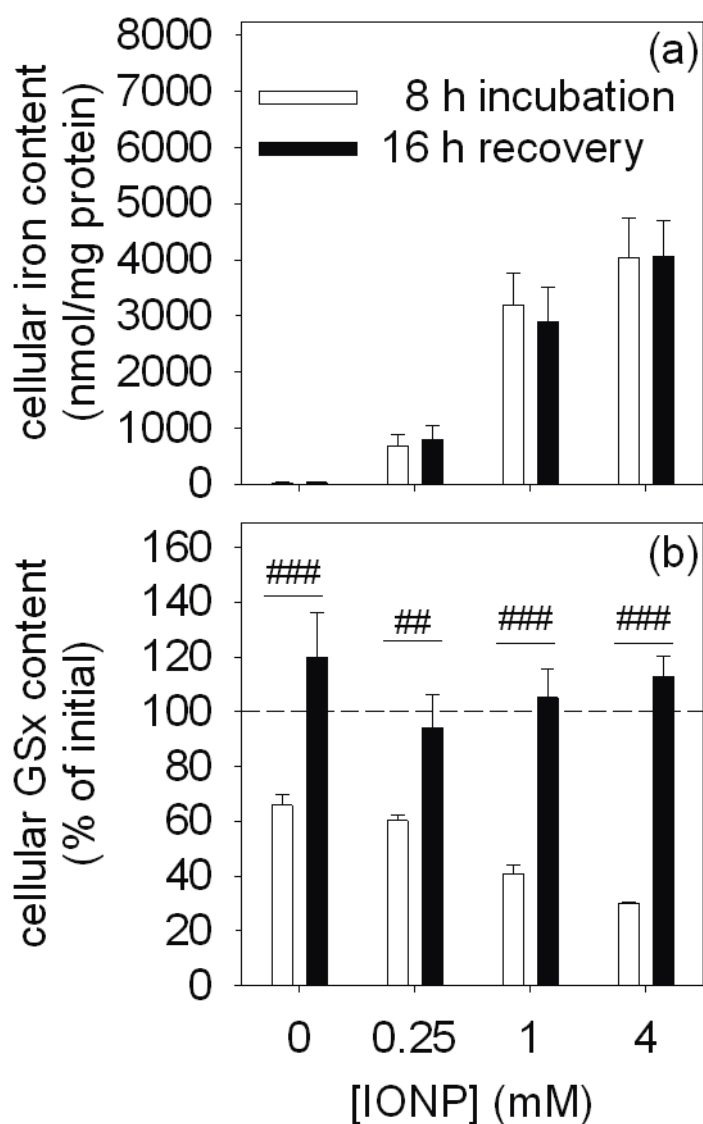
Fig 6 Effects of a recovery phase on the specific cellular iron (a) and GSx (b) contents of IONP-treated OLN-93 cells. The cells were incubated for 8 h with IONP in the indicated concentrations. Some cultures were directly analyzed after 8 h of incubation (white bars), while others were subsequently incubated for additional 16 h (recovery) in culture medium without IONP (black bars). The 100% GSx content corresponds to 57.6 ± 3.4 nmol/mg protein. The significance of differences between the values obtained for cells after exposure for 8 h to IONP and for cells after the 16 h recovery phase are indicated by [##]p<0.01 and [###]p<0.001.

Tab 1 Cellular and extracellular GSx and GSSG contents of OLN-93 cells before and after exposure to IONP for 8 h.

	0 h	8 h incubation with IONP			
	(initial)	0 mM	0.25 mM	1 mM	4 mM
Cells					
GSx					
(nmol/mg)	47.0 ± 6.5***	31.5 ± 5.6	31.0 ± 5.4	20.5 ± 3.6**	16.3 ± 2.3**
(nmol/well)	2.8 ± 0.5***	1.9 ± 0.3	1.8 ± 0.4	1.2 ± 0.2**	1.0 ± 0.2***
GSSG					
(nmol GSx/mg)	1.69 ± 0.28	0.86 ± 0.56	1.14 ± 0.24	0.88 ± 1.20	1.19 ± 0.05
(nmol GSx/well)	0.01 ± 0.01	0.05 ± 0.04	0.07 ± 0.01	0.06 ± 0.08	0.07 ± 0.01
Media					
GSx					
(nmol/well)	n.d.	0.5 ± 0.1	0.3 ± 0.1***	0.2 ± 0.1***	n.d.
GSSG					
(nmol GSx/well)	n.d.	n.d.	n.d.	n.d.	n.d.

OLN-93 cells were incubated for 8 h in the absence or the presence of IONP in the indicated concentrations. The levels of significance of differences compared to the control values (0 mM IONP) are indicated with **$p<0.01$ and ***$p<0.001$. (n.d., not detectable).

Tab 2 Effects of phenanthrolines on the viability and the GSx content of IONP-treated OLN-93 cells.

Compound	Extracellular LDH activity (% initial cellular LDH activity)	Cellular GSx content (nmol/mg protein)
None (1% DMSO)	0.1 ± 0.2	16.5 ± 1.1
1,10-phenanthroline	0.5 ± 0.9	16.3 ± 1.5
4,7-phenanthroline	0.7 ± 1.2	20.6 ± 0.8

OLN-93 cells were incubated with 4 mM IONP for 8 h in the absence (none) or in the presence of the iron chelator 1,10-phenanthroline or its non-chelating structural isomer 4,7-phenanthroline. DMSO was used as solvent for the phenanthrolines in a final concentration of 1%. The initial cellular GSx and protein contents were 52.6 ± 5.8 nmol/mg protein and 58 ± 9 µg/well, respectively. The values obtained for phenanthroline-treated cells did not differ significantly from those of control cells (none).

Discussion

OLN-93 cells efficiently accumulated iron after exposure to DMSA-coated IONP, confirming the reported potential of oligodendroglial cells to accumulate nanosized iron oxide particles such as citrate-coated IONP (Hohnholt et al. 2010a), magnetite nanoparticles (Busch et al. 2011) or magnetodendrimers (Bulte et al. 2001). The amount of iron accumulated by the cells during exposure to IONP were not lowered during a 16 h recovery phase in IONP-free medium, demonstrating that OLN-93 cells under the conditions used do not release IONP or IONP-derived iron. Despite of the very strong increase in the specific cellular iron content, the exposure of OLN-93 cells to IONP was not acutely toxic and did also not severely compromize cell viability during a subsequent recovery phase in IONP-free medium, demonstrating that these cells are remarkably resistant towards a potential toxicity of IONP. This resistance may be a general property of glial cells, since also cultured brain astrocytes are not acutely damaged by high concentrations of IONP (Ding et al. 2010; Geppert et al. 2009; Geppert et al. 2011; Hohnholt et al. 2010b; Pickard and Chari 2010). Nevertheless, accumulation of IONP caused severe alterations in cell morphology, lowered the cellular GSH content and accelerated the generation of ROS in OLN-93 cells.

The bipolar morphology of OLN-93 cells (Buckinx et al. 2009; Richter-Landsberg and Heinrich 1996) with elongated processes disappeared after exposure to millimolar concentrations of IONP and large bright vesicles appeared in the cytosol of IONP-treated cells. This may be a consequence of endocytotic uptake of the nanoparticles into the cells (Busch et al. 2011) and subsequent fusion of smaller vesicles with each other to larger vesicles as previously shown by the increased appearance of Lysotracker red dye-stained vesicles for A549 human lung epithelial cells after exposure to IONP in combination with carbon black nanoparticles (Berg et al. 2010). Also an alteration of the cytoskeleton, as recently described for primary human endothelial cells after exposure to IONP (Soenen et al. 2010), could be involved in the observed alteration in cell morphology of IONP-treated OLN-93 cells. However, during a 16 h recovery, the vesicles observed in IONP-treated OLN-93 cells disappeared, suggesting that at least the observed vesicle formation is a reversible process.

Incubation of OLN-93 cells in amino acid-free medium without IONP caused a moderate loss in the cellular GSx level that was accelerated by IONP in millimolar concentrations. Under all these conditions the contribution of GSSG to the GSx values determined remained very low. Thus, loss of cellular GSx reflects exclusively loss of cellular GSH. The low rate of GSH

export observed for control OLN-93 cells is similar to values observed for secondary oligodendrocyte cultures (Hirrlinger et al. 2002b), while the accelerated loss of cellular GSH from OLN-93 cells in presence of IONP is consistent with GSH loss reported for a human lung fibroblast cell line after treatment with hematite (Radu et al. 2010).

The disappearance of cellular GSH during incubation of OLN-93 cells without or with IONP was completely prevented by the presence of amino acids that provide the cellular substrates for GSH synthesis. This demonstrates that presence of IONP, in contrast to the GSH synthesis inhibitor BSO, does not inhibit GSH synthesis in OLN-93 cells and that the observed loss of cellular GSH was fully compensated by GSH synthesis in the presence of amino acid precursors.

Presence of IONP lowered also the amount of detectable GSH in the medium. Since the DMSA-coating of the IONP used contain disulfide bridges (Fauconnier et al. 1997; Valois et al. 2010), the formation of mixed disulfides between the DMSA-coat and GSH could contribute to the observed loss of detectable GSH from the medium. Indeed, results from preliminary cell-independent experiments demonstrate that GSH but not GSSG can react with DMSA-coated IONP (data not shown), suggesting that at least the lowered amounts of extracellular GSH found in the presence of IONP could be a consequence of a reaction between the coat of the nanoparticles and GSH. Whether such a reaction may also contribute to the observed cellular loss of GSH from IONP-treated OLN-93 cells remains to be elucidated.

Iron-mediated oxidative stress has to be considered as potential negative consequence of a treatment of cells with IONP (Nel et al. 2006). Indeed, as recently reported for other cell types (Apopa et al. 2009; Buyukhatipoglu and Clyne 2011; Soenen et al. 2011), also IONP-exposed OLN-93 cells showed accelerated formation of ROS as demonstrated by the concentration-dependent increase in the staining intensity for rhodamine 123. This ROS-formation depends on the presence of low molecular weight iron, since it was almost completely prevented by the ferrous iron chelator 1,10-phenanthroline, but was not affected by its non-chelating structural isomer. The inhibition of ROS formation by 1,10-phenanthroline demonstrates that OLN-93 cells are able to generate chelatable low molecular weight iron from IONP.

Detection of increased ROS formation can be a consequence of accelerated ROS production and/or of a decreased antioxidative defense. Since the amounts of detectable ROS were not lowered in IONP-treated OLN-93 cells that maintained the GSH level in the presence of amino acids (data not shown), a lowered antioxidative defense in cells partially deprived of

GSH appears not to accelerate ROS production. Despite of the detection of ROS in IONP-treated OLN-93 cells, the cells appear not to suffer from a severe oxidative stress. At least the viability of the cells was not acutely compromized in IONP-treated cells and the GSSG levels remained very low and were not increased as expected for cells that do not suffer from oxidative stress (Hirrlinger and Dringen 2010; Lewinski et al. 2008).

In summary, the accumulation of large amounts of iron in IONP-treated OLN-93 cells is not acutely toxic but leads to changes in cell morphology, to an increase in iron-catalyzed cellular ROS production and to a decrease in the specific cellular GSH content. Most of the effects observed for IONP-treated cells disappeared during a recovery phase. Thus, OLN-93 cell appear to cope quite well with even a 600fold increased cellular iron content, if the iron had been applied as IONP. These observations demonstrate that DMSA-coated IONP are even in high concentrations biocompatible with oligodendroglial cells, suggesting that also oligodendroglial cells in brain have the potential to deal with IONP that are applied for neurobiological and medical reasons.

References

Apopa PL, Qian Y, Shao R, Guo NL, Schwegler-Berry D, Pacurari M, Porter D, Shi X, Vallyathan V, Castranova V, Flynn DC (2009) Iron oxide nanoparticles induce human microvascular endothelial cell permeability through reactive oxygen species production and microtubule remodeling. Part Fibre Toxicol 6:1. doi:10.1186/1743-8977-6-1

Baud O, Greene AE, Li J, Wang H, Volpe JJ, Rosenberg PA (2004) Glutathione peroxidase-catalase cooperativity is required for resistance to hydrogen peroxide by mature rat oligodendrocytes. J Neurosci 24 (7):1531-1540.   doi:10.1523/JNEUROSCI.3989-03.2004

Benkovic SA, Connor JR (1993) Ferritin, transferrin, and iron in selected regions of the adult and aged rat brain. J Comp Neurol 338 (1):97-113. doi:10.1002/cne.903380108

Berg JM, Ho S, Hwang W, Zebda R, Cummins K, Soriaga MP, Taylor R, Guo B, Sayes CM (2010) Internalization of carbon black and maghemite iron oxide nanoparticle mixtures leads to oxidant production. Chem Res Toxicol 23 (12):1874-1882. doi:10.1021/tx100307h

Bradl M, Lassmann H (2010) Oligodendrocytes: biology and pathology. Acta Neuropathol 119 (1):37-53. doi:10.1007/s00401-009-0601-5

Buckinx R, Smolders I, Sahebali S, Janssen D, Smets I, Ameloot M, Rigo JM (2009) Morphological changes do not reflect biochemical and functional differentiation in OLN-93 oligodendroglial cells. J Neurosci Methods 184 (1):1-9. doi:10.1016/j.jneumeth.2009.07.004

Bulte JW, Douglas T, Witwer B, Zhang SC, Strable E, Lewis BK, Zywicke H, Miller B, van Gelderen P, Moskowitz BM, Duncan ID, Frank JA (2001) Magnetodendrimers allow endosomal magnetic labeling and in vivo tracking of stem cells. Nat Biotechnol 19 (12):1141-1147. doi:10.1038/nbt1201-1141

Busch W, Bastian S, Trahorsch U, Iwe M, Kühnel D, Meißner T, Springer A, Gelinsky M, Richter V, Ikonomidou C (2011) Internalisation of engineered nanoparticles into mammalian cells in vitro: influence of cell type and particle properties. J Nanopart Res 13:293-310. doi:10.1007/s11051-010-0030-3

Buyukhatipoglu K, Clyne AM (2011) Superparamagnetic iron oxide nanoparticles change endothelial cell morphology and mechanics via reactive oxygen species formation. J Biomed Mater Res A 96 (1):186-195. doi:10.1002/jbm.a.32972

Chertok B, Moffat BA, David AE, Yu F, Bergemann C, Ross BD, Yang VC (2008) Iron oxide nanoparticles as a drug delivery vehicle for MRI monitored magnetic targeting of brain tumors. Biomaterials 29 (4):487-496. doi:10.1016/j.biomaterials.2007.08.050

Connor JR, Menzies SL (1996) Relationship of iron to oligodendrocytes and myelination. Glia 17 (2):83-93. doi:10.1002/(SICI)1098-1136(199606)17:2<83::AID-GLIA1>3.0.CO;2-7

Ding J, Tao K, Li J, Song S, Sun K (2010) Cell-specific cytotoxicity of dextran-stabilized magnetite nanoparticles. Colloids Surf B Biointerfaces 79 (1):184-190. doi:10.1016/j.colsurfb.2010.03.053

Dringen R, Hamprecht B (1996) Glutathione content as an indicator for the presence of metabolic pathways of amino acids in astroglial cultures. J Neurochem 67 (4):1375-1382. doi:10.1046/j.1471-4159.1996.67041375.x

Dringen R, Hamprecht B (1998) Glutathione restoration as indicator for cellular metabolism of astroglial cells. Dev Neurosci 20 (4-5):401-407. doi:10.1159/000017338

Dringen R, Kranich O, Hamprecht B (1997) The γ-glutamyl transpeptidase inhibitor acivicin preserves glutathione released by astroglial cells in culture. Neurochem Res 22 (6):727-733. doi:10.1023/A:1027310328310

Dringen R, Kussmaul L, Hamprecht B (1998) Detoxification of exogenous hydrogen peroxide and organic hydroperoxides by cultured astroglial cells assessed by microtiter plate assay. Brain Res Brain Res Protoc 2 (3):223-228. doi:10.1016/S1385-299X(97)00047-0

Dringen R, Pawlowski PG, Hirrlinger J (2005) Peroxide detoxification by brain cells. J Neurosci Res 79 (1-2):157-165. doi:10.1002/jnr.20280

Fauconnier N, Pons JN, Roger J, Bee A (1997) Thiolation of maghemite nanoparticles by dimercaptosuccinic acid. J Colloid Interface Sci 194 (2):427-433. doi:10.1006/jcis.1997.5125

Galaris D, Pantopoulos K (2008) Oxidative stress and iron homeostasis: mechanistic and health aspects. Crit Rev Clin Lab Sci 45 (1):1-23.   doi:10.1080/10408360701713104

Geppert M, Hohnholt M, Gaetjen L, Grunwald I, Bäumer M, Dringen R (2009) Accumulation of iron oxide nanoparticles by cultured brain astrocytes. J Biomed Nanotechnol 5 (3):285-293. doi:10.1166/jbn.2009.1033

Geppert M, Hohnholt MC, Thiel K, Nürnberger S, Grunwald I, Rezwan K, Dringen R (2011) Uptake of dimercaptosuccinate-coated magnetic iron oxide nanoparticles by cultured brain astrocytes. Nanotechnology 22 (14):145101-145111. doi:10.1088/0957-4484/22/14/145101

Hagens WI, Oomen AG, de Jong WH, Cassee FR, Sips AJ (2007) What do we (need to) know about the kinetic properties of nanoparticles in the body? Regul Toxicol Pharmacol 49 (3):217-229. doi:10.1016/j.yrtph.2007.07.006

Hirrlinger J, Dringen R (2010) The cytosolic redox state of astrocytes: maintenance, regulation and functional implications for metabolite trafficking. Brain Res Rev 63 (1-2):177-188. doi:10.1016/j.brainresrev.2009.10.003

Hirrlinger J, Resch A, Gutterer JM, Dringen R (2002a) Oligodendroglial cells in culture effectively dispose of exogenous hydrogen peroxide: comparison with cultured neurones, astroglial and microglial cells. J Neurochem 82 (3):635-644. doi:10.1046/j.1471-4159.2002.00999.x

Hirrlinger J, Schulz JB, Dringen R (2002b) Glutathione release from cultured brain cells: multidrug resistance protein 1 mediates the release of GSH from rat astroglial cells. J Neurosci Res 69 (3):318-326. doi:10.1002/jnr.10308

Hoepken HH, Korten T, Robinson SR, Dringen R (2004) Iron accumulation, iron-mediated toxicity and altered levels of ferritin and transferrin receptor in cultured astrocytes during incubation with ferric ammonium citrate. J Neurochem 88 (5):1194-1202. doi:10.1046/j.1471-4159.2003.02236.x

Hohnholt M, Geppert M, Dringen R (2010a) Effects of iron chelators, iron salts, and iron oxide nanoparticles on the proliferation and the iron content of oligodendroglial OLN-93 cells. Neurochem Res 35 (8):1259-1268. doi:10.1007/s11064-010-0184-5

Hohnholt MC, Geppert M, Nürnberger S, Von Byern J, Grunwald I, Dringen R (2010b) Advanced biomaterials accumulation of citrate-coated magnetic iron oxide

nanoparticles by cultured brain astrocytes. Adv Eng Mater 12 (12):B690-B694. doi:10.1002/adbi.201000055

Jordan A, Scholz R, Maier-Hauff K, van Landeghem FK, Waldoefner N, Teichgraeber U, Pinkernelle J, Bruhn H, Neumann F, Thiesen B, von Deimling A, Felix R (2006) The effect of thermotherapy using magnetic nanoparticles on rat malignant glioma. J Neurooncol 78 (1):7-14. doi:10.1007/s11060-005-9059-z

Lewinski N, Colvin V, Drezek R (2008) Cytotoxicity of nanoparticles. Small 4 (1):26-49. doi:10.1002/smll.200700595

Lowry OH, Rosebrough NJ, Farr AL, Randall RJ (1951) Protein measurement with the folin phenol reagent. J Biol Chem 193 (1):265-275

McTigue DM, Tripathi RB (2008) The life, death, and replacement of oligodendrocytes in the adult CNS. J Neurochem 107 (1):1-19. doi:DOI 10.1111/j.1471-4159.2008.05570.x

Moller P, Jacobsen NR, Folkmann JK, Danielsen PH, Mikkelsen L, Hemmingsen JG, Vesterdal LK, Forchhammer L, Wallin H, Loft S (2010) Role of oxidative damage in toxicity of particulates. Free Radic Res 44 (1):1-46. doi:10.3109/10715760903300691

Nel A, Xia T, Mädler L, Li N (2006) Toxic potential of materials at the nanolevel. Science 311 (5761):622-627. doi:10.1126/science.1114397

Pickard M, Chari D (2010) Enhancement of magnetic nanoparticle-mediated gene transfer to astrocytes by 'magnetofection': effects of static and oscillating fields. Nanomedicine (Lond) 5 (2):217-232. doi:10.2217/nnm.09.109

Radu M, Munteanu MC, Petrache S, Serban AI, Dinu D, Hermenean A, Sima C, Dinischiotu A (2010) Depletion of intracellular glutathione and increased lipid peroxidation mediate cytotoxicity of hematite nanoparticles in MRC-5 cells. Acta Biochim Pol 57 (3):355-360. doi:20101975

Richardson DR, Baker E (1994) Two saturable mechanisms of iron uptake from transferrin in human melanoma cells: the effect of transferrin concentration, chelators, and metabolic probes on transferrin and iron uptake. J Cell Physiol 161 (1):160-168. doi:10.1002/jcp.1041610119

Richter-Landsberg C, Heinrich M (1996) OLN-93: a new permanent oligodendroglia cell line derived from primary rat brain glial cultures. J Neurosci Res 45 (2):161-173. doi:10.1002/(SICI)1097-4547(19960715)45:2<161::AID-JNR8>3.0.CO;2-8

Riemer J, Hoepken HH, Czerwinska H, Robinson SR, Dringen R (2004) Colorimetric ferrozine-based assay for the quantitation of iron in cultured cells. Anal Biochem 331 (2):370-375. doi:10.1016/j.ab.2004.03.049

Scheiber IF, Schmidt MM, Dringen R (2010) Zinc prevents the copper-induced damage of cultured astrocytes. Neurochem Int 57 (3):314-322. doi:10.1016/j.neuint.2010.06.010

Silva GA (2007) Nanotechnology approaches for drug and small molecule delivery across the blood brain barrier. Surg Neurol 67 (2):113-116. doi:10.1016/j.surneu.2006.08.033

Soenen SJ, Himmelreich U, Nuytten N, De Cuyper M (2011) Cytotoxic effects of iron oxide nanoparticles and implications for safety in cell labelling. Biomaterials 32 (1):195-205. doi:10.1016/j.biomaterials.2010.08.075

Soenen SJ, Nuytten N, De Meyer SF, De Smedt SC, De Cuyper M (2010) High intracellular iron oxide nanoparticle concentrations affect cellular cytoskeleton and focal adhesion kinase-mediated signaling. Small 6 (7):832-842. doi:10.1002/smll.200902084

Thiessen A, Schmidt MM, Dringen R (2010) Fumaric acid dialkyl esters deprive cultured rat oligodendroglial cells of glutathione and upregulate the expression of heme oxygenase 1. Neurosci Lett 475 (1):56-60. doi:10.1016/j.neulet.2010.03.048

Valois CR, Braz JM, Nunes ES, Vinolo MA, Lima EC, Curi R, Kuebler WM, Azevedo RB (2010) The effect of DMSA-functionalized magnetic nanoparticles on transendothelial migration of monocytes in the murine lung via a β_2 integrin-dependent pathway. Biomaterials 31 (2):366-374. doi:10.1016/j.biomaterials.2009.09.053

Wang J, Chen Y, Chen B, Ding J, Xia G, Gao C, Cheng J, Jin N, Zhou Y, Li X, Tang M, Wang XM (2010) Pharmacokinetic parameters and tissue distribution of magnetic Fe_3O_4 nanoparticles in mice. Int J Nanomedicine 5:861-866. doi:10.2147/IJN.S13662

Weinstein JS, Varallyay CG, Dosa E, Gahramanov S, Hamilton B, Rooney WD, Muldoon LL, Neuwelt EA (2010) Superparamagnetic iron oxide nanoparticles: diagnostic magnetic resonance imaging and potential therapeutic applications in neurooncology and central nervous system inflammatory pathologies, a review. J Cereb Blood Flow Metab 30 (1):15-35. doi:10.1038/jcbfm.2009.192

Yang H (2010) Nanoparticle-mediated brain-specific drug delivery, imaging, and diagnosis. Pharm Res 27 (9):1759-1771. doi:10.1007/s11095-010-0141-7

2.2.   Consequences of an exposure of cultured astrocytes to iron oxide nanoparticles

2.2.1.   Publication 4

Hohnholt MC, Geppert M, Nürnberger S, von Byern J, Grunwald I, Dringen R (2010) Advanced Biomaterials: Accumulation of citrate-coated magnetic iron oxide nanoparticles by cultured brain astrocytes. Adv Eng Mater 12:B690-B694

2.2.2.   Publication 5

Geppert M, Hohnholt M, Gaetjen L, Grunwald I, Bäumer M, Dringen R (2009) Accumulation of iron oxide nanoparticles by cultured brain astrocytes. J Biomed Nanotechnol 5:285-293

2.2.3.   Publication 6

Geppert M, Hohnholt MC, Thiel K, Nürnberger S, Grunwald I, Rezwan K, Dringen R (2011) Uptake of dimercaptosuccinate-coated magnetic iron oxide nanoparticles by cultured brain astrocytes. Nanotechnology 22:145101-145111

2.2.1.   Publication 4

Hohnholt MC, Geppert M, Nürnberger S, von Byern J,

Grunwald I, Dringen R

(2010)

Advanced Biomaterials: Accumulation of citrate-coated magnetic iron oxide

nanoparticles by cultured brain astrocytes.

Adv Eng Mater 12:B690-B694

Contribution of Michaela C. Hohnholt:

- Concept of this publication.

- Performance of the Perls´ staining and preparation of Fig. 3.

- Coordination of sample preparation for electron microscopy of cell samples.

- Preparation of the first version of the manuscript.

Mark Geppert synthesized the iron oxide nanoparticles and obtained the data shown in Figs. 1 and 2.

Sylvia Nürnberger performed the sample preparation for electron microscopy and generated Fig. 4.

ADVANCED BIOMATERIALS

Advanced Biomaterials Accumulation of Citrate-Coated Magnetic Iron Oxide Nanoparticles by Cultured Brain Astrocytes**

By *Michaela C. Hohnholt, Mark Geppert, Sylvia Nürnberger, Janek von Byern, Ingo Grunwald* and *Ralf Dringen**

Magnetic iron oxide nanoparticles (Fe-NP) are considered for various applications in the brain. However, little is known so far on the uptake and the metabolism of such nanoparticles in brain cells. Since astrocytes are strategically localized between capillaries and neurons, astrocytes are of particular interest concerning uptake and fate of nanoparticles in the brain. Using astrocyte-rich primary cultures as model system we have investigated the accumulation of citrate-coated Fe-NP by astrocytes. Viable cultured astrocytes accumulate iron from citrate-coated Fe-NP in a time-, concentration-, and temperature-dependent manner. The cellular iron content determined after 4 h of incubation increases proportional to the concentration of Fe-NP, if the particles were applied in concentrations of up to 1000×10^{-6} M of total iron. The iron accumulation from 500 or 1000×10^{-6} M iron as Fe-NP is significantly slowed by lowering the incubation temperature from 37 to 4 °C. Transmission electron microscopy of the cells revealed that most of the cellular Fe-NP are present in intracellular vesicles. These data demonstrate that astrocytes accumulate efficiently citrate-coated Fe-NP, most likely by an endocytotic pathway.

Magnetic iron oxide nanoparticles (Fe-NP) contain an iron oxide core (Fe_3O_4 or γ-Fe_2O_3) and a ligand shell which consists of small organic molecules, polymers, or proteins and is

[*] Prof. R. Dringen, M. C. Hohnholt, M. Geppert
Center for Biomolecular Interactions Bremen and Center for Environmental Research and Sustainable Technology, University of Bremen,
PO. Box 330440, D-28334 Bremen, Germany
E-mail: ralf.dringen@uni-bremen.de
S. Nürnberger
Department of Traumatology, Medical University of Vienna, Waehringer Guertel 18-20, 1090 Vienna, Austria
Dr. J. von Byern
Faculty of Life Sciences, University of Vienna, Research Unit Cell Imaging and Ultrastructure
Althanstrasse 14, 1090 Vienna, Austria
Dr. I. Grunwald
Fraunhofer Institute for Manufacturing Technology and Applied Materials Research
Wiener Strasse, D-28359 Bremen, Germany

essential for the stable dispersion of such nanoparticles in physiological media.[1–3] Due to their small size Fe-NP are considered for many applications. Especially in medicine and brain cell biology, Fe-NP have already been used as contrast agent,[4] as carriers for drug delivery,[5] for magnetic hyperthermia approaches,[6] and for magnetic transfection of cells.[7] However, despite such important applications little is known so far about the uptake of Fe-NP into brain cells and on the fate of these particles in brain or in cultured brain cells.

The brain contains in addition to neurons also different types of glial cells. Among these glial cells, astrocytes are quantitatively the largest population of cells.[8] Astrocytes fulfill a variety of very important functions for the brain, e.g., in the regulation of ion, pH and transmitter homeostasis, in supporting synapse function and in giving metabolic support to other types of brain cells.[9–12] Endfeet of astrocytes are covering the surface of brain capillaries that consist of capillary endothelial cells which constitute the blood-brain barrier. Thus, astrocytes will be the first parenchymal brain cell type that encounters nanoparticles that have crossed the blood-brain barrier. Due to this strategically important location astrocytes can control the flow of metabolites and metal ions from the blood into the brain and vice versa.[9] Due to their potential to take up and release iron, astrocytes have been discussed to play an important role in the iron metabolism of the brain.[13] Thus, astrocytes should also be considered concerning the accumulation and the fate of Fe-NP in the brain. Application of different types of Fe-NP to

M. C. Hohnholt et al./Advanced Biomaterials Accumulation of Citrate-Coated Magnetic...

ADVANCED BIOMATERIALS

cultured astrocytes appears not to be acutely toxic to these cells.[7,14,15] These cells accumulate iron even better from Fe-NP than from identical amounts (100×10^{-6} M total iron) of low molecular weight iron sources.[14]

Here, we report that cultured astrocytes accumulate iron efficiently from citrate-coated Fe-NP in a time-, concentration-, and temperature dependent manner. Presence of cellular iron after exposure of astrocytes to Fe-NP was demonstrated by iron quantification, by cytochemical Perls' staining for iron as well as by transmission electron microscopy (TEM) of Fe-NP in the cells.

Experimental

Synthesis and Coating of Fe-NP

Magnetic Fe-NP were synthesized by using a wet chemical method as described previously[14] using the method initially described by Bee et al.[16]. The stock solution of Fe-NP in water (80×10^{-3} M total iron concentration) was diluted with an equal volume of 80×10^{-3} M freshly prepared aqueous tri-sodium citrate, resulting in an aqueous stable dispersion of citrate-coated Fe-NP that contained 40×10^{-3} M of total iron. The presence of the citrate as coating molecule on the surface of such Fe-NP has previously been demonstrated.[17,18] The dispersion of citrate-coated Fe-NP was sterile filtered and stored at 4 °C. All concentrations of Fe-NP given here refer to the concentration of total iron in the diluted Fe-NP dispersions and not to the concentration of the nanoparticles.

Cell Culture and Experimental Incubations

Astrocyte-rich primary cultures in wells of 24-well plates were prepared from the brains of newborn Wistar rats and maintained as described previously.[14] Cells were exposed to citrate-coated Fe-NP in 1 mL incubation buffer (20×10^{-3} M HEPES, 145×10^{-3} M NaCl, 1.8×10^{-3} M CaCl$_2$, 5.4×10^{-3} M KCl, 1×10^{-3} M MgCl$_2$, 5×10^{-3} M glucose, 10×10^{-3} M tri-sodium citrate) that had been adjusted to pH 7.4 at the desired temperature. After the given incubation periods, the cells were washed twice with 1 mL of ice-cold phosphate-buffered saline (PBS: 10×10^{-3} M potassium phosphate buffer pH 7.4, containing 150×10^{-3} M NaCl) and dry cells were stored frozen until quantification of their iron and protein contents. Increasing the number of washing steps, washing the cells in presence of the iron chelator deferoxamine (10×10^{-3} M in PBS) or washing the cells with 10×10^{-3} M HCl did not lower the amount of detectable cellular iron after incubation with 1000×10^{-6} M Fe-NP for 4 h (data not shown), demonstrating that washing the cells twice with PBS is sufficient to remove all loosely bound Fe-NP from the cell membranes.

Determination of Cell Viability and Quantification of Cellular Contents of Protein and Iron

Cell viability was analyzed by comparison of the activities of extracellular and cellular lactate dehydrogenase (LDH) as described previously.[19,20] For quantification of the cellular

protein content, cells were lysed in 400 µL 50×10^{-3} M NaOH and the protein content was determined according to the Lowry method [21] with bovine serum albumin as standard. Iron contents in media and cells were quantified by the ferrozine-based colorimetric assay [22] in the modification described previously.[14,19]

Visualization of Cellular Iron and Fe-NP by Perls' Staining and TEM

Cellular iron was visualized by the cytochemical Perls' staining [23] as described previously.[14,19] For TEM analysis, cells grown on Aclarfilm (Ted Pella, Redding, USA) in wells of 24-well dishes were incubated with 1000×10^{-6} M citrate-coated Fe-NP, washed with ice-cold PBS and prefixed with 2.5% w/v glutaraldehyde in 0.1 M sodium cacodylate buffer pH 7.3 for 60 min. After rinsing in prefixation buffer, fixation was carried out in 1% w/v osmium tetroxide and 1% w/v potassium ferrocyanide (in sodium cacodylate buffer) for 2 h. The samples were subsequently washed with cacodylate buffer, dehydrated in a graded series of increasing ethanol concentrations, infiltrated with Agar Low Viscosity Resin (Agar Scientific, Stansted, UK) and polymerized at 60 °C. Ultrathin sections of 70 nm were stained with uranyl acetate and lead citrate. Sections were examined in an FEI Morgagni electron microscope (Eindhoven, Netherlands) operated at 80 kV. Results were documented with a Morada CCD-camera (Olympus, Vienna, Austria).

Presentation of Data

The data shown are means ± standard deviation from values obtained on three independently prepared cultures. Significance of differences between two sets of data was analyzed by paired t-test. $p > 0.05$ was considered as not significant.

Results

To test for the ability of astrocytes to accumulate iron from Fe-NP, astrocyte-rich primary cultures were incubated with citrate-coated Fe-NP (Fig. 1). While no alteration of the cellular iron content was observed for cells treated without Fe-NP at 37 °C, the content of cell-associated iron increased almost linearly after exposure to Fe-NP from initial 18 ± 10 nmol iron/mg protein to 1075 ± 138 nmol mg^{-1} protein (500×10^{-6} M) and 1915 ± 93 nmol mg^{-1} protein (1000×10^{-6} M) [Fig. 1(A)]. Cells that were incubated with Fe-NP at 4 °C under otherwise identical conditions contained at each time point investigated less iron than cells that had been incubated at 37 °C [Fig. 1(A)]. The almost linear increases of the specific cellular iron contents between 1 and 6 h were used to calculate specific iron accumulation rates. For both Fe-NP concentrations used, the iron accumulation rate at 4 °C was with $44.4 \pm 2.3\%$ (500×10^{-6} M) and $41.2 \pm 2.9\%$ (1000×10^{-6} M) significantly lower than that determined for 37 °C [Fig. 1(B)], suggesting that a membrane dependent

M. C. Hohnholt et al./Advanced Biomaterials Accumulation of Citrate-Coated Magnetic ...
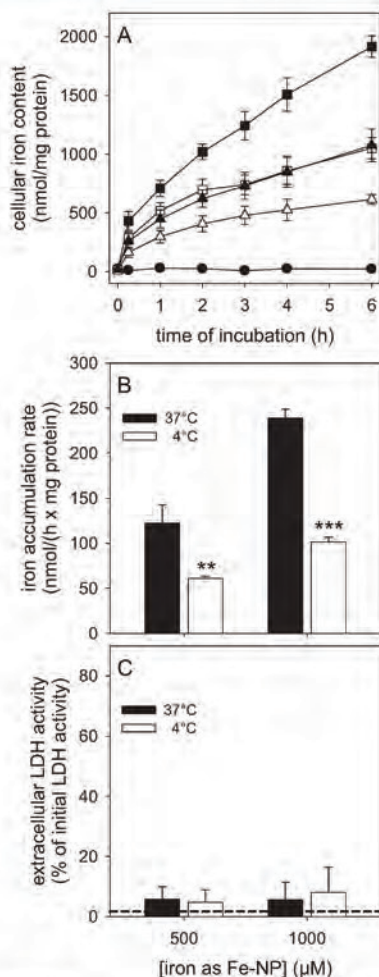
Fig. 1. (A) Time- and temperature-dependency of the accumulation of iron by cultured astrocytes after exposure to Fe-NP. The cells were incubated without (circles) or with 500×10^{-6} M (triangles) or 1000×10^{-9} M (squares) iron as citrate-coated Fe-NP for up to 6 h at 37 °C (filled symbols) or 4 °C (open symbols). (B) Iron accumulation rates that were calculated from the almost linear increases of the cellular iron contents between 1 and 6 h of incubation. (C) Extracellular LDH activity after 6 h of incubation as indicator for cell viability. Stars in B indicate the significance of differences between the values obtained for incubation at 37 and 4 °C (**$p < 0.01$, ***$p < 0.001$). The dashed line in C represents the extracellular LDH activity of cells that had been incubated without Fe-NP.

uptake process is involved in iron accumulation from Fe-NP. None of the conditions used compromised cell viability, since after 6 h of incubation no significant increases in extracellular LDH activity were observed [Fig. 1(C)].

To investigate the concentration dependency of the iron accumulation from Fe-NP, astrocyte cultures were incubated with citrate-coated Fe-NP of various concentrations for 4 h (Fig. 2). The content of cell-associated iron increased almost linearly with the concentration of citrate-coated Fe-NP in the concentration range of $0-1000 \times 10^{-6}$ M iron (Fig. 2).
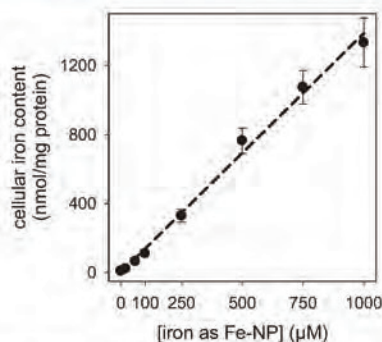

Fig. 2. Concentration dependency of the accumulation of iron from Fe-NP by cultured astrocytes. The cells were incubated for 4 h at 37 °C with iron supplied as citrate-coated Fe-NP in the indicated concentrations. Linear regression of the data revealed a correlation of 0.995.

The strong accumulation of iron from citrate-coated Fe-NP by cultured astrocytes was confirmed by cytochemical Perls' staining for iron (Fig. 3). Astrocytes that had been exposed to 1000×10^{-6} M citrate-coated Fe-NP for 4 h at 37 °C showed an intense dark staining [Fig. 3(C)] which was not detectable for cells that were incubated without Fe-NP [Fig. 3(A)]. The staining was punctuated and predominantly located around the cell nuclei [Fig. 3(C)]. In contrast, when cells were incubated at 4 °C hardly any Perls' staining was detectable both for cells that were incubated without or with citrate-coated Fe-NP [Fig. 3(B,D)].

To investigate whether the measured cell-associated iron represents intracellular Fe-NP, the cells were analyzed by TEM after incubation for 4 h with 1000×10^{-6} M citrate-coated Fe-NP at 37 °C (Fig. 4). Cells exposed to Fe-NP contained electron-dense particles that were predominately located as aggregates in intracellular membrane vesicle and to a lesser extent in the cytosol of the cells [Fig. 4(A,B)]. In addition,
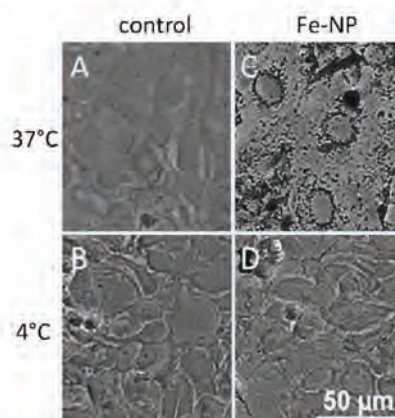

Fig. 3. Perls' iron staining of cultured astrocytes after exposure to Fe-NP. The cells were incubated without (control) or with 1000×10^{-6} M citrate-coated Fe-NP at 37 °C or at 4 °C. The size bar in D applies to all panels.
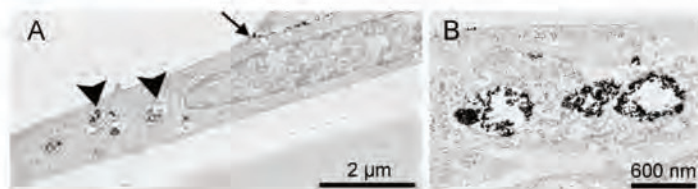
ADVANCED BIOMATERIALS

Fig. 4. TEM images of cultured astrocytes after exposure to Fe-NP. The cells were incubated at 37 °C with 1000×10^{-6} M iron as citrate-coated Fe-NP. Electron-dense particles are predominately visible in intracellular vesicles (A, arrowhead) and at the cell surface between cells (A, arrow).

electron-dense material was observed to be present between cells [Fig. 4(A), arrow].

Discussion

Exposure of cultured astrocytes to citrate-coated magnetic Fe-NP did not cause any acute damage, confirming published data for the exposure of astrocytes with different types of coated Fe-NP.[7,14] Cultured astrocytes accumulated iron efficiently to yield high specific iron contents of up to 2 μmol iron/mg protein within 6 h. This demonstrates the high capacity of astrocytes to accumulate iron from Fe-NP and is in line with the observation that astrocytes accumulate iron better from Fe-NP than from low molecular weight iron.[14] The concentration dependency of iron accumulation was almost linear for concentrations up to 1000×10^{-6} M Fe-NP, indicating that at least in this range the iron accumulation from citrate-coated Fe-NP is not saturable.

The iron quantification method used cannot discriminate between intracellular iron and iron that is extracellularly bound as Fe-NP to cell membranes. To discriminate between these two options, the iron accumulation from citrate-coated Fe-NP at 37 °C was compared to that at 4 °C, since membrane dependent uptake processes are strongly slowed by lowering the incubation temperature. Results from such experiments suggest that after exposure of astrocytes to Fe-NP around 40% of the cell-associated iron represents extracellularly bound iron, while around 60%, calculated as difference of the cellular iron contents determined after incubations at 37 and 4 °C, had been taken up into the cells. The view that cell-associated iron represents the sum of intracellular iron plus extracellularly bound iron is strongly supported by TEM images of astrocytes after exposure to Fe-NP, which revealed presence of Fe-NP in cells as well as between cells and on the cell surface. The temperature dependency of iron accumulation from 1000×10^{-6} M citrate-coated Fe-NP resembles results obtained for the cellular uptake of low molecular weight iron,[24–26] hemine iron,[27] or a low concentration (100×10^{-6} M) of citrate-coated Fe-NP.[14] Also in these studies, the amounts of cell-associated iron determined after incubation at 4 °C was considered to reflect extracellularly bound material.

Most of the electron-dense material observed by TEM for Fe-NP-treated astrocytes was localized within vesicle-like structures, confirming previous reports.[7,14] This observation

suggests that astrocytes internalize Fe-NP by an endocytotic uptake process, as it has been suggested for non-phagocytotic cells.[28] In addition, the Perls' iron staining of astrocytes that had been exposed to citrate-coated Fe-NP at 37 °C revealed presence of substantial amounts of iron in the cells, while cells that were incubated at 4 °C were not Perls'-positive. These data support the view that the temperature dependent part of the cellular iron reflects the amount of iron that has been taken up into the cells after exposure to citrate-coated Fe-NP, whereas the amount of cell-associated iron determined for cells that were incubated at 4 °C represents predominantly Fe-NP that had bound extracellularly to cell membranes. The absence of Perls' staining from cells that were exposed to Fe-NP at 4 °C is likely to be a consequence of the known poor sensitivity of this assay.[14]

In summary, cultured brain astrocytes are highly efficient to accumulate iron from citrate-coated Fe-NP in a time-, concentration-, and temperature dependent manner into intracellular vesicles by a mechanism that is likely to involve endocytosis, a process which is well known to occur in astrocytes in vitro.[29–31] However, further studies are required to investigate whether the observed accumulation of Fe-NP in cultured astrocytes is also a property of astrocytes in brain. Since astrocytes have important functions for the iron homeostasis of the brain,[13] the fate of the internalized Fe-NP particles will be interesting to study. If the iron of the accumulated Fe-NP is available for the cellular metabolism, it could support iron-dependent processes or, alternatively, induce iron-mediated toxicity in brain cells.

[1] S. Laurent, D. Forge, M. Port, A. Roch, C. Robic, L. Vander Elst, R. N. Muller, *Chem. Rev.* **2008**, *108*, 2064.

[2] A. H. Lu, E. L. Salabas, F. Schuth, *Angew. Chem, Int. Ed. Engl.* **2007**, *46*, 1222.

[3] B. Samanta, H. Yan, N. O. Fischer, J. Shi, D. J. Jerry, V. M. Rotello, *J. Mater. Chem.* **2008**, *18*, 1204.

[4] J. S. Weinstein, C. G. Varallyay, E. Dosa, S. Gahramanov, B. Hamilton, W. D. Rooney, L. L. Muldoon, E. A. Neuwelt, *J. Cereb. Blood Flow Metab.* **2010**, *30*, 15.

[5] B. Chertok, B. A. Moffat, A. E. David, F. Yu, C. Bergemann, B. D. Ross, V. C. Yang, *Biomaterials* **2008**, *29*, 487.

[6] A. Jordan, R. Scholz, K. Maier-Hauff, F. K. van Landeghem, N. Waldoefner, U. Teichgraeber, J. Pinkernelle, H. Bruhn, F. Neumann, B. Thiesen, A. von Deimling, R. Felix, *J. Neurooncol.* **2006**, *78*, 7.

[7] M. Pickard, D. Chari, *Nanomedicine (Lond)* **2010**, 5, 217.

[8] M. Nedergaard, B. Ransom, S. A. Goldmann, *Trends Neurosci.* **2003**, 26, 523.

[9] M. V. Sofroniew, H. V. Vinters, *Acta Neuropathol.* **2010**, 119, 7.

[10] J. Hirrlinger, R. Dringen, *Brain Res. Rev.* **2010**, 63, 177.

[11] M. M. Halassa, P. G. Haydon, *Annu. Rev. Physiol.* **2010**, 72, 335.

[12] C. Giaume, A. Koulakoff, L. Roux, D. Holcman, N. Rouach, *Nat. Rev. Neurosci.* **2010**, 11, 87.

[13] R. Dringen, G. M. Bishop, M. Koeppe, T. N. Dang, S. R. Robinson, *Neurochem. Res.* **2007**, 32, 1884.

[14] M. Geppert, M. Hohnholt, L. Gaetjen, I. Grunwald, M. Baumer, R. Dringen, *J. Biomed. Nanotechnol.* **2009**, 5, 285.

[15] C. Au, L. Mutkus, A. Dobson, J. Riffle, J. Lalli, M. Aschner, *Biol. Trace Elem. Res.* **2007**, 120, 248.

[16] A. Bee, R. Massart, S. Neveu, *J. Magn. Magn. Mater.* **1995**, 149, 6.

[17] N. Fauconnier, A. Bee, R. Massart, F. Dardoize, *J. Liq. Chromatogr. Relat. Technol.* **1996**, 19, 783.

[18] N. Fauconnier, A. Bee, J. Roger, J. N. Pons, *Prog. Colloid Polym. Sci.* **1996**, 100, 212.

[19] M. Hohnholt, M. Geppert, R. Dringen, *Neurochem. Res.* **2010**, 35, 1259.

[20] R. Dringen, L. Kussmaul, B. Hamprecht, *Brain Res. Protoc.* **1998**, 2, 223.

[21] O. H. Lowry, N. J. Rosebrough, A. L. Farr, R. J. Randall, *J. Biol. Chem.* **1951**, 193, 265.

[22] J. Riemer, H. H. Hoepken, H. Czerwinska, S. R. Robinson, R. Dringen, *Anal. Biochem.* **2004**, 331, 370.

[23] M. Perls, *Virchows Arch.* **1867**, 39, 42.

[24] Z. M. Qian, Q. K. Liao, Y. To, Y. Ke, Y. K. Tsoi, G. F. Wang, K. P. Ho, *Cell Mol. Biol. (Noisy-le-grand)* **2000**, 46, 541.

[25] D. R. Richardson, *Biochim. Biophys. Acta* **2001**, 1536, 43.

[26] D. Trinder, E. Morgan, *Am. J. Physiol.* **1998**, 275, G279.

[27] T. N. Dang, G. M. Bishop, R. Dringen, S. R. Robinson, *Glia* **2010**, 58, 55.

[28] J. Rejman, V. Oberle, I. S. Zuhorn, D. Hoekstra, *Biochem. J.* **2004**, 377, 159.

[29] W. Noske, H. Letzen, K. Lange, K. Keller, *Exp. Cell Res.* **1982**, 142, 437.

[30] L. Megias, C. Guerri, E. Fornas, I. Azorin, E. Bendala, M. Sancho-Tello, J. M. Duran, M. Tomas, M. J. Gomez-Lechon, J. Reanu-Piqueras, *Int. J. Dev. Biol.* **2000**, 44, 2009.

[31] M. Jiang, G. Chen, *J. Neurosci.* **2009**, 29, 8063.

196

2.2.2.   Publication 5

Geppert M, Hohnholt M, Gaetjen L, Grunwald I,

Bäumer M, Dringen R

(2009)

Accumulation of iron oxide nanoparticles by cultured brain astrocytes.

J Biomed Nanotechnol 5:285-293

Contribution of Michaela C. Hohnholt:

- Performance of the Perls´ staining and preparation of Fig. 5.

- Coordination of sample preparation for electron microscopy of cell samples.

Mark Geppert synthesized the iron oxide nanoparticles and obtained the data shown in Figs. 1-4, Fig. 6 and Table 1.

Linda Gaetjen performed the sample preparation and staining of cell samples for electron microscopy (Fig. 4).

Accumulation of Iron Oxide Nanoparticles by Cultured Brain Astrocytes

Mark Geppert[1,2], Michaela Hohnholt[1,2], Linda Gaetjen[3], Ingo Grunwald[3],
Marcus Bäumer[4], and Ralf Dringen[1,2,5,*]

[1] Center for Biomolecular Interactions Bremen, University of Bremen, PO. Box 330440, D-28334 Bremen, Germany
[2] Center for Environmental Research and Sustainable Technology, Leobener Strasse, D-28359 Bremen, Germany
[3] Fraunhofer Institute for Manufacturing Technology and Applied Materials Research,
Wiener Strasse 12, D-28395 Bremen, Germany
[4] Institute for Applied and Physical Chemistry, University of Bremen, PO. Box 330440, D-28359 Bremen, Germany
[5] School of Psychology, Psychiatry, and Psychological Medicine, Monash University,
Wellington Rd., Clayton, Victoria 3800, Australia

Magnetic iron oxide nanoparticles are considered for various diagnostic and therapeutic applications in brain including their use as contrast agent for magnetic resonance imaging or as tool for magnetic drug delivery. However, little is known so far on the consequences of a treatment of brain cells with such nanoparticles. In order to study the biocompatibility of iron oxide nanoparticles and the accumulation of iron from such particles in brain cells, we have used astrocyte-rich primary cultures as model system. Iron oxide nanoparticles were chemically synthesized with a yield of about 80% regarding the iron content. Transmission electron microscopy revealed that the synthesized iron oxide nanoparticles had a diameter of about 10 nm. Exposure of astrocyte cultures to 100 μM iron that were supplied as citrate-coated iron oxide nanoparticles did not cause any acute loss in cell viability but resulted in an almost linear increase in the cellular iron content that reached after 6 h of incubation at 37 °C a total cellular iron content of about 300 nmol/mg protein. The rate of iron accumulation from iron oxide nanoparticles was significantly higher than that from the low molecular weight iron complex ferric ammonium citrate (FAC). Lowering the incubation temperature from 37 °C to 4 °C reduced the iron accumulation rate from iron oxide nanoparticles or FAC by about 60%. In addition, presence of ferric or ferrous iron chelators did not affect the cellular iron accumulation from iron oxide nanoparticles. These data suggest that cultured astrocytes are able to accumulate intact iron oxide nanoparticles.

Keywords: Accumulation, Astrocytes, Brain, Iron, Nanoparticles, Oxidative Stress, Uptake.

1. INTRODUCTION

Magnetic iron oxide nanoparticles are considered for a wide range of biomedical applications, for example for targeted drug delivery, as contrast agents in magnetic resonance imaging or for the elimination of tumors by magnetically mediated hyperthermia.[1-4] Magnetic iron oxide nanoparticles consist of an iron oxide core (Fe_3O_4 or γ-Fe_2O_3) and are surrounded by a ligand shell of polymers, proteins or small organic molecules.[4,5] This coating with ligands is important for the stability and for the chemical properties of the nanoparticles.[5] Typical diameters of chemically synthesized magnetic iron oxide nanoparticles are around 10 nm, but methods have also been described

to obtain iron oxide nanoparticles of other sizes.[6,7] The magnetic behaviour of aqueous dispersions of iron oxide nanoparticles relies on the small size of the particles and the resulting superparamagnetism.[5]

Astrocytes are the most abundant cell type of the brain.[8] These cells cover with their endfeet almost completely the brain capillaries.[9] In addition, astrocytes have contact with neurons and other types of brain cells. This strategic important localization of astrocytes in the brain allows a controlled transport of nutrients from blood to the brain parenchyma and a controlled export of waste products from the brain. Astrocytes have important functions for the brain in the supply of nutrients to neurons,[10,11] in the detoxification of reactive oxygen species and xenobiotics[12-14] as well as in the metabolism of iron and other metals in the brain.[15-17]

---

* Author to whom correspondence should be addressed.

Little information is currently available on the consequences of a treatment of brain cells with iron oxide nanoparticles. Exposure of cultured astrocytes with iron oxide nanoparticles did not lower cell viability but affected cell adhesion after exposure of the cells for days to nanoparticles.[18] In contrast, when PC12 cells—a frequently used model system for neurons–were exposed to iron oxide nanoparticles for days, a severe loss in cell viability was observed.[19]

Quantitative data on the biocompatibility and accumulation of iron oxide nanoparticles in brain cells are currently not available. Since astrocytes cover the endothelial cells of the brain capillaries, these cells would have the first contact to iron oxide nanoparticles after entering the brain from blood. Astrocytes have the capacity to effectively accumulate iron from various extracellular iron sources, are able to store large amounts of iron and are able to release iron.[16] Thus, this cell type is of especial interest to study the consequences of a treatment of brain cells with iron oxide nanoparticles. Therefore, we have synthesized and characterised iron oxide nanoparticles and have studied the consequences of an exposure of astrocyte-rich primary cultures to the synthesized nanoparticles. Incubation of cultured astrocytes with iron oxide nanoparticles caused a time dependent increase in cellular iron content that depended on the incubation temperature and was not prevented by the presence of iron chelators. In addition, no acute cell toxicity was observed, if cultured astrocytes were exposed to iron oxide nanoparticles.

2. MATERIALS AND METHODS

2.1. Materials

Fetal calf serum (FCS) and penicillin/streptomycin solution were obtained from Biochrom (Berlin, Germany). Dulbecco's modified Eagle's medium (DMEM) was from Gibco (Karlsruhe, Germany). Acetonitrile, bathophenanthroline disulfonate (BPS), deferoxamine (DFX), diaminobenzidine, glutaraldehyde, lead citrate, neocuproine, osmium tetroxide, paraformaldehyde, sodium ascorbate, sodium cacodylate, Trizma base and uranyl acetate were purchased from Sigma (Steinheim, Germany). Bovine serum albumin and NADH were purchased from Applichem (Darmstadt, Germany). All other chemicals of the highest purity available were from either Fluka (Buchs, Switzerland), Merck (Darmstadt, Germany), or Riedel-deHaen (Seelze, Germany). 96-well microtiter plates were from Nunc (Wiesbaden, Germany) and 24-well cell culture plates from Sarstedt (Nümbrecht, Germany).

2.2. Synthesis of Iron Oxide Nanoparticles

Iron oxide nanoparticles were prepared using a modification of a published method.[6] Briefly, 380 mL of an aqueous solution containing 8.89 g $FeCl_3 \cdot 6\ H_2O$, 3.28 g $FeCl_2 \cdot 4\ H_2O$ and 1 mL 37% HCl was mixed under vigorous stirring with 25 mL 25% (w/v) ammonium hydroxide solution. The resulting black magnetic precipitate was isolated with the aid of a permanent magnet (S-30-10-N, Webcraft (Uster, Switzerland)) and washed twice with 100 mL deionized water. The precipitate was then boiled with 40 mL 2 M HNO_3 for 5 min, isolated from the supernatant by magnetic separation and incubated with 60 mL 0.34 M $Fe(NO_3)_3$ in water for 30 min at 90 °C. After magnetic separation from the supernatant, the particles were dispersed with deionized water to a final volume of 50 mL. The iron content of this aqueous dispersion was determined and the dispersion was diluted with water to a final concentration of 20 mM of total iron.

2.3. Citrate-Coating of Iron Oxide Nanoparticles

The synthesized iron oxide nanoparticles were coated with citrate to stabilize them in incubation buffer at physiological pH. Ten milliliter of the aqueous dispersion of iron oxide nanoparticles (total iron concentration of 20 mM) were mixed with 10 mL sodium citrate solution (200 mM) in water. The mixture was incubated for 10 min at 80 °C and then cooled down to room temperature. Before application to the cells the coated iron oxide nanoparticles were filtered through a 200 nm syringe filter (Renner, Darmstadt, Germany).

2.4. Transmission Electron Microscopy of Iron Oxide Nanoparticles

The transmission electron microscopy (TEM) of the synthesized iron oxide nanoparticles was performed using a Tecnai F20 STwin (FEI, Hillsboro, Oregon, USA) at 200 kV. The particles were analyzed in the bright-field imaging mode and in high angle annular dark-field (HAADF) STEM mode. The point resolution in TEM mode is 0.24 nm and 0.19 nm in HAADF-STEM mode. Samples were spotted on carbon-copper grids (Plano, Wetzlar, Germany), washed with ultrapure water and were dried to completeness before the analysis.

2.5. Cell Cultures

Astrocyte-rich primary cultures were prepared from the brains of newborn Wistar rats.[20] The cells were seeded in culture medium (90% DMEM, 10% FCS, 1 mM pyruvate, 20 units/mL penicillin G and 20 μg/mL streptomycin sulfate) in wells of 24-well plates (300,000 cells in 1 mL) and incubated in the humidified atmosphere of a Sanyo (Osaka, Japan) incubator with 10% CO_2. The cultures were maintained by renewing the culture medium every seventh day. The cultures were used for experiments at an age between 15 and 27 days.

2.6. Experimental Incubation

Cells in wells of 24-well plates were washed twice with 1 mL pre-warmed (37 °C) or cold (4 °C) incubation buffer (IB: 20 mM HEPES, 145 mM NaCl, 1.8 mM CaCl$_2$, 5.4 mM KCl, 1 mM MgCl$_2$, 0.8 mM Na$_2$HPO$_4$, 5 mM glucose) that had been adjusted to pH 7.4 at the desired temperature. Different concentrations of iron as iron oxide nanoparticles or as ferric ammonium citrate (FAC, a soluble ferric iron complex) in the incubation buffer were attained by diluting stock solutions (10 mM) to the desired final iron concentration in IB. The main incubation of the cells was started by application of 1 mL incubation buffer of the desired temperature with or without iron oxide nanoparticles, FAC and/or iron chelators. After incubation of cells for the indicated incubation time at 4 °C or 37 °C the media were collected and the cells were washed twice with 1 mL ice-cold phosphate-buffered saline (PBS, 10 mM potassium phosphate buffer pH 7.4, containing 150 mM NaCl) and stored frozen until further analysis of protein and iron contents.

2.7. Quantification of Total Iron

The total iron content of incubation buffers or cells was determined by a modification of the ferrozine (FZ) method previously described.[21] For estimation of iron in solutions, 100 μL of the sample was mixed with 100 μL 50 mM NaOH and 100 μL freshly prepared iron-releasing reagent (1:1 mixture of 1.4 M HCl and 4.5% KMnO$_4$ in water). After incubation over night at 60 °C, 30 μL freshly prepared iron-detection reagent (6.5 mM ferrozine, 6.5 mM neocuproine, 2.5 M ammonium acetate, 1 M ascorbate) was added. For estimation of the total iron content in cells, 200 μL 50 mM NaOH, 200 μL 10 mM HCl and 200 μL iron-releasing reagent was added to each well of a 24-well plate and incubated over night at 60 °C in a water-saturated environment. Thereafter, 60 μL iron-detection reagent was added to each well. As iron standards, 100 μL of FeCl$_3$ (0 to 300 μM FeCl$_3$ in 10 mM HCl) were mixed with 100 μL 50 mM NaOH, 100 μL iron-releasing reagent and 30 μL iron-detection reagent. After 30 min incubation with the iron-detection reagent at room temperature the absorbance at 540 nm of the ferrous iron-FZ complex in 280 μL reaction mixture was recorded in wells of a microtiter plate using a Sunrise RC microtiterplate photometer (Tecan, Crailsheim, Germany). Iron contents were determined by comparison of absorbance of reaction mixtures containing samples to those containing iron standards.

2.8. Perls' Staining of Cultured Cells for Iron

Ferric iron was visualized in cells by a modification of the histochemical Perls' stain.[22, 23] Following incubation, cells were washed thrice with 1 mL ice cold PBS, fixed in 300 μL 4% paraformaldehyde in phosphate buffer (PB; 0.1 M potassium phosphate buffer pH 7.4) for 30 min and then washed thrice with 1 mL PB for 10 min. The Perls' reaction was performed by incubating cells with 500 μL 5% (w/v) potassium ferrocyanide in PB for 30 min, followed by incubation with 500 μL of a solution that contains 5% (w/v) potassium ferrocyanide and 5% HCl in PB for 30 min. Cells were washed once with 1 mL PB for 20 min and the Perls' reaction was intensified by incubation with 500 μL of a solution that contained 0.05% (w/v) 3'3'-diaminobenzidine and 0.1% (w/v) nickel sulphate for 15 min and subsequent incubation with 500 μL of a solution that contained 0.05% (w/v) 3'3'-diaminobenzidine, 0.1% (w/v) nickel sulphate and 0.002% H$_2$O$_2$ for 15 min. The stained cells were washed twice with 1 mL of PB for 10 min and incubated at 4 °C over night in 1 mL PB to obtain a clear staining. The cellular staining was visualized using the Eclipse TS2000U microscope (Nikon, Düsseldorf, Germany) with a DS-Qi1Mc digital camera (Nikon, Düsseldorf, Germany).

2.9. TEM of Iron Oxide Nanoparticles in Cultured Astrocytes

To obtain TEM images of cultured astrocytes that had been exposed to iron oxide nanoparticles the cells were washed twice with 1 mL PBS. The cells were scratched of the culture dish with a rubber policemen and the cell suspension was centrifuged at 500 g for 3 minutes. The cell pellet was fixed using a modification of a published method.[24] Briefly, the cells were fixed with 2.5% (w/v) glutaraldehyde in 0.1 M sodium cacodylate buffer pH 7.3 (SCB) at 4 °C over night, washed with SCB and post-fixed in 2% (w/v) osmium tetroxide in SCB for 2 h at room temperature. After washing with SCB, the fixed cells were dehydrated by incubation in solutions of increasing ethanol concentration (up to 100%), washed in acetonitrile, embedded in the Agar low viscosity resin R1078 (Agar Scientific, Stansted, England) and sliced with a microtome (Ultracut UCT, Leica, Germany). The slices were stained with uranyl acetate and lead citrate before they were analysed using the FEI Tecnai F20 S-Twin.

2.10. Determination of Cell Viability and Protein Content

Cell viability was analyzed by determining the activity of lactate dehydrogenase (LDH) in the incubation buffers using the microtiter plate assay described previously[25] with the modification that 20 μL of lysates or incubation buffers were used. The protein content was determined after solubilization of the cells in 200 μL 0.5 M NaOH according to the Lowry method,[26] using bovine serum albumin as a standard.

Accumulation of Iron Oxide Nanoparticles by Cultured Brain Astrocytes

Geppert et al.

2.11. Presentation of Data

With the exception of the TEM analysis and the Perls' staining, the data presented are means $\pm$ SD of triplicate values obtained in a representative experiment or they represent means $\pm$ SD of data that were obtained in n independent experiments that were performed in triplicates. All cell culture experiments were performed on at least three independently prepared cultures with comparable results. Significance of differences between two sets of data was analyzed by paired t-test, analysis of significance between groups of data was performed by ANOVA followed by the Bonferroni *post-hoc* tests. $p > 0.05$ was considered as not significant.

3. RESULTS

Magnetic iron oxide nanoparticles were synthesized by coprecipitation of ferrous and ferric iron and subsequent oxidation as described in Methods. The product obtained was a concentrated ferrofluid which showed strong magnetic properties in an external magnetic field (Fig. 1). The yield of the synthesis was determined by measuring the iron content of the ferrofluid. In three independent syntheses the amount of iron quantified in the iron oxide nanoparticles was $78 \pm 10\%$ of the amount of total iron that was used as substrate of the reaction.

Transmission electron microscopy (TEM) revealed that the ferrofluid contained spherical particles that were polydisperse and had diameters between 5 and 20 nm (Fig. 2). The average particle diameter was about 10 nm. The agglomerates of the particles observed by TEM (Fig. 2) are likely to be a direct consequence of the drying process that was required for the sample preparation for the TEM, since the synthesized nanoparticle solution was filtered through
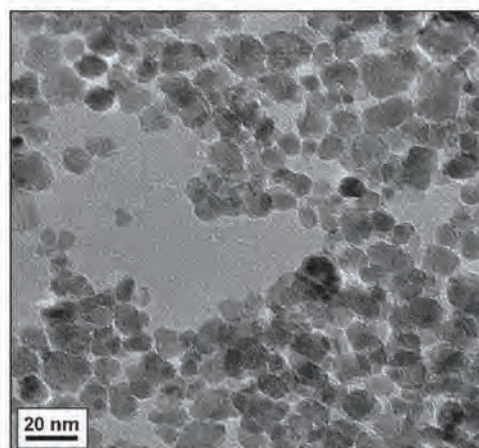

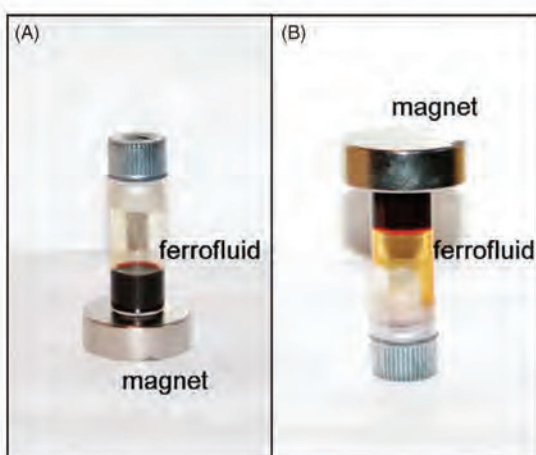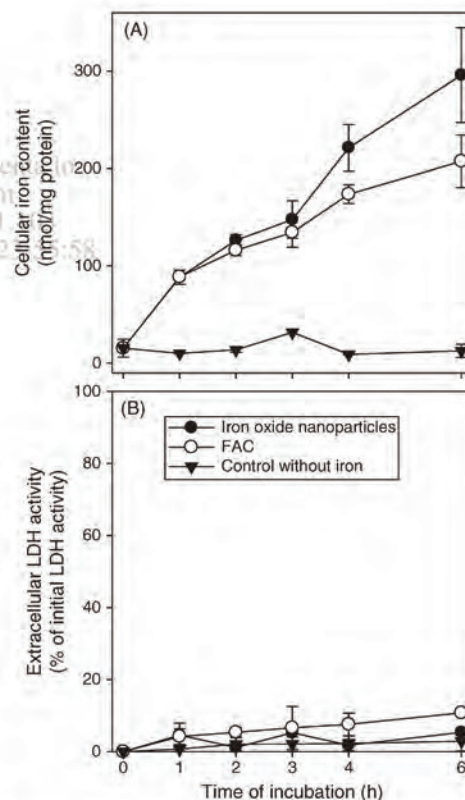**Fig. 2.** TEM image of the synthesized iron oxide nanoparticles.

Fig. 3. Time-dependent accumulation of iron from iron oxide nanoparticles or FAC. Cultured astrocytes were incubated for up to 6 hours without or with iron (100 μM) as iron oxide nanoparticles or FAC. For the given incubation periods the cellular iron content (A) and the extracellular LDH activity (B) was measured. The data represent mean values $\pm$ SD of a representative experiment that was performed in triplicates on a 20-day-old culture that contained 143 ± 18 μg protein per well.

Fig. 1. Aqueous dispersion of iron oxide nanoparticles (ferrofluid) in a magnetic field.

288

Accumulation of Iron Oxide Nanoparticles by Cultured Brain Astrocytes

Table I. Temperature dependency of iron accumulation of iron from iron oxide nanoparticles or FAC.

| Iron source	Temperature (°C)	Iron accumulation rate (nmol/(h×mg))	Extracellular LDH activity (% of initial LDH activity)
Iron oxide	37	36.1±4.1	4.7±3.3
nanoparticles	4	13.9±1.2***	3.2±1.5
FAC	37	26.1±1.7**	11.5±3.8
	4	7.4±1.9***	6.7±2.4

Notes: Astrocyte-rich primary cultures were incubated with 100 μM iron as iron oxide nanoparticles or as FAC for up to 4 h. The cellular iron accumulation was calculated from the linear increase in the values of the cellular iron contents between 1 and 4 h of incubation. The extracellular LDH activity was measured after 4 h of incubation. The data represent means±SD of values that were obtained in 3 individual experiments performed in triplicates. Indicated is the significance of differences between the data obtained for cells that were incubated at 4 °C or 37 °C with one extracellular iron source (***$p < 0.001$) or the difference between the data that were obtained for the incubation at 37 °C with iron oxide nanoparticles or FAC (**$p < 0.05$).

a 200 nm filter. Dilution of the ferrofluid in the physiological incubation buffer caused immediate aggregation and precipitation of the particles (data not shown). In order to disperse the synthesized iron oxide nanoparticles in such a buffer, the particles were coated with citrate.

To test for the ability of cultured astrocytes to accumulate iron from iron oxide nanoparticles, astrocyte-rich primary cultures were incubated without iron (control), with 100 μM iron in the form of iron oxide nanoparticles or with 100 μM iron supplied as FAC for up to 6 h (Fig. 3). In the absence of exogenous iron, the cellular iron content remained unchanged during the incubation. In contrast, after application of iron as iron oxide nanoparticles

or as FAC, the cellular iron content increased almost linearly during incubation for up to 6 h (Fig. 3(A)). The cellular iron content after 6 h of incubation with iron oxide nanoparticles and FAC was about 300 and 200 nmol/mg protein, respectively (Fig. 3(A)). None of these conditions caused a significant loss in cell viability as indicated by the almost complete absence of extracellular LDH activity (Fig. 3(B)).
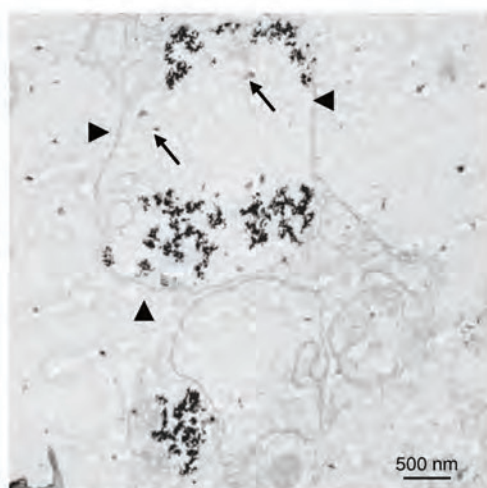
Fig. 4. TEM image of cultured astrocytes that had been exposed for 4 h to 100 μM iron as iron oxide nanoparticles. Small aggregates of iron oxide nanoparticles of a diameter of about 50 nm (arrows) as well as large agglomerates of particles are located in a membrane (arrowheads)-surrounded compartment.
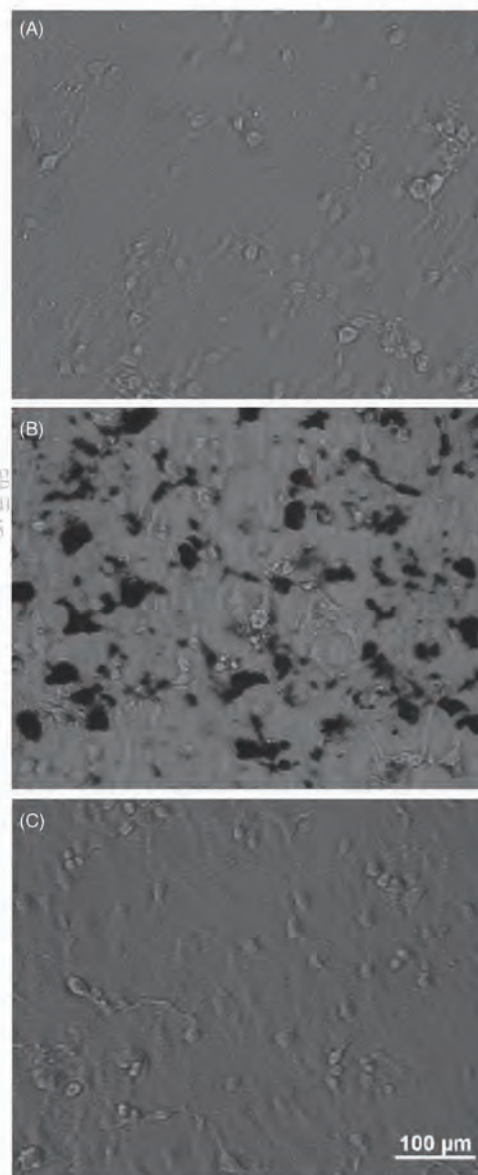
Fig. 5. Perls' staining of cultured astrocytes for ferric iron after exposure to iron oxide nanoparticles. Cultured astrocytes were incubated for 4 h without (A) or with (B, C) iron oxide nanoparticles (100 μM total iron) at 37 °C (A, B) or 4 °C (C). The size bar in (C) applies to all panels.
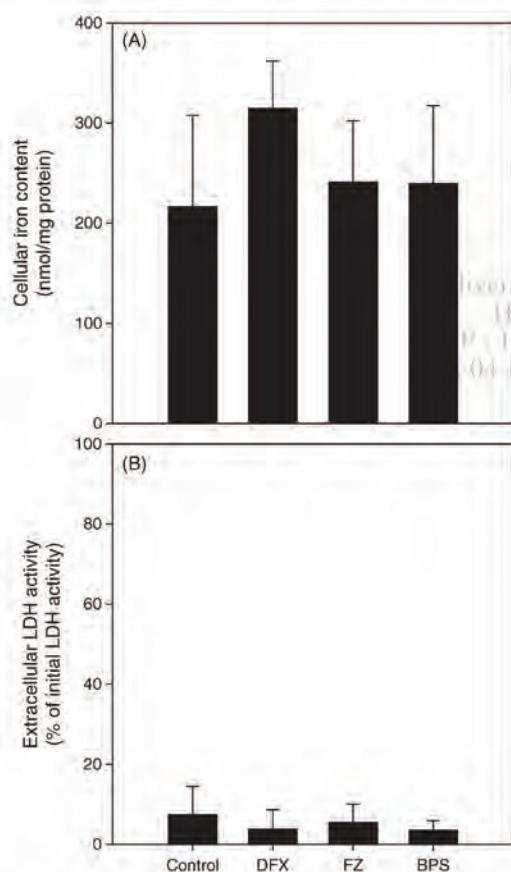
The linear increase in cellular iron content after application of iron oxide nanoparticles or FAC was used to calculate specific accumulation rates for iron. The specific accumulation rate of iron after application of iron oxide nanoparticles was with 36.1 ± 4.1 nmol/(h × mg protein) significantly ($p < 0.05$) higher than that calculated for cells that were exposed to equimolar amounts of low molecular iron in form of FAC (26.1 ± 1.7 nmol/(h × mg protein)) (Table I).

To confirm that the iron accumulation from exogenous iron oxide nanoparticles or FAC was due to membrane-dependent uptake mechanisms, iron accumulation by astrocytes was compared for incubation temperatures of 37 °C and 4 °C. When astrocyte cultures were incubated for up to 4 h at 4 °C with iron oxide nanoparticles and FAC,

the iron accumulation rate was significantly decreased to approximately 40% and 30%, respectively, of the values obtained for incubations at 37 °C (Table I). Also for these conditions the viability of the cells was not compromised as indicated by the absence of any substantial increase in extracellular LDH activity (Table I).

TEM pictures of astrocyte cultures that had been exposed for 4 h with 100 μM iron as iron oxide nanoparticles revealed the presence of small aggregates (diameter of about 50 nm) and of large agglomerates of iron oxide nanoparticles in compartments that appeared to be surrounded by a membrane (Fig. 4). Cellular accumulation of iron from iron oxide nanoparticles was also demonstrated by the cytochemical Perls' staining for iron of astrocyte cultures that have been exposed for 4 h to iron oxide nanoparticles (100 μM of total iron). While no staining for iron was observed for cultures that were incubated in the absence of iron oxide nanoparticles (Fig. 5(A)), many but not all cells in the cultures that were exposed to iron oxide nanoparticles were intensively stained for iron as indicated by the very dark colour (Fig. 5(B)). In contrast, if cells were incubated with iron oxide nanoparticles (100 μM total iron) for 4 h at 4 °C, hardly any cellular iron was detected by the cytochemical Perls' staining (Fig. 5(C)).

In order to investigate whether the accumulation of iron by astrocyte cultures from exogenous iron oxide nanoparticles was due to uptake of intact iron oxide nanoparticles or a consequence of uptake of low molecular weight iron that was released from the iron oxide nanoparticles, the iron chelators deferoxamine, ferrozine or bathophenanthroline disulfonate (BPS) were applied to the cells together with iron oxide nanoparticles. Under the conditions used, none of the chelators affected significantly the iron accumulation (Fig. 6(A)) or the viability of the cells (Fig. 6(B)).

4. DISCUSSION

Iron oxide nanoparticles were synthesized by coprecipitation of ferric and ferrous iron and subsequent oxidation using a modification of a published method[6] to obtain maghemite iron oxide nanoparticles. The yield of the synthesis was about 80% regarding the amount of iron used as substrate for the synthesis and we obtained spherical polydisperse iron oxide nanoparticles with a mean diameter of around 10 nm. It can be assumed that the iron oxide nanoparticles produced contain predominately maghemite,[6] since oxygen was not excluded during synthesis. However, we can not preclude that the particles may also have contained some magnetite, since iron oxide nanoparticles can contain mixtures of the two magnetic iron oxides.[27]

The uncoated iron oxide nanoparticles aggregated and precipitated quickly in incubation buffer at physiological pH. To avoid this process, iron oxide nanoparticles have to be coated with low molecular weight compounds

Fig. 6. Effects of iron chelators on the iron accumulation (A) and viability (B) of cultured astrocytes after exposure to iron oxide nanoparticles. The cells were incubated with 100 μM iron as iron oxide nanoparticles in the absence (control) or presence of 500 μM of the ferric iron chelator deferoxamine (DFX) or the ferrous iron chelators ferrozine (FZ) or bathophenanthroline disulfonate (BPS). After 4 h of incubation the cellular iron content (A) and the extracellular LDH activity (B) were measured. The data represent mean values ± SD of three individual experiments performed in triplicates.

such as sodium oleate,[28] dimercaptosuccinic acid[19, 29] or citrate[6, 30, 31] or with organic polymers.[32] Since citrate is a physiological compound that is produced and release in substantial amounts by astrocytes[33] we have used citrate as coating ligand for the iron oxide nanoparticles that were applied to cultured astrocytes.

Application of citrate-coated iron oxide nanoparticles to cultured astrocytes did not cause any acute cell toxicity, if the cells were incubated for up to 6 h with iron amounts of 100 μM. This result confirms literature data.[18] Thus, the conditions used were considered suitable to investigate the accumulation of iron from iron oxide nanoparticles by viable astrocytes.

During an incubation of astrocytes with iron oxide nanoparticles, the cellular iron content increased strongly from about 10 nmol/mg protein to about 300 nmol/mg protein within 6 h. This increase was even stronger than that observed after application of ferric ammonium citrate (FAC), a compound that has previously been reported as a good extracellular iron source for astrocytes.[21, 34] The accumulation of iron in cultured astrocytes after exposure to iron oxide nanoparticles was confirmed by TEM and by cytochemical Perls' staining. TEM revealed that most of the cell-associated particles were present in small aggregates or in large agglomerates that were surrounded by a membrane.

The Perls' iron staining has already been used before to demonstrate the presence of iron oxide nanoparticles in cells.[35] Interestingly, not all cells in astrocyte cultures were Perls' positive after exposure to iron oxide nanoparticles and several cells appeared not to be stained. However, it should be noted here that the sensitivity of the Perls' staining for fixed cells is still a matter of debate.[36] Even cells in brain sections are very heterogeneously stained for iron,[37,38] although the brain contains large amounts of iron.[38] The differences in the intensity of the observed cellular Perls' iron staining could be a consequence of the presence of different types of astrocytes in the total brain cultures used that differ in the expression level of proteins that are involved in the accumulation of iron oxide nanoparticles.

To further investigate whether the cellular accumulation of iron after exposure of astrocytes to iron oxide nanoparticles was completely caused by the accumulation of particles and not in part by the known uptake of ferrous or ferric iron ions into astrocytes,[16] the cells were exposed to iron oxide nanoparticles in the presence of iron chelators. Presence of the ferric iron chelator deferoxamine and the ferrous iron chelators ferrozine or bathophenanthroline disulfonate prevent almost completely the uptake by cultured astrocytes of iron from FAC[34] or from ferrous iron (K. Tulpule and R. Dringen, unpublished results), respectively. Since none of these iron chelators prevented the cellular accumulation of iron from iron oxide nanoparticles, an extracellular liberation of ferric or ferrous iron

ions from the iron oxide nanoparticles during the incubation with the cells and subsequent uptake of low molecular weight iron can be excluded.

Since the method used to quantify iron does not allow discriminating between intracellular iron and iron that is bound extracellularly to the cells, the temperature dependency of the iron accumulation was investigated. The accumulation of iron by astrocyte-rich primary cultures after exposure to iron oxide nanoparticles (or FAC) was strongly attenuated by lowering the incubation temperature to 4 °C. This finding confirms that the accumulation of iron from iron oxide nanoparticles at 37 °C is due to a membrane-dependent uptake process rather than being due to the non-specific extracellular binding of the nanoparticles. The strong reduction by lowering the temperature on the ability of astrocytes to accumulate iron from iron oxide nanoparticles or FAC confirms literature data that report that lowering the incubation temperature reduces cellular accumulation of iron[39–42] or of silica-coated nanoparticles.[43]

The effects of the magnetic properties of the citrate-coated iron oxide particles on the accumulation of the nanoparticles was not investigated here and the cultured astrocytes were exposed to the nanoparticles in the absence of an exogenous high magnetic field. However, it should be noted that the uptake of polymer-coated superparamagnetic iron oxide nanoparticles by HELA cells was strongly accelerated by an exogenous magnetic field.[44] Whether such a magnetic field will also enhance the accumulation of citrate-coated iron oxide nanoparticles in cultured brain astrocytes under the conditions used here remains to be elucidated.

Iron in redox active form catalyses the generation of hydroxyl radicals by the Fenton reaction. The iron-dependent generation of cell-damaging reactive oxygen species has also been reported for cultured astrocytes. Exposure of astrocytes to low molecular weight iron in the form of FAC causes radical formation and moderate toxicity[34] which was severely increased by subsequent application of hydrogen peroxide.[45] In contrast, iron chelators completely prevented the iron-mediated toxicity of astrocytes in the absence or presence of peroxides.[34, 45, 46] Although cultured astrocytes efficiently accumulated the nanoparticles, the cells were not acutely damaged by iron oxide nanoparticles under the conditions used. Thus, cellular damage by iron-mediated production of radicals[34] appears not to occur after exposure to the iron oxide nanoparticles. This suggests that for the conditions used an increased formation of reactive oxygen species by a catalytic action of iron in the nanoparticles,[47] or a quick intracellular mobilization of iron from the particles and subsequent formation of radicals by low molecular weight iron[34] does not take place.

In summary, we report that cultured astrocytes rapidly accumulate iron oxide nanoparticles in a temperature-dependent process. It would be interesting to study the

Accumulation of Iron Oxide Nanoparticles by Cultured Brain Astrocytes   *Geppert et al.*

accumulation of iron oxide nanoparticles in astrocytes in the brain to demonstrate the *in vivo* relevance of the data that were obtained on cultured astrocytes. Further studies will also be necessary to test whether the iron accumulated in astrocytes after exposure to iron oxide nanoparticles is bioavailable and can be mobilised from the particles to serve as source for cellular iron metabolism. If iron in cellular iron oxide nanoparticles is bioavailable, the delivery of iron in redox-inactive form as iron oxide nanoparticles could be an interesting approach to load cells with a depot of iron without risking a quick mobilisation of iron that would subsequently lead to iron-catalyzed generation of reactive oxygen species and to oxidative cell damage.

References and Notes

1. S. Laurent, D. Forge, M. Port, A. Roch, C. Robic, L. V. Elst, and R. N. Muller, Magnetic iron oxide nanoparticles: Synthesis, stabilization, vectorization, physicochemical characterizations and biological applications. *Chem. Rev.* 108, 2064 (**2008**).
2. J. Kreuter, Application of nanoparticles for the delivery of drugs to the brain. *Int. Congr. Ser.* 1277, 85 (**2005**).
3. C. Corot, P. Robert, J. M. Idée, and M. Port, Recent advances in iron oxide nanocrystal technology for medical imaging. *Adv. Drug Deliv. Rev.* 58, 1471 (**2006**).
4. B. Samanta, H. Van, N. O. Fischer, M. Shi, D. J. Jerry, and V. M. Rotello, Protein-passivated Fe$_3$O$_4$-nanoparticles: Low toxicity and rapid heating for thermal therapy. *J. Mater. Chem.* 18, 1204 (**2008**).
5. F. Schüth, A. H. Lu, and E. L. Salabas, Magnetische nanopartikel: Synthese, stabilisierung, funktionalisierung und anwendung. *Angew. Chem.* 119, 1242 (**2007**).
6. A. Bee, R. Massart, and S. Neveu, Synthesis of very fine maghemite particles. *J. Magn. Magn. Mater.* 149, 6 (**1995**).
7. S. Sun, H. Zeng, Size-controlled synthesis of magnetite nanoparticles. *J. Am. Chem. Soc.* 124, 8204 (**2002**).
8. I. Markiewicz and B. Lukomska, The role of astrocytes in the physiology and pathology of the central nervous system. *Acta Neurobiol. Exp.* 66, 343 (**2006**).
9. M. Nedergaard, B. Ransom, and S. A. Goldman, New roles for astrocytes: Redefining the functional architecture of the brain. *Trends Neurosci.* 26, 532 (**2003**).
10. F. Kirchhoff, R. Dringen, and C. Giaume, Pathways of neuron-astrocyte interactions and their possible role in neuroprotection. *Eur. Arch. Psychiatr. Clin. Neurosci.* 251, 159 (**2001**).
11. E. E. Benarroch, Neuron-astrocyte interactions: Partnership for normal function and disease in the central nervous system. *Mayo Clin. Proc.* 80, 1326 (**2005**).
12. A. J. L. Cooper, The Role of Glutathione in the Nervous System, edited by C. A. Shaw. Taylor and Francis, Washington (**1998**), pp. 91–115.

13. R. Dringen, P. G. Pawlowski, and J. Hirrlinger, Peroxide detoxification by brain cells. *J. Neurosci. Res.* 79, 157 (**2005**).
14. R. Dringen, The New Encyclopedia of Neuroscience. edited by L. Squire, T. Albright, F. Bloom, F. Gage, and N. Spitzer, Elsevier, Oxford (**2009**), pp. 733–737.
15. E. Tiffany-Castiglioni and Y. Qian, Astroglia as metal depots: Molecular mechanisms for metal accumulation, storage and release. *Neurotoxicology* 22, 577 (**2001**).
16. R. Dringen, G. M. Bishop, M. Koeppe, T. N. Dang, and S. R. Robinson, The pivotal role of astrocytes in the metabolism of iron in the brain. *Neurochem. Res.* 32, 1884 (**2007**).
17. T. Moos, T. Rosengren Nielsen, T. Skjørringe, and E. H. Morgan, Iron trafficking inside the brain. *J. Neurochem.* 103, 1730 (**2007**).
18. C. Au, L. Mutkus, A. Dobson, J. Riffle, J. Lalli, and M. Aschner, Effects of nanoparticles on the adhesion and cell viability on astrocytes. *Biol. Trace Elem. Res.* 120, 248 (**2007**).
19. T. R. Pisanic II, J. D. Blackwell, V. I. Shubayev, R. R. Finones, and S. Jin, Nanotoxicity of iron oxide nanoparticles internalization in growing neurons. *Biomaterials* 28, 2572 (**2007**).
20. B. Hamprecht and F. Löffler, Primary glial cultures as model for studying hormone action. *Methods Enzymol.* 109, 341 (**1985**).
21. J. Riemer, H. H. Hoepken, H. Czerwinska, S. R. Robinson, and R. Dringen, Colorimetric ferrozine-based assay for the quantification of iron in cultured cells. *Anal. Biochem.* 331, 370 (**2004**).
22. G. M. Bishop and S. R. Robinson, Quantitative analysis of cell death and ferritin expression in response to cortical iron: Implications for hypoxia-ischemia and stroke. *Brain Res.* 907, 175 (**2001**).
23. T. Moos and K. Mollgrad, A sensitive post-DAB enhancement technique for demonstration of iron in the central nervous system. *Histochemistry* 99, 471 (**1993**).
24. M. Grusch, D. Polgar, S. Gfatter, K. Leuhuber, S. Huettenbrenner, C. Leisser, G. Fuhrmann, F. Kassie, H. Steinkellner, K. Smid, G. J. Peters, H. N. Jayaram, W. Klepal, T. Szekeres, S. Knasmüller, and G. Krupitza, Maintenance of ATP favours apoptosis over necrosis triggered by benzamide riboside. *Cell Death Differ.* 9, 169 (**2002**).
25. R. Dringen, L. Kussmaul, and B. Hamprecht, Detoxification of endogenous hydrogen peroxide and organic hydroperoxides by cultured astroglia cells assessed by microtiter plate assay. *Brain Res. Protoc.* 2, 223 (**1998**).
26. O. H. Lowry, N. J. Rosebrough, A. L. Farr, and R. J. Randall, Protein measurements with the Folin phenol reagent. *J. Biol. Chem.* 193, 265 (**1951**).
27. D. Maity and D. C. Agrawal, Synthesis of iron oxide nanoparticles under oxidizing environment and their stabilization in aqueous and non-aqueous media. *J. Magn. Magn. Mater.* 308, 46 (**2007**).
28. A. K. Gupta and M. Gupta, Synthesis and surface engineering of iron oxide nanoparticles for biomedical applications. *Biomaterials* 26, 3995 (**2005**).
29. N. Fauconnier, J. N. Pons, J. Roger, and A. Bee, Thiolation of maghemite nanoparticles by dimercaptosuccinic acid. *J. Colloid Interface Sci.* 194, 427 (**1997**).
30. N. Fauconnier, A. Bee, J. Roger, and J. N. Pons, Synthesis of aqueous magnetic liquids by surface complexation of maghemite nanoparticles. *J. Mol. Liq.* 83, 233 (**1999**).
31. H. Pilgrimm, Superparamagnetic particles with increased R1 relaxivity, process for producing said particles and use thereof. U.S. Patent 6,634,494, October (**2003**).
32. A. Petri-Fink, B. Steitz, A. Finka, J. Salaklang, and H. Hofmann, Effect of cell media on polymer coated superparamagnetic iron oxide nanoparticles (SPIONs): Colloidal stability, cytotoxicity, and cellular uptake studies. *Eur. J. Pharm. Biopharm.* 86, 129 (**2008**).
33. N. Westergaard, U. Sonnewald, G. Unsgard, L. Peng, L. Hertz, and A. Schousboe, Uptake, release, and metabolism of citrate in neurons and astrocytes in primary cultures. *J. Neurochem.* 62, 1727 (**1994**).
34. H. H. Hoepken, T. Korten, S. R. Robinson, and R. Dringen, Iron accumulation, iron-mediated toxicity and altered levels of ferritin

Accumulation of Iron Oxide Nanoparticles by Cultured Brain Astrocytes

and transferrin receptor in cultured astrocytes during incubation with ferric ammonium citrate. *J. Neurochem.* 88, 1194 (**2004**).

35. A. Naveau, P. Smirnov, C. Ménager, F. Gazeau, O. Clément, A. Lafont, and B. Gogly, Phenotypic study of human gingival fibroplasts labeled with superparamagnetic anionic nanoparticles. *J. Periodontol.* 77, 238 (**2006**).

36. M. F. Falangola, S. P. Lee, R. A. Nixon, K. Duff, and J. A. Helpern, Histological co-localization of iron in Aβ plaques of PS/APP transgenic mice. *Neurochem. Res.* 30, 201 (**2005**).

37. J. R. Burdo, J. Martin, S. L. Menzies, K. G. Dolan, M. A. Romano, R. J. Fletcher, M. D. Garrick, L. M. Garrick, and J. R. Connor, Cellular distribution of iron in the brain of the Belgrade rat. *Neuroscience* 93, 1189 (**1999**).

38. D. J. Piñero and J. R. Connor, Iron in the brain: An important contributor in normal and diseased states. *Neuroscientist* 6, 435 (**2000**).

39. D. Trinder and E. Morgan, Mechanisms of ferric citrate uptake by human hepatoma cells. *Am. J. Physiol. Gastrointest. Liver. Physiol.* 275, 279 (**1998**).

40. Z. M. Qian, Q. K. Liao, Y. To, Y. Ke, Y. K. Tsoi, G. F. Wang, and K. P. Ho, Transferrin-bound and transferrin free iron uptake by cultured rat astrocytes. *Cell. Mol. Biol.* 46, 541 (**2000**).

41. D. R. Richardson, Iron and gallium increase iron uptake from transferrin by human melanoma cells: Further examination of the ferric ammonium citrate-derived iron uptake process. *Biochim. Biophys. Acta* 1536, 43 (**2001**).

42. M. Arreedondo, J. Kloosterman, S. Núñez, F. Segovia, V. Candia, S. Flores, S. Le Blanc, M. Olivares, and F. Pizarro, Heme iron uptake by Caco-2 cells is a saturable, temperature sensitive and modulated by extracellular pH and potassium. *Biol. Trace Elem. Res.* 125, 109 (**2008**).

43. J. S. Kim, T. J. Yoon, K. N. Yu, M. S. Noh, M. Woo, B. G. Kim, K. H. Lee, B. H. Sohn, S. B. Park, J. K. Lee, and M. H. Cho, Cellular uptake of magnetic nanoparticles is mediated through energy-dependent endocytosis in A549 cells. *J. Vet. Sci.* 7, 321 (**2006**).

44. A. Petri-Fink and H. Hoffmann, Superparamagnetic iron oxide nanoparticles (SPIONs): From synthesis to *in vivo* studies—a summary of the synthesis, characterization, *in vitro* and *in vivo* investigations of SPIONs with particular focus on surface and colloidal properties. *IEEE Transact. Nanobiosci.* 6, 289 (**2007**).

45. J. R. Liddell, H. H. Hoepken, P. J. Crack, S. R. Robinson, and R. Dringen, Glutathione peroxidase 1 and glutathione are required to protect mouse astrocytes from iron-mediated hydrogen peroxide toxicity. *J. Neurosci. Res.* 84, 578 (**2006**).

46. J. R. Liddell, S. R. Robinson, and R. Dringen, Endogenous glutathione and catalase protect cultured rat astrocytes from the iron-mediated toxicity of hydrogen peroxide. *Neurosci. Lett.* 364, 164 (**2004**).

47. A. Nel, T. Xia, L. Mädler, and L. Ning, Toxic potential of materials at the nanolevel. *Science* 311, 622 (**2006**).

208

2.2.3. Publication 6

Geppert M, Hohnholt MC, Thiel K, Nürnberger S, Grunwald I, Rezwan K,

Dringen R

(2011)

Uptake of dimercaptosuccinate-coated magnetic iron oxide nanoparticles by

cultured brain astrocytes.

Nanotechnology 22:145101-145111

Contribution of Michaela C. Hohnholt:

- Performance of the Perls´ staining and of Fig. 4.

- Coordination of sample preparation for electron microscopy of cell samples.

Mark Geppert synthesized the iron oxide nanoparticles and obtained the data shown in Figs. 2, 3, 5, 6 and Table 1.

Karsten Thiel performed electron microscopy and energy dispersive x-ray analysis of iron oxide nanoparticles (Fig. 1).

Sylvia Nürnberger performed the sample preparation for electron microscopy and designed Figs. 5 and 6.

Uptake of dimercaptosuccinate-coated magnetic iron oxide nanoparticles by cultured brain astrocytes

Mark Geppert[1,2], Michaela C Hohnholt[1,2], Karsten Thiel[3], Sylvia Nürnberger[4,5], Ingo Grunwald[3], Kurosch Rezwan[6] and Ralf Dringen[1,2,7,8]

[1] Center for Biomolecular Interactions Bremen, University of Bremen, PO Box 330440, D-28334 Bremen, Germany
[2] Center for Environmental Research and Sustainable Technology, Leobener Strasse, D-28359 Bremen, Germany
[3] Fraunhofer Institute for Manufacturing Technology and Advanced Materials, Wiener Strasse 12, D-28359 Bremen, Germany
[4] Department of Traumatology, Medical University of Vienna, Waehringer Guertel 18-20, 1090 Vienna, Austria
[5] Ludwig Boltzmann Institute for Clinical and Experimental Traumatology, Austrian Cluster for Tissue Regeneration, 1200 Vienna, Austria
[6] Advanced Ceramics, University of Bremen, Am Biologischen Garten 2, D-28359 Bremen, Germany
[7] School of Psychology and Psychiatry, Monash University, Wellington Road, Clayton, Victoria 3800, Australia

E-mail: ralf.dringen@uni-bremen.de

Abstract

Magnetic iron oxide nanoparticles (Fe-NP) are currently considered for various diagnostic and therapeutic applications in the brain. However, little is known on the accumulation and biocompatibility of such particles in brain cells. We have synthesized and characterized dimercaptosuccinic acid (DMSA) coated Fe-NP and have investigated their uptake by cultured brain astrocytes. DMSA-coated Fe-NP that were dispersed in physiological medium had an average hydrodynamic diameter of about 60 nm. Incubation of cultured astrocytes with these Fe-NP caused a time- and concentration-dependent accumulation of cellular iron, but did not lead within 6 h to any cell toxicity. After 4 h of incubation with 100–4000 μM iron supplied as Fe-NP, the cellular iron content reached levels between 200 and 2000 nmol mg^{-1} protein. The cellular iron content after exposure of astrocytes to Fe-NP at 4 °C was drastically lowered compared to cells that had been incubated at 37 °C. Electron microscopy revealed the presence of Fe-NP-containing vesicles in cells that were incubated with Fe-NP at 37 °C, but not in cells exposed to the nanoparticles at 4 °C. These data demonstrate that cultured astrocytes efficiently take up DMSA-coated Fe-NP in a process that appears to be saturable and strongly depends on the incubation temperature.

1. Introduction

Magnetic iron oxide nanoparticles (Fe-NP) are available with various functionalizations and have a wide range of

[8] Address for correspondence: Center for Biomolecular Interactions Bremen, University of Bremen, PO Box 330440, D-28334 Bremen, Germany.

potential applications [1–3]. Among these, the most important applications for biology and medicine are the utilization of Fe-NP as contrast agents in magnetic resonance imaging [4, 5], as carrier for drug delivery or transfection [6–8] and as therapeutic agents in cancer therapy by magnetic field-mediated hyperthermia [9]. Fe-NP contain an iron oxide core

(Fe_3O_4 or γ-Fe_2O_3) that is surrounded by a ligand shell which consists of small organic or inorganic molecules, polymers or proteins. These ligand shells are essential for the stabilization of the nanoparticles in physiological media [2, 3, 10].

Astrocytes are the most abundant cells in the brain [11]. They have a strategically very important localization between the blood vessels and neurons [11]. Thus, astrocytes are the first cells in brain that encounter substances which have passed the blood–brain barrier. Astrocytes have a variety of essential functions in the brain that include the uptake and release of transmitters [12, 13] and the supply of metabolites to neurons [14]. In addition, astrocytes contribute substantially to the antioxidative defense of the brain [14] and to the regulation of iron homeostasis [15].

Very recently it was shown that peripherally applied Fe-NP are able to pass the blood–brain barrier [16]. However, despite the promising potential of Fe-NP for brain-related approaches, surprisingly little is known about the consequences of an exposure of brain cells to Fe-NP. Such particles appear not to be acutely toxic to cultured astrocytes [8, 17, 18] or oligodendroglial cells [19], while PC12 cells, a frequently used cell model system for neurons, show an altered morphology and a severe loss in cell viability after exposure to Fe-NP [20]. In addition, cultured astrocytes have been shown to accumulate carboxyl-modified fluorescent Fe-NP [21] and citrate-coated Fe-NP [18, 22].

To investigate the characteristics of the uptake of Fe-NP into astrocytes in more detail, we have synthesized and characterized Fe-NP that were coated with dimercaptosuccinic acid (DMSA) and have used astrocyte-rich primary cultures as cell model system. DMSA-coated Fe-NP (D-Fe-NP) remained dispersed in physiological media after complete removal of unbound DMSA and could be applied to the cells for many hours without inducing toxicity. During the exposure, cultured astrocytes accumulated D-Fe-NP efficiently in a time-, concentration- and temperature-dependent manner.

2. Materials and methods

2.1. Materials

Fetal calf serum (FCS) and penicillin/streptomycin solution were obtained from Biochrom (Berlin, Germany). Dulbecco's modified Eagle's medium (DMEM) was from Gibco (Karlsruhe, Germany). Bovine serum albumin and NADH were purchased from Applichem (Darmstadt, Germany). All other chemicals of the highest purity available were from Sigma (Steinheim, Germany), Fluka (Buchs, Switzerland), Merck (Darmstadt, Germany) or Riedel-de Haen (Seelze, Germany). 96-well microtiter plates were from Nunc (Wiesbaden, Germany) and 24-well cell culture plates from Sarstedt (Nümbrecht, Germany).

2.2. Synthesis and coating of Fe-NP

Magnetic Fe-NP (γ-Fe_2O_3) were synthesized using a wet chemical method as described previously [18, 23]. In six independent experiments, the average yield of the synthesis regarding iron content was $68 \pm 7\%$. To disperse the synthesized Fe-NP in physiological media, the nanoparticles were coated with DMSA as previously described [20, 24]. Briefly, 0.13 g of DMSA was dissolved in 150 ml pure water and added under vigorous stirring to 100 ml of an aqueous dispersion of Fe-NP (40 mM total iron concentration). After 30 min, the resulting precipitate was centrifuged (5 min; 800g) and resuspended in 80 ml of pure water. The pH value was adjusted with NaOH to pH 10 and the solution was stirred for an additional 30 min before lowering the pH to 7.4 by adding HCl. To remove larger aggregates, the nanoparticle dispersion was centrifuged (10 min, 1000g) and sterile filtered through a 0.2 μm filter. The solution was diluted with water to a final iron concentration of 40 mM (3.5 g particle l^{-1}) before storing the solution at 4 °C. Concentrations of D-Fe-NP are given as concentration of the iron present in the nanoparticle dispersion used and not as concentration of particles.

2.3. Transmission electron microscopy (TEM)

Preparation of TEM samples was done by dropping 1 μl of a diluted solution of D-Fe-NP (1 mM total iron) onto a carbon-coated copper-grid. After airdrying at room temperature, TEM imaging was carried out using a FEI Tecnai F20 S-TWIN (Hillsboro, Oregon, USA) operated at 200 kV. Images were recorded using a GATAN GIF2001 SSC-CCD camera. Element analysis by energy dispersive x-ray spectrometry (EDX) was carried out while operating the microscope in scanning mode (STEM) at a spatial resolution of about 1 nm. STEM images were recorded using a high-angle-annular-dark-field (HAADF)-STEM detector. EDX analysis was performed using an EDAX r-TEM-EDX-Detector with an energy resolution of 136 eV. Preparation for TEM analysis of cultured astrocytes that had been incubated without or with D-Fe-NP was performed as previously described [22].

2.4. Determination of the hydrodynamic diameter and the zeta-potential of the particles

The hydrodynamic diameter of the Fe-NP in solution was determined by dynamic light scattering at a scattering angle of 90° using a L.i.SA light scattering machine (Fraunhofer IFAM, Bremen, Germany). The zeta-potential and hydrodynamic particle diameter at a scattering angle of 165° were determined with a Delsa™ Nano C Analyzer (Beckmann Coulter, Krefeld, Germany).

2.5. Cell cultures and experimental incubations

Astrocyte-rich primary cultures were prepared from the brains of newborn Wistar rats and cultured to confluency as described previously [18, 25]. For incubation with D-Fe-NP, the cells were washed twice with 1 ml pre-warmed (37 °C) or cold (4 °C) incubation buffer (IB: 20 mM HEPES, 145 mM NaCl, 1.8 mM CaCl₂, 5.4 mM KCl, 1 mM MgCl₂, 5 mM glucose, adjusted to pH 7.4 at the desired temperature). Subsequently, the cells were incubated at the indicated temperature with 1 ml of IB containing D-Fe-NP. After the desired incubation period, the media were collected and the cells were washed twice with 1 ml each of ice-cold phosphate-buffered saline (PBS: 10 mM
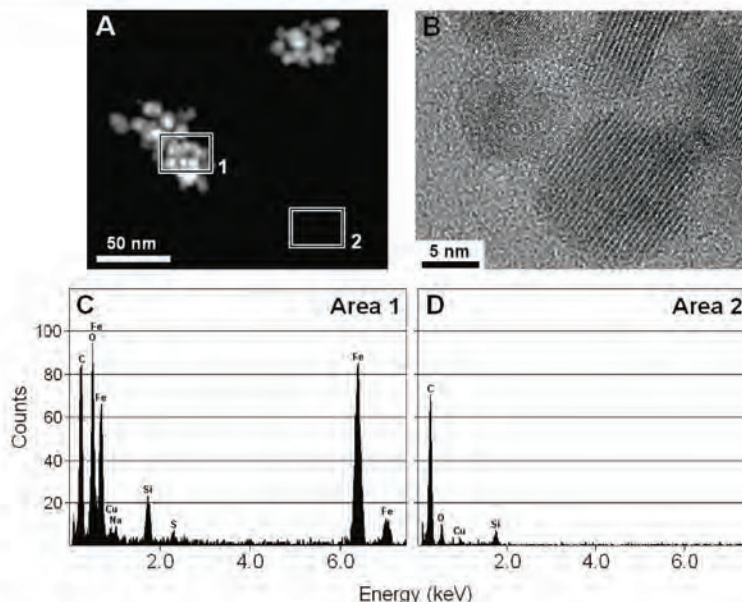
Figure 1. TEM-EDX analysis of DMSA-coated Fe-NP. The nanoparticles were diluted with water to a final concentration of 1 mM total iron, dried and investigated by TEM ((A), (B)). The EDX profiles of the contents of the frames 1 and 2 in (A) are presented as panels (C) and (D), respectively.

potassium phosphate buffer pH 7.4, containing 150 mM NaCl). The dry cells were stored frozen until determination of their iron and protein contents.

2.6. Iron quantification and histochemical Perls' staining for iron

The total iron content of the incubation buffers and cells was determined by a modification of the ferrozine-based colorimetric iron assay [26] as described previously [18]. Specific cellular iron contents were obtained by normalizing the total cellular iron content per well to the total cellular protein content per well. Ferric iron was visualized in cells by a modification of the histochemical Perls' iron staining as described previously [18, 19].

2.7. Determination of cell viability and protein content

Cell viability was analyzed by determining the activity of lactate dehydrogenase (LDH) in the incubation buffers using the microtiter plate assay described previously [27] with the modification that 20 μl of lysates or incubation buffers were used. The protein content per well was determined according to the Lowry method [28] after solubilization of the cells in 400 μl 50 mM NaOH, using bovine serum albumin as a standard.

2.8. Presentation of data

If not stated otherwise, the data are presented as means $\pm$ SD of values from at least three experiments that were performed on independently prepared cultures. Significance of difference between two sets of data was analyzed by the paired t-test; analysis of significance between groups of data was performed by ANOVA followed by the Bonferroni *post hoc* tests. $p > 0.05$ was considered as not significant.

3. Results

3.1. Characterization of the synthesized DMSA-coated Fe-NP

The D-Fe-NP were synthesized as described in section 2. TEM of the nanoparticles revealed the presence of spherical particles with a diameter of about 5–20 nm which formed larger agglomerates of up to 70 nm diameter (figure 1(A)). High resolution TEM confirmed [3, 29] the presence of monocrystalline nanoparticles (figure 1(B)). By EDX analysis of the particles intensive signals for iron and oxygen as well as a small signal for sulfur were detected (figure 1(C)), which were not present in areas of the TEM grid that did not contain nanoparticles (figure 1(D)).

Investigation of diluted solutions (1 mM total iron in water) of uncoated or DMSA-coated Fe-NP by dynamic light scattering revealed for both types of particles a monomodal particle size distribution with d_{50} values of around 60 nm (table 1). Diluting the D-Fe-NP with incubation buffer (IB) did

3

not cause any significant change in the average hydrodynamic particle diameter (table 1), whereas dilution of uncoated Fe-NP in IB led immediately to aggregation and precipitation of the particles (table 1). Measurements of the zeta-potential of the nanoparticles revealed a positive value of 43 ± 14 mV for uncoated nanoparticles in water and negative values of -77 ± 18 mV and -26 ± 3 mV for DMSA-coated nanoparticles in water and IB, respectively. Uncoated nanoparticles aggregated in IB as expected for particles that show a zeta-potential of around zero (table 1).
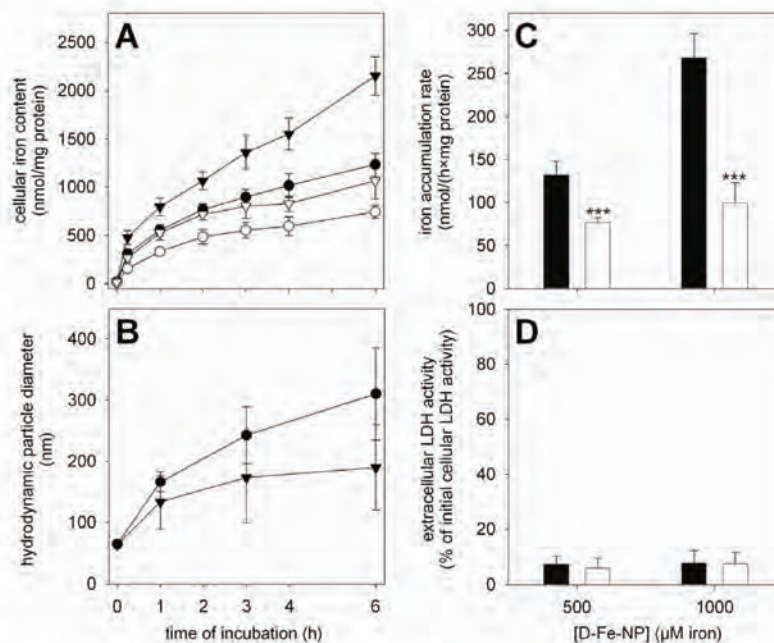
3.2. Accumulation of iron from DMSA-coated Fe-NP by cultured astrocytes

To test for the ability of astrocytes to accumulate iron from Fe-NP, astrocyte cultures were incubated with D-Fe-NP and the amount of cell-associated iron was quantified for incubation periods of up to 6 h (figure 2). The cells accumulated iron as a function of time and concentration. After a 6 h incubation with 500 and 1000 μM D-Fe-NP, the specific cellular iron content had increased from an initial value of 18 ± 10 nmol mg^{-1} to 1232 ± 122 and 2151 ± 198 nmol mg^{-1} cellular protein, respectively (means $\pm$ SD of data from six experiments). The cellular iron content increased almost linearly between 1

Table 1. Hydrodynamic particle diameter and zeta-potential of uncoated and DMSA-coated Fe-NP. (Note: uncoated or DMSA-coated Fe-NP were dispersed in either water or incubation buffer (IB) to a final concentration of 1 mM total iron and the hydrodynamic particle diameter (at scattering angles of 90° or 165°) as well as the zeta-potential were measured. The numbers in brackets represent the number of measurements performed on individually prepared Fe-NP dispersions.)

Coating	Solvent	Hydrodynamic particle diameter (nm)		Zeta-potential (mV)
		90°	165°	
Uncoated	H$_2$O	64 ± 32 (5)	53 ± 6 (3)	$+43 \pm 14$ (3)
Uncoated	IB	>1000 (3)	>1000 (3)	-1 ± 1 (3)
DMSA	H$_2$O	59 ± 9 (4)	51 ± 7 (3)	-77 ± 18 (3)
DMSA	IB	74 ± 10 (12)	64 ± 14 (3)	-26 ± 3 (3)

and 6 h after application of D-Fe-NP (figure 2(A)), whereas the cellular iron content was not altered during incubation of the cells in the absence of nanoparticles (data not shown). The linear increase in the cellular iron content of D-Fe-NP-treated astrocytes between 1 and 6 h was used to calculate iron accumulation rates. Astrocytes that were exposed to 500 and 1000 μM D-Fe-NP accumulated iron with rates of 122 ± 16

Figure 2. Time- and temperature-dependence of the iron accumulation of cultured astrocytes after exposure to DMSA-coated Fe-NP. The cells were incubated with 500 μM (circles in (A) and (B)) or 1000 μM (triangles in (A) and (B)) D-Fe-NP for up to 6 h at 37 °C (filled symbols and bars) or 4 °C (open symbols and bars) and the cellular iron content (A) and the hydrodynamic particle diameter (B) were determined. The iron accumulation rates (C) were calculated from the linear increases of the cellular iron contents between 1 and 6 h incubation. Extracellular LDH activity (D) was determined after 6 h of incubation as an indicator for a potential loss in cell viability. The extracellular LDH activities of cells incubated in the absence of D-Fe-NP were $5.5 \pm 4.9\%$ (37 °C) and $4.3 \pm 1.7\%$ (4 °C) of the initial cellular LDH activity. The data shown represent mean values $\pm$ SD of 3–6 experiments performed on independently prepared cultures. The stars in (C) indicate the significance of differences between the values obtained for incubation at 37 and 4 °C (*** $p < 0.001$).

4
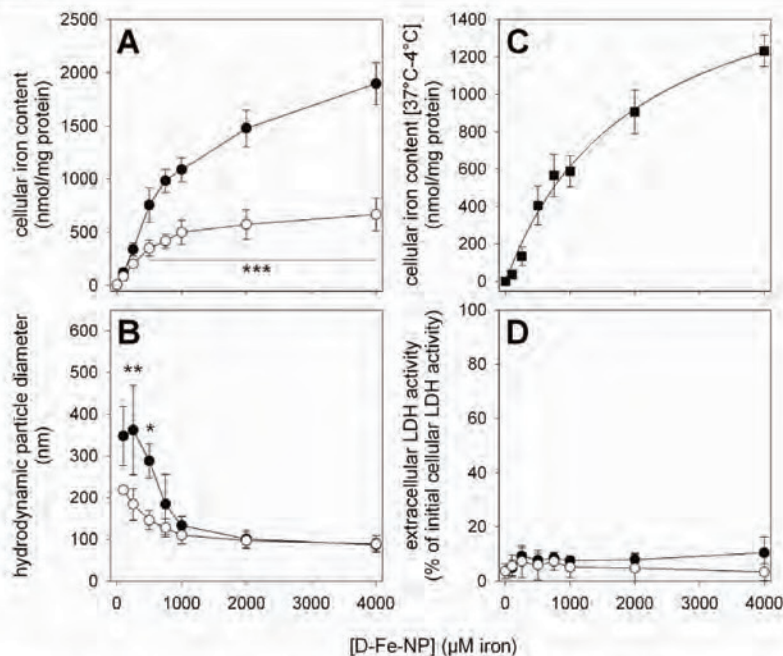
Figure 3. Concentration- and temperature-dependence of the iron accumulation from DMSA-coated Fe-NP by cultured astrocytes. The cells were incubated for 4 h with D-Fe-NP containing the indicated concentrations of iron at 37 °C (filled circles) or at 4 °C (open circles) and the cellular iron content (A), the hydrodynamic diameter of the nanoparticles in the supernatant (B) and the extracellular LDH activity (D) were measured. (C) shows the difference of cellular iron contents of cells that were exposed to Fe-NP at 37 °C and at 4 °C. Hyperbolic regression of the data shown in (C) using the Michaelis Menten equation gave a correlation of 0.989. The data represent means ± SD of values obtained in 3–4 experiments performed on independently prepared cultures. The significance of differences between the values obtained for cells that were incubated at 37 °C and at 4 °C is indicated ($^*p < 0.05$; $^{**}p < 0.01$; $^{***}p < 0.001$).

and 268 ± 28 nmol/(h × mg protein), respectively (figure 2(C)). Compared to incubation at 37 °C, astrocytes that were exposed at 4 °C to 500 and 1000 μM D-Fe-NP accumulated iron slower (figure 2(A)) with significantly lower rates that accounted for 58 ± 4 % and 37 ± 9 %, respectively, of the values calculated for the 37 °C conditions (figure 2(C)). Cell viability was not affected for these conditions, as indicated by the absence of any significant increase in extracellular LDH activity (figure 2(D)).

During incubation of cells with 500 and 1000 μM D-Fe-NP for 6 h, the average hydrodynamic diameter of the particles in the incubation medium increased significantly from an initial value of 66 ± 5 nm to values of 310 ± 75 (500 μM D-Fe-NP; $p < 0.01$) and 190 ± 70 nm (1000 μM D-Fe-NP; $p < 0.05$) (figure 2(B)). In contrast, incubation of D-Fe-NP under identical incubation conditions in the absence of cells did not lead to an increase in hydrodynamic particle diameter (data not shown).

To investigate the concentration- and temperature-dependence of the iron accumulation from D-Fe-NP as well as the agglomeration of the particles in the presence of cells in more detail, astrocyte cultures were incubated for 4 h with up to 4000 μM D-Fe-NP at 37 °C or at 4 °C (figure 3). While at 4 °C the amount of cell-associated iron already reached a plateau

of about 600 nmol mg^{-1} cellular protein after incubation for 4 h with around 1000 μM D-Fe-NP, significantly higher cellular iron contents were observed for cells that had been incubated at 37 °C with D-Fe-NP in concentrations above 200 μM (figure 3(A)). Specific cellular iron contents reached after incubation with 4000 μM D-Fe-NP values of around 1900 nmol iron mg^{-1} protein. None of these conditions affected cell viability as indicated by the lack of any significant increase in extracellular LDH activity (figure 3(D)).

The temperature-sensitive part of the iron accumulation from D-Fe-NP was calculated as the difference of the cellular iron contents determined for cells that were incubated at 37 and 4 °C. The temperature-sensitive iron accumulation increased hyperbolically with the concentration of D-Fe-NP applied (figure 3(C)). Analysis of these data by hyperbolic regression demonstrated that the cellular accumulation of iron from D-Fe-NP followed an apparent Michaelis Menten kinetic with apparent K_M and V_{Max} values of 2.1 ± 0.6 mM and 1871 ± 231 nmol iron/(mg × 4 h) (means ± SD of four independent experiments).

The average hydrodynamic diameter of the D-Fe-NP in the media was increased during the incubation with cells. While the diameter of the nanoparticles was at best slightly
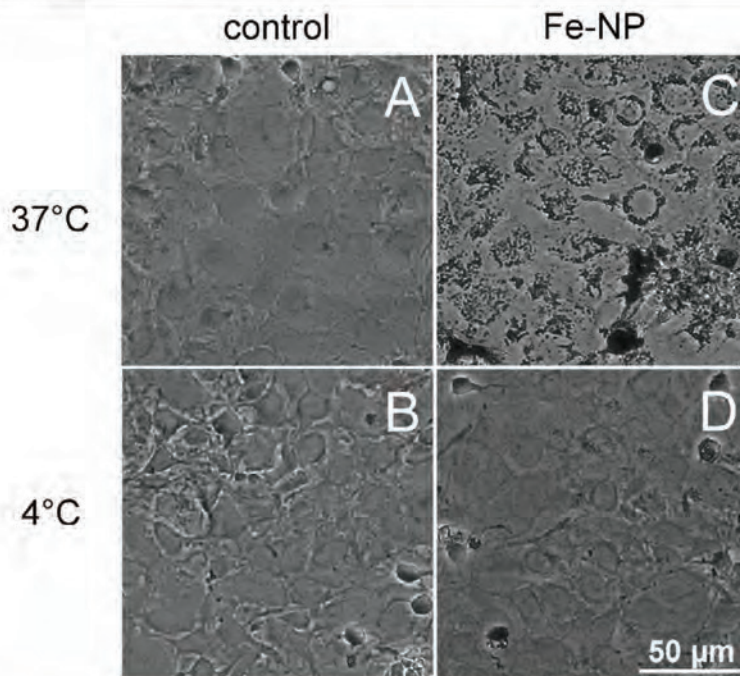
Figure 4. Perls' iron staining of cultured astrocytes after exposure to DMSA-coated Fe-NP. Cultured astrocytes were incubated without (control) or with 1000 μM of iron as D-Fe-NP at 37 °C or at 4 °C. The size bar in (D) applies to all panels.

increased from an initial value of 68 ± 4 to 87 ± 17 nm (37 °C) or 89 ± 20 nm (4 °C) during a 4 h incubation of cells with 4000 μM D-Fe-NP, their size increased significantly to 348 ± 71 nm (37 °C; $p < 0.01$) and 218 ± 19 nm (4 °C; $p < 0.01$) when cells were exposed to only 100 μM D-Fe-NP (figure 3(B)). At low D-Fe-NP concentrations of 200 and 500 μM the hydrodynamic diameter of nanoparticles that were exposed to cells at 37 °C was significantly larger than that of particles incubated with cells at 4 °C (figure 3(B)). In contrast, incubation of D-Fe-NP in media in the absence of cells did not cause any alteration of the hydrodynamic diameter during incubation at 4 or 37 °C (data not shown).

Cellular iron accumulation after exposure of astrocytes to D-Fe-NP was also investigated by the cytochemical Perls' staining which visualizes the presence of large amounts of cellular iron as black precipitate (figure 4). While cells that were incubated without D-Fe-NP were not Perls' positive (figures 4(A) and (B)), exposure of cells for 4 h with 1000 μM D-Fe-NP led to an intense staining for iron that was indicated by the dark color, especially visible around the nuclei of the cells (figure 4(C)). In contrast, when the cells were exposed to D-Fe-NP at 4 °C, hardly any cellular iron was detectable by Perls' staining (figure 4(D)).

3.3. Detection of intracellular Fe-NP by TEM

To investigate whether intact nanoparticles are present in the cells after exposure of astrocytes to D-Fe-NP, the cells were analyzed by TEM after incubation for 4 h without or with 1000 μM D-Fe-NP at 37 or 4 °C (figures 5 and 6). Control cells that were incubated in the absence of D-Fe-NP showed the normal medium electron density of all cellular structures, whereas hardly any dark electron-dense particles were present intra- or extracellularly (figure 5(A)). In contrast, cells exposed to D-Fe-NP at 37 °C contained large vesicles loosely or densely filled with electron-dense particles (figure 5(B) arrowheads; figure 6). Some vesicles contained additionally cellular residuals between the particles (figure 6(C)). In contrast to an incubation at 37 °C, hardly any intracellular vesicles that contained electron-dense material were observed for astrocytes that were incubated with D-Fe-NP at 4 °C (figure 5(C)). However, after exposure to D-Fe-NP at both 37 °C (figure 5(B)) and 4 °C (figure 5(C)), the cells were contoured with nanoparticles at their surface and between the cells.

4. Discussion

Magnetic D-Fe-NP were synthesized with good yield and reproducibility, using a modification of a previously published wet chemical method [18, 23]. The particles were spherical and polydisperse with an average diameter of about 10 nm observed by TEM, confirming previously published results [18]. The synthesized nanoparticles contained large amounts of iron and oxygen, as shown by TEM-EDX analysis,
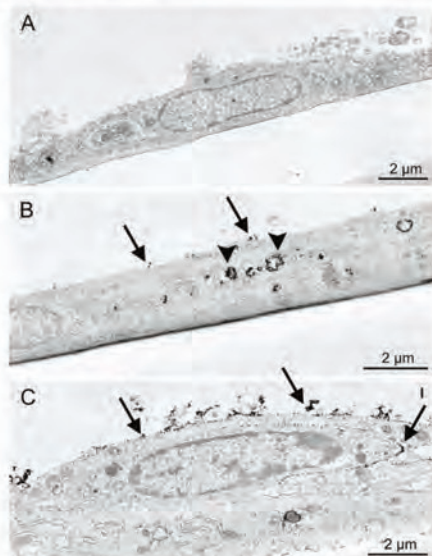
Figure 5. TEM images of astrocytes that were incubated with DMSA-coated Fe-NP. The cells were incubated at 37 °C ((A), (B)) or 4 °C (C) for 4 h without (A) or with ((B), (C)) 1000 μM of iron as D-Fe-NP. Electron-dense particles are visible in intracellular vesicles ((B), arrowhead) and contour the cell surface ((B) and (C), arrows) and the intercellular space (arrow labeled I in (C)).

as well as sulfur, which demonstrates that the particles are indeed coated with the sulfur containing DMSA. This treatment of the synthesized Fe-NP with DMSA allowed stable dispersion of the nanoparticles at physiological pH, as indicated by the absence of any increase in hydrodynamic particle diameter of the diluted D-Fe-NP. Thus, in contrast to citrate-coated Fe-NP [18], the presence of an excess of ligand was not required for dispersion of D-Fe-NP in physiological media, excluding potential side effects of an excess of the ligand DMSA on cells. Binding of the carboxyl groups of DMSA to the nanoparticle surface and formation of disulfide bridges between adsorbed DMSA molecules to form a cage-like structure around the Fe-NP core has been discussed as a mechanism of the DMSA stabilization [30]. The importance of the suggested formation of disulfide bridges for the stabilization of Fe-NP by DMSA is strongly supported by the observation that monomercaptosuccinate was unable to stabilize Fe-NP in physiological media (data not shown).

Uncoated and DMSA-coated nanoparticles showed a monomodal size distribution with average hydrodynamic particle diameters around 60 nm, and thus are substantially larger than the diameter of the individual particles observed by TEM. These agglomerates of Fe-NP are most likely formed due to magnetostatic interactions between the individual particles [31, 32]. However, even with an average diameter of around 60 nm the small agglomerates of dispersed D-Fe-NP were considered as well suited to investigate the uptake of nanoparticles by astrocytes. The zeta-potential of uncoated nanoparticles in water indicates a positively charged surface
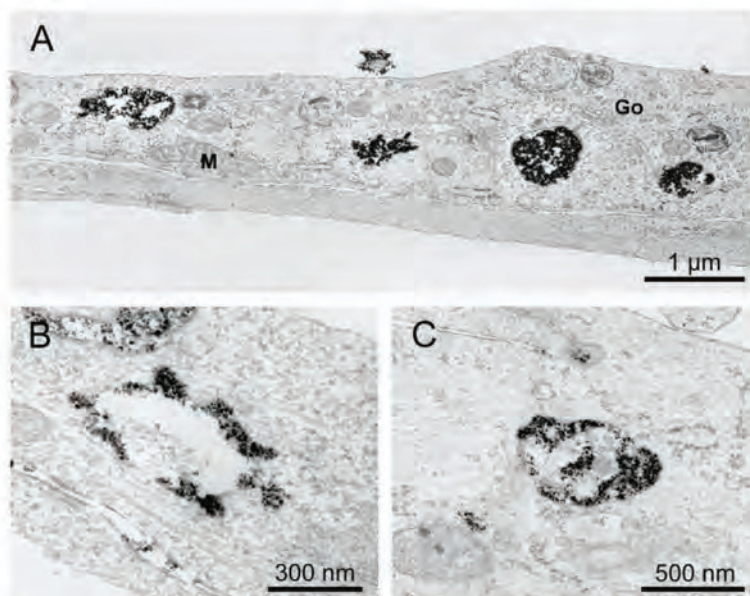
Figure 6. TEM images of astrocytes after treatment with DMSA-coated Fe-NP. The cells were incubated for 4 h with 1000 μM iron as D-Fe-NP at 37 °C. (A) shows a cross section through a cell showing four vesicles filled with electron-dense particles at different densities. Intact mitochondria (M) and the golgi apparatus (Go) are indicated. (B) Nanoparticle containing vesicles that may have fused with a larger vesicle. (C) Vesicle containing heterogeneous cellular debris and Fe-NP.

7

which is in line with the suggested stabilization by protonated surface hydroxyl groups at acidic pH [23]. This positive charge is removed after dispersion in physiological buffer, thereby changing the zeta-potential to around zero which subsequently causes the particles to flocculate out. The DMSA-coat stabilizes D-Fe-NP at physiological pH [23, 24, 33] by introducing a negative surface charge as indicated by the negative zeta-potential.

Incubation of astrocyte cultures with D-Fe-NP did not lead to acute cell death within 6 h, which confirms previously published results for citrate-coated Fe-NP [18, 22] and commercially available Fe-NP [8, 17]. The almost linear increase of cellular iron content observed during 6 h of incubation of cultured astrocytes with D-Fe-NP to values of up to 2000 nmol iron mg^{-1} protein demonstrates the high capacity of these cells to accumulate iron from D-Fe-NP, confirming that astrocytes accumulate iron better from Fe-NP than from low molecular weight iron complexes [18, 34, 35]. The amounts of iron accumulated from D-Fe-NP by cultured astrocytes are similar to those reported for citrate-coated Fe-NP [18, 22]. However, the use of D-Fe-NP has the strong advantage that presence of unbound DMSA is not required for dispersion of D-Fe-NP in physiological media. This contrasts with the situation for citrate-coated Fe-NP [22], since these nanoparticles require for their stability the presence of a high molar excess of the ligand citrate. Such high concentrations of citrate are likely to affect the properties of the cultured astrocytes [36], for example by chelation of extracellular Ca^{2+}-ions. Therefore, especially if higher concentrations of Fe-NP have to be applied to cells, D-Fe-NP appear to be better suited to investigation of the consequences of a treatment of cells with Fe-NP than citrate-coated particles.

After application of D-Fe-NP, the amount of cellular iron increased drastically. To test whether the cell-associated iron is intracellular or extracellularly bound to the cell surface, the iron accumulation from D-Fe-NP at 37 °C was compared to that at 4 °C. Iron accumulation at 4 °C was significantly lower than that observed at 37 °C, suggesting that a temperature-dependent transport process is involved in the iron accumulation from D-Fe-NP in astrocytes. However, the amounts of cell-associated iron that were still found after incubation at 4 °C demonstrate that a substantial part of the cell-associated iron represents extracellularly bound iron. Similar temperature dependences of metal uptake have also been reported for low molecular weight iron [37–39], for hemine iron [40], and for copper [41] as well as for citrate- or silica-coated Fe-NP [18, 22, 42]. Also in these studies the amounts of cell-associated metals determined after incubation at 4 °C were considered to reflect extracellularly bound material. For D-Fe-NP this hypothesis was experimentally confirmed by TEM images of astrocytes that were exposed to the nanoparticles. While, after incubation at both 37 and 4 °C, D-Fe-NP were found decorating the cell membrane extracellularly, the presence of large amounts of intracellular vesicles that contained D-Fe-NP was only observed for the 37 °C condition. In addition, also the Perls' iron staining of astrocytes that had been exposed to D-Fe-NP at 37 °C revealed the presence of substantial amounts of iron in the cells, while

cells that were incubated at 4 °C were not Perls'-positive. These data demonstrate that indeed the temperature-dependent part of the cellular iron reflects the amount of iron that has been taken up into the cells after exposure to D-Fe-NP, whereas the amount of cell-associated iron determined for cells that were incubated at 4 °C represents predominantly the amount of D-Fe-NP that had bound extracellularly to cell membranes. The absence of large, nanoparticle-filled vesicles in the 4 °C condition is in accord with the reduced physiological activity of vesicle transport systems at low temperatures [42].

While the amounts of cellular iron after incubation with D-Fe-NP at 37 °C increased at least up to a concentration of 4000 μM, the cellular iron accumulation at 4 °C already reached a plateau after incubation of the cells with around 1000 μM D-Fe-NP. This suggests a limited capacity of the cells to bind D-Fe-NP extracellularly, whereas the maximum of the uptake of D-Fe-NP into the cells at 37 °C has not been reached even after application of 4000 μM D-Fe-NP. The difference of the iron contents of cells treated with D-Fe-NP at 37 °C versus 4 °C was calculated to get further information on the temperature-dependent transport process that leads to the occurrence of intracellular D-Fe-NP. Uptake of D-Fe-NP appears to be saturable with apparent K_M and V_{Max} values of 2.1 $\pm$ 0.6 mM and 1871 $\pm$ 231 nmol iron/(mg × 4 h), respectively. Considering the fact that each nanoparticle contains at least several thousand iron atoms, it has to be expected that the apparent K_M value for iron accumulation from D-Fe-NP differs by orders of magnitude from those reported for example for ferrous iron which is taken up into astrocytes with K_M values of about 1 μM [37].

Uptake of D-Fe-NP into astrocytes is likely to involve a membrane-dependent uptake process. Free diffusion of D-Fe-NP through the plasma membrane is unlikely to occur, since the particles are negatively charged as indicated by their zeta-potential. The cellular localization of D-Fe-NP in astrocytes by TEM revealed that these cells contained large vesicles filled with substantial amounts of electron-dense nanoparticles. The presence of Fe-NP in intracellular vesicles in astrocytes confirms previous reports for other types of Fe-NP [18, 21, 22] and suggests that endocytotic mechanisms [43, 44] are involved in the uptake process. Indeed, inhibitors of endocytosis have been reported to lower cellular uptake of fluorescent Fe-NP into astrocytes [21]. The occurrence of several large aggregates of Fe-NP in one vesicle is likely to be a consequence of fusion of several endosomes.

During the incubation of D-Fe-NP with astrocytes, but not in the absence of cells, a significant increase in the hydrodynamic diameter of the particles in the medium was observed. Interestingly, this increase was strongest when D-Fe-NP were applied in low concentrations. In addition, the increase in hydrodynamic diameter was significantly lowered by a decrease in the incubation temperature to 4 °C. These observations suggest that compound(s) that are released from astrocytes in a temperature-dependent manner at limited amounts foster the agglomeration of the dispersed D-Fe-NP to larger aggregates. Thus, regarding the interactions of nanoparticles with astrocytes, not only binding to and uptake of nanoparticles into cells have to be considered, but also the

8

219

alteration of the properties of the dispersed nanoparticles by cell-derived compounds.

5. Conclusions

DMSA-coated iron oxide nanoparticles (D-Fe-NP) were efficiently taken up into cultured astrocytes and were found predominately in intracellular vesicles, which supports literature data [21] that endocytotic uptake mechanisms are involved in Fe-NP uptake. Since incubation with D-Fe-NP at 4 °C prevented the occurrence of Fe-NP in intracellular vesicles, this temperature control appears to be well suited to determine the amount of Fe-NP that is bound extracellularly to cell membranes. This allows us to discriminate the amount of Fe-NP that is attached to the cells from the amount of Fe-NP that has been internalized into the cells. Astrocytes are highly efficient at strongly increasing their iron content after application of D-Fe-NP. If astrocytes are able to liberate iron from Fe-NP, this iron would be available for the cells and could subsequently be used for iron-dependent processes. Alternatively, since iron can be liberated from Fe-NP under conditions that resemble the intracellular environment [45], cell damage by iron-mediated radical formation could also be a consequence of a long time exposure of astrocytes to Fe-NP. Thus, further studies are also required to investigate the fate of D-Fe-NP in astrocytes, especially in the context of the suggested supply and regulatory function of astrocytes in the iron homeostasis of the brain [15].

References

[1] Gupta A K and Gupta M 2005 Synthesis and surface engineering of iron oxide nanoparticles for biomedical applications *Biomaterials* **26** 3995–4021
[2] Laurent S, Forge D, Port M, Roch A, Robic C, Elst L V and Muller R N 2008 Magnetic iron oxide nanoparticles: synthesis, stabilization, vectorization, physicochemical characterizations, and biological applications *Chem. Rev.* **108** 2064–110
[3] Lu A H, Salabas E L and Schuth F 2007 Magnetic nanoparticles: synthesis, protection, functionalization, and application *Angew. Chem. Int. Edn* **46** 1222–44
[4] Corot C, Robert P, Idee J M and Port M 2006 Recent advances in iron oxide nanocrystal technology for medical imaging *Adv. Drug Deliv. Rev.* **58** 1471–504

[5] Weinstein J S, Varallyay C G, Dosa E, Gahramanov S, Hamilton B, Rooney W D, Muldoon L L and Neuwelt E A 2010 Superparamagnetic iron oxide nanoparticles: diagnostic magnetic resonance imaging and potential therapeutic applications in neurooncology and central nervous system inflammatory pathologies, a review *J. Cereb. Blood Flow Metab.* **30** 15–35
[6] Chertok B, Moffat B A, David A E, Yu F Q, Bergemann C, Ross B D and Yang V C 2008 Iron oxide nanoparticles as a drug delivery vehicle for MRI monitored magnetic targeting of brain tumors *Biomaterials* **29** 487–96
[7] Jain T K, Morales M A, Sahoo S K, Leslie-Pelecky D L and Labhasetwar V 2005 Iron oxide nanoparticles for sustained delivery of anticancer agents *Mol. Pharmacol.* **2** 194–205
[8] Pickard M and Chari D 2010 Enhancement of magnetic nanoparticle-mediated gene transfer to astrocytes by 'magnetofection': effects of static and oscillating fields *Nanomedicine* **5** 217–32
[9] Jordan A et al 2006 The effect of thermotherapy using magnetic nanoparticles on rat malignant glioma *J. Neurooncol.* **78** 7–14
[10] Samanta B, Yan H, Fischer N O, Shi J, Jerry D J and Rotello V M 2008 Protein-passivated Fe(3)O(4) nanoparticles: low toxicity and rapid heating for thermal therapy *J. Mater. Chem.* **18** 1204–8
[11] Sofroniew M V and Vinters H V 2010 Astrocytes: biology and pathology *Acta Neuropathol.* **119** 7–35
[12] Eulenburg V and Gomeza J 2010 Neurotransmitter transporters expressed in glial cells as regulators of synapse function *Brain Res. Rev.* **63** 103–12
[13] Parpura V and Zorec R 2010 Gliotransmission: exocytotic release from astrocytes *Brain Res. Rev.* **63** 83–92
[14] Hirrlinger J and Dringen R 2010 The cytosolic redox state of astrocytes: maintenance, regulation and functional implications for metabolite trafficking *Brain Res. Rev.* **63** 177–88
[15] Dringen R, Bishop G M, Koeppe M, Dang T N and Robinson S R 2007 The pivotal role of astrocytes in the metabolism of iron in the brain *Neurochem. Res.* **32** 1884–90
[16] Wang J et al 2010 Pharmacokinetic parameters and tissue distribution of magnetic Fe₃O₄ nanoparticles in mice *Int. J. Nanomed.* **5** 861–6
[17] Au C, Mutkus L, Dobson A, Riffle J, Lalli J and Aschner M 2007 Effects of nanoparticles on the adhesion and cell viability on astrocytes *Biol. Trace Elem. Res.* **120** 248–56
[18] Geppert M, Hohnholt M, Gaetjen L, Grunwald I, Bäumer M and Dringen R 2009 Accumulation of iron oxide nanoparticles by cultured brain astrocytes *J. Biomed. Nanotechnol.* **5** 285–93
[19] Hohnholt M, Geppert M and Dringen R 2010 Effects of iron chelators, iron salts and iron oxide nanoparticles on the proliferation and the iron content of oligodendroglial OLN-93 cells *Neurochem. Res.* **35** 1259–68
[20] Pisanic T R II, Blackwell J D, Shubayev V I, Finones R R and Jin S 2007 Nanotoxicity of iron oxide nanoparticle internalization in growing neurons *Biomaterials* **28** 2572–81
[21] Pickard M R, Jenkins S I, Koller C J, Furness D N and Chari D M 2010 Magnetic nanoparticle labeling of astrocytes derived for neural transplantation *Tissue Eng.* C *Methods* **17** 89–99
[22] Hohnholt M C, Geppert M, Nürnberger S, von Byern J, Grunwald I and Dringen R 2010 Advanced biomaterials: accumulation of citrate-coated magnetic iron oxide nanoparticles by cultured brain astrocytes *Adv. Eng. Mater.* **12** B690–4
[23] Bee A, Massart R and Neveu S 1995 Synthesis of very fine maghemite particles *J. Magn. Magn. Mater.* **149** 6–9

9

[24] Fauconnier N, Pons J N, Roger J and Bee A 1997 Thiolation of maghemite nanoparticles by dimercaptosuccinic acid *J. Colloid Interface Sci.* **194** 427–33

[25] Hamprecht B and Löffler F 1985 Primary glial cultures as a model for studying hormone action *Methods Enzymol.* **109** 341–5

[26] Riemer J, Hoepken H H, Czerwinska H, Robinson S R and Dringen R 2004 Colorimetric ferrozine-based assay for the quantitation of iron in cultured cells *Anal. Biochem.* **331** 370–5

[27] Dringen R, Kussmaul L and Hamprecht B 1998 Detoxification of exogenous hydrogen peroxide and organic hydroperoxides by cultured astroglial cells assessed by microtiter plate assay *Brain Res. Prot.* **2** 223–8

[28] Lowry O H, Rosebrough N J, Farr A L and Randall R J 1951 Protein measurement with the Folin phenol reagent *J. Biol. Chem.* **193** 265–75

[29] Petri-Fink A and Hofmann H 2007 Superparamagnetic iron oxide nanoparticles (SPIONs): from synthesis to *in vivo* studies—a summary of the synthesis, characterization, *in vitro*, and *in vivo* investigations of SPIONs with particular focus on surface and colloidal properties *IEEE Trans. Nanobiosci.* **6** 289–97

[30] Valois C R, Braz J M, Nunes E S, Vinolo M A, Lima E C, Curi R, Kuebler W M and Azevedo R B 2010 The effect of DMSA-functionalized magnetic nanoparticles on transendothelial migration of monocytes in the murine lung via a beta2 integrin-dependent pathway *Biomaterials* **31** 366–74

[31] Chantrell R W, Bradbury A, Popplewell J and Charles S W 1982 Agglomerate formation in a magnetic fluid *J. Appl. Phys.* **53** 2742–4

[32] Maity D and Agrawal D C 2007 Synthesis of iron oxide nanoparticles under oxidizing environment and their stabilization in aqueous and non-aqueous media *J. Magn. Magn. Mater.* **308** 46–55

[33] Fauconnier N, Bee A, Roger J and Pons J N 1999 Synthesis of aqueous magnetic liquids by surface complexation of maghemite nanoparticles *J. Mol. Liq.* **83** 233–42

[34] Hoepken H H, Korten T, Robinson S R and Dringen R 2004 Iron accumulation, iron-mediated toxicity and altered levels of ferritin and transferrin receptor in cultured astrocytes during incubation with ferric ammonium citrate *J. Neurochem.* **88** 1194–202

[35] Tulpule K, Robinson S R, Bishop G M and Dringen R 2010 Uptake of ferrous iron by cultured rat astrocytes *J. Neurosci. Res.* **88** 563–71

[36] Westergaard N, Sonnewald U, Unsgard G, Peng L, Hertz L and Schousboe A 1994 Uptake, release, and metabolism of citrate in neurons and astrocytes in primary cultures *J. Neurochem.* **62** 1727–33

[37] Qian Z M, Liao Q K, To Y, Ke Y, Tsoi Y K, Wang G F and Ho K P 2000 Transferrin-bound and transferrin-free iron uptake by cultured rat astrocytes *Cell. Mol. Biol.* **46** 541–8

[38] Richardson D R 2001 Iron and gallium increase iron uptake from transferrin by human melanoma cells: further examination of the ferric ammonium citrate-activated iron uptake process *Biochim. Biophys. Acta* **1536** 43–54

[39] Trinder D and Morgan E 1998 Mechanisms of ferric citrate uptake by human hepatoma cells *Am. J. Physiol. Gastrointest. Liver Physiol.* **275** G279–86

[40] Dang T N, Bishop G M, Dringen R and Robinson S R 2010 The putative heme transporter HCP1 is expressed in cultured astrocytes and contributes to the uptake of hemin *Glia* **58** 55–65

[41] Scheiber I F, Mercer J F and Dringen R 2010 Copper accumulation by cultured astrocytes *Neurochem. Int.* **56** 451–60

[42] Kim J S *et al* 2006 Cellular uptake of magnetic nanoparticle is mediated through energy-dependent endocytosis in A549 cells *J. Vet. Sci.* **7** 321–6

[43] Kumari S, Mg S and Mayor S 2010 Endocytosis unplugged: multiple ways to enter the cell *Cell. Res.* **20** 256–75

[44] Megías L, Guerri C, Fornas E, Azorin I, Bendala E, Sancho-Tello M, Durán J M, Tomás M, Gomez-Lechon M J and Renau-Piqueras J 2000 Endocytosis and transcytosis in growing astrocytes in primary culture. Possible implications in neural development *Int. J. Dev. Biol.* **44** 209–21

[45] Levy M, Lagarde F, Maraloiu V A, Blanchin M G, Gendron F, Wilhelm C and Gazeau F 2010 Degradability of superparamagnetic nanoparticles in a model of intracellular environment: follow-up of magnetic, structural and chemical properties *Nanotechnology* **21** 395103

221

3. Discussion

3.   Discussion

Iron is an important trace metal for mammals due to its involvement in essential processes such as the transport of oxygen (Jensen 2009) and the catalysis of redox reactions (Babcock 1999, Rouault and Tong 2008). However, since ferrous iron is redox active and can catalyze the formation of ROS (Halliwell and Gutteridge 2007, Kell 2009), iron metabolism has to be tightly regulated on the cellular level. In addition to physiological iron sources, the consequences of an exposure to Fe-NP have to be considered for the brain, since Fe-NP have a promising potential for neurological applications such as magnetic resonance imaging of the brain and drug delivery to the brain (Laurent *et al.* 2008, Weinstein *et al.* 2010, Yang 2010). Therefore, the knowledge about uptake and fate of Fe-NP in brain cells is important for further neurobiological applications in order to allow successful treatment but to avoid toxic consequences (Nel *et al.* 2006, Lewinski *et al.* 2008, Oberdörster 2010).

In the brain, oligodendrocytes form and maintain the myelin sheaths around axons of neurons (chapter 1.1.1.; Miron *et al.* 2011). To fulfill these functions, oligodendrocytes are considered to have a high metabolic activity (Piñero and Connor 2000) and hence an increased need for iron, since this metal is essential for a number of metabolic pathways which are involved in myelin production (Connor and Menzies 1996, McTigue and Tripathi 2008). In contrast to oligodendrocytes, brain astrocytes have important functions in brain metabolism and homeostasis (Kimelberg 2010, Sofroniew and Vinters 2010). Due to the localization of astrocytes in the brain and the coverage of the brain capillaries by astrocytic endfeet, astrocytes have been suggested to be especially important for the GSH-mediated detoxification of xenobiotics (Dringen 2000, Ballatori *et al.* 2009) and for distribution of metals in the brain (Tiffany-Castiglioni and Qian 2001, Dringen *et al.* 2007).

In this thesis the metabolism of iron and Fe-NP in brain cells was investigated, using the oligodendroglial OLN-93 cell line and astrocyte-rich primary cultures as model systems for oligodendrocytes and astrocytes, respectively. The consequences of an exposure to low molecular weight iron and Fe-NP were studied for OLN-93 cells. In addition, the expression of proteins involved in iron metabolism was investigated to gain knowledge on the potential of OLN-93 cells to take up, store and export iron. Furthermore, the consequences of Fe-NP exposure on cell viability and iron contents of astrocyte-rich primary cultures were examined.
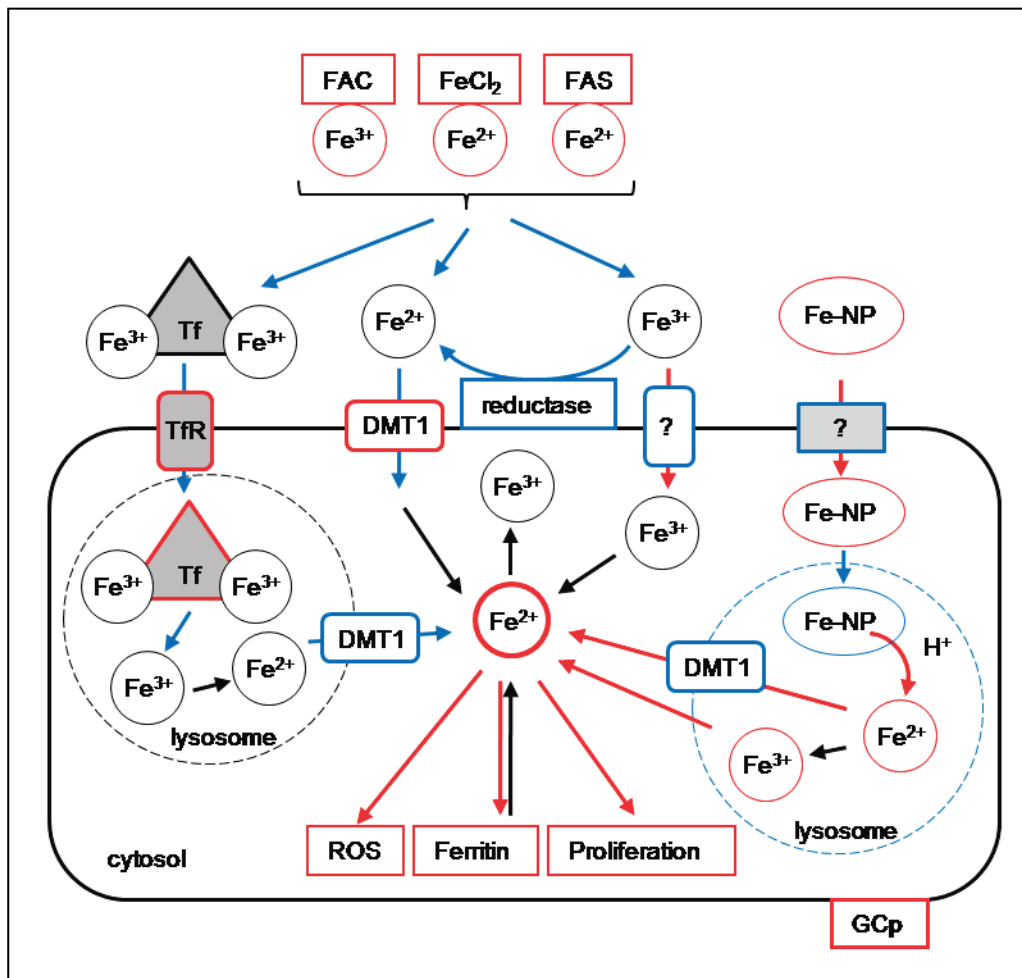
3.1.   Iron metabolism of OLN-93 cells

In this thesis new information on the expression of the mRNAs of proteins involved in iron metabolism, on accumulation of iron from low molecular weight iron salts and on the consequences of iron accumulation on cell viability and ferritin upregulation were obtained for OLN-93 cells. Figure 1 gives an overview about the current knowledge on the iron metabolism in OLN-93 cells, and includes the results obtained in this thesis. OLN-93 cells possess basal mechanisms for the uptake of protein-bound and non-protein-bound iron (chapters 2.1.1. and 2.1.2.). Although the transporters involved in the iron accumulation remain to be elucidated, iron uptake from low molecular weight iron in serum-containing incubation medium is very likely mediated by the Tf/TfR system since OLN-93 express the mRNAs of Tf (chapter 2.1.1.) and TfR (chapter 2.1.1.; Brand *et al.* 2008). Tf is present in serum and is able to bind ferric iron from iron salts due to its very high iron binding affinity (Moos and Morgan 2000, Munoz *et al.* 2009). Extracellularly applied ferrous iron from ferrous ammonium sulfate and $FeCl_2$ is quickly oxidized to ferric iron in the physiological medium (Schröder *et al.* 2003, Tulpule *et al.* 2010) and might therefore also be taken up after binding of ferric iron to Tf. Intracellularly, iron is released from Tf in the lysosomes and can become part of the labile iron pool for cellular metabolism (Figure 1; Moos and Morgan 2000). In addition to Tf, the metal-binding protein albumin is present in serum (Kasvosve and Delanghe 2002) and can bind excess of iron. Whether albumin-bound iron is taken up by OLN-93 cells remains to be elucidated.

As an alternative to protein-bound iron, iron could be taken up by a transporter for low molecular weight iron. The uptake of ferric iron (chapter 2.1.1.) could be mediated by a trivalent cation-specific transport mechanism or the β_3-integrin/mobilferrin pathway (Attieh *et al.* 1999, Conrad *et al.* 2000). Ferric iron could also be reduced by extracellular reductases that have been reported to be expressed at least in astrocytes (Jeong and David 2003, Dringen *et al.* 2007, Tulpule *et al.* 2010), and subsequently be taken up as ferrous iron by DMT1 as this transporter is also expressed by OLN-93 cells (chapter 2.1.1.; Brand *et al.* 2008).

In addition to protein-bound iron and low molecular weight iron, OLN-93 cells are also able to accumulate iron from Fe-NP (chapter 2.1.). Fe-NP are very likely to be taken up by OLN-93 cells into lysosomes as this has been reported previously for other types of nanoparticles (Busch *et al.* 2011). Since release of iron from Fe-NP has been suggested to take place in the

lysosomes (Arbab *et al.* 2005, Huang *et al.* 2009, Levy *et al.* 2010, Soenen *et al.* 2010a), iron mobilization from Fe-NP in OLN-93 cells is likely to take place in these organelles.

Figure 1: Iron metabolism of OLN-93 cells. The presence of mRNA of proteins involved in iron metabolism is considered as indicator for the presence of the respective protein (red: knowledge confirmed in the present thesis; black: knowledge from the current literature; blue: presence of proteins or pathways assumed). Abbreviations: DMT1, divalent metal transporter 1; FAC, ferric ammonium citrate; FAS, ferric ammonium sulfate, Fe-NP, iron oxide nanoparticles; G-Cp, glycosylphosphatidylinositol-anchored ceruloplasmin; ROS, reactive oxygen species; Tf, transferrin; TfR, transferrin receptor; ?, transporter/transport mechanism has not yet been shown for OLN-93 cells.

The uptake of Fe-NP by oligodendroglial cells might be mediated by a similar mechanism as the uptake of ferritin by these cells (Todorich *et al.* 2009, Todorich *et al.* 2011). Ferritin is composed of an iron oxide core surrounded by protein chains (Arosio *et al.* 2009). Similarly,

Fe-NP are likely to be coated by serum proteins in serum-containing medium, suggesting that protein-coated Fe-NP resemble ferritin for OLN-93 cells.

It is currently not clear, whether OLN-93 cells are able to export iron. Although the presence of the iron exporter ferroportin in oligodendrocytes *in vivo* has been shown (Burdo *et al.* 2001, Wu *et al.* 2004, Wang *et al.* 2007), the mRNA of ferroportin has not been detected in OLN-93 cells in the present thesis (chapter 2.1.1.). Nevertheless, preliminary experiments suggest that OLN-93 cells are able to release iron after preloading with FAC (data not shown), but whether this is a transporter-mediated export has to be further investigated. Moreover, OLN-93 cells have the mRNA of the ferroxidase G-Cp (chapter 2.1.1.), although oligodendrocytes *in vivo* express neither soluble Cp nor G-Cp (Mollgard *et al.* 1988). The activity of this ferroxidase is crucial for iron export by ferroportin, at least for astrocytes (Jeong and David 2003). Therefore, the function of the G-Cp protein in the absence of ferroportin in OLN-93 cells remains to be elucidated.

The present thesis describes for the first time the iron-dependency of OLN-93 cell proliferation. As shown in detail in chapter 2.1.2., the iron content of standard culture medium with 10% FCS offers a sufficient amount of iron, since the proliferation of OLN-93 cells was not accelerated by supplementation with additional iron. Therefore, the Tf-mediated pathway of iron uptake appears to be sufficient for optimal proliferation of these cells. Although the culture medium contains enough iron for proliferation, this process depends on the extracellular availability of iron. The decrease of available iron by iron chelators inhibits the proliferation of OLN-93 cells in a time- and concentration-dependent manner as demonstrated by the absence of any increase in cell density, cellular protein content and also the cellular LDH activity in the presence of the iron chelator DFX (chapter 2.1.2.). The inhibition of cell proliferation by the iron chelator was bypassed by an excess of extracellularly applied iron (chapter 2.1.2.), demonstrating that the DFX-mediated inhibition of proliferation was indeed an iron-dependent effect. Interestingly, the inhibition of proliferation was also partially prevented by coincubation with Fe-NP (chapter 2.1.3.) suggesting that OLN-93 cells are able to mobilize iron from Fe-NP to support proliferation.

3.2.   Iron accumulation from different iron sources in OLN-93 cells

The ability of OLN-93 cells to accumulate iron from different low molecular weight iron salts and from Fe-NP was shown for the first time in the present thesis (chapter 2.1.). Table 1 compares the cellular iron contents of OLN-93 cells after exposure to FAC and Fe-NP. Within

48 h, these cells accumulated 3 to 4 times more iron after exposure to 300 µM citrate- or DMSA-coated Fe-NP as compared to a treatment with 300 µM iron as FAC (Table 1). Iron accumulation from Fe-NP is most likely due to the uptake of intact particles, since OLN-93 cells have been shown to take up nanoparticles (Busch *et al.* 2011) and the iron chelator DFX does not prevent the uptake of Fe-NP (chapters 2.1.1. to 2.1.3.). As a consequence of the high number of iron atoms contained in one particle of Fe-NP, the iron content of OLN-93 cells exposed to Fe-NP is likely to increase strongly, even if the number of individual uptake processes is much lower for Fe-NP than for low molecular weight iron complexes or Tf-bound iron. Higher iron accumulation from Fe-NP than from FAC was also found for astrocytes (chapter 2.2.1.) and was correlated with the intracellular presence of Fe-NP in these cells by electron microscopy (chapter 2.2.).

Table 1: Iron content of OLN-93 cells after exposure to FAC or Fe-NP.

Iron source	Iron content (nmol/mg protein)	Significance of differences	Data from chapter
FAC	54 ± 9		2.1.2.
Citrate-coated Fe-NP	159 ± 34	**	2.1.2.
DMSA-coated Fe-NP	212 ± 30	***	2.1.3.

The cellular iron contents of OLN-93 cells were determined after 48 h exposure to 300 µM iron in form of the indicated iron sources in serum-containing incubation medium. Statistical analysis of significance of differences of data to those of the FAC-treated cells were analyzed by ANOVA followed by Bonferroni post hoc test (**$p<0.01$ and ***$p<0.001$).

The accumulation of iron in the presence of serum from 300 µM citrate- and DMSA-coated Fe-NP by OLN-93 cells did not differ significantly between the two different coatings (Table 1). Differences in the uptake of iron from Fe-NP due to different coatings have been reported (Villanueva *et al.* 2009, Soenen *et al.* 2010b). However, serum proteins that bind to the surface of Fe-NP (Mu *et al.* 2009, Nel *et al.* 2009, Wiogo *et al.* 2011) are able to mask these coating-dependent differences in the iron uptake from Fe-NP (Chen *et al.* 2009). Both, citrate and DMSA contain negatively charged carboxylate groups at physiological pH which form a negatively charged coating as shown at least for DMSA-coated Fe-NP in the absence of serum by a negative zeta-potential (chapter 2.2.3.). Thus, citrate- and DMSA-coated Fe-NP are likely to have a similar surface charge in the physiological medium which will interact

with medium components and with the cell surface. Investigation of the hydrodynamic particle diameter of DMSA-coated Fe-NP revealed a two-fold increase of the particle diameter in the presence of serum compared to the absence of serum in incubation buffer (Mark Geppert, personal communication). This observation suggests that medium or serum components interact with the coating of Fe-NP or the surface of Fe-NP. Cations present in the culture medium may electrostatically attach to the negatively charged coating of Fe-NP thereby forming a positively charged layer. To this layer of cations, proteins could subsequently bind, for example albumin which is negatively charged at physiological pH as shown for bovine serum albumin at a pH of 7 (Rezwan *et al.* 2004). Therefore, electrostatic interactions of medium components and proteins with the surface of Fe-NP could result in a very similar surface for Fe-NP with different coatings in the physiological medium.

The iron accumulation from Fe-NP by OLN-93 cells was also studied in the absence and presence of serum (chapters 2.1.2. and 2.1.3.). During an exposure to 1000 µM DMSA-coated Fe-NP in the absence of serum about three times higher iron levels were accumulated by the cells (8 h; 2829 ± 517 nmol/mg protein; chapter 2.1.4.) compared to an incubation in the presence of serum (48 h; 957 ± 179 nmol/mg protein; chapter 2.1.3.). This indicates that the presence of serum does indeed strongly influence the accumulation of Fe-NP as also observed for the accumulation of Fe-NP by astrocytes (Mark Geppert, personal communication) and human cervix carcinoma cells (Petri-Fink and Hofmann 2007) and of polystyrene nanoparticles by macrophages (Lunov *et al.* 2011).

The iron accumulation by astrocytes was also investigated in serum-free incubation medium. Astrocytes accumulated almost identical amounts of iron from citrate- and DMSA-coated Fe-NP with about 1000 nmol/mg protein from 500 µM Fe-NP and about 2000 nmol/mg protein from 1000 µM Fe-NP after exposure for 6 h in serum-free incubation medium (chapters 2.2.1. and 2.2.3.). Moreover, the iron accumulation rates of astrocytes were also in a comparable range (chapters 2.2.1. and 2.2.3.). Thus, the small molecules used to coat Fe-NP seem to have only a minor influence on the amounts of iron accumulated under the conditions used in this thesis.

3.3.   Mobilization of iron from iron oxide nanoparticles by OLN-93 cells

The present thesis describes for the first time the consequences of an exposure of OLN-93 cells to Fe-NP. Table 2 lists various parameters that were investigated after exposure of OLN-

93 cells to DMSA-coated Fe-NP in incubation buffer (IB) or incubation medium containing serum (DMEM with 10% FCS). In both incubation conditions, OLN-93 cells accumulated substantial amounts of iron, whereas no increase in ROS was observed and the cell viability was not compromised after exposure to 300 µM Fe-NP in DMEM with 10% FCS or 250 µM Fe-NP in IB (Table 2). Effects on the other parameters investigated, such as protein content and cellular GSH content differed between these incubation conditions, suggesting that the observed effects depend on the incubation conditions. For example, medium components such as amino acids alter the metabolism of OLN-93 cells. In the absence of amino acids in incubation buffer the cellular GSH content of control OLN-93 cells decreased within 8 h of incubation (chapter 2.1.4.), whereas the cellular GSH content remains constant in culture medium containing amino acids for up to 48 h (data not shown). Furthermore, in a 16 h recovery incubation in the presence of amino acids OLN-93 cells restored the lowered cellular GSH content caused by an incubation in the absence of amino acids (chapter 2.1.4.).

Table 2: Consequences of DMSA-coated Fe-NP on OLN-93 cells.

Parameter investigated	DMEM + 10% FCS (300 µM; 48 h)	IB (250 µM; 8 h)	IB (4000 µM; 8 h)
Iron content	+ 210 fold	+ 170 fold	+ 260 fold
Ferritin content	+ 4 fold	n.i.	n.i.
Protein content	- 11%	$\pm 0^{\#}$	$\pm 0^{\#}$
Number of nuclei	- 9%	n.i.	n.i.
Extracellular LDH	± 0	± 0	± 0
PI-positive cells	± 0	± 0	↑
MTT reduction	- 16%	n.i.	n.i.
ROS	± 0	± 0	↑
GSH content	- 8%	- 37%	- 37%
Data from chapter	2.1.3.	2.1.4.	2.1.4.

n.i., not investigated; ± 0, parameter not altered; #, data not shown in chapter; ↑, number of positive cells increased.

Although different consequences of Fe-NP on OLN-93 cell metabolism were observed, all effects were minor such as the decreased MTT reduction capacity (chapter 2.1.3.) or reversible such as the decrease in cellular GSH content of cells exposed to Fe-NP in incubation buffer (chapter 2.1.4.). Fe-NP have been reported to affect cellular signaling

pathways (Soenen *et al.* 2010b) and microtubule-remodeling (Apopa *et al.* 2009). Such processes might account for the observed alteration of cellular morphology of these cells (chapters 2.1.3. and 2.1.4.), but do not seem to strongly influence the parameters investigated for Fe-NP-treated OLN-93 cells. Therefore, OLN-93 cells seem to be remarkably resistant against potential negative consequences of Fe-NP. This supports literature data for oligodendrocyte progenitor cells labeled with Fe-NP which were transplanted into the brain of experimental animals. These cells survived, migrated and were detected by MRI after several weeks (Bulte *et al.* 2001).

Iron that has been taken up by OLN-93 cells is used for cellular metabolism as shown by three different approaches: the increase of OLN-93 cell proliferation following iron restriction (chapter 2.1.3.), the upregulation of ferritin (chapter 2.1.3.) and the inhibition of Fe-NP-dependent ROS formation by the iron chelator 1,10-phenanthroline (chapter 2.1.4.). The proliferation of OLN-93 cells depends on the availability of iron and can be inhibited by iron chelators such as DFX (chapter 2.1.2.). This chelator makes the extracellular iron unavailable for cell proliferation, since it is likely to chelate transferrin-bound iron and low molecular weight iron in the medium. The iron chelator-inhibited proliferation of OLN-93 cells was partially bypassed by the presence of Fe-NP, demonstrating that OLN-93 cells are able to use iron derived from these Fe-NP for the proliferation. The release of iron from Fe-NP is further supported by the observed protein synthesis-dependent upregulation of the iron storage protein ferritin, because the ferritin synthesis is induced by increased availability of low molecular weight iron in the cytosol (Arosio *et al.* 2009).

Fe-NP uptake is very likely mediated by an endocytotic uptake of the particles as was recently demonstrated for other types of nanoparticles (Busch *et al.* 2011). The low pH of the lysosomal compartment has been suggested to help mobilizing ferric iron from Fe-NP (Weissleder *et al.* 1995, Arbab *et al.* 2005, Huang *et al.* 2009, Levy *et al.* 2010, Soenen *et al.* 2010a) that might be subsequently reduced to ferrous iron in the lysosomal compartment (Levy *et al.* 2010) for example by a reductase as suggested for reticulocytes (Garrick and Garrick 2009) or by ascorbate that might be present in this compartment. Ferrous iron could then be transported from the lysosomal/endosomal compartment into the cytosol by DMT1, which is expressed by OLN-93 cells (chapter 2.1.1.; Brand *et al.* 2008), as it is known for the Tf/TfR-mediated uptake of iron (Figure 1; Moos and Morgan 2000). Finally, after reaching the cytosol, iron is available for incorporation into proteins for the cellular metabolism, proliferation and also for the storage in ferritin.

The increased staining for ROS after exposure of OLN-93 cells to 4000 µM Fe-NP for 8 h (chapter 2.1.4.) serves as a further evidence for the iron mobilization from Fe-NP. Since this increase in ROS generation was completely prevented by the iron chelator 1,10-phenanthroline, but not by the non-chelating structural isomer 4,7-phenanthroline, it is very likely mediated by low molecular weight iron derived from the Fe-NP, further supporting the view that OLN-93 cells are able to mobilize iron from Fe-NP.

3.4. Comparison of the consequences of a treatment with iron oxide nanoparticles on OLN-93 cells and astrocytes

In this thesis, the two glial cell types oligodendrocytes and astrocytes have been investigated with respect to their ability to accumulate iron from Fe-NP. Interestingly, OLN-93 cells and astrocyte-rich primary cultures accumulated similar amounts of 2829 ± 517 nmol/mg protein (chapter 2.1.4.) and 2151 ± 198 nmol/mg protein iron (chapter 2.2.3.) from 1000 µM DMSA-coated Fe-NP after exposure for 6 h under identical incubation conditions, respectively. This contradicts literature data that different cell types accumulated different amounts of Fe-NP (Mailänder and Landfester 2009, Soenen *et al.* 2010a). However, the uptake of comparable amounts of polystyrene nanoparticles has also been reported for primary human macrophages and a human leukemia cell line in the absence of serum (Lunov *et al.* 2011). Furthermore, the accumulation of iron from DMSA-coated Fe-NP was not saturable for OLN-93 cells (chapter 2.1.4.) and also not for astrocytes in concentrations of up to 1 mM iron (chapter 2.2.3.). Thus, these two glial cell types seem to accumulate iron from Fe-NP in a very similar manner, suggesting that the mechanisms involved in uptake of Fe-NP might be identical for oligodendrocytes and astrocytes.

Also in other aspects, OLN-93 cells and astrocytes reacted quite similar to an exposure with Fe-NP. 1) Increased formation of ROS was observed after exposure to 4000 µM DMSA-coated Fe-NP in serum-free incubation buffer within 8 h for OLN-93 cells (chapter 2.1.4.) and in a preliminary experiment within 4 h for astrocytes (data not shown). 2) The upregulation of the iron storage protein ferritin was observed for OLN-93 cells (chapter 2.1.1.) and astrocytes (data not shown) after exposure to 1000 µM Fe-NP for 4 h and subsequently 20 h in the absence of Fe-NP. 3) The viability of OLN-93 cells and astrocytes was not compromised within 6 h of incubation with 4000 and 1000 µM DMSA-coated Fe-NP, respectively, in serum-free incubation buffer (chapters 2.1.4. and 2.2.3.).

An increased formation of ROS has also been reported for differently coated Fe-NP (Buyukhatipoglu and Clyne 2011, Soenen *et al.* 2011) and might occur on the surface of Fe-NP (Nel *et al.* 2006) or due to low molecular weight iron released from these Fe-NP. The increase in ROS formation in OLN-93 cells and in astrocytes is likely to be mediated by low molecular weight iron released from Fe-NP, since the iron chelator 1,10-phenanthroline prevented the increase in ROS formation in OLN-93 cells as discussed above (chapter 2.1.4.). In astrocytes, low molecular weight iron has been shown to induce a transient iron-dependent increase in ROS after exposure to FAC which decreases when the iron storage protein ferritin is upregulated (Hoepken *et al.* 2004), since this protein stores iron in a redox-inactive form (Arosio *et al.* 2009). The upregulation of ferritin in OLN-93 cells and astrocytes supports the suggested release of iron from Fe-NP because the upregulation of this protein depends on the presence of low molecular weight iron in the cytosol (Arosio *et al.* 2009) as discussed before (chapter 2.1.3.). Since the viability of OLN-93 cells and astrocytes was not compromised after exposure to Fe-NP under the conditions used, both cell types seem to be able to cope with the observed increased ROS formation very well. Already, a low level of ferritin present in OLN-93 cells and astrocytes at the onset of an incubation with Fe-NP may be sufficient to store some iron released from Fe-NP within a short time frame before ferritin synthesis is started. Storage in ferritin of at least part of the iron released from Fe-NP is likely to prevent the accumulation of high amounts of intracellular redox-active iron and extensive ROS formation that could induce severe cellular damage. In summary, the comparison of OLN-93 cells and primary astrocyte-rich cultures regarding the consequences of Fe-NP exposure suggests that these two glial cell types accumulate Fe-NP, liberate iron from Fe-NP and store Fe-NP-derived iron by similar mechanisms.

3.5.   Future perspectives

The uptake of iron from low molecular iron salts and the intracellular ferritin upregulation by iron in proliferating OLN-93 cells has been examined in detail in this thesis, but the involved transporters have not been identified so far. Further studies should therefore investigate the mechanisms responsible for iron uptake by OLN-93 cells and identify the iron transporters involved. The ability of OLN-93 cells to take up Tf-bound iron could be studied by application of commercially available Tf in serum-free medium. Preloading of Tf with iron in presence of FAC or other iron salts should reveal whether iron from FAC is taken up by the Tf/TfR system as shown before for astrocytes (Qian *et al.* 2000). Iron accumulation studies with low molecular weight iron sources in absence of serum should address the involvement

of an iron transporter such as DMT1. Since the iron transport of DMT1 is coupled to a cotransport of protons (Gunshin *et al.* 1997), an alteration of the pH of the incubation buffer would alter the amount of DMT1-transported iron as reported before for astrocytes (Tulpule *et al.* 2010). Final proof for the involvement of an iron transporter in iron uptake by OLN-93 cells should be obtained by gene silencing techniques, as reported before for DMT1-mediated iron uptake into renal cells (Abouhamed *et al.* 2007).

Ferroportin mRNA was not observed for OLN-93 cells, although the presence of ferroportin has been reported for oligodendrocytes *in vivo* (Burdo *et al.* 2001, Wu *et al.* 2004, Wang *et al.* 2007). To elucidate the ability of OLN-93 cells to export iron, the cells should be preloaded with low molecular weight iron. Iron export by the cells during the subsequent main incubation would be demonstrated by a decrease in cellular iron content and a matching increase in the extracellular iron content as shown before for hepatocytes (Chua *et al.* 2006).

Iron accumulation from Fe-NP by OLN-93 cells has been shown by quantification of cell-associated iron and by Perls´ iron staining (chapters 2.1.1. to 2.1.3.). Although these two methods strongly suggest, that OLN-93 cells have taken up intact Fe-NP, final proof of the intracellular presence of Fe-NP in OLN-93 cells should be obtained by electron microscopy, as shown before for Fe-NP-treated astrocytes (chapter 2.2.) and for OLN-93 cells that have taken up other types of nanoparticles (Busch *et al.* 2011). Since endocytotic processes are involved in the uptake of different kinds of nanoparticles by OLN-93 cells (Busch *et al.* 2011), endocytosis inhibitors should be applied to further characterize the endocytotic pathways involved in the uptake of the Fe-NP used here. As discussed in chapter 2.1.1., protein-coated Fe-NP might resemble the uptake of ferritin as a physiological iron source by oligodendrocytes (Todorich *et al.* 2009, Todorich *et al.* 2011). A comparison of the iron accumulation from serum protein-coated Fe-NP with the iron accumulation from commercially available ferritin could reveal whether OLN-93 cells take up similar amounts of iron from these two iron sources and whether these cells used similar pathways for the uptake of both types of particles.

Mobilization of iron from Fe-NP in OLN-93 cells was shown by inhibition of proliferation by iron restriction (chapter 2.1.3.), by the upregulation of ferritin (chapter 2.1.3.) and by the inhibition of the Fe-NP-dependent ROS formation by an iron chelator (Chapter 2.1.4.). Despite of the high amounts of accumulated iron no severe negative consequences of an exposure of OLN-93 cells to Fe-NP were observed. Therefore, the rate of iron liberated from Fe-NP in cells should be investigated in further detail. Differently coated Fe-NP release iron

with different velocities in a cell-free system and also the rate of cellular degradation of Fe-NP depends on the type of Fe-NP investigated (Soenen *et al.* 2010a). Thus, for OLN-93 cells that have accumulated large amounts of Fe-NP, the complete degradation of these Fe-NP may take quite some time. In addition potential negative consequences of this process may not be observable in the time frame investigated here. To address such questions, the presence of low molecular weight iron derived from internalized Fe-NP should be visualized and quantified by fluorescence indicators such as Phen Green[TM] or calcein which alter their fluorescence depending on the concentration of low molecular weight iron (Kakhlon and Cabantchik 2002, Petrat *et al.* 2002). In this context, the fluorescence-dye-labeled Fe-NP should be used to colocalize the Fe-NP with the low molecular weight iron fluorescence indicators.

Internalized Fe-NP and other types of nanoparticles have been shown to be localized in vesicular structures (chapters 2.2.1 and 2.2.3.; Busch *et al.* 2011) which are considered to be part of the lysosomal compartment where iron release is facilitated by a low pH (Arbab *et al.* 2005, Huang *et al.* 2009, Soenen *et al.* 2010a). Staining of the lysosomes, for example by uptake of fluorescent transferrin (Soenen *et al.* 2010a) or by dyes that accumulate in lysosomes (Berg *et al.* 2010, Busch *et al.* 2011) should reveal whether these particles are indeed taken up into the lysosomal compartment in cells that have been exposed to fluorescence-dye-labeled Fe-NP.

Fe-NP are considered for various applications in neuroscience (Silva 2007, Yang 2010). Therefore, the consequences of an exposure to brain cells *in vivo* are of particular importance. OLN-93 cells are a cell line that has been derived from primary glial cultures (Richter-Landsberg and Heinrich 1996). Thus, the results obtained about the consequences of Fe-NP exposed to OLN-93 cells should be confirmed for oligodendroglial-rich secondary cultures, since these cells are more comparable to the *in vivo* situation. Oligodendroglial-rich secondary cultures were established during the work on this thesis by Anette Thiessen and myself according to a published method (Hirrlinger *et al.* 2002) and were successfully used to study the consequences of fumaric acid esters on oligodendroglial cells (Thiessen *et al.* 2010). Key results on the accumulation of Fe-NP and on consequences of such treatments on cell viability and on cellular metabolism of OLN-93 cells should be verified on such cultures.

The toxicity and fate of Fe-NP *in vivo* is of importance for medical applications of Fe-NP (Yang 2010, Kunzmann *et al.* 2011). Although Fe-NP have been reported to cross the BBB and to enter the brain (Wang *et al.* 2010) no information is available concerning the uptake and distribution of Fe-NP among the different cell types in brain. Astrocytes might be the first

cells of the brain to come in contact with Fe-NP, when the BBB remains intact, especially as these cells efficiently accumulate Fe-NP in culture (chapter 2.2.; Au *et al.* 2007, Pickard *et al.* 2010) and since these cells have been discussed as sink for metal ions (Tiffany-Castiglioni and Qian 2001, Dringen *et al.* 2007). Microglial cells, the immune-competent cells of the brain (Graeber and Streit 2010), have also been reported to take up Fe-NP (Pickard and Chari 2010). Therefore, these cells might accumulate substantial amounts of Fe-NP when these particles cross the BBB and pass astrocytes. Therefore, uptake of Fe-NP by different brain cell types in brain slices and *in vivo* should be investigated. An ideal tool for these investigations would be again fluorescence-dye-labeled Fe-NP as mentioned above, since the fluorescence signal could be correlated to immunohistochemical stainings of cell type specific markers to identify the cell types that have taken up the Fe-NP in brain slices. This would improve the understanding of consequences of a treatment of the brain with Fe-NP for medical diagnostics or disease treatment.

3.6.   References

Abouhamed M, Wolff NA, Lee WK, Smith CP, Thevenod F (2007) Knockdown of endosomal/lysosomal divalent metal transporter 1 by RNA interference prevents cadmium-metallothionein-1 cytotoxicity in renal proximal tubule cells. Am J Physiol Renal Physiol 293:F705-712.

Apopa PL, Qian Y, Shao R, Guo NL, Schwegler-Berry D, Pacurari M, Porter D, Shi X, Vallyathan V, Castranova V, Flynn DC (2009) Iron oxide nanoparticles induce human microvascular endothelial cell permeability through reactive oxygen species production and microtubule remodeling. Part Fibre Toxicol 6:1.

Arbab AS, Wilson LB, Ashari P, Jordan EK, Lewis BK, Frank JA (2005) A model of lysosomal metabolism of dextran coated superparamagnetic iron oxide (SPIO) nanoparticles: implications for cellular magnetic resonance imaging. NMR Biomed 18:383-389.

Arosio P, Ingrassia R, Cavadini P (2009) Ferritins: a family of molecules for iron storage, antioxidation and more. Biochim Biophys Acta 1790:589-599.

Attieh ZK, Mukhopadhyay CK, Seshadri V, Tripoulas NA, Fox PL (1999) Ceruloplasmin ferroxidase activity stimulates cellular iron uptake by a trivalent cation-specific transport mechanism. J Biol Chem 274:1116-1123.

Au C, Mutkus L, Dobson A, Riffle J, Lalli J, Aschner M (2007) Effects of nanoparticles on the adhesion and cell viability on astrocytes. Biol Trace Elem Res 120:248-256.

Babcock GT (1999) How oxygen is activated and reduced in respiration. Proc Natl Acad Sci USA 96:12971-12973.

Ballatori N, Krance SM, Marchan R, Hammond CL (2009) Plasma membrane glutathione transporters and their roles in cell physiology and pathophysiology. Mol Aspects Med 30:13-28.

Berg JM, Ho S, Hwang W, Zebda R, Cummins K, Soriaga MP, Taylor R, Guo B, Sayes CM (2010) Internalization of carbon black and maghemite iron oxide nanoparticle mixture leads to oxidant production. Chem Res Toxicol 23:1874-1882.

Brand A, Schonfeld E, Isharel I, Yavin E (2008) Docosahexaenoic acid-dependent iron accumulation in oligodendroglia cells protects from hydrogen peroxide-induced damage. J Neurochem 105:1325-1335.

Bulte JW, Douglas T, Witwer B, Zhang SC, Strable E, Lewis BK, Zywicke H, Miller B, van Gelderen P, Moskowitz BM, Duncan ID, Frank JA (2001) Magnetodendrimers allow endosomal magnetic labeling and *in vivo* tracking of stem cells. Nat Biotechnol 19:1141-1147.

Burdo JR, Menzies SL, Simpson IA, Garrick LM, Garrick MD, Dolan KG, Haile DJ, Beard JL, Connor JR (2001) Distribution of divalent metal transporter 1 and metal transport protein 1 in the normal and Belgrade rat. J Neurosci Res 66:1198-1207.

Busch W, Bastian S, Trahorsch U, Iwe M, Kühnel D, Meißner T, Springer A, Gelinsky M, Richter V, Ikonomidou C (2011) Internalisation of engineered nanoparticles into mammalian cells *in vitro*: influence of cell type and particle properties. J Nanopart Res 13:293-310.

Buyukhatipoglu K, Clyne AM (2011) Superparamagnetic iron oxide nanoparticles change endothelial cell morphology and mechanics via reactive oxygen species formation. J Biomed Mater Res A 96:186-195.

Chen ZP, Xu RZ, Zhang Y, Gu N (2009) Effects of proteins from culture medium on surface property of silanes-functionalized magnetic nanoparticles. Nanoscale Res Lett 4:204-209.

Chua AC, Drake SF, Herbison CE, Olynyk JK, Leedman PJ, Trinder D (2006) Limited iron export by hepatocytes contributes to hepatic iron-loading in the Hfe knockout mouse. J Hepatol 44:176-182.

Connor JR, Menzies SL (1996) Relationship of iron to oligodendrocytes and myelination. Glia 17:83-93.

Conrad ME, Umbreit JN, Moore EG, Hainsworth LN, Porubcin M, Simovich MJ, Nakada MT, Dolan K, Garrick MD (2000) Separate pathways for cellular uptake of ferric and ferrous iron. Am J Physiol Gastrointest Liver Physiol 279:767-774.

Dringen R (2000) Metabolism and functions of glutathione in brain. Prog Neurobiol 62:649-671.

Dringen R, Bishop GM, Koeppe M, Dang TN, Robinson SR (2007) The pivotal role of astrocytes in the metabolism of iron in the brain. Neurochem Res 32:1884-1890.

Garrick MD, Garrick LM (2009) Cellular iron transport. Biochim Biophys Acta 1790:309-325.

Graeber MB, Streit WJ (2010) Microglia: biology and pathology. Acta Neuropathol 119:89-105.

Gunshin H, Mackenzie B, Berger UV, Gunshin Y, Romero MF, Boron WF, Nussberger S, Gollan JL, Hediger MA (1997) Cloning and characterization of a mammalian proton-coupled metal-ion transporter. Nature 388:482-488.

Halliwell B, Gutteridge JMC (2007) Free Radicals in Biology and Medicine. Oxford, UK: Oxford University Press.

Hirrlinger J, Resch A, Gutterer JM, Dringen R (2002) Oligodendroglial cells in culture effectively dispose of exogenous hydrogen peroxide: comparison with cultured neurones, astroglial and microglial cells. J Neurochem 82:635-644.

Hoepken HH, Korten T, Robinson SR, Dringen R (2004) Iron accumulation, iron-mediated toxicity and altered levels of ferritin and transferrin receptor in cultured astrocytes during incubation with ferric ammonium citrate. J Neurochem 88:1194-1202.

Huang DM, Hsiao JK, Chen YC, Chien LY, Yao M, Chen YK, Ko BS, Hsu SC, Tai LA, Cheng HY, Wang SW, Yang CS (2009) The promotion of human mesenchymal stem cell proliferation by superparamagnetic iron oxide nanoparticles. Biomaterials 30:3645-3651.

Jensen FB (2009) The dual roles of red blood cells in tissue oxygen delivery: oxygen carriers and regulators of local blood flow. J Exp Biol 212:3387-3393.

Jeong SY, David S (2003) Glycosylphosphatidylinositol-anchored ceruloplasmin is required for iron efflux from cells in the central nervous system. J Biol Chem 278:27144-27148.

Kakhlon O, Cabantchik ZI (2002) The labile iron pool: characterization, measurement, and participation in cellular processes. Free Radic Biol Med 33:1037-1046.

Kasvosve I, Delanghe J (2002) Total iron binding capacity and transferrin concentration in the assessment of iron status. Clin Chem Lab Med 40:1014-1018.

Kell DB (2009) Iron behaving badly: inappropriate iron chelation as a major contributor to the aetiology of vascular and other progressive inflammatory and degenerative diseases. BMC Med Genomics 2:2.

Kimelberg HK (2010) Functions of mature mammalian astrocytes: a current view. Neuroscientist 16:79-106.

Kunzmann A, Andersson B, Thurnherr T, Krug H, Scheynius A, Fadeel B (2011) Toxicology of engineered nanomaterials: focus on biocompatibility, biodistribution and biodegradation. Biochim Biophys Acta 1810:361-373.

Laurent S, Forge D, Port M, Roch A, Robic C, Vander Elst L, Muller RN (2008) Magnetic iron oxide nanoparticles: synthesis, stabilization, vectorization, physicochemical characterizations, and biological applications. Chem Rev 108:2064-2110.

Levy M, Lagarde F, Maraloiu VA, Blanchin MG, Gendron F, Wilhelm C, Gazeau F (2010) Degradability of superparamagnetic nanoparticles in a model of intracellular environment: follow-up of magnetic, structural and chemical properties. Nanotechnology 21:395103-395114.

Lewinski N, Colvin V, Drezek R (2008) Cytotoxicity of nanoparticles. Small 4:26-49.

Lunov O, Syrovets T, Loos C, Beil J, Delacher M, Tron K, Nienhaus GU, Musyanovych A, Mailänder V, Landfester K, Simmet T (2011) Differential uptake of functionalized polystyrene nanoparticles by human macrophages and a monocytic cell line. ACS Nano 5:1657-1669.

Mailänder V, Landfester K (2009) Interaction of nanoparticles with cells. Biomacromolecules 10:2379-2400.

McTigue DM, Tripathi RB (2008) The life, death, and replacement of oligodendrocytes in the adult CNS. J Neurochem 107:1-19.

Miron VE, Kuhlmann T, Antel JP (2011) Cells of the oligodendroglial lineage, myelination, and remyelination. Biochim Biophys Acta 1812:184-193.

Mollgard K, Dziegielewska KM, Saunders NR, Zakut H, Soreq H (1988) Synthesis and localization of plasma proteins in the developing human brain. integrity of the fetal blood-brain barrier to endogenous proteins of hepatic origin. Dev Biol 128:207-221.

Moos T, Morgan EH (2000) Transferrin and transferrin receptor function in brain barrier systems. Cell Mol Neurobiol 20:77-95.

Mu Q, Li Z, Li X, Mishra SR, Zhang B, Si Z, Yang L, Jiang W, Yan B (2009) Characterization of protein clusters of diverse magnetic nanoparticles and their dynamic interactions with human cells. J Phys Chem C 113:5390-5395.

Munoz M, Villar I, Garcia-Erce JA (2009) An update on iron physiology. World J Gastroenterol 15:4617-4626.

Nel A, Xia T, Mädler L, Li N (2006) Toxic potential of materials at the nanolevel. Science 311:622-627.

Nel AE, Mädler L, Velegol D, Xia T, Hoek EM, Somasundaran P, Klaessig F, Castranova V, Thompson M (2009) Understanding biophysicochemical interactions at the nano-bio interface. Nat Mater 8:543-557.

Oberdörster G (2010) Safety assessment for nanotechnology and nanomedicine: concepts of nanotoxicology. J Intern Med 267:89-105.

Petrat F, de Groot H, Sustmann R, Rauen U (2002) The chelatable iron pool in living cells: a methodically defined quantity. Biol Chem 383:489-502.

Petri-Fink A, Hofmann H (2007) Superparamagnetic iron oxide nanoparticles (SPIONs): from synthesis to *in vivo* studies-a summary of the synthesis, characterization, *in vitro*, and *in vivo* investigations of SPIONs with particular focus on surface and colloidal properties. IEEE Trans Nanobioscience 6:289-297.

Pickard MR, Chari DM (2010) Robust uptake of magnetic nanoparticles (MNPs) by central nervous system (CNS) microglia: implications for particle uptake in mixed neural cell populations. Int J Mol Sci 11:967-981.

Pickard MR, Jenkins SI, Koller CJ, Furness DN, Chari DM (2010) Magnetic nanoparticle labeling of astrocytes derived for neural transplantation. Tissue Eng Part C Methods 17:89-99.

Piñero DJ, Connor JR (2000) Iron in the brain: an important contributor in normal and diseased states. Neuroscientist 6:435-453.

Qian Z, Liao Q, To Y, Ke Y, Tsoi Y, Wang G, Ho K (2000) Transferrin-bound and transferrin free iron uptake by cultured rat astrocytes. Cell Mol Biol (Noisy-le-Grand) 46:541-548.

Rezwan K, Meier LP, Rezwan M, Voros J, Textor M, Gauckler LJ (2004) Bovine serum albumin adsorption onto colloidal Al_2O_3 particles: a new model based on zeta potential and UV-Vis measurements. Langmuir 20:10055-10061.

Richter-Landsberg C, Heinrich M (1996) OLN-93: a new permanent oligodendroglia cell line derived from primary rat brain glial cultures. J Neurosci Res 45:161-173.

Rouault TA, Tong WH (2008) Iron-sulfur cluster biogenesis and human disease. Trends Genet 24:398-407.

Schröder I, Johnson E, de Vries S (2003) Microbial ferric iron reductases. FEMS Microbiol Rev 27:427-447.

Silva GA (2007) Nanotechnology approaches for drug and small molecule delivery across the blood brain barrier. Surg Neurol 67:113-116.

Soenen SJ, Himmelreich U, Nuytten N, Pisanic TR, 2nd, Ferrari A, De Cuyper M (2010a) Intracellular nanoparticle coating stability determines nanoparticle diagnostics efficacy and cell functionality. Small 6:2136-2145.

Soenen SJ, Nuytten N, De Meyer SF, De Smedt SC, De Cuyper M (2010b) High intracellular iron oxide nanoparticle concentrations affect cellular cytoskeleton and focal adhesion kinase-mediated signaling. Small 6:832-842.

Soenen SJ, Himmelreich U, Nuytten N, De Cuyper M (2011) Cytotoxic effects of iron oxide nanoparticles and implications for safety in cell labelling. Biomaterials 32:195-205.

Sofroniew MV, Vinters HV (2010) Astrocytes: biology and pathology. Acta Neuropathol 119:7-35.

Thiessen A, Schmidt MM, Dringen R (2010) Fumaric acid dialkyl esters deprive cultured rat oligodendroglial cells of glutathione and upregulate the expression of heme oxygenase 1. Neurosci Lett 475:56-60.

Tiffany-Castiglioni E, Qian Y (2001) Astroglia as metal depots: molecular mechanisms for metal accumulation, storage and release. Neurotoxicology 22:577-592.

Todorich B, Pasquini JM, Garcia CI, Paez PM, Connor JR (2009) Oligodendrocytes and myelination: the role of iron. Glia 57:467-478.

Todorich B, Zhang X, Connor JR (2011) H-ferritin is the major source of iron for oligodendrocytes. Glia 59:927-935.

Tulpule K, Robinson SR, Bishop GM, Dringen R (2010) Uptake of ferrous iron by cultured rat astrocytes. J Neurosci Res 88:563-571.

Villanueva A, Canete M, Roca AG, Calero M, Veintemillas-Verdaguer S, Serna CJ, Morales Mdel P, Miranda R (2009) The influence of surface functionalization on the enhanced internalization of magnetic nanoparticles in cancer cells. Nanotechnology 20:115103-115112.

Wang J, Jiang H, Xie JX (2007) Ferroportin1 and hephaestin are involved in the nigral iron accumulation of 6-OHDA-lesioned rats. Eur J Neurosci 25:2766-2772.

Wang J, Chen Y, Chen B, Ding J, Xia G, Gao C, Cheng J, Jin N, Zhou Y, Li X, Tang M, Wang XM (2010) Pharmacokinetic parameters and tissue distribution of magnetic Fe_3O_4 nanoparticles in mice. Int J Nanomedicine 5:861-866.

Weinstein JS, Varallyay CG, Dosa E, Gahramanov S, Hamilton B, Rooney WD, Muldoon LL, Neuwelt EA (2010) Superparamagnetic iron oxide nanoparticles: diagnostic magnetic resonance imaging and potential therapeutic applications in neurooncology and central nervous system inflammatory pathologies, a review. J Cereb Blood Flow Metab 30:15-35.

Weissleder R, Bogdanov A, Neuwelt EA, Papisov M (1995) Long-circulating iron-oxides for MR imaging. Adv Drug Deliver Rev 16:321-334.

Wiogo HT, Lim M, Bulmus V, Yun J, Amal R (2011) Stabilization of magnetic iron oxide nanoparticles in biological media by fetal bovine serum (FBS). Langmuir 27:843-850.

Wu LJ, Leenders AG, Cooperman S, Meyron-Holtz E, Smith S, Land W, Tsai RY, Berger UV, Sheng ZH, Rouault TA (2004) Expression of the iron transporter ferroportin in synaptic vesicles and the blood-brain barrier. Brain Res 1001:108-117.

Yang H (2010) Nanoparticle-mediated brain-specific drug delivery, imaging, and diagnosis. Pharm Res 27:1759-1771.

4.   Appendix

4.1.   Curriculum vitae

Born 19th February 1983 in Bremen, Germany

Education:

12/2007 – 06/2011	Doctoral thesis under supervision of Prof. Ralf Dringen
	"Metabolism of iron and iron oxide nanoparticles in glial cells"
	University of Bremen, Germany
10/2007	Diploma in Chemistry
	"Development of an enzymatic method for the measurement of the hepatocellular enzyme activity of pyruvate carboxylase"
	University of Bremen, Germany
02/2007 – 05/2007	Laboratory work on the Diploma thesis with Dr. Claudia Zwingmann at the "Research Centre of the Centre Hospitalier de L´Université de Montréal", Montreal, Canada
06/2006 – 10/2006	Practical laboratory training with Dr. Claudia Zwingmann at the "Research Centre of the Centre Hospitalier de L´Université de Montréal", Montreal, Canada
10/2002 – 10/2007	Studies of Chemistry
	University of Bremen, Germany
07/2002	Abitur (University entrance diploma)
	Hermann-Böse-Gymnasium, Bremen, Germany

Teaching experience:

12/2006 – 06/2011	Supervisor for laboratory courses in biochemistry for students of chemistry and biology
10/2005 – 01/2006	Supervisor for laboratory course in basal chemistry for students of chemistry
09/2004 – 12/2004	Supervisor for laboratory course in organic chemistry for students of biology

4.2. List of publications

Justus E, Awad D, **Hohnholt M**, Edwards K, Karlsson G, Gabel D (2007) Synthesis, liposomal preparation, and *in vitro* toxicity of two novel dodecaborate cluster lipids for boron neutron capture therapy. Bioconjugate Chem 18:1287-1293.

Geppert M, **Hohnholt M**, Gaetjen L, Grunwald I, Bäumer M, Dringen R (2009) Accumulation of iron oxide nanoparticles by cultured brain astrocytes. J Biomed Nanotechnol 5:285-293.

Hohnholt M, Geppert M, Dringen R (2010) Effects of iron chelators, iron salts, and iron oxide nanoparticles on the proliferation and the iron content of oligodendroglial OLN-93 cells. Neurochem Res 35:1259-1268.

Hohnholt MC, Geppert M, Nürnberger S, von Byern J, Grunwald I, Dringen R (2010) Advanced Biomaterials: Accumulation of citrate-coated magnetic iron oxide nanoparticles by cultured brain astrocytes. Adv Eng Mater 12:B690-B694.

Geppert M, **Hohnholt MC**, Thiel K, Nürnberger S, Grunwald I, Rezwan K, Dringen R (2011) Uptake of dimercaptosuccinate-coated magnetic iron oxide nanoparticles by cultured brain astrocytes. Nanotechnology 22:145101-145111.

Hohnholt MC, Geppert M, Dringen R; Mobilization of iron from iron oxide nanoparticles in oligodendroglial cells. *Revised manuscript submitted for publication*

Hohnholt MC, Dringen R; Iron-dependent formation of reactive oxygen species and glutathione depletion after accumulation of magnetic iron oxide nanoparticles by oligodendroglial cells. *Submitted for publication*